ДОКЛАДЫ
АКАДЕМИИ НАУК СССР

SOVIET PHYSICS

"Doklady"

VOLUME 1 NUMBER 6

A Translation
of the
"Physics Section"
of the

Proceedings of the Academy of Sciences of the USSR

(RUSSIAN ORIGINAL VOL. 111, NOS. 1-6)

Published by the
AMERICAN INSTITUTE OF PHYSICS
INCORPORATED

SOVIET PHYSICS

"Doklady"

A translation of the "Physics Section" of the Proceedings of the Academy of Sciences of the USSR.

A publication of the

AMERICAN INSTITUTE OF PHYSICS

Governing Board

ALLEN V. ASTIN
ROBERT F. BACHER
W. S. BAIRD
H. A. BETHE
R. T. BIRGE
FRANK D. DEXTER
I. C. GARDNER
S. A. GOUDSMIT
CHARLES KITTEL
HUGH S. KNOWLES
R. B. LINDSAY
WILLIAM F. MEGGERS
HARRY F. OLSON
R. R. PALMER
R. F. PATON
ERIC RODGERS
RALPH A. SAWYER
FREDERICK SEITZ
H. D. SMYTH
MARK W. ZEMANSKY

Officers and Staff

FREDERICK SEITZ
Chairman, Governing Board
HENRY A. BARTON
Director
WALLACE WATERFALL
Executive Secretary
MARK W. ZEMANSKY
Treasurer
THEODORE VORBURGER
Advertising Manager
RUTH F. BRYANS
Publication Manager
KATHRYN SETZE
Assistant Treasurer
ALICE MASTROPIETRO
Circulation Manager
EUGENE H. KONE
Director of Public Relations

American Institute of Physics Advisory Board on Russian Translations

ELMER HUTCHISSON, *Chairman*
DWIGHT GRAY, MORTON HAMERMESH, VLADIMIR ROJANSKY,
VICTOR WEISSKOPF

SOVIET PHYSICS—"Doklady" is a bi-monthly journal published by the American Institute of Physics for the purpose of making available in English reports of current Soviet research in physics as contained in the "Physics Section" of the Proceedings of the Academy of Sciences of the USSR. The Proceedings appears thirty-six times per year and the "Physics Sections" are accumulated and English translations of them are published in six issues per year.

Transliteration of the names of Russian authors follows the system employed by the Library of Congress.

This translating and publishing project was undertaken by the Institute in the conviction that dissemination of the results of research everywhere in the world is invaluable to the advancement of science. The National Science Foundation of the United States encouraged the project initially and is supporting it in large part by a grant. Translation and printing are being handled by Consultants Bureau, Inc.

The American Institute of Physics and its translators propose to translate faithfully all of the scientific material in the "Physics Section" of the Proceedings of the Academy of Sciences of the USSR appearing after January 1, 1956. The views expressed in the translated material, therefore, are intended to be those expressed by the original authors, and not those of the translators nor of the American Institute of Physics.

One volume is published annually. Volume 1 will consist of six issues and will contain all scientific material published in the "Physics Section" of the original Russian journal during the 1956 calendar year.

Subscription Prices:

Per year (6 issues)	
United States and Canada	$25.00
Elsewhere	27.50
Back Numbers	
Single copies	$ 6.00

Subscriptions should be addressed to the American Institute of Physics, 57 East 55th Street, New York 22, N. Y.

Copyright by American Institute of Physics 1957

SOVIET PHYSICS
"Doklady"

A translation of the "Physics Section" of the Proceedings of the Academy of Sciences of the USSR.

VOLUME 1, NUMBER 6 NOVEMBER-DECEMBER, 1956

POLARIZATION OF LOW-ENERGY PROTONS SCATTERED BY CARBON

B. V. Gavrilovskii, V. Ia. Golovnia, K. V. Karadzhev,

A. P. Kliucharev and V. I. Man'ko

(Presented by Academician A. P. Aleksandrov, June 16, 1956)

We have studied the polarization of protons elastically scattered by C^{12}. $C^{12}(p, p)$ elastic scattering was very carefully investigated by Jackson et al.[1] in the range 0.4-4.3 Mev for four scattering angles. These results were analyzed and the levels of N^{13} were identified in reference [2]. Using the data of [2] I. T. Diatlov and L. N. Rozentsveig have calculated the degree of polarization in $C^{12}(p, p)$ scattering for various angles in the range 1.2-2.4 Mev. For 60° the degree of polarization P increases smoothly from + 0.2 at 2.4 Mev to + 0.5 at 1.8 Mev. Near 1.7 Mev the polarization changes sign sharply and reaches a value of -0.65 at 1.6 Mev.

For the purpose of investigating the function P(E) we performed an experiment on double proton scattering in solid carbon targets. We measured the azimuthal asymmetry of secondary scattering for different energies of the primary proton beam. The experimental results were compared with calculations of the asymmetry according to [3]. This comparison makes it possible to verify the correctness of the phase analysis of $C^{12}(p, p)$ scattering in [2].

The work was done with an electrostatic generator. The scheme and geometry of the experiment are shown in Fig. 1. The apparatus consists of two vacuum chambers. Chamber I is a steel cylinder with a cover which can be turned through the angle β with respect to the cylinder axis without affecting the vacuum. The cover contains a tube a to which the cylindrical steel chamber II is attached. The axis of the tube forms the angle $\alpha = 19°$ with the plane of chamber I. Fig. 1 shows a vertical section of the apparatus corresponding to $\beta = 0$ and mutually perpendicular planes of primary and secondary scattering.

The proton beam from the electrostatic generator enters the inlet tube b to reach the first carbon target M_I in the center of chamber I. Protons scattered by target M_I pass through tube a to enter chamber II and are scattered by target M_{II} in the center of chamber II. Doubly scattered protons are registered by photographic plates with a 100 μ emulsion. These plates are at identical distances from the center of chamber II at positions which correspond to definite angles of secondary scattering. The primary scattering angle Θ_1 was 60° in the c. m. system. This angle was chosen because at 60° there is considerable polarization over a broad energy range. The secondary scattering angles Θ_2 were ± 60 ± 120 ± 150° in the c. m. system. The primary and secondary scattering planes were mutually adjusted by rotating chamber II around the axis of tube a. In the course of irradiation 6 plates were exposed simultaneously to correspond to selected values of the angle Θ_2.

A system of circular diaphragms in tubes a and b insured good collimation of the primary and scattered proton beams and protected the plates from protons scattered by the chamber walls and holders of the carbon targets.

The entire apparatus was carefully adjusted. The diameter of the proton beam which impinged on target M_I was ~ 6 mm. The scattered proton beam had a diameter of ~ 14 mm at target M_{II}. The diameter of target M_I was 14 mm; that of target M_{II} was 22 mm.

We paid special attention to the preparation of the solid carbon targets. Because of the strong functional relationship P(E) for $C^{12}(p, p)$ scattering the targets had to be very thin and uniform in thickness. We develped the following method of producing thin carbon targets. To a brass ring we cemented a very thin (~ 0,2-0.3 μ) film of nitrocellulose, on which we poured a colloidal solution of graphite (aquadag). The ring was kept in a horizontal position until the solution was completely dried. After the drying the organic backing was carefully burned off. In this way we obtained carbon films which were of uniform thickness (~ 5%). For different exposures the thickness of target M_I was between 0.75 and 1.05 mg/cm². Such targets were exposed to proton currents up to 2 μa for many hours. Target M_{II} was from 0.5 to 0.65 mg/cm² in thickness. The error in determining the thickness of the targets did not exceed ± 5%.

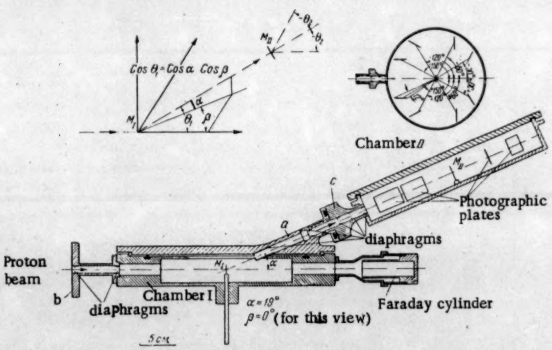

Fig. 1. Scheme and geometry of the experiment. α) angle of inclination of scattered beam to horizontal plane; β) scattering angle in the horizontal plane, read from the chamber scale; Θ_1) primary scattering angle; Θ_2) secondary scattering angle; Θ_1 and Θ_2 are in the same plane.

The presence of impurities in the colloidal graphite of which the targets were made was investigated by burning the graphite and weighing the ash. The impurities constituted ~ 2%.

We ran a series of exposures at the following energies E_0 of protons striking target M_I: 1.9, 2.0, 2.1, 2.2, 2.3 and 2.4 Mev. The exposures lasted from 5 to 20 hours with a current of from 1 to 2 μa.

By control exposures in the absence of a carbon film in chamber II it was shown that the extraneous tracks of protons scattered by the metal chamber walls and by the target and plate holders comprise a very small fraction of the effect (~ 1%). For individual exposures we determined the energy spectrum of protons scattered by target M_{II}. Fig. 2 shows the spectrum for scattering at angle $\Theta_2 = 60°$ and initial proton energy of 2.1 Mev. The thickness of the targets was 0.80 mg/cm² for M_I and 0.65 mg/cm² for M_{II}.

E_0, Mev	Δ_1, mg/cm²	Δ_2, mg/cm²	$R_{\text{av exp}}$	$R_{\text{av theor}}$
$\Theta_2 = 60°$				
1.9	0.80	0.50	1.41±0.14	1.33
2.0	0.80	0.50	1.50±0.10	1.34
2.1	0.80	0.65	1.01±0.07	0.90
2.2	0.75	0.65	1.00±0.11	0.85
2.3	0.80	0.65	0.81±0.10	0.89
2.4	0.80	0.60	0.77±0 20	0.90
$\Theta_2 = 120°$				
2.0	0.80	0.50	1.43±0.10	1.41
2.1	0.80	0.50	1.27±0 11	1.36
2.2	1.05	0.65	1.1 ±0.07	1.05
$\Theta_2 = 150°$				
2.1	0.80	0.50	1.2±0.07	1.4
2.1	1.05	0.65	1.19±0.06	1.31

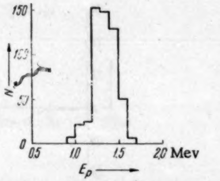

Fig. 2. Double-scattering proton spectrum for $\Theta_1 = 60°$, $\Theta_2 = 60°$ and $E_0 = 2.1$ Mev.

The number of protons recorded in the plates averaged from 300 to 1000 for individual exposures. Scattering at the angles $\Theta_2 = +60°, +120°$ and $+150°$ according to Fig. 1 constitutes scattering to the right. Scattering to the left corresponds to the angles $-60°, -120°$ and $-150°$. The ratio of scattering to the right and to the left for each absolute value of Θ_2 is a measure of the azimuthal asymmetry of proton scattering by target M_{II} and is thus a measure of polarization in $C^{12}(p, p)$ scattering.

Due to the fact that ionization losses of proton energy in the targets are between 100 and 150 kev our measurements of the azimuthal asymmetry are averaged over this energy range.

In the experiments we measured

$$R_{\text{av}}(E_0, \Delta_1, \Delta_2, \Theta_1, \Theta_2) = \frac{1 - P_{1\text{av}}P_{2\text{av}}}{1 + P_{1\text{av}}P_{2\text{av}}}. \tag{1}$$

Here E_0 is the initial proton energy; Δ_1 and Δ_2 are the thicknesses of targets M_I and M_{II}, respectively; Θ_1 and Θ_2 are the angles of primary and secondary scattering; $P_{1\text{av}}$ and $P_{2\text{av}}$ are the average values of the polarization calculated from the relation

$$P_{\text{av}} = \frac{\int\limits_{\delta E} \sigma(E)\, P(E)\, dE \Big/ \frac{dE}{dx}}{\int\limits_{\delta E} \sigma(E)\, dE \Big/ \frac{dE}{dx}}, \tag{2}$$

where $\sigma(E)$ is the energy dependence of the differential $C^{12}(p, p)$ scattering cross section; $\delta(E)$ is the energy range which corresponds to ionization losses of energy in the targets.

We investigated with most care the energy dependence of right-to-left asymmetry for $\Theta_2 = 60°$. Experimental data for this case averaged over the individual exposures are given in Table 1 and Fig. 3.

With initial proton energies from 1.9 to 2.4 Mev and $\Theta_2 = 60°$ for our targets the asymmetry measurement enables us to investigate proton polarization in $C^{12}(p, p)$ scattering in the range 1.6-2.4 Mev.

In order to determine the instrumental asymmetry we ran control exposures in which the right and left halves of the chamber were interchanged by rotation of the plane of chamber II around the axis of tube a. Within the limits of error the values obtained for the asymmetry coincided for both positions of the chamber.

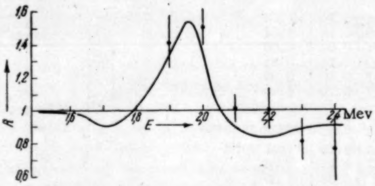

Fig. 3. This curve represents the values of R_{Av} calculated theoretically. The dots represent experimental results.

The solid curve in Fig. 3 represents the values of R_{Av} calculated by the method indicated above on the basis of information given in reference [3] for the targets used in our measurements.

Evaluation of the asymmetry for $\Theta_1 = 60°$, $\Theta_2 = 120°$ and 150° under the conditions of this experiment can be regarded as only approximate. This is due to the very strong dependence P(E) for 120° and 150°, as was shown in [3].

We obtained R_{Av} for $\Theta_2 = 120°$ and 150° in a few exposures. The results are given in the table. The theoretical values of R_{Av} calculated from the curves P(E) and σ(E) are given in [3].

The results of our experiments on double scattering of protons from C^{12} are in satisfactory agreement with theoretical calculations for proton polarization and thus confirm the correctness of the phase analysis of C^{12}(p,p) scattering in [2]. It was shown that scattering is accompanied by strong polarization of protons from 1.6 to 2.4 Mev.

The authors thank A. S. Emlianinov for great assistance with the experiment, also A. A. Tsygikalo and the crew of the electrostatic generator for maintaining stability of the generator during long exposures.

Physico-Technical Institute, Academy of
Sciences, Ukrainian SSR

Received June 14, 1956

LITERATURE CITED

[1] H. L. Jackson, A. I. Galonsky et al., Phys. Rev. 89, 365 (1953).

[2] H. L. Jackson and A. I. Galonsky, Phys. Rev. 89, 370 (1953).

[3] I. T. Diatlov and L. N. Rosentsveig, Trans. Physico-Math. Faculty Kharkov State Univ. 1955, No. 6, 81.

ON THE THEORY OF A REAL GAS WITH NONCENTRAL PARTICLE INTERACTION

A. E. Glauberman

(Presented by Academician N. N. Bogoliubov, April 12, 1956)

Let us consider a gas that consists of axially symmetrical molecules with a constant electric moment (dipole, quadrupole). We shall assume that the interaction between two particles is of the form

$$L_{ij}(|\mathbf{q}_i - \mathbf{q}_j|,\ \vartheta_i, \varphi_i, \vartheta_j, \varphi_j, \vartheta_{ij}, \varphi_{ij}), \tag{1}$$

where $\mathbf{q}_i$ is a vector which determines the position of the center of gravity of a molecule; ϑ_i and φ_i are angles which give the orientation of the molecular electric moment vector in space; ϑ_{ij} and φ_{ij} are the corresponding angles for the line of centers of the two molecules under consideration.

Bogoliubov's equations [1] for the distribution law of groups of particles can easily be seen in this case to be

$$\frac{\partial F_s}{\partial q_1^\alpha} + \frac{1}{\theta}\frac{\partial U_s}{\partial q_1^\alpha} F_s + \frac{1}{4\pi v\theta}\int \frac{\partial}{\partial q_1^\alpha}(L_{1,s+1}) F_{s+1} d\mathbf{q}_{s+1} d\Omega_{s+1} = 0, \tag{2}$$
$$\alpha = 1, \ldots, s, \quad \theta = kT,$$

$\mathbf{q}_1(q_1^1, q_1^2, q_1^3)$; $q_1^4 = \vartheta_1$, $q_1^5 = \varphi_1$, $d\Omega$ is an element of solid angle; U_s is the potential energy of the group of s particles:

$$U_s = \sum_{1 \leqslant i < j \leqslant s} L_{ij} + \sum_{1 \leqslant i \leqslant s} \varphi_i, \tag{3}$$

where φ_i is the potential energy of the i-th molecule in an external field.

Expanding, as usual, in powers of the density n of the system:

$$F_s = F_s^0 + nF_s^1 + \ldots \tag{4}$$

with weakened correlation it is possible to solve the corresponding set of equations. We obtain

$$F_s^0 = C_s^0 \exp(-U_s/\theta), \tag{5}$$

where $C_s^0 = (C_1^0)^s$; $C_1^0 = [(1/4\pi)\int \exp(-\varphi_1/\theta)\, d\Omega_1]^{-1}$. Representing the first approximation of the unary function as $F_1^1 = C_1' \exp(-\varphi_1/\theta)$ we obtain

$$F_1^1 = \frac{1}{4\pi}\int f_{13}F_1^0(1)\,F_1^0(3)\,d\mathbf{q}_3\,d\Omega_3 - \left(\frac{1}{4\pi}\right)^2 F_1^0(1)\int f_{13}F_1^0(1)\,F_1^0(3)\,d\mathbf{q}_3 d\Omega_1 d\Omega_3 \tag{6}$$

(for brevity, instead of $F_1^0(\vartheta_1\ \varphi_1)$ we have written $F_1^0(1)$ etc.), where $f_{13} = \exp(-L_{13}/\theta) - 1$.

Considering the equation for the first approximation of the s-th distribution function

$$\frac{\partial F_s^1}{\partial q_1^\alpha} + \frac{1}{\theta}\frac{\partial U_s}{\partial q_1^\alpha}F_s^1 + \frac{1}{4\pi\theta}\int\frac{\partial}{\partial q_1^\alpha}(L_{1,s+1})\,F_{s+1}^0 d\mathbf{q}_{s+1}d\Omega_{s+1} = 0 \tag{7}$$

and representing the desired function F_s^1 as $F_s^1 = C_s' \exp(-U_s/\theta)$, we obtain

$$C_s' = \frac{1}{4\pi}\int (C_1^0)^s \prod_{1\leqslant i\leqslant s}(1 + f_{i,s+1})\,F_1^0(s+1)\,d\mathbf{q}_{s+1}d\Omega_{s+1} + k_s', \tag{8}$$

and from weakened correlation

$$k_s' = -\frac{1}{4\pi}\int\left\{1 + \frac{(C_1^0)^s}{4\pi}\sum_{i=1}^{s}\int f_{i,s+1}F_1^0(s+1)\,d\Omega_i\right\}d\mathbf{q}_{s+1}\,d\Omega_{s+1}. \tag{9}$$

The higher approximations can be determined analogously. In the particular case of a dipolar gas $\varphi_1 = pE\cos\vartheta_1$, where p is the molecular dipole moment; E is the electric field strength. In this case, retaining only the terms which contain the first power of the density of the system, we obtain

$$\begin{aligned} F_1 = \left(\frac{\beta}{\sinh\beta}\right)e^{\beta\cos\vartheta_1} + \frac{n}{4\pi}\left(\frac{\beta}{\sinh\beta}\right)^2 e^{\beta\cos\vartheta_1}\Big\{\int f_{13}e^{\beta\cos\vartheta_3}\,d\mathbf{q}_3 d\Omega_3 - \\ - \frac{1}{4\pi}\left(\frac{\beta}{\sinh\beta}\right)\int f_{13}e^{\beta\cos\vartheta_1}e^{\beta\cos\vartheta_3}\,d\mathbf{q}_3 d\Omega_3 d\Omega_1\Big\}; \end{aligned} \tag{10}$$

$$\begin{aligned} F_2 = e^{-L_{12}/\theta}e^{\beta(\cos\vartheta_1 + \cos\vartheta_2)}\left(\frac{\beta}{\sinh\beta}\right)^2\Big[1 + \frac{1}{4\pi}\int f_{13}f_{23}F_1^0(3)\,d\mathbf{q}_3\,d\Omega_3 + \\ + \frac{1}{4\pi}\int f_{13}F_1^0(3)\,d\mathbf{q}_3\,d\Omega_3 + \frac{1}{4\pi}\int f_{23}F_1^0(3)\,d\mathbf{q}_3\,d\Omega_3 - \\ - \left(\frac{1}{4\pi}\right)^2\int f_{13}F_1^0(1)\,F_1^0(3)\,d\mathbf{q}_3 d\Omega_3 d\Omega_1 - \left(\frac{1}{4\pi}\right)^2\int f_{23}F_1^0(2)\,F_1^0(3)\,d\mathbf{q}_3 d\Omega_3 d\Omega_2\Big], \end{aligned} \tag{11}$$

where $\beta = pE/kT$.

By virtue of the properties of the oriented part of the dipole potential the logarithmically divergent term which arises from integration over $\mathbf{q}_3$ vanishes, and the series for the distribution functions of groups of particles converge well for sufficiently small density of the system.

A knowledge of the unary and binary distribution functions in first approximation is sufficient for calculation of the mean potential energy of the system to terms which contain the square of the small parameter:

$$\begin{aligned} \overline{U}_N = \frac{N(N-1)}{2(4\pi v)^2}\int L_{12}(F_2^0 + nF_2^1)\,d\mathbf{q}_1\,d\mathbf{q}_2\,d\Omega_1\,d\Omega_2 - \\ - \frac{N}{4\pi v}\int\beta\cos\vartheta_1\,(F_1^0 + nF_1^1)\,d\mathbf{q}_1\,d\Omega_1. \end{aligned} \tag{12}$$

The mean potential energy $\overline{U}_N$ can be used in the usual way to express the corresponding part of the free energy and to determine all equilibrium characteristics of the dipolar gas; in particular, we in this way derive a rigorous theory of the polarization properties of a dipolar gas. The interaction potential L_{ij} for this case is taken in the form (Stockmayer)

$$L_{ij} = \chi_{ij} + \frac{\mathbf{p}_i \mathbf{p}_j}{r_{ij}^3} - 3\frac{(\mathbf{p}_i \mathbf{r}_{ij})(\mathbf{p}_j \mathbf{r}_{ij})}{r_{ij}^5}, \tag{13}$$

where χ_{ij} is the Lennard-Jones short-range potential.

A similar method is used to construct the theory of a gas which consists of molecules possessing a higher electric moment such as a quadrupole.

From the above formulas it is easy to derive the theory of a gas consisting of nonpolar axially symmetrical molecules such as diatomic molecules with weak orientation interaction. We take the interaction potential for such molecules in the form

$$L_{ij} = \Phi_{ij}(|\mathbf{q}_i - \mathbf{q}_j|)\,[1 + \lambda g_{ij}(\vartheta_i, \varphi_i, \vartheta_j, \varphi_j, \vartheta_{ij}, \varphi_{ij})], \tag{14}$$

where Φ_{ij} is the short-range potential which corresponds to central forces; $g_{ij}(\vartheta_i, \varphi_i, \vartheta_j, \varphi_j, \vartheta_{ij}, \varphi_{ij})$ is the part which describes the orientation interaction; λ is a small parameter. In the absence of external fields after expanding in powers of λ we obtain from the general equations as the first approximation of the binary distribution function:

$$\begin{aligned} F_2^1 = F_2^{10} + \lambda \Big\{ &-\frac{U_2'}{\theta} F_2^{10} - \frac{1}{4\pi\theta}\int \Big(\sum_{i=1} \Phi_{i3} g_{i3}\Big) \exp\Big(-\frac{U_3^0}{\theta}\Big) d\mathbf{q}_3\, d\Omega_3 + \\ &+ a_2^{11} \exp\Big(-\frac{U_2^0}{\theta}\Big)\Big\} + \lambda^2 \Big\{ -\frac{1}{2}\Big(\frac{U_2'}{\theta}\Big)^2 F_2^{10} - \Big(\frac{U_2'}{\theta}\Big) F_2^{11} + \\ &+ \frac{1}{4\pi\theta^2}\int \frac{1}{2}\Big(\sum_{i=1}^{2} \Phi_{i3} g_{i3}\Big)^2 \exp\Big(-\frac{U_3^0}{\theta}\Big) d\mathbf{q}_3\, d\Omega_3 + a_2^{12} \exp\Big(-\frac{U_2^0}{\theta}\Big)\Big\} + \dots \end{aligned} \tag{15}$$

where

$$a_s^{11} = \frac{1}{(4\pi)^2\theta} \sum_{i=1}^{s} \int \exp\Big(-\frac{\Phi_{i,s+1}}{\theta}\Big) \Phi_{i,s+1} g_{i,s+1} d\mathbf{q}_{s+1} d\Omega_i d\Omega_{s+1}, \tag{16}$$

$$a_s^{12} = -\frac{1}{2}\Big(\frac{1}{4\pi\theta}\Big)^2 \sum_{i=1}^{s} \int \exp\Big(-\frac{\Phi_{i,s+1}}{\theta}\Big) (\Phi_{i,s+1} g_{i,s+1})^2\, d\mathbf{q}_{s+1} d\Omega_i d\Omega_{s+1},$$

$$U_s' = \sum_{1 \leqslant i < j \leqslant s} \Phi_{ij}(|\mathbf{q}_i - \mathbf{q}_j|)\, g_{ij}(\vartheta_i, \varphi_i, \vartheta_j, \varphi_j, \vartheta_{ij}, \varphi_{ij}),$$

$$U_s^0 = \sum_{1 \leqslant i < j \leqslant s} \Phi_{ij}(|\mathbf{q}_i - \mathbf{q}_j|), \tag{17}$$

$$F_s^{10} = \exp\Big(-\frac{U_s^0}{\theta}\Big) \int \Big\{ \prod_{1 \leqslant i \leqslant s} (1 + f_{i,s+1}) - 1 - \sum_{1 \leqslant i \leqslant s} f_{i,s+1} \Big\} d\mathbf{q}_{s+1} \tag{18}$$

with $f_{ij} = \exp\left(-\varphi_{ij}\left(|\mathbf{q}_i - \mathbf{q}_j|\right)/\theta\right) - 1,$

$$F_s^{11} = -\frac{U_s'}{\theta} F_s^{10} - \frac{1}{4\pi\theta} \sum_{1 < i < s} \int \Phi_{i,s+1} g_{i,s+1} F_{s+1}^{00} d\mathbf{q}_{s+1} d\Omega_{s+1} + \\ + a_s^{11} \exp\left(-\frac{U_s^0}{\theta}\right), \tag{19}$$

$$F_s^{00} = \exp\left(-\frac{U_s^0}{\theta}\right), \quad F_s^{01} = -\frac{U_s'}{\theta} F_s^{00} \text{ etc.} \tag{20}$$

In all of the equations the first superscript in F_s^{kl} denotes the order of the approximation with respect to density; the second superscript denotes the order with respect to λ.

Using a binary function up to first-order terms in both parameters one can calculate the equilibrium properties of such a system to a satisfactory approximation. Thus, for example, it is relatively easy to calculate the second and third virial coefficients:

$$B = B^c\left[1 - \lambda\overline{g}\theta \frac{d}{d\theta} \ln \beta_1 - \lambda^2 \overline{g}^2 \left(1 + \theta \frac{d}{d\theta} \ln \beta_1\right)\right], \tag{21}$$

$$C = C^c\Big[1 - \lambda\overline{g}\theta \frac{d}{d\theta} \ln \beta_2 - \lambda^2 \overline{g}^2 \Big\{1 + \theta \frac{d}{d\theta} \ln \beta_2 + \\ + 6\left(\frac{\overline{g_{12}g_{13}}}{\overline{g}^2} - 1\right) \frac{1}{\beta_2} \int \theta\gamma \, d\theta + 6 \frac{\overline{g_{12}g_{13}} - \overline{g}^2}{\overline{g^2}} \frac{1}{\beta_2} \int \theta \left(\frac{d\beta_1}{d\theta}\right)^2 d\theta\Big\}\Big], \tag{22}$$

where B^c and C^c are the second and third virial coefficients, which were obtained by neglecting the central interaction, i. e., for the interaction potential $\Phi_{ij}(|\mathbf{q}_i - \mathbf{q}_j|)$; β_1 and β_2 are, respectively, the first irreducible integral and double the second irreducible integral also for the case of purely central forces

$$\overline{g^n} = \left(\frac{1}{4\pi}\right)^3 \int g_{12}^n \, d\Omega_1 \, d\Omega_2 \, d\Omega_{12};$$

$$\gamma = \int \frac{\partial f_{12}}{\partial \theta} \frac{\partial f_{13}}{\partial \theta} f_{23} d\mathbf{q}_2 \, d\mathbf{q}_3.$$

Thus the distribution function method for groups of particles [1] enables us to construct a rigorous theory of real gases which takes into consideration not only the central interaction but all forms of orientation interaction, and which possesses a number of advantages over other theories [2-8].

I. Franko Lvov State University

Received April 11, 1956

LITERATURE CITED

[1] N. N. Bogoliubov, Problems of Dynamical Theory in Statistical Physics (Moscow-Leningrad, 1946).

[2] P. Debye, Physik. Z. 36, 193 (1935).

[3] L. Onsager, J. Am. Chem. Soc. 58, 1986 (1936).

[4] J. H. van Vleck, J. Chem. Phys. 5, 999 (1937).

[5] J. G. Kirkwood, J. Chem. Phys. 7, 911 (1939).

[6] J. H. Rowlinson, J. Chem. Phys. 19, 827 (1951).

[7] J. A. Pople, Proc. Roy. Soc. (London) A215, 67 (1952).

[8] J. A. Barker, Proc. Roy. Soc. (London) A219, 367 (1953).

ON THE SCATTERING MATRIX OF AN INTERMEDIATE SYSTEM

M. S. Livshits

(Presented by Academician N. N. Bogoliubov, April 12, 1956)

In this article a nonselfadjoint energy operator is derived for the intermediate system that is formed in an elastic collision between two particles taking into consideration the relativistic mass-velocity relation. It is established that there is a close relationship between the scattering matrix and the so-called characteristic matrix-function [1-4] of the corresponding nonselfadjoint energy operator, which makes it possible in some cases to establish the energy operator for a given scattering matrix. The familiar Wigner-Eisenbud equation [5] is extended to the continuous spectrum of an intermediate system. As an example we obtain the energy operator for the Heisenberg elementary-particle model [6].

In order to show the essence of the method we confine ourselves to elastic collisions of two uncharged particles $a_1 + a_2 \rightarrow C \rightarrow a_2 + a_1$, where C is the "intermediate" or "compound" system. We assume that the angular momentum l of the particles and their spins are zero.

The wave function of the system can be represented conveniently as a vector with two components $\begin{pmatrix} u(r) \\ v(r) \end{pmatrix}$ where u(r) and v(r) are defined by

$$u(r) = \begin{cases} \dfrac{a_0}{r}\left\{e^{-i\frac{p}{\hbar}r} - S(W)\, e^{i\frac{p}{\hbar}r}\right\} & (r > R); \\ 0 & (r < R); \end{cases} \tag{1}$$

$$v(r) = \begin{cases} 0 & (r > R); \\ \sum\limits_{k=1}^{\infty} f_k v_k(r) & (r < R). \end{cases} \tag{2}$$

Here $v_k(r)$ is the complete orthonormalized system of wave functions of the intermediate system in the interval (O, R); $f_k (k = 1, 2, \ldots)$ are constant coefficients; R is the radius of the reaction channel [7].

The Hamiltonian is written correspondingly as a second-order matrix $\left\| \begin{matrix} W & \Gamma \\ \Gamma^* & A \end{matrix} \right\|$ where $W = W_1 + W_2 = c\left[\sqrt{m_1^2c^2 + p^2} + \sqrt{m_2^2c^2 + p^2}\right]$ is the energy operator of the (a_1, a_2) system (with respect to the center of mass) for $r > R$; A is an operator which acts on the wave functions $v_k(r)$ $(r < R)$ in the intermediate system, and the operators Γ and Γ^* determine the probability of decay and formation of the intermediate system.

The function u(r) can also be written as

$$u(r) = \frac{\text{const}}{r}\left\{e^{-i\frac{p}{\hbar}(r-R)} - S_0(W)\, e^{i\frac{p}{\hbar}(r-R)}\right\} \quad (r > R), \tag{3}$$

where $S_0(W) = e^{2i\frac{p}{\hbar}R} S(W)$ describes scattering which is associated with the formation of the intermediate system. The function $S_0(W)$ will be called the reduced (one-dimensional) scattering matrix. Introducing

$$F_p(r) = \frac{1}{r} \sin \frac{p}{\hbar} (r - R) \text{ and } G_p(r) = \frac{i}{r} \cos \frac{p}{\hbar} (r - R) \quad (r > R)$$

$(F_p(r) = G_p(r) = 0$ for $r < R)$ we can represent u(r) as

$$u(r) = aF_p(r) + b[G_p(r) + iF_p(r)]. \tag{4}$$

In order to take into consideration the relativistic mass-velocity dependence of the particles, we pass to the representation in momentum space. The representative (r|) and (p|) of any state are related by

$$(r|) = \frac{1}{r} \sqrt{\frac{2}{\pi\hbar}} \int_0^\infty (p|) \sin \frac{p(r-R)}{\hbar} p\, dp \quad (r > R).$$

Hence it follows that in the p-representation the states $F_{p'}(r)$ and $G_{p'}(r)$ are given by

$$\begin{aligned} \tilde{F}_{p'}(p) &= \sqrt{\frac{\pi\hbar}{2}} c^2 \left(\frac{1}{W'_1} + \frac{1}{W'_2}\right) \delta(W' - W); \\ \tilde{G}_{p'}(p) &= -\sqrt{\frac{2\hbar}{\pi}} \frac{1}{p'^2 - p^2}. \end{aligned} \tag{5}$$

From (5) it follows that

$$(W' - W) \tilde{F}_{p'}(p) = 0. \tag{6}$$

We shall now consider the wave equation $\begin{Vmatrix} W & \Gamma \\ \Gamma^* & A \end{Vmatrix} \begin{pmatrix} u \\ v \end{pmatrix} = W' \begin{pmatrix} u \\ v \end{pmatrix}$, which is divided into two equations:

$$Wu + \Gamma v = W'u, \tag{7}$$

$$\Gamma^* u + Av = W'v. \tag{8}$$

From (4), (6) and (7) it follows that

$$b\Phi_{p'}(p) = \sum_{k=1}^\infty f_h \Gamma v_h, \quad \tilde{\Phi}_{p'}(p) = -\sqrt{\frac{2\hbar}{\pi}} \frac{W' - W}{p'^2 - p^2}. \tag{9}$$

In accordance with (9) we shall assume that

$$\Gamma v_h = \gamma_k \tilde{\Phi}_{p'}(p), \tag{10}$$

where γ_k (k = 1, 2,...) are numerical factors. It follows that b is a linear function of the f_k (k = 1, 2, ...)

$$b = \sum_{k=1}^{\infty} f_k \gamma_k. \tag{11}$$

We also obtain the scalar products

$$(\tilde{\Phi}_{p'}(p),\ \tilde{F}_{p'}(p)) = -\frac{\hbar}{2} c^2 \left(\frac{1}{W'_1} + \frac{1}{W'_2}\right) p' = -\frac{\hbar}{2}(V'_1 + V'_2);$$
$$(\tilde{\Phi}_{p'}(p),\ \tilde{G}_{p'}(p)) = 0. \tag{12}$$

Through scalar multiplication of both sides of (8) by $v_k(r)$ ($k = 1, 2, \ldots$) and using (4), (10) and (11) we shall have

$$-a\gamma_k^{*} \frac{\hbar}{2}(V'_1 + V'_2) - i \sum_{j=1}^{\infty}{}' f_j \gamma_j^{*} \gamma_k \frac{\hbar}{2}(V'_1 + V'_2) + \sum_{j=1}^{\infty} A_{jk} f_j = W' f_k, \tag{13}$$

where $A_{jk} = (Av_j, v_k)$.

We introduce the vectors $\mathbf{f} = \{f_k\}$ with the components $f_1, f_2, \ldots$ and the operators A, B, H, H^*, defined by

$$[A\mathbf{f}]_k = \sum_{j=1}^{\infty} A_{jk} f_j, \quad [B\mathbf{f}]_k = \sum_{j=1}^{\infty} f_j \beta_j^{*} \beta_k \quad \left(\beta_k = \gamma_k^{*} \sqrt{\frac{\hbar}{2}(V_1 + V_2)}\right),$$
$$H = A + iB, \quad H^{*} = A - iB, \tag{14}$$

where $[A\mathbf{f}]_k$, $[B\mathbf{f}]_k$ ($k = 1, 2, \ldots$) are the components **f** of the vectors $A\mathbf{f}$ and $B\mathbf{f}$. By the use of (14) the equation which defines the state **f** of the intermediate system can be written as

$$H^{*}\mathbf{f} - W\mathbf{f} = \frac{a}{2}\sqrt{\frac{\hbar}{2}(V_1 + V_2)}\,\mathbf{1}, \quad \mathbf{1} = \{\sqrt{2}\,\beta_k\}. \tag{15}$$

Using (4), (11) and (15) we obtain the following expression for the scattering matrix:

$$S(W) = e^{-2i\frac{p}{\hbar}R} S_0(W), \quad S_0(W) = 1 + i\,((H^{*} - WI)^{-1}\mathbf{1},\ \mathbf{1}). \tag{16}$$

The function $S_0(W)$, which is associated with the operator H by (16), is called the characteristic function of H. It has been studied in a number of papers on the theory of nonselfadjoint operators [1-4].

From $i\hbar \frac{d\mathbf{f}}{dt} = H^{*}\mathbf{f}$ it follows that $\frac{d(\mathbf{f}, \mathbf{f})}{dt} = -\frac{1}{\hbar}|(\mathbf{f}, \mathbf{1})|^2$.

Thus the total probability P of the decay (per unit time) of an intermediate system is defined by

$$P = \frac{1}{\hbar}(\mathbf{1}, \mathbf{1}) = \frac{2}{\hbar}\sum_{j=1}^{\infty}|\beta_j|^2. \tag{17}$$

By the use of (16) we can obtain a new expression for $S_0(W)$ which is a generalization of the familar equation of Wigner and Eisenbud:

$$S_0(W) = \frac{1 + \frac{iP\hbar}{2}\varphi(W)}{1 - \frac{iP\hbar}{2}\varphi(W)}, \quad \varphi(W) = ((A - WI)^{-1}\mathbf{l}_0, \mathbf{l}_0). \tag{18}$$

We also have $\varphi(W) = \int\limits_a^b \frac{d\sigma(t)}{t - W}$ $(\mathbf{l}_0 = \mathbf{l}/(\mathbf{l},\mathbf{l})^{1/2})$, where $\sigma(t) = (E_t\mathbf{l}_0, \mathbf{l}_0)$ is a nondecreasing function; E_t is the spectral family [8] of the self-adjoint operator A.

It is noteworthy that from a knowledge of $S_0(W)$ and the nature of the dependence of P on the energy W it is possible to obtain $\varphi(W)$, and from $\varphi(W)$ by using the Stieltjes conversion formula to obtain $\sigma(t)$ $(a \leq t \leq b)$. A knowledge of $\sigma(t)$ is sufficient for the construction of the energy operator A in different representations.

As an example we consider the scattering function

$$S_0(W) = -\frac{iW - \alpha\sqrt{W^2 - (2m)^2}}{iW + \alpha\sqrt{W^2 - (2m)^2}} \quad (c = 1)$$

for the elastic collisions of two identical particles which differs only in sign from the Heisenberg function[6] in the simplest elementary particle model. Rewriting $S_0(W)$ as

$$S_0(W) = \frac{1 - \frac{iW}{\alpha}\frac{1}{\sqrt{W^2 - (2m)^2}}}{1 + \frac{iW}{\alpha}\frac{1}{\sqrt{W^2 - (2m)^2}}}$$

and comparing it with (18) we set

$$\varphi(W) = \frac{-1}{\sqrt{W^2 - (2m)^2}}, \quad P = \frac{2W}{\alpha\hbar} \tag{19}$$

In [9] it was shown that the operator A, for which $\varphi(W)$ is given by (19), can be reduced by a unitary transformation to the form

$$2m \begin{Vmatrix} 0 & \sqrt{1/2} & 0 & 0 & \dots \\ \sqrt{1/2} & 0 & 1/2 & 0 & \dots \\ 0 & 1/2 & 0 & 1/3 & \dots \\ \cdot & \cdot & \cdot & \cdot & \dots \end{Vmatrix}. \tag{20}$$

The vector $\mathbf{l}_0$ in this transformation becomes $\mathbf{l}_0 = (1, 0, 0, \dots)$.

Thus the energy operator of the intermediate system in the Heisenberg model is

$$H^{*} = A - \frac{iW}{\alpha\hbar}J_0, \quad J_0 = \begin{Vmatrix} 1 & 0 & 0 & \dots \\ 0 & 0 & 0 & \dots \\ \cdot & \cdot & \cdot & \dots \\ \cdot & \cdot & \cdot & \dots \end{Vmatrix}. \tag{21}$$

In [9] it is proved that A has a purely continuous spectrum which fills the interval $(-2m, 2m)$.

Odessa Hydrometeorological Institute Received February 28, 1956

LITERATURE CITED

[1] M. S. Livshits, Math. Collection 34, (76), 145 (1954).

[2] M. S. Livshits, Math. Collection 19 (61), 239 (1946).

[3] V. P. Potapov, Doklady Akad. Nauk SSSR 72, 5, 849 (1950).

[4] M. S. Brodskii, Doklady Akad. Nauk SSSR 97, 5 (1954).

[5] E. P. Wigner and L. Eisenbud, Phys. Rev. 72, 29 (1947).

[6] W. Heisenberg, Z. Physik. 123, 1-2 (1944).

[7] J. Blatt and W. Weisskopf, Theoretical Nuclear Physics (For. Lit. Press, 1954) (Russian Translation).

[8] V. I. Smirnov, Course of Higher Mathematics 5 (Moscow-Leningrad, 1947).

[9] M. S. Livshits, Doklady Akad. Nauk SSSR 97, 3 (1954).

AN INVESTIGATION OF THE N COMPONENT OF EXTENSIVE AIR SHOWERS

S. N. Nikol'skii, Iu. N. Vavilov and V. V. Batov

(Presented by Academician D. V. Skobel'tsyn May 23, 1956)

According to the prevailing concept [1] N particles (those which interact with nuclei) are the basis for the development of an extensive air shower (e. a. s). But at present only very meager experimental information is available concerning the energy, composition, spatial distribution and number of N particles in a shower. The present article presents the results of experiments which studied the spatial distribution and number of N particles with energies $\gtrsim 10^9$ ev.

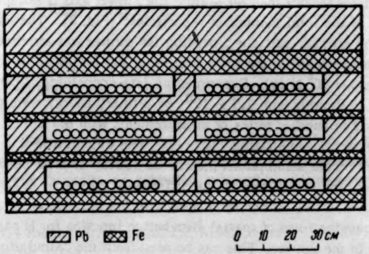

Fig. 1.

The measurements were performed at 3860 m above sea level (in Pamir) during the summer and autumn of 1954. The experimental apparatus, which was similar to that used in [2], permitted determination within 1 m of the location of the axis in each instance when an e. a. s. was recorded. Simultaneous measurement of the flux density of shower particles at various distances from the shower axis made it possible to compute the total number of charged particles in each shower with a relative error of $\leq 10\%$.

The flux density of N particles and non-N particles was determined by a detector of penetrating particles using the methods described in [3, 4]. The construction of the detector with three rows of hodoscopic counters is shown in Fig. 1.

The passage of a charged non-N particle (muon) through the area covered by the middle row of counters produced a discharge in a single counter of not less than two rows of the detector. The formation, in the matter of the detector, of an electron-nuclear shower by an N particle or of a δ shower by muons was distinguished by discharges in two or more counters of a single row. The number of δ showers associated with the passage of the non-N component of an e. a. s. was related to the number of passages without formation of a recorded δ shower. The probability for the formation and recording of δ showers produced by muons of the e. a. s. was determined in these experiments.

In the analysis of the experimental results all of the e. a. s. recorded during the period of observation were divided into groups of showers which differed in their total number of particles. For each group we determined the spatial distribution function of the N particles at distances from 1 to 40 m from the shower axis. In all cases the function could be represented in the form $\sim r^{-b}$, where r is the distance from the axis. The values of the exponent b for 9 groups of showers are given in Table 1.

TABLE 1

Total number $\overline{N}$ of charged particles b	$0.4 \cdot 10^5$ 1.3 ± 0.5	$0.65 \cdot 10^5$ 1.6 ± 0.25	$0.9 \cdot 10^5$ 1.6 ± 0.22	$1.5 \cdot 10^5$ 1.6 ± 0.16	$3 \cdot 10^5$ 1.75 ± 0 2
Total number $\overline{N}$ of charged particles b	$5 \cdot 10^5$ 0.9 ± 0 18	$7 \cdot 10^5$ 1.4 ± 0.12	$9 \cdot 10^5$ 0.85 ± 0.25	$12 \cdot 10^6$ 1.2 ± 0.13	

If we neglect the noticeable tendency of b to decrease as the primary particle energy increases, then by averaging b we obtain b = 1.4 ± 0.1. Fig. 2 shows the experimental results for the spatial distribution of N particles in the second and ninth groups of Table 1.

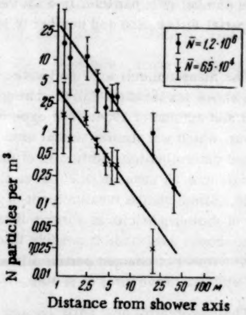

Fig. 2.

On the basis of the data on the spatial distribution of N particles we computed the number of N particles in e. a. s. of different primary energies. It was assumed that the form of the spatial distribution is independent of the primary particle energy of the shower ($\overline{b}$ - 1.4) and the number of N particles farther than 40 m from the shower axis is not greater 20% of the total number of N particles* (Fig. 3). The energy of the primary particle producing the shower was assumed to be proportional to the total number of shower particles ($E_0 = 5 \times 10^9 \overline{N}$ ev). Experimental data concerning N particles in showers with 1.7×10^{13} ev primary energy were obtained in another series of measurements with the same detectors of penetrating particles. The calculation was based on the assumptions mentioned above. It must be indicated, first of all, that the peculiarity of the curve in Fig. 3 at $E_0 \simeq 10^{15}$ ev is not associated with the assumption of an unchanging form of spatial distribution function for N particles in the shower. This can be seen from the calculation of the number of N particles without use of this assumption. The corresponding values, whose statistical errors are very large, are shown by crosses in Fig. 3.

The experimental data were also treated subject to a more rigorous selection of electron-nuclear showers in the matter of the detector. Discharges were required in at least two pairs of hodoscopic counters located in different rows. This criterion required the formation of not less than two penetrating particles in an act of nuclear interaction, which raises the average energy of the selected events and practically excludes the possibility of recording δ showers produced by muons. The calculated numbers of N particles causing such an occurrence and from 2 to 8 m distant from the shower axis are given in agreement with Fig. 3 (see Fig. 4). Fig. 4 contains two triangles to represent converted data taken from [5], which were obtained at 3260 m and by different methods but using the above N-particle criterion.**

As can be seen from the curves of Figs. 3 and 4 in the primary particle energy region below 10^{15} ev the number of N particles is proportional to $\sim E_0^{0.2}$. For higher primary particle energies the number of N particles is proportional to $\sim E_0$. We believe that it is most reasonable to associate the sharp change of slope of the curves at $\sim 10^{15}$ ev (Figs. 3 and 4) with a possible change of character of the elementary act of particle interaction at

---

*This was obtained by comparing the data of the present work with the results of our earlier work [3].

**In [5] a third group of e. a. s. is found, the data for which it is difficult to convert, as the spatial distribution of all charged particles in this group of showers contradicts our results [2].

$\sim 10^{15}$ ev. The slow rise of the number of N particles with increasing energy up to $\sim 10^{15}$ ev corresponds to the formation in the first act of nuclear interaction of one energetically distinguished particle which retains its distinct status in succeeding interactions. In the majority of cases the formation of secondary particles with lower energies is only slightly dependent on the energy of the interacting particle ($\lesssim E^{1/4}$). The experimental data do not conflict with this view [6]. Above $\sim 10^{15}$ ev in the first act of nuclear collision the primary particle energy is distributed among a few secondary particles each of which possesses $\lesssim 10^{15}$ ev and retains its distinct status in succeeding interactions. The number of such secondary particles is proportional to the primary particle energy.

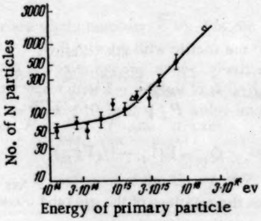

Fig. 3.

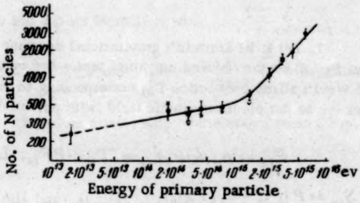

Fig. 4.

In conclusion the authors wish to thank N. A. Dobrotin and G. T. Zatsepin for valuable discussions of the results.

This work was assisted by many staff members of the Physics Institute of the Academy of Sciences, USSR, and the students of the Moscow State University. To all these collaborators, and especially to O. I. Dovzhenko, E. I. Tukish and V. Ia. Iakovlev, the authors are deeply grateful.

P. N. Lebedev Physics Institute, Academy of
Sciences, USSR

Received May 18, 1956

LITERATURE CITED

[1] N. A. Dobrotin, G. T. Zatsepin et al., Progr. Phys. Sci. (USSR) 49, 185 (1953).

[2] Iu. N. Vavilov, S. I.Nikol'skii and E. I. Tukish, Doklady Akad. Nauk SSSR 93, 233 (1953).

[3] Iu. N. Vavilov, S. I.Nikol'skii and V. P. Sarantsev, J. Exptl.-Theoret. Phys. (USSR) 28, 505 (1955).

[4] A. T. Abrosimov, V. I. Zatsepin et al., Bull. Acad. Sci. USSR, Phys. Ser. 19, 677 (1955).

[5] H. Kasnitz, K. Sitte, Phys. Rev. 94, 977 (1954).

[6] N. A. Dobrotin, G. T. Zatsepin et al., Bull. Acad. Sci. USSR, Phys. Ser. 19, 666 (1955).

NONLINEARITY AND CONFORMAL RECIPROCITY

Andrei Popovich

(Presented by Academician N. N. Bogoliubov, April 12, 1956)

1. Let $\underline{k}$ be Einstein's gravitational constant and $ds^2 = g_{ik}dx^i dx^k$ the metric with $g_{ik} = |g_{ki}|$ $(i, k = 0, \ldots, 3)$. Let Γ_{ik}, Γ be the reduced curvature tensor and curvature scalar, respectively, which are composed of components of Weyl's affine connection Γ^i_{kl} corresponding to the metric $\hat{g}_{ik} = \psi g_{ik}$ (ψ is of weight -1 with respect to g_{ik}). Let P_{ik} be the electromagnetic field (with potential p_i) with the absolute value $P/\sqrt{2} = P'\sqrt{k/2} = P'_r/\sqrt{2}$,

$$P_{ik} = p_{ir}p^r_k/P,\ L_{ik} = \Gamma\Gamma_{ik} + PP_{ik},\ L = L^r_r = \Gamma^2 + P^2.\quad Q_{ik} = \Gamma(\Gamma_{ik} - {}^1\!/_4\Gamma g_{ik}),$$

$S_{ik} = P(P_{ik} - {}^1\!/_4 P g_{ik})$. Γ_{ik}, P_{ik} (and also p_{ik}) depend only on the relations of the g_{ik} (and consequently on $\hat{g}_{ik}$); the variation of $L\sqrt{g}$ with respect to g_{ik}, p_i gives [16, 17] the conformally covariant equations

$$Q_{ik} = -S_{ik}\quad (\text{or}\quad L_{ik} = {}^1\!/_4 L g_{ik})\ \ (1a);\qquad \partial(p^{ik}\sqrt{g})/\partial x^k = 0$$

(1a) presents the gravitational equations and (1b) the electromagnetic equations. We have $(Q^k_i\sqrt{g})_{;k} + (S^k_i\sqrt{g})_{;k} = 0$. In other articles [20] the gravitational equations $Q_{ik} = 0$ are derived from $\Gamma^2\sqrt{g}$ in the special case $\psi \equiv \Gamma$.

2. Let

$$\begin{aligned} U = L/2\Gamma = -if,\quad V = L/2P = in;\quad \Gamma_{ik}/J_{ik} = J_{ik}/N_{ik} = \\ = P_{ik}/H_{ik} = H_{ik}/F_{ik}\,(= p_{ik}/h_{ik} = h_{ik}/f_{ik}) = \Gamma/J = J/N = P/H = H/F = \\ = \gamma/j = j/n = p/h = h/f = \sqrt{\varepsilon} = 1/\sqrt{\mu},\qquad g^{\bullet}_{ik} = g_{ik}U,\ g^{\bullet\bullet}_{ik} = -ig_{ik}V, \\ \varepsilon = (1 + P^2/f^2)^{1/2} = (1 - F^2/f^2)^{-1/2} = (1 + \Gamma^2/n^2)^{1/2} = (1 - N^2/n^2)^{-1/2} \end{aligned} \tag{2}$$

$$L = \Gamma^2 + P^2 = 2\Gamma U = 2PV,\quad L^{\bullet} = 2\Gamma^{\bullet},\quad L^{\bullet\bullet} = 2iP^{\bullet\bullet}\ (\Gamma^{\bullet\bullet} = -iP^{\bullet}) \tag{3}$$

(3) gives the pairs of solutions

$$\begin{aligned} \underset{1}{\Gamma} = \underset{1}{U}(1+\varepsilon),\ \underset{1}{P} = \underset{1}{V}(1-\varepsilon),\ \underset{00}{L} = 2\underset{1}{U^2}(1+\varepsilon) = \\ = 2\underset{1}{V^2}(1-\varepsilon) = 4h'_1 = 4\varepsilon l'_1\ \&\ \underset{2}{\Gamma} = \underset{1}{U}(1-\varepsilon),\ \underset{1}{P} = \underset{2}{V}(1+\varepsilon),\ \underset{01}{L} = 2\underset{1}{U^2}(1-\varepsilon) = \\ = 2\underset{2}{V^2}(1+\varepsilon) = 4h'_2 = -4\varepsilon l'_2.\ \text{The relation}\quad (1b)\,\&\,(2)\,(\&\,P, F, f = iU)\ \&\ \underset{01}{L} = 2\underset{1}{U^2}(1-\varepsilon) \end{aligned}$$

agree with the formulas of the first form of Born and Infeld's nonlinear electrodynamics [7, 11]; $U/\sqrt{2} = if/\sqrt{2}$ is the "maximum electromagnetic field"; $-iV/\sqrt{2} = n/\sqrt{2}$ is the "maximum gravitational field." The Hamiltonian h'_2 and the Lagrangian $l'_2 = -\mu h'_2$ of the Born-Infeld theory correspond to the conformal Lagrangian L.

3. Let

$$s = 1/w = (\varepsilon+1)/(\varepsilon-1),\ \varepsilon = 1/\mu = (s+1)/(s-1).$$

$$\underset{\beta\alpha}{L} = \underset{\beta\alpha}{A^2} + \underset{\beta,\alpha+1}{A^2} = -2i\underset{\beta\alpha}{A}\ \underset{\beta+2,\alpha+1}{a} = 2i\underset{\beta,\alpha+1}{A}\ \underset{\beta+2,\alpha}{a} = \underset{\beta\alpha}{L^r_r},$$

$$\underset{\beta\alpha}{L^k_i} = \underset{\beta\alpha}{A}\ \underset{\beta\alpha}{A^k_i} + \underset{\beta,\alpha+1}{A}\ \underset{\beta,\alpha+1}{A^k_i},\quad \underset{\beta,\alpha-1}{A^k_i} + \underset{\beta,\alpha+1}{A^k_i} = -(1-s)\,(\underset{\beta\alpha}{A^k_i} - {}^1/_2\,\underset{\beta\alpha}{A}\delta^k_i)/i\sqrt{s},$$

$$\underset{\beta,\alpha-1}{A^k_i} - \underset{\beta,\alpha+1}{A^k_i} = -(1+s)\,\underset{\beta\alpha}{A^k_i}/i\sqrt{s},\quad \underset{\beta\alpha}{A} = \underset{\beta\alpha}{A^r_r}$$

(β, α are whole numbers $\gtreqless 0$). For the indices β = 0, 1, 2 and 2α we identify A with $\underset{\alpha+1}{\Gamma},\ \underset{\alpha+1}{J},\ \underset{\alpha+1}{N},$ respectively and indices $\underset{\beta,2\alpha}{a}$ with $\underset{\alpha+1}{\gamma},\ \underset{\alpha+1}{j},\ \underset{\alpha+1}{n} = -i\underset{\alpha+1}{V}$ For β = 0,1,2 and $2\alpha+1$ $\underset{\beta,2\alpha+1}{A}$ is identified with c $\underset{\alpha+1}{P},\ \underset{\alpha+1}{H},\ \underset{\alpha+1}{F}$, and $\underset{\beta,2\alpha+1}{a}$ with $\underset{\alpha+1}{p},\ \underset{\alpha+1}{h},\ \underset{\alpha+1}{f} = i\underset{\alpha+1}{U}$. The close relationship of the above tensors Γ_{ik}, P_{ik} (or f_{ik}) is analogous to the theory of V. A. Fok [9]. We have

$$s = (1 - 4\underset{\beta,\alpha-1}{a^2}/\underset{\beta-1,\alpha}{A^2})^{1/2} = (1 + 4\underset{\beta,\alpha+1}{a^2}/\underset{\beta-1,\alpha}{A^2})^{1/2};$$

$$\varepsilon = (1 + \underset{\beta-2,\alpha}{A^2}/\underset{\beta\alpha}{a^2})^{1/2} = (1 - \underset{\beta\alpha}{A^2}/\underset{\beta\alpha}{a^2})^{-1/2};$$

$$\underset{\beta\alpha}{A^2} - \underset{\beta\alpha}{a^2} + \underset{\beta+2,\alpha}{a^2} = 0;\quad 4\underset{\beta+1,\alpha}{a^2} - \underset{\beta,\alpha+1}{A^2} + \underset{\beta,\alpha-1}{A^2} = 0. \tag{4}$$

We have $\underset{00}{L} = 4h_1',\ \underset{10}{L} = 4l_1' = \mu\underset{00}{L},\ \underset{01}{L} = -w\underset{00}{L} = 4h_2',\ \underset{11}{L} = 4l_2' = \mu w\underset{00}{L}.$ (5)

4. In Kalantarov's system of dimensions let $\epsilon_0\epsilon'$ be the dielectric constant; q_0 and $\varphi_0' = c\varphi_0$ be the electric and magnetic (canonically conjugate) units of charge; $e_0 = e/\delta$ is the mechanical ("gravitational") unit of charge; a is the radius of an elementary charged particle; $W = m/\delta^2$ is its energy; $\delta = \sqrt{k}/c$. We have the "conformal" relations

$$a/e_0 = e_0/W = \lambda\delta\ (a/e = e/m = \lambda);\text{(6a)};\ q_0/e_0 = e_0/\varphi_0' = (\varepsilon'\varepsilon_0)^{1/2} = (c^2\mu'\mu_0)^{-1/2}$$

and relations similar to (6a) for the quanta of time [1], "momentum" and current. We have the correspondences $\underset{\alpha}{P},\ \underset{\alpha}{F},\ \underset{\alpha}{H} \leftrightarrow \underset{\alpha}{\Gamma},\ \underset{\alpha}{N},\ \underset{\alpha}{J}$ и $\underset{\alpha}{P},\ \underset{\alpha+1}{P} \leftrightarrow \underset{\alpha}{\Gamma},\ \underset{\alpha+1}{\Gamma}$, defined by the conformal factors $\sqrt{\epsilon}$, $i\sqrt{s}$ (and similarly for all $\underset{\beta\alpha}{A}$ and $\underset{\beta\alpha}{a}$). The change of the dielectric constant $\epsilon'\epsilon_0$ which is postulated in nonlinear electrodynamics and the change of the gravitational constant k postulated by Dirac and the projective theory of relativity [13] thus result automatically from the conformal character, i. e., the quadratic character of the Lagrangian L with respect to Γ and P and, consequently, of equations (1a) or (3); $\epsilon'\epsilon_0$ and $k\lambda^2$ (or $\sqrt{\epsilon'\epsilon_0}$ and $\delta\lambda$) become the variable quantities $c\epsilon\epsilon_0 = (c\mu\mu_0)^{-1} = \epsilon_1 = \epsilon_2^{-1}$ and $sk = k_1 = k_2^{-1}$. These nonlinearities of the "second kind" reflect the interaction of the different fields, i. e., the reciprocity principle [see below (8) and (9)] and the existence of several maximum fields; they differ from the nonlinearity of the "first kind" of the curvature tensor with respect to Γ^i_{kl}. The "maximum fields" $\underset{\alpha}{U}$ (unlike the Born-Infeld theory) and $-i\underset{\alpha}{V}$ are variables which are defomed by Equations (1a) and (1b), i. e., (3), like the variable maximum relativistic velocity (the velocity of light) v_0, $U^{*} = -iV^{**} = 1$; L is linearized [see/(3)] (Γ^{*} is Einstein's Lagrangian); (1a) becomes $L_i^{*h} - {}^1/_2\,\Gamma^{*}\delta_i^h = 0$ or $L_i^{**h} - {}^1/_2\,P^{**}\delta_i^h = 0$. As in de Broglie's [8] (nonconformal) theory of a dual solution the continuous fields and fields with singularities are solutions of the same conformal equations.

5. The ratios of the components of $\underset{\beta\alpha}{A}$ are the elements of the isomorphic dihedral cubic (projective) groups D_6. We have the groups of elements $z_a(\varepsilon)$, $z_a(-\varepsilon)$, $z_a(\varepsilon^2)$, $z_a(s)$, $z_a(-s)$, $z_a(s^2)$ $(a = 1, \ldots, 6)$. For arbitrary distributions and motion of matter the group D_6 appears in other articles [15] independently of nonlinear electrodynamics as the basis of a group algebra of C_6.

6. In the electrostatic spherical case $\rho = C\exp(\mp\omega/2)$ is the radius-vector; $\rho_2^2 = \cos h\,\omega$; $\rho_1^2 = \sin h\,\omega$; $C = (e\sqrt{2}/C')^{1/2}$ is the constant of integration. We have $\underset{1}{P} = 2P_1^1 = 2P_4^4$; $P_2^2 = P_3^3 = 0$; $\Gamma_2^2 = \Gamma_3^3 = U/2$; $\Gamma_1^1 = \Gamma_4^4 = \varepsilon\underset{1}{U}/2$; $s = \rho^4/C^4$; $\varepsilon = \pm\cot h\omega > 0$. In the metrics $\hat{g}_{ik} = \psi g_{ik}$, $\underset{\bullet}{g}{}^{*}_{ik} = \hat{g}_{ik}\underset{1}{\hat{U}}$,

$$g_{ik}^{**} = -ig_{ik}\underset{2}{\hat{V}} \text{ we have } \underset{1}{\hat{\Gamma}} = 2(\hat{\Gamma}_1^1 + \hat{\Gamma}_2^2) = \mp C', \quad \underset{2}{\hat{\Gamma}} = -2\,(\hat{\Gamma}_1^1 - \hat{\Gamma}_2^2) = \mp \hat{P}_1^2/C'$$
$$\underset{1}{\hat{P}}{}^2 = -C'^2/s = -2e^2/\rho^4,\ \underset{1}{\hat{U}} = \mp e\rho_1^2\sqrt{2}/\rho^2,\ \underset{1}{\hat{V}} = \mp i\rho_1^2 C',\ -i\underset{1}{F}{}^{*} = \underset{2}{N}{}^{**} = \rho_2^{-2},$$
$$-\ i\underset{1}{P}{}^{*} = \underset{2}{\Gamma}{}^{**} = \rho_1^{-2}.$$

7. Let $ds = ds_1/f$, $\bar{ds} = i\bar{ds}_1$, $\bar{\bar{ds}} = (ds\,\bar{ds})^{1/2}$ be, respectively, the kinematic (space-time), dynamical (momentum-energy), charge (3-current − charge) metrics (all are "world" metrics) and $dS = i\,dS_1/f$, $d\bar{S} = d\bar{S}_1$, $d\bar{\bar{S}} = (dSd\bar{S})^{1/2}$ the corresponding "intrinsic" metrics ($\underset{1}{f} \equiv f$, $\underset{1}{p} \equiv p$, $\underset{1}{F} \equiv F$, $\underset{1}{P} \equiv P$). Let the total metric be $d\tau^2 = d\bar{s}_1^2 + ds_1^2 + 2\overset{1}{g}_1\,d\bar{s}_1\,ds_1 = -(d\bar{S}_1^2 + dS_1^2 + 2G_1\,d\bar{S}_1\,dS_1) = -dT^2$ or $d\tau'^2 = d\tau^2 + dT^2 = 0$. When $g_1 = G_1 = 0$, $d\tau^2$ is of the "kinematic" type (C), of the "dynamical" type (D) or "isobaric" (for $d\tau^2 < 0$, $d\tau^2 > 0$, $d\tau^2 = 0$). When $d\tau^2 < 0$ [16], or $d\tau^2 > 0$, respectively, a coordinate system exists in which

$$(C)\quad d\bar{S} = 0,\ ds_1/p^{*} = d\bar{s}_1/iP^{*} = dS_1\ \ (ds = \varepsilon\,dS,\ \bar{ds} = F ds = PdS) \tag{7}$$

$$(D)\ ds = 0,\ d\bar{S}_1/p^{*} = dS_1/iP^{*} = d\bar{s}_1\ \ (d\bar{S} = \varepsilon\,d\bar{s},\ dS = F\,d\bar{S}/f^2 = P\,d\bar{s}/f^2) \tag{8}$$

The metric $d\tau'^2$ is equivalent to (5); In the interchange of "universal" and "intrinsic," kinematic and dynamical quantities (7) and (8) are interchanged.

8. $g_1 = G = 0$ is analogous to the static relativistic case $\overline{ds^2} = dW^2 - v_0^2dl^2$, $ds^2 = d\psi^2 - v_0^2dt^2$ (dW, dl, $d\psi$, dt are the metrics of energy, momentum, coordinates and time). We have correspondence between the "intrinsic" field (with affine components $F = \overline{ds}/ds$, f, $q = f/\epsilon$) and the intrinsic velocity ($v = d\psi/dt = dW/dl$, v_0, $w_0 = v_0/\alpha$), the "world" fields ($P = \varepsilon F = \bar{ds}/dS$, $p = \varepsilon f = f\,ds/dS$, $f = p/\varepsilon$) and the world velocity ($u = \alpha v = d\psi/ds' = dW/d\bar{s}$, $u_0 = \alpha v_0 = dt/ds' = v_0 dl/d\bar{s}$, $v_0 = u_0/\alpha$) so that

$ds = iv_0 ds'$ and [see (5)] $F^2 - f^2 + q^2 = 0$ $(P^2 - p^2 + f^2 = 0)$, similarly $v^2 - v_0^2 + w_0^2 = 0$ $(u^2 - u_0^2 + v_0^2 = 0)$, and $\alpha = (1 + u^2/v_0^2)^{1/2} = (1 - v^2/v_0^2)^{-1/2}$ and $\chi = (\alpha + 1)/(\alpha - 1)$ correspond to ϵ and $\underline{s}$ [see (4)]. $\overline{ds} = \mu d\overline{S}$ [see (8)] reflects the mass defect of a particle which interacts with a set (field) and $ds = \epsilon dS$ [see (7)] is the corresponding expansion of the metric dS; this is similar to the contraction of lengths and expansion of time for a moving particle.

9. In the more general case let $\overset{\beta\alpha}{V_4}$ be a manifold with the metric $\overset{\beta\alpha}{ds_1}$ $(\beta, \alpha = 0, 2, 4)$; let $\overset{\beta\alpha}{ds_1} = \overset{\beta\alpha}{ds'} f^{(\alpha+\beta-4)/4}$ [case (C)] or $\overset{\beta\alpha}{ds_1} = \overset{\beta\alpha}{ds'} f^{-(\alpha+\beta)/4}$ [case (D)]. For $\beta, \alpha = 00, 04, 40, 44$ $\overset{\beta\alpha}{ds_1}$ is identical with, respectively, $d\bar{S}_1$, dS_1, $\overline{ds}_1$, ds_1. $\overset{\beta 4}{V_4}$, $\overset{\beta 2}{V_4}$, $\overset{\beta 0}{V_4}$ and $\overset{4\alpha}{V_4}$, $\overset{2\alpha}{V_4}$, $\overset{0\alpha}{V_4}$ are, respectively, the kinematic, charge, dynamical and electrical ("world"), gravitational ("mixed"), magnetic ("intrinsic") manifolds. In case (C) [see (7)] $\overset{44}{ds'}$, $\overset{42}{ds'}$, $\overset{40}{ds'}$ и $\overset{44}{ds'}$, $\overset{24}{ds'}$, $\overset{04}{ds'}$ are derived from $ds = \overset{44}{ds'}$ through multiplication by the affine factors 1, $F^{1/2}$, $F = \underset{0}{F}W$ and 1, $q^{1/2}$ $q = f\mu$ in accordance with (6a) and (6b). In case (D) [see (8)] the indices 0 and 4 are interchanged; consequently $\overset{44}{ds'} = ds$ and $\overset{00}{ds'} = d\bar{S}$. In case (C):

$$\overset{\beta 4}{ds'} / \overset{\beta 2}{ds'} = \overset{\beta 2}{ds'} / \overset{\beta 0}{ds'} (= 1/F); \ (9a) \ \overset{4\alpha}{ds'} / \overset{2\alpha}{ds'} = \overset{2\alpha}{ds'} / \overset{0\alpha}{ds'} (= 1/q). \qquad (9b)$$

For any relative tensor we have $\overset{\beta 4}{T}\overset{\beta 0}{T} = (\overset{\beta 2}{T})^2$, $\overset{4\alpha}{T}\ \overset{0\alpha}{T} = (\overset{2\alpha}{T})^2$ $(\overset{42}{F} = \overset{02}{F} \Rightarrow \overset{24}{q} = \overset{20}{q} = i)$, where $\overset{\beta\alpha}{T}$ (for example, $\overset{\beta\alpha}{g_{ik}}$) depends on p $\gtrless$ 4 variables. The affine relations (9a) and (9b) and $ds\,\overline{ds} = dSd\bar{S}$ [(7) and (8)] generalize (6a) and (6b) and the indeterminacy relations; they in a certain sense reflect the indeterminacy of the field quantities (see N. N. Bogoliubov et al. [3, 4]; M. A. Markov [14], M. Born, J. Reyski [18], Yukawa and others).

10. The above affine theory is a generalization of the law of reciprocity [5, 6, 15-17, 19] leading to covariance of physical laws (see (1a) and (1b), $d\tau'^2$) with respect to the variables of the manifolds $\overset{\beta\alpha}{V_4}$, and consequently with respect to the following pairs: I – space and time; I' – world and intrinsic; II – kinematic and dynamical; II' – "world" (electrical) and "intrinsic" (magnetic) variables. Each pair corresponds to canonically conjugate quantities; the corresponding mixed products are thus elements of the type $dx^{\gamma}dt$ (space-time); dtds (world-intrinsic element), ds $\overline{ds}$ (charge) and dsdS ("gravitational" element) correspond to "self-adjoint" quantities. II can be decomposed with respect to I, I' and II'. The affine factor $\delta s^{1/2} = \delta w^{-1/2}$ thus relates the variables II and the charges, and the affine factor $(c\epsilon\epsilon_0)^{1/2} = (c\mu\mu_0)^{-1/2}$ relates the variables II' and the mixed (gravitational) variables. The theory can be extended to the case of complex Lagrangians [22], unsymmetrical g_{ik} [7, 11], and meson and spinor fields [2, 10, 12, 21].

Bucharest, Rumanian People's Republic

Received February 16, 1956

LITERATURE CITED

[1] V. Ambartsumian and D. Ivanenko, Z. Physik, 64, 563 (1936).

[2] D. Blokhintsev, Progr. Phys. Sci. (USSR) 42, 76 (1950);

[3] N. N. Bogoliubov, V. Ch. Bonch-Bruevich and B. V. Medvedev, Doklady Akad. Nauk SSSR 74, 681 (1950).

[4] V. Ch. Bonch-Bruevich and B. V. Medvedev, J. Exptl.-Theoret. Phys. (USSR) 22, 4 (1952).

[5] M. Born, Proc. Roy. Soc. Edinburgh 59, 219 (1939).

[6] M. Born and K. Fuchs, Proc. Roy. Soc. Edinburgh 60, 141, 147 (1940).

[7] M. Born, Ann. Inst. Henri Poincare 7, 155 (1937).

[8] L. de Broglie, J. Phys. 27, 225 (1927).

[9] V. A. Fok, Z. Physik 57, 261 (1929).

[10] B. Hoffmann, Phys. Rev. 72, 458 (1947); 73, 30 (1947).

[11] L. Infeld, Proc. Cambridge Phil. Soc. 32, 127 (1936); 33, 70 (1937).

[12] D. Ivanenko and A. Brodskii, Doklady Akad. Nauk SSSR 84, 4 (1951).

[13] G. Ludwig, Fortschritte der projektiven Relativitatstheori (Braunschweig, 1951).

[14] M. A. Markov, Doklady Akad. Nauk SSSR 75, 5 (1950).

[15] A. Popovici, Bul. Polytehn. Iassi 3, 2, 543 (1948).

[16] A. Popovici, Rev. Univ. C. I. Parhon si Politehn, Bucuresti 3, 78 (1953).

[17] A. Popovici, Bul. Sect. I. Acad. RPR 1, 6, 65 (1954).

[18] J. Reyski, Acta Phys. Pol. 10, 1-2 (1950).

[19] J. Reyski, J. Exptl.-Theoret. Phys. (USSR) 22, 2, 194 (1950).

[20] E. Reichenbacher, Z. Physik 45, 663 (1929).

[21] J. A. Schouten, Rev. Mod. Phys. 21 (1949).

[22] P. Weiss, Proc. Cambridge Phil. Soc. 33, 79 (1937).

ON THE THEORY OF CONCENTRATION QUENCHING OF FLUORESCENT SOLUTIONS

B. Ia. Sveshnikov

(Presented by Academician A. N. Terenin, June 21, 1956)

It is well known that in the majority of cases of concentration quenching of fluorescent solutions the fluorescence yield decreases more rapidly than the duration of emission. There are a number of hypotheses which attempt to explain this phenomenon. The present article examines critically the hypothesis of Foerster [1] and Galanin [2], according to which the inconsistency results from the fact that fluorescence decay of concentrated solutions is not exponential.

We briefly summarize Foerster's argument. In agreement with other earlier theories of concentration quenching Foerster assumes that the frequency of the energy transfer from an excited molecule to an unexcited molecule is independent of the interaction time and changes inversely with the 6th power of the distance between the interacting molecules, i. e.,

$$f(R,t) = f(R) = \frac{1}{\tau_0}\left(\frac{R_0}{R}\right)^6, \tag{1}$$

where τ_0 is the mean time spent by a molecule in an excited state in the absence of quenching; R is the distance between molecules; R_0 is the distance at which the frequency of transfer is $1/\tau_0$.

Then for the time dependence of the excitation probability $\rho(t)$ of any excited molecule Foerster obtains

$$-\frac{d\rho(t)}{dt} = \left\{\frac{1}{\tau_0} + \frac{1}{\tau_0}\sum_{k=1}^{N}\left(\frac{R_0}{R_k}\right)^6\right\}\rho(t), \tag{2}$$

where N is the number of unexcited molecules in a finite volume $\underline{v}$ of the solution; R_k is the distance of the k-th unexcited molecule from the excited molecule.

Integrating (2) over time with the initial condition $\rho(0) = 1$, we have

$$\rho(t) = \exp\left\{-\left[1 + \sum_{k=1}^{N}\left(\frac{R_0}{R_k}\right)^6\right]\frac{t}{\tau_0}\right\} = \exp\left[-\frac{t}{\tau_0}\right]\prod_{k=1}^{N}\exp\left[-\left(\frac{R_0}{R_k}\right)^6\frac{t}{\tau_0}\right]. \tag{3}$$

Thus the decay of excitation of a single molecule is exponential.

But in reality, as Foerster shows, one must examine the decay of a set of molecules with a statistical distribution of their separations R_k. Foerster obtains this quantity $\overline{\rho(t)}$ as follows:

$$\begin{aligned}\overline{\rho(t)} \doteq \exp\left[-\frac{t}{\tau_0}\right]\prod_{k-1}^{N}\int_0^{R_g}\exp\left[-\left(\frac{R_0}{R_k}\right)^6\frac{t}{\tau_0}\right]w(R_k)\,dR_k = \\ = \exp\left[-\frac{t}{\tau_0}\right][J(t)]^N,\end{aligned} \tag{4}$$

where

$$J(t) = \int_0^{R_g} \exp\left[-\left(\frac{R_0}{R}\right)^6 \frac{t}{\tau_0}\right] w(R)\,dR, \quad v = \frac{4}{3}\pi R_g^3. \tag{5}$$

The form of w(R), which is the distribution of quenching molecules, must depend on the intermolecular forces, but since these are unknown, Foerster assumes a uniform molecular distribution:

$$w(R)\,dR = \frac{4\pi R^2 dR}{v}. \tag{6}$$

Then

$$J(t) = \frac{1}{2}\sqrt{\zeta_g}\int_{\zeta_g}^{\infty} e^{-\zeta}\frac{d\zeta}{\sqrt{\zeta^3}} = 1 - \sqrt{\pi\zeta_g} - 3\zeta_g, \tag{7}$$

where

$$\zeta = \left(\frac{R_0}{R}\right)^6 \frac{t}{\tau_0}, \quad \zeta_g = \left(\frac{R_0}{R_g}\right)^6 \frac{t}{\tau_0}. \tag{8}$$

Since R_0 is very small compared with the macroscopic radius R_g, $\zeta_g \ll 1$. Therefore in (7) we can neglect the higher powers of ζ_g and from (4) and (7) we have

$$\overline{\rho(t)} = \exp\left[-\frac{t}{\tau_0}\right](1 - \sqrt{\pi\zeta_g})^N. \tag{9}$$

For sufficiently large N we obtain

$$\overline{\rho(t)} = \exp\left[-\frac{t}{\tau_0}\right]\lim\left(1 - \frac{1}{N}N\sqrt{\pi\zeta_g}\right)^N = \exp\left[-\frac{t}{\tau_0} - N\sqrt{\pi\zeta_g}\right]. \tag{10}$$

Replacing ζ_g by its value according to (8) we obtain

$$\overline{\rho(t)} = \exp\left[-\frac{t}{\tau_0} - 2q\sqrt{\frac{t}{\tau_0}}\right], \text{ where } q = \frac{\sqrt{\pi}}{2}\frac{NR_0^3}{R_g^3}. \tag{11}$$

Thus according to Foerster the fluorescence decay law for an ensemble of excited molecules is not exponential.

From the knowldege of the change with time in the number of excited molecules it is possible to obtain the change of fluorescence yield and mean duration for concentration quenching. The formulas are quite complicated,* but show clearly that the duration changes considerably more slowly than the yield.

---

*See the articles of Foerster [1] and Galanin [2]. It should be noted that in the formula for the fluorescence yield obtained by Foerster the limits of the tabulated integral $\int e^{-x^2}dx$ are erroneously given as q and ∞, but should be 0 and q.

The error in Foerster's argument is easily shown. In the derivation of Equation (2) Foerster assumes some definite distribution of N quenching molecules in the volume v̲ around a given excited molecule and derives therefrom the law of excitation energy decrease of one molecule (3). He assumes also that the transition from (3) to (4) gives the average decay over all molecules. But it is clear that this process should be written differently:

$$\overline{\rho(t)} = \frac{1}{n_0} \exp\left[-\frac{t}{\tau_0}\right] \sum_{i=1}^{n_0} \prod_{k=1}^{N} \exp\left[-\left(\frac{R_0}{R_{ki}}\right)^6 \frac{t}{\tau_0}\right], \tag{12}$$

where the index i̲ denotes that the given distribution of quenching molecules refers to the i-th excited molecule.

The definite distribution of quenching molecules around an excited molecule was also incorrectly replaced by the probable distribution. The distribution function $w_i(R)$ should clearly have been introduced in connection with (2), i. e., instead of (2) we should have

$$-\frac{d\rho_i(t)}{dt} = \left\{\frac{1}{\tau_0} + \frac{c}{\tau_0} \int_0^\infty \left(\frac{R_0}{R}\right)^6 w_i(R)\, dR\right\} \rho_i(t), \tag{13}$$

where c̲ is the concentration of quenching molecules.

We shall now consider the derivation of Equation (11) which was proposed by M. D. Galanin* and shall reproduce it almost in its entirety.

If n(t) denotes the concentration of excited M_1^* molecules as a function of time; n(r, t) is the concentration of excited molecules at distance r̲ from M_2 damping molecules; N(r, t) is the concentration of M_2 molecules at distance r̲ from the M_1^*; f(r) is the transfer probability per unit time** from M_1^* to M_2 at distance r;*** N_0 is the M_2 concentration; $1/\tau_0$ is the emission probability; then

$$-\frac{dn(t)}{dt} = \left\{\frac{1}{\tau_0} + \int_0^\infty N(r,t) f(r)\, dv\right\} n(t). \tag{14}$$

If at initial time the M_1 and M_2 molecules are distributed statistically with respect to each other, then for n(r, t) we can write an equation which represents the decrease of the number of pairs of M_1 and M_2 molecules at a given distance r̲:

$$-\frac{dn(r,t)}{dt} = \left\{\frac{1}{\tau_0} + \int_0^\infty N(r,t) f(r)\, dv + f(r)\right\} n(r,t). \tag{15}$$

Keeping in mind that

$$n(t)\, N(r,t) = N n(r,t), \tag{16}$$

---

*It should be noted that Galanin, like Foerster, considers very viscous solutions.

**Galanin denotes this probability by w(r). We have changed the notation in order to avoid confusion with (13).

***In the concentration quenching of fluorescence M_1 and M_2 are identical molecules.

from (14) and (15) we obtain

$$n(t) = n_0 \exp\left\{-\frac{t}{\tau_0} - N\int_0^\infty (1 - \exp[-f(r)\,t])\,dv\right\}, \tag{17}$$

where f(r) is defined by (1) and N_0 is the concentration of M_2 quenching molecules.

We note first of all that it is easily shown that Galanin's solution

$$N(r, t) = N_0 \exp[-f(r)\,t] \tag{18}$$

is not in accord with the problem which he had formulated. Indeed, from the fact that those excited molecules will be quenched, primarily, which are close to a high concentration of quenching molecules by virtue of fluctuations of the molecular distribution, it follows that the remaining unquenched excited molecules will have a low concentration of quenchers close to each excited molecule and a higher than average concentration at greater distances. This latter circumstance is not allowed for by (18) and N cannot for any r and t be greater than N_0.

It can thus be seen at once that Galanin's affirmation to the effect that n(r, t) changes more rapidly than n(t) is generally untrue. But he uses this idea as a basis for introducing the additional probability f(r) n(r, t) dt* in (14).

The incorrectness of the calculations of these authors does not, of course, mean that their fundamental assumption is wrong – to the effect that because of fluctuations of molecular distribution the fluorescence decay of concentrated solutions can be nonexponential. At the same time our discussion has shown that the theoretical solution of this problem is very difficult. Therefore it would be very desirable, with the aid of fluorometric measurements, which have attained considerable precision, to determine the upper limit of the possible nonexponential deviation of fluorescence decay of concentrated solutions.

Received May 8, 1956

LITERATURE CITED

[1] Th. Förster, Z. Naturforsch. 4a, 321 (1949).

[2] M. D. Galanin, J. Exptl.-Theoret. Phys. (USSR) 28, 485 (1955).

[3] V. V. Antonov-Romanovskii, Doklady Akad. Nauk SSSR 2, 93 (1936).

---

*This term, which the author borrowed from the "impoverishment" formula of V. V. Antonov-Romanovskii [3] is altogether incomprehensible. Unfortunately V. V. Antonov-Romanovskii does not give a full proof of this formula.

THE POLARIZATION OF PROTONS SCATTERED ELASTICALLY BY C^{12}

P. V. Sorokin and A. Ia. Taranov

(Presented by Academician A. P. Aleksandrov, June 16, 1956)

The elastic scattering of protons by C^{12} nuclei has been investigated by Jackson and Galonsky [1, 2]. Using the results of the phase analysis in [2], Diatlov and Rosentsveig [3] showed that the scattered protons are partially polarized and calculated the curves representing the dependence of the polarization P on proton energy for several scattering angles. The present communication is devoted to an experimental verification of these results: at the same time a check is provided for the correctness of the phase analysis [2], which is based on a generalization of the Wigner-Eisenbud dispersion formula [4].

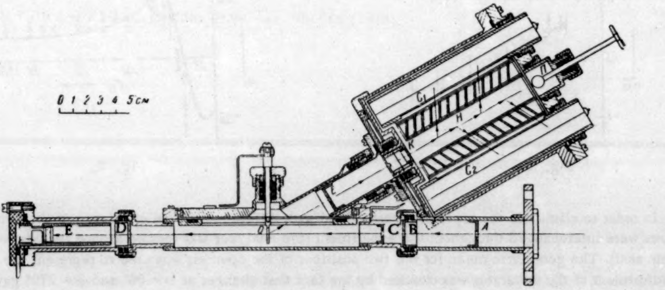

Fig. 1.

For measurements of the degree of polarization P we used the apparatus which is represented schematically in Fig. 1. Protons accelerated by an electrostatic generator passed through a system of collimating apertures A, B and C (6, 7 and 6 mm) and struck a solid carbon target O. The primary beam current was measured by a Faraday cylinder E and current integrator; all measurements referred to a definite number of integrator counts. The protons that were scattered through the aperture K (5 mm) which was sealed with a caprone film (0.8 mg/cm^2) entered an analyzer filled with helium at 40 mm Hg. Protons which were scattered by He^4 passed through 7 μ Al windows into the proportional counters C_1 and C_2.

The counter windows measured $3 \cdot 80$ mm^2; the length of the scattering space of the analyzer and collimating system H were such that the counters could receive protons scattered by a column of He 8 cm high within the angular range 55-105° in the c. m. system. The thickness of the scattering gas layer and the large solid angle of the counters, while somewhat reducing the effective polarization value of the helium analyzer, make the analyzer a quite sensitive instrument which is able to detect the polarization of proton beams with an intensity of 10^4 protons per second.

In the scattering of spin 1/2 particles by nuclei with zero spin the azimuthal asymmetry is given by

$$\sigma(\Theta,\varphi) = \sigma_0(\Theta)\,[1 + PP_{\text{ef}}\cos\varphi], \tag{1}$$

where P is the polarization of the protons elastically scattered by C^{12} nuclei; P_{ef} is the effective polarization of protons scattered in the helium analyzer; φ is the angle between the normals to the planes of first and second scattering. The ratio of the intensities at $\varphi = 0°$ and $\varphi = 180°$ is given by

$$R = \frac{1 - PP_{\text{ef}}}{1 + PP_{\text{ef}}}. \tag{2}$$

(2) makes it possible to determine P if P_{ef} is known.

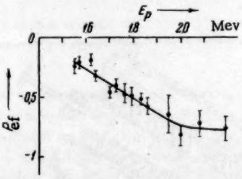

Fig. 2.

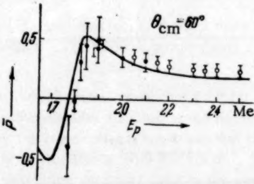

Fig. 3.

In order to eliminate the asymmetry associated with differences in the efficiency of the two detectors the counters were interchanged throughout the experiment (the analyzer was rotated around its axis on a movable vacuum seal). The geometric mean for the two positions of the counters was used to represent the asymmetry R. The adjustment of the apparatus was checked by the fact that changes at $\varphi = 90°$ and $\varphi = 270°$ gave asymmetry $R = 1$ within the limits of statistical error.

Because of the poor geometry of the analyzer the calculation of P_{ef} would be very complicated. We therefore obtained P_{ef} from an experiment on double scattering of protons in He^4. The chamber where the primary scattering occurred was separated from the vacuum system of the electrostatic generator by a 7μ mica film covered with a semitransparent film of aquadag. The chamber was filled with He^4 at 40 mm Hg. In this experiment we determined the product $P_{\text{He}}\,P_{\text{ef}}$, where P_{He} is the proton polarization from the primary scattering, which is characterized by good geometry (solid angle $1.5 \cdot 10^{-3}$ sterad). P_{He} was calculated from the phases [5]. The values of P_{ef} obtained in this way as a function of the energy with which the protons reach the analyzer foil are shown in Fig. 2. This curve was used for determination of the degree of polarization of protons scattered elastically by C^{12}.

Our values for the polarization of protons scattered by C^{12} at 60° in the c. m. system are shown in Fig. 3. The dots represent measurements taken with a 0.6 mg/cm^2 target; the open circles represent a 1.1 mg/cm^2 target. The solid curve was computed from the formula

$$\overline{P}(E) = \int\limits_{E}^{E-\Delta E} P(E)\,\sigma(E)\,\frac{dE}{F(E)} \Bigg/ \int\limits_{E}^{E-\Delta E} \sigma(E)\,\frac{dE}{F(E)}, \tag{3}$$

where P(E) and σ(E) were given in Fig. 3. In [3] F(E) is the stopping power of the carbon target (we consider this constant in the energy interval ΔE).

The observed agreement of the experimental and theoretical data confirms the phase analysis of [2] and energy level scheme of the N^{13} nucleus in [2].

We take this opportunity to thank A. K. Val'ter and L. N. Rozentsveig for valuable discussions during the preparations for the experiment and for discussions of the results, and V. I. Man'ko for assistance with the measurements.

Physico-Technical Institute, Academy of Sciences,
Ukrainian SSR

Received June 14, 1956

LITERATURE CITED

[1] H. L. Jackson, A. I. Galonsky et al., Phys. Rev. 89, 365 (1953).

[2] H. L. Jackson, A. I. Galonsky, Phys. Rev. 89, 370 (1953).

[3] I. T. Diatlov and L. N. Rozentsveig, Trans. Physico-Math. Faculty Kharkov State Univ. 6, 81 (1955).

[4] E. P. Wigner, L. Eisenbud, Phys. Rev. 72, 29 (1947).

[5] C. L. Critchfield, D. C. Dodder, Phys. Rev. 76, 602 (1949).

THE EFFECT OF A LONGITUDINAL MAGNETIC FIELD ON IMPULSIVE GAS DISCHARGES WITH LARGE CURRENTS

A. L. Bezbatchenko, I. N. Golovin, D. P. Ivanov,
V. D. Kirillov and N. A. Iavlinskii

(Presented by Academician L. A. Artsimovich, November 22, 1956)

Gas discharges with large currents have recently attracted much attention. In [1, 2] it was shown that the discharge column, which is constricted by the intrinsic field of the current, undergoes 1-2 rapid radial oscillations of small amplitude, after which it loses its stability and collapses in one-half to one-third of a microsecond after the discharge begins.

We investigated the effect of a longitudinal magnetic field on the stability of a plasma column produced by impulsive current transmission through deuterium. The gas pressure was from 0.05 to 0.4 mm Hg. The current strength reached 700 ka; the longitudinal magnetic field was 12,000 oersted. The discharge chamber was a porcelain or glass tube of radius a_0 = 10 cm; the inter-electrode distance was $\underline{l}$ = 70 cm. The apparatus is shown schematically in Fig. 1. The experiments recorded simultaneously as a function of time, the discharge current, the inter-electrode potential, the radius of the discharge column and the mean value of the longitudinal magnetic field in the plasma. The radius of the discharge column was determined from high-speed photographs of the discharge. The speed was 2×10^6 frames per second.

Fig. 2 contains photographs of the discharge column during the first 10 μ sec. It can be seen that in the presence of a longitudinal magnetic field during the first 5-6 μ sec the column is constricted but remains uniform lengthwise. A comparison of photographs of the discharge column subjected to a longitudinal field with photographs in the absence of the field shows that as the field strength increases to 6000 oersted the construction is noticeably slowed down. Further increase of the field has little effect on the constriction of the column. At fields of 700 and 2,000 oersted, radial oscillations of the discharge column are visible. Fig. 3 represents the dependence of a/a_0 (a is the radius of the column; a_0 is the radius of the discharge chamber) on time, determined by measuring the luminous region in the photographs, samples of which are given in Fig. 2.

The photographs in Fig. 2 show that the time of the existence of a sharply outlined column in the presence of a longitudinal magnetic field is considerably greater than in its absence. In weak longitudinal fields during the 8th microsecond the column is distorted but remains sharply outlined, while in the absence of a longitudinal field by the 5th microsecond it has completely lost its outline but during the preceding intervals of time is not distorted on the whole. It is easily seen from Fig. 3 that the period of existence of a sharply outlined column increases more strongly under the effect of a longitudinal field than the rate of its constriction diminishes.

The elementary theory of the contraction of a discharge column under the influence of its own magnetic field in the presence of a longitudinal magnetic field was constructed on the assumption that a) the gas pressure can be neglected compared with magnetic forces and inertial forces; b) the discharge column retains the shape of a circular cylinder; c) the longitudinal magnetic field is frozen into the plasma column; d) the mass which participates in the motion is constant. The equation of motion was integrated electronically.

A comparison of the theoretical curves with the experimental curves in Fig. 3 showed us that there is satisfactory agreement for a field of 2,000 oersted, while for 6,000 and 12,000 oersted the calculated constriction is a few times smaller than the observed value. This indicates that a strong longitudinal field is not frozen in and that a considerable portion of its flux goes outside the column during the constriction of the latter. Assuming that the longitudinal field flux is proportional to the radius of the column we obtained a solution of the equation of motion which is in good agreement with the measurements. For fields $H_z > 3000$ oersted the inertial term can be neglected, so that the constriction takes place practically with equilibrium of the magnetic stresses, i. e.,

$$\overline{H}_{zi}^2 - H_{ze}^2 = H_\varphi^2, \tag{1}$$

where H_φ, H_{zi} and H_{ze} are the intrinsic field of the current, the longitudinal field inside the column and the longitudinal field outside the column, respectively.

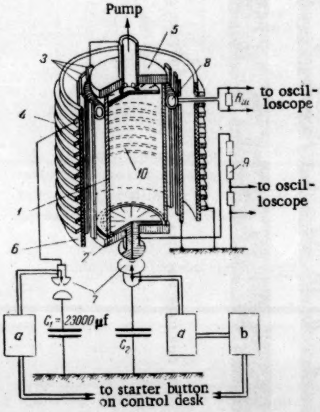

Fig. 1. Schematic diagram of apparatus. For the capacitance C_2 of 30 and 180 μf the frequency is 43 and 17 kc, respectively, and the maximum current through the discharge chamber is 330 and 700 ka. 1) glass chamber; 2) copper electrode; 3) return wire; 4) coil for longitudinal magnetic field; 5) porcelain flange; 6) coil support; 7) needle-point dischargers; 8) Rogovskii belt; 9) voltage divider; 10) window for photographing; a) trigger circuit; b) delay circuit.

The magnetic equilibrium given by (1) can be checked by direct measurements. During the constriction of the plasma column an emf $\mathcal{E}$ is induced in a coil of wire surrounding the discharge chamber; this can be recorded by an oscilloscope. Simple calculation shows that from a knowledge of

$$\int_0^t \mathcal{E}\;dt,$$

the initial longitudinal magnetic field H_0 and the dimensions and electrical parameters of the apparatus it is possible to calculate H_e and the mean value of $\overline{H}_{zi}$.

The values of the field strength which are obtained satisfy (1) within the limits of experimental accuracy.

When the gas pressure is not neglected it is necessary to add the term 2 nkT to the left-hand side of (1) (n is the number of free electrons and electrons bound to atoms per cm^3 of hydrogen, T is an assumed mean plasma temperature). Within the limits of error this equality is satisfied for $T \leq 20$ ev at $H_z \geq 6000$ oersted. Allowances for the gas pressure at $H_z = 2000$ oersted improves the correspondence of theory and experiment at $T \sim 20$-30 ev. We thus see that the longitudinal magnetic field, although it increases the stability of the column, does not permit heating of the column to ~ 100 ev as in the absence of the longitudinal field (see [1]).

From the rate at which the longitudinal magnetic field leaves the column we can obtain the conductivity σ of the plasma using the relation

$$\frac{d\Phi_{zi}}{dt} = \frac{ac^2}{2\sigma}\left(\frac{\partial H_z}{\partial r}\right)_{r=a} \tag{2}$$

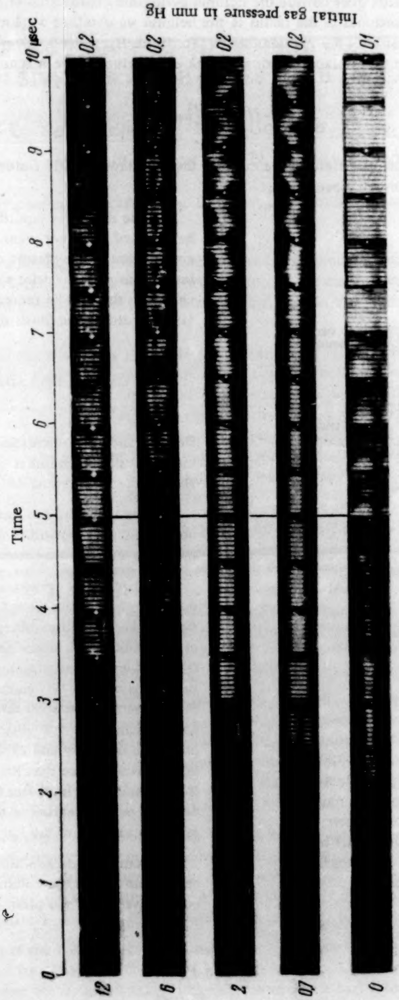
Initial gas pressure in mm Hg
0.2
0.2
0.2
0.2
0.1
Time
0
1
2
3
4
5
6
7
8
9
10 µsec
12
6
2
0.7
0
Field strength in thousands of oersteds

Fig. 2. High-speed photographs of the gas discharge. The dark transverse lines are shadows of the coil which generated the magnetic field.

$d\Phi_{zi}/dt$ and $\underline{a}$ are measured experimentally as a function of time. $H_z(r)$ and its derivative $\partial H_z/\partial r$ are unknown but $H_z(r)$ can be represented by a formula containing one or two parameters which are easily expressed in terms of measurable quantities. Calculations showed that within the limits of error in measurements of all quantities in (2) a one-parametric parabolic approximation of H_z inside the discharge is sufficiently accurate. The calculated values of the conductivity to this approximation are given in Fig. 4. When H_z is approximated by a two-parameter formula the calculated values of σ change by a factor of less than 2.

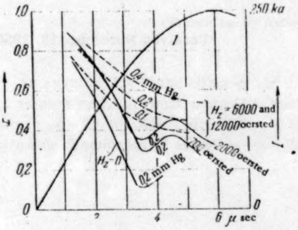

Fig. 3. Time dependence of the relative radius $x = a/a_0$ of the discharge column in hydrogen for different H_z and initial gas pressure.

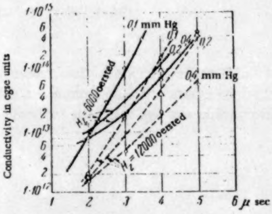

Fig. 4. Conductivity of the plasma calculated from the measured rate at which the longitudinal field left the discharge column.

Assuming that electrons are scattered by H_z molecules and by the Coulomb fields of the ions it is easy to obtain

$$\sigma = \frac{4\cdot 10^{15}}{1/\eta - 1 + 122/T_e^{3/2}},$$

where η is the ionization constant of the plasma, T_e is the electron temperature in electron volts (σ is given in cgse units). With a conductivity of 4×10^{14} cgse we find that for an electron temperature of less than 10 ev the ionization constant is above 15%, which is in agreement with the data in [3].

In every weak magnetic fields ($H_z \leq 500$ oersted) an interesting effect is observed: the longitudinal field flux inside the column does not decrease, but increases during constriction. This could be explained by twisting of the column in a spiral. But in not a single photograph were we able to detect a distortion of the column during the first 3 microseconds, when the effect considerably exceeds the experimental error. The theory developed by S. I. Braginskii shows that when the mean free time of an electron depends on its velocity the stationary conductivity is different along and transversely to the magnetic lines of force. For example, in Coulomb scattering the longitudinal conductivity is twice as great as the transverse. It is easily seen that this anisotropy of the conductivity always leads to such twisting of the direction of the current that the longitudinal magnetic field flux increases inside the plasma. A calculation by S. I. Braginskii and V. D. Shafranov gives for the Coulomb anisotropy a smaller increase of longitudinal magnetic field flux inside the column than the experimentally observed value. Incomplete ionization should only weaken the effect. Therefore, the increased longitudinal magnetic field flux can evidently be explained not only by anisotropy but by azimuthal inhomogeneity of the conductivity whereby inside a column with a regular cylindrical surface there are twisted helical filaments with increased current density.

LITERATURE CITED

[1] L. A. Artsimovich, A. M. Andrianov, O. A. Bazilevskaia, Iu. G. Prokhorov and N. V. Filippov, Atomic Energy 1956, No. 3, 76.

[2] M. A. Leontovich and S. M. Osovets, Atomic Energy 1956, No. 3, 81.

[3] S. Iu. Luk'ianov and V. I. Sinitsyn, Atomic Energy 1956, No. 3, 97.

Received November 18, 1956

THE ENERGY SPECTRUM OF He³ DISSOLVED IN He II

N. G. Berezniak and B. N. Esel'son

(Presented by Academician L. D. Landau, May 28, 1956)

An examination of the effect of He^3 admixtures on the thermodynamic properties of He II has been carried through by I. Ia. Pomeranchuk [1] based, as we know, on the assumption that the atoms of the impurity are associated with additional elementary excitations which obey classical statistics and are characterized by the following dependence of energy on momentum:

$$E = E_0 + \frac{(p-p_0)^2}{2\mu}, \tag{1}$$

where μ is the effective mass of the impurity. The energy minimum can correspond to either $p_0 = 0$ or $p_0 \neq 0$.

The change of the thermodynamic properties of He II caused by the presence of impurities will of course depend on the form of the energy spectrum. In particular, there is strong dependence on the form of the spectrum in the case of the contribution of the impurity ($\rho_{n\ imp}$) to the density of the normal component of He II ($\rho_n = \rho_{n_0} + \rho_{n\ imp}$), which, according to Pomeranchuk, can be written as follows:

$$\rho_n = \rho_{n0} + \frac{\rho}{m}\mu x \qquad \text{for} \quad p_0 = 0, \tag{2}$$

or

$$\rho_n = \rho_{n0} + \frac{\rho}{m}\frac{p_0^2}{3kT}x \qquad \text{for} \quad p_0 \neq 0, \tag{3}$$

where ρ_{n_0} is the density of the normal component of He II and $\underline{x}$ is the molar concentration of He^3 in the solution.

This shows directly that the experimental study of the temperature dependence of $\rho_{n\ imp}$ enables us to establish uniquely the form of the energy spectrum, since such dependence is absent for $p_0 = 0$ and is very strong for $p_0 \neq 0$.

For this purpose we measured the density of the normal component of a solution of He^3 in He^4 with the concentration $x = 3.0\%$ of He^3. As in the case of a similar problem for He^4 [2, 3], we determined the temperature dependence of the moment of inertia of a stack of parallel light disks immersed in a solution of helium isotopes; 53 disks with radius $R = 1.5$ cm and made of aluminum foil 1.2×10^{-3} cm thick were separated from each other by the distance $a = 1.5 \times 10^{-2}$ cm. This separation was less than twice the depth of penetration of a viscous wave under the given oscillatory conditions for all the temperatures employed, which insured complete entrainment of the normal component of the liquid between the disks. The stack of disks was firmly fastened in a pail surrounding it, which was hung by a phosphor bronze filament and was able to perform torsional oscillations around an axis perpendicular to the plane of the disks.

From the change of the moment of inertia of the apparatus it was possible to determine the temperature dependence of the oscillatory period θ of the apparatus in the liquid, which was obtained from the over-all time of 15-20 oscillations and in a vacuum was $\theta_0 = 21.51$ sec.

The relation between the period of oscillation of the system and the density of the liquid which participated in the motion can be established, as is usually done, by solving the corresponding hydrodynamical problem [4, 5]. But it is necessary to take into consideration that the liquid is entrained not only by the disks but by the outer surfaces of the pail. In our apparatus the separation of the moving and motionless surfaces due to the limited quantity of the isotope mixture (9 liters of gas) was about 0.1 cm, which is comparable with the depth of penetration. Therefore in solving the hydrodynamical problem it is necessary to consider these characteristics of the experiment by imposing suitable boundary conditions. As a result two equations can be obtained, one of which,*

$$\frac{\dfrac{\operatorname{sh}\frac{a}{\delta}+\sin\frac{a}{\delta}}{\operatorname{ch}\frac{a}{\delta}+\cos\frac{a}{\delta}}+\dfrac{1}{2N}\dfrac{R_1^4}{R^4-r^4}\left[\dfrac{\operatorname{sh}\frac{2h}{\delta}-\sin\frac{2h}{\delta}}{\operatorname{ch}\frac{2h}{\delta}-\cos\frac{2h}{\delta}}+\dfrac{\operatorname{sh}\frac{2l}{\delta}+\sin\frac{2l}{\delta}}{\operatorname{ch}\frac{2l}{\delta}+\cos\frac{2l}{\delta}}+\dfrac{4L}{R_1}\dfrac{\operatorname{sh}\frac{2d}{\delta}-\sin\frac{2d}{\delta}}{\operatorname{ch}\frac{2d}{\delta}-\cos\frac{2d}{\delta}}\right]}{\dfrac{\operatorname{sh}\frac{a}{\delta}-\sin\frac{a}{\delta}}{\operatorname{ch}\frac{a}{\delta}+\cos\frac{a}{\delta}}+\dfrac{1}{2N}\dfrac{R_1^4}{R^4-r^4}\left[\dfrac{\operatorname{sh}\frac{2h}{\delta}+\sin\frac{2h}{\delta}}{\operatorname{ch}\frac{2h}{\delta}-\cos\frac{2h}{\delta}}+\dfrac{\operatorname{sh}\frac{2l}{\delta}-\sin\frac{2l}{\delta}}{\operatorname{ch}\frac{2l}{\delta}+\cos\frac{2l}{\delta}}+\dfrac{4L}{R_1}\dfrac{\operatorname{sh}\frac{2d}{\delta}+\sin\frac{2d}{\delta}}{\operatorname{ch}\frac{2d}{\delta}-\cos\frac{2d}{\delta}}\right]}= \frac{\theta^2-\theta_0^2}{\gamma-\gamma_0}\,\frac{\pi}{\theta\theta_0^2} \tag{4}$$

provides the possibility of determining the depth of penetration δ, while the second gives the density of the normal component:

$$\rho_n=\frac{2I(\theta^2-\theta_0^2)}{\pi N\theta_0^2\delta(R^4-r^4)}\left\{\frac{\operatorname{sh}\frac{a}{\delta}+\sin\frac{a}{\delta}}{\operatorname{ch}\frac{a}{\delta}+\cos\frac{a}{\delta}}+\right.$$
$$\left.+\frac{1}{2N}\frac{R_1^4}{R^4-r^4}\left[\frac{\operatorname{sh}\frac{2h}{\delta}-\sin\frac{2h}{\delta}}{\operatorname{ch}\frac{2h}{\delta}-\cos\frac{2h}{\delta}}+\frac{\operatorname{sh}\frac{2l}{\delta}+\sin\frac{2l}{\delta}}{\operatorname{ch}\frac{2l}{\delta}+\cos\frac{2l}{\delta}}+\frac{4L}{R_1}\frac{\operatorname{sh}\frac{2d}{\delta}-\sin\frac{2d}{\delta}}{\operatorname{ch}\frac{2d}{\delta}-\cos\frac{2d}{\delta}}\right]\right\}^{-1} \tag{5}$$

Here γ and γ_0 are the damping of the system in the liquid within a vacuum; I is the moment of inertia of the instrument; N is the number of disks; L and R_1 are the height and outside radius of the pail; d and h are the separation of the lateral surface of the pail and of its bottom from the motionless walls; l is the thickness of the layer of liquid above the top disk; r is the radius of the axis. In order to eliminate a temperature effect due to changed instrumental dimensions it is most convenient to determine the ratio of the density of the normal component to the density at the λ point, as was done in the case of He^4 [2], i. e., the ratio ρ_n/ρ_λ, for which by using (5) we obtain

$$\frac{\rho_n}{\rho_\lambda}=\frac{\theta^2-\theta_0^2}{\theta_\lambda^2-\theta_0^2}\,\frac{\delta_\lambda}{\delta}\times$$
$$\times\frac{\dfrac{\operatorname{sh}\frac{a}{\delta_\lambda}+\sin\frac{a}{\delta_\lambda}}{\operatorname{ch}\frac{a}{\delta_\lambda}+\cos\frac{a}{\delta_\lambda}}+\dfrac{1}{2N}\dfrac{R_1^4}{R^4-r^4}\left[\dfrac{\operatorname{sh}\frac{2h}{\delta_\lambda}-\sin\frac{2h}{\delta_\lambda}}{\operatorname{ch}\frac{2h}{\delta_\lambda}-\cos\frac{2h}{\delta_\lambda}}+\dfrac{\operatorname{sh}\frac{2l}{\delta_\lambda}+\sin\frac{2l}{\delta_\lambda}}{\operatorname{ch}\frac{2l}{\delta_\lambda}+\cos\frac{2l}{\delta_\lambda}}+\dfrac{4L}{R_1}\dfrac{\operatorname{sh}\frac{2d}{\delta_\lambda}-\sin\frac{2d}{\delta_\lambda}}{\operatorname{ch}\frac{2d}{\delta_\lambda}-\cos\frac{2d}{\delta_\lambda}}\right]}{\dfrac{\operatorname{sh}\frac{a}{\delta}+\sin\frac{a}{\delta}}{\operatorname{ch}\frac{a}{\delta}+\cos\frac{a}{\delta}}+\dfrac{1}{2N}\dfrac{R_1^4}{R^4-r^4}\left[\dfrac{\operatorname{sh}\frac{2h}{\delta}-\sin\frac{2h}{\delta}}{\operatorname{ch}\frac{2h}{\delta}-\cos\frac{2h}{\delta}}+\dfrac{\operatorname{sh}\frac{2l}{\delta}+\sin\frac{2l}{\delta}}{\operatorname{ch}\frac{2l}{\delta}+\cos\frac{2l}{\delta}}+\dfrac{4L}{R_1}\dfrac{\operatorname{sh}\frac{2d}{\delta}-\sin\frac{2d}{\delta}}{\operatorname{ch}\frac{2d}{\delta}-\cos\frac{2d}{\delta}}\right]}. \tag{6}$$

---

* [Here 'sh' ≡ 'sinh', 'ch' ≡ 'cosh'].

With the above-described apparatus we measured the temperature dependence of the normal component density of pure He^4 in a solution of helium isotopes with the content $x = 3.0\%$ He^3.* The results obtained for He^4 were in quite good agreement with the data of E. L. Andronikashvili [2] and Hollis-Hallett [3] and are shown in Fig. 1 (Curve 1). Curve 2 in the same figure characterizes the results for a solution of helium isotopes. The accuracy of determination of ρ_n / ρ_λ was 3 % for the lowest temperatures and greater for higher temperatures.

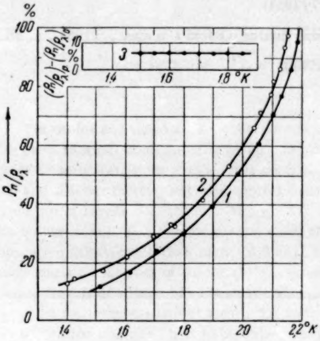

Fig. 1. Temperature dependence of ρ_n / ρ_λ 1) He; 2) solution with 3.0 % He^3; 3) variation of $(\rho_n / \rho_\lambda)_p - (\rho_n / \rho_\lambda)_0$ with temperature.

These results are evidence of the fact that the density of the normal component of the solution is considerably higher than for He^4, as follows from the theory of I. Ia. Pomeranchuk. Thus, for example, at 1.5°K, ρ_n / ρ_λ for a solution is 50% greater than for He^4.

Fig. 1 also shows the variation with temperature of the difference between $(\rho_n / \rho_\lambda)_p$ of a solution and $(\rho_n / \rho_\lambda)_0$ of pure He^4. It is clearly evident that between 1.5 and 1.85°K this quantity remains constant. This circumstance enables us to conclude that the energy spectrum of elementary excitations corresponding to the impurity is characterized by $p_0 = 0$. At higher temperatures the difference increases somewhat (this is not shown in Fig. 1), but this does not contradict the theory, which is incorrect near the λ point.

By using (2) and the experimentally determined values of $(\rho_n / \rho_\lambda)_p$ for a solution and $(\rho_n / \rho_\lambda)_0$ for pure He^4 we can calculate the effective mass of the impurity in the solution. This calculation yields the value $\mu = 2.5\ m_3$, where m_3 is the mass of a He^3 atom.

Our conclusion regarding the character of the energy spectrum, which was based on the temperature dependence of ρ_n / ρ_λ, agrees with conclusions derived from measurements of the velocity of second sound in solutions of helium isotopes [7-10]. To be sure, there is still no explanation of the temperature dependence of μ which was detected in such investigations. Our value for the effective mass of He^3 is in satisfactory agreement with the calculation of μ from the results of recently published work by Pellam [11].

At the present time experimental work is being conducted to determine ρ_n / ρ_λ for more highly concentrated mixtures.

We take this opportunity to thank Professor B. G. Lazarev for a number of suggestions and Professor I. M. Lifshits and M. I. Kaganov for discussions of the results.

Physico-Technical Institute, Academy of Sciences,
Ukrainian SSR

Received April 12, 1956

LITERATURE CITED

[1] I. Pomeranchuk, J. Exptl.-Theoret. Phys. (USSR) 19, 42 (1949).

[2] E. L. Andronikashvili, J. Exptl.-Theoret. Phys. (USSR) 18, 424 (1948).

[3] A. C. Hollis-Hallett, Proc. Roy. Soc. (London) A 210, 404 (1952).

---

*The concentration of the mixture was determined from the vapor pressure of the solution using the liquid-vapor phase diagram [6].

[4] L. D. Landau and E. M. Lifshits, Mechanics of Continuous Media (1953), p. 117.

[5] E. L. Andronikashvili, Dissertation, Inst. Phys. Prob., Acad. Sci. USSR (1948).

[6] B. N. Esel'son and N. G. Berezniak, Doklady Akad. Nauk SSSR 105, 454 (1955).

[7] E. A. Lynton and H. A. Fairbank, Phys. Rev. 80, 1043 (1950).

[8] I. M. Khalatnikov, Doklady Akad. Nauk SSSR 79, 57 (1951).

[9] E. A. Lynton and H. A. Fairbank, Conf. on Low Temp. Physics, Oxford University (1951), p. 88.

[10] J. C. King, and H. A. Fairbank, Phys. Rev. 93, 21 (1954).

[11] J. R. Pellam, Phys. Rev. 99, 1327 (1955).

TRIPLET-QUINTET TRANSITIONS IN THE ATOMIC SPECTRUM OF SILICON

Academician N. A. El'iashevich of the Academy of Sciences Byelorussian SSR and O. N. Nikitina

For atoms and ions with an even normal electronic configuration of the type ns^2np^2, among which are the carbon atom (normal configuration $2s^2 2p^2$) and the silicon atom (normal configuration $3s^2 3p^2$), excitation results in the odd configuration $nsnp^3$ [1]. This configuration, as we know, is associated with the tetravalent state of carbon and silicon; therefore it is of special interest to find the corresponding levels. The configuration $nsnp^3$ gives the set of levels ${}^1P^\circ_1$, ${}^1D^\circ_0$, ${}^3S^\circ_1$, ${}^3P^\circ_{0,1,2}$, ${}^3D^\circ_{1,2,3}$, ${}^5S^\circ_2$, of which the lowest according to Hund's rules must be the quintet level ${}^5S^\circ_2$. For the carbon atom this level is known and is, consequently, the deepest level for the configuration $2s2p^3$ (excitation energy 4.2 ev). For the silicon atom the ${}^5S^\circ_2$ level has thus far not been found although the arc spectrum of silicon (SiI) has been well studied and essentially interpreted [2, 3]. Only singlet and triplet levels of silicon have been found, especially all the levels of the normal configuration $3s^2 3p^2$, namely, ${}^3P_{0,1,2}$ (the fundamental triplet term), ${}^1D_2$ and ${}^1S_0$ and the triplet term ${}^3D^\circ_{1,2,3}$ of the $3s3p^3$ configuration (with 6.0 ev excitation energy). It is to be expected that the ${}^5S^\circ_2$ level of the configuration $3s3p^3$ will lie lower than ${}^3D^\circ_{1,2,3}$.

In investigating the silicon spectrum excited in a dc carbon arc through the burning of SiO_2 out of the anode, one of the authors (O. N. Nikitina) was able to detect the two weak spectral lines $\lambda_1 = 3006.72$ A ($\nu_{1vac} = 33249.16$ cm^{-1}) and $\lambda_2 = 3020.00$ A ($\nu_{2vac} = 33102.95$ cm^{-1}), which are not found in Harrison's Wavelength Tables [4] nor in the table given by Kiess [3].*

It was carefully verified that these lines belong to the silicon spectrum. They always appear in the spectrum of a sample containing a considerable amount of silicon – in the burning of siliceous materials in a dc carbon arc and in an ac arc between electrodes of elementary silicon. The pure silica and carbon electrodes as well as elementary silicon contained slight Al, Ca and Mg impurities; traces of the most intense lines of these elements were present in the spectra. However, according to the tables the investigated portions of the spectrum (3006.72 and 3020.00 A) do not contain strong lines of Al, Ca and Mg nor any lines of carbon and weak lines of other elements. Therefore, the lines 3006.72 and 3020.00 A cannot be ascribed to impurities of the sample or carbon electrodes. These lines do not belong to the molecular spectrum of SiO which is observed in the region 2400-3100 A when the silicon spectrum is excited in air nor to the molecular spectrum of any other silicon compounds. This was shown by exciting the silicon spectrum under conditions which excluded the possibility of the formation of SiO molecules or any other silicon compounds. For this purpose the silicon spectrum was excited in dc and ac arcs in an inert gas atmosphere (argon). The resulting silicon spectra were free of all molecular bands and the lines 3006.72 and 3020.00 A were present.

3006.72 and 3020.00 A always appear together and the ratio of their intensities remains constant within the limits of experimental accuracy. The difference of their wavelengths is 146.21 cm^{-1} and within the limits of accuracy, 0.01 A (i. e., 0.1 cm^{-1}), agrees with the difference of the wavelengths of the levels ${}^3P_2$ and ${}^3P_1$ of the fundamental triplet term ${}^3P$ of silicon, which is 146.16 cm^{-1} [1]. It is reasonable to interpret these lines as transitions from an odd upper level to the even levels $^3P_1$ and $^3P_2$. From the fact that there is no transition to the level $^3P_0$ it follows that the quantum number J for the upper level is 2, and the low intensity of the lines indicates that these are intercombination transitions. The level lies 33326.28 cm^{-1} above the normal level $3s^2 3p^2\ ^3P_0$ (the excitation energy is 4.13 ev), i. e., below all known odd levels of atomic silicon; the excitation energy of the next in order odd levels $3s^2 3p(^3P^0) 4s\ ^3P^\circ_{0,1,2}$ is 4.95 ev. All expected deep odd levels are known except $^5S^\circ_2$. Therefore the 33326.28 cm^{-1} level can be interpreted uniquely as the quintet level $^5S^\circ_2$. Then 3006.72 and 3020.00 A are interpreted as triplet-quintet transitions:

---

*The line 3020.00 A was previously indicated as doubtful in the silicon spectrum by Fowler [5] (3020.01 A) and in the Atlas of Eder and Valenta [6] (3020.13 A).

$$3006.72\ \text{A} \quad 3s3p^3\ ^5S^\circ_2 - 3s^2 3p^2\ ^3P_1{}^\circ;$$
$$3020.00\ \text{A} \quad 3s3p^3\ ^5S^\circ_2 - 3s^2 3p^2\ ^3P_2.$$

This interpretation agrees fully with all experimental data and theoretical considerations. Table 1 gives the data for the intensities of 3006.72 and 3020.00 A compared with the line 2970.35 A ($3s^2 3p(^3P^\circ) 4s\ ^3P^\circ_2 - 3s^2 3p^2\ ^1D_2$, excitation energy 4.95 ev) and the line 2577.13 A ($3s^2 3p(^3P^\circ) 4d\ ^3D^\circ_1 - 3s^2 3p^2\ ^1S_0$, excitation energy 6.7 ev). These data were obtained under different conditions of excitations. They show the relative intensities I_{3020}/I_{2970}, I_{3006}/I_{2970} are more stable than the relative intensities I_{3020}/I_{2577}, I_{3006}/I_{2577}. This is to be expected considering the excitation energy of 2970.35 A (4.95 ev) is closer to the excitation energy of 3020.00 and 3006.72 A (4.13 ev) than the excitation energy of 2577.13 A (6.7 ev).* The intensities of the lines 3020.00 and 3006.72 A (triplet-qunitet transitions), although lower than the intensities of 2970.35 and 2577.13 A (singlet-triplet transitions), are not of the same order of magnitude, which is as it should be. The fact that 3020.00 A is more intense than 3006.72 A is in qualitative agreement with the greater statistical weight of the $^3P_2$ level compared with the $^3P_1$ level; the theoretical intensity ratio is 5 : 3 = 1.67. Quantitative agreement cannot be expected in such cases.

TABLE 1

Relative Line Intensities

Conditions under which the silicon spectrum was obtained in a dc carbon arc	$\frac{I_{3020}}{I_{2970}}$	$\frac{I_{3006}}{I_{2970}}$	$\frac{I_{3020}}{I_{2577}}$	$\frac{I_{3006}}{I_{2577}}$	$\frac{I_{3020}}{I_{3006}}$
in an argon atmosphere	0.21	0.081	0.44	0.17	2.6
in a nitrogen atmosphere	0.22	0.087	0.59	0.24	2.5
in air*	0.21	0.098	0.56	0.26	2.2

*There is a SiO background which is insignificant in the region 2970-3020 A and more noticeable at 2577 A.

The difference in excitation energy between the levels $^3D^\circ_{1,2,3}$ and $^5S^\circ_2$ of the $3s3p^3$ configuration of atomic silicon is 6.0-4.13 = 1.9 ev, which is smaller than the corresponding difference for the levels $^3D^\circ_{1,2,3}$ and $^5S^\circ_2$ of the $2s2p^3$ configuration of atomic carbon, which is 8.0-4.2 = 3.8 ev. This agrees with the general decrease of binding energy of the outer electrons when we go from carbon to silicon.

It can finally be concluded that 3020.00 and 3006.72 A correspond to triplet-quintet transitions from the level $3s3p^3\ ^5S^\circ_2$ 33326.28 cm^{-1} with excitation energy 4.13 ev.

It would, of course, be desirable to find combinations of this level with other levels besides $^3P_2$ and $^3P_1$ of the normal configuration. However, as is shown by an examination of the different possible combinations, only extremely weak lines can be expected.

---

*In accordance with the higher ionization potential of argon compared with nitrogen and oxygen, in argon the line 2577 A should be excited instead, which explains the smaller ratios I_{3020}/I_{2577}, I_{3006}/I_{2577} in this case.

LITERATURE CITED

[1] C. Moore, Atomic Energy Levels 1 (1949).

[2] H. Babcock, C. Moore and W. Hoge, Astrophys. J. 83, 118 (1936).

[3] C. Kiess, J. Research Nat. Bur. Standards 21, 185 (1938).

[4] G. Harrison, Wavelength Tables (New York, 1939).

[5] A. Fowler, Proc. Roy. Soc. (London) 123 A, 422 (1929).

[6] J. Eder, E. Valenta, Atlas typischen Spectra (Wien, 1911).

Physics and Mathematics Institute, Academy of
Sciences, Byelorussian SSR Institute for Silicate
Chemistry Academy of Sciences, USSR

Received June 25, 1956

ON THE INTERMOLECULAR TRANSFER OF EXCITATION ENERGY IN CRYSTALS

E. K. Zavoiskii, Corresponding Member of the
Academy of Sciences USSR, and G. E. Smolkin

I. Recently the literature on the theory of luminescence has contained frequent discussions of the mechanism for the intermolecular transfer of excitation energy in crystals. For example, one of the relatively new theories is the so-called "theory of primary photons" of Birks [1]. According to this theory when an ionizing particle passes through a crystal high electronic states are excited. Transitions from these states are accompanied by emission of primary hard quanta of $\sim$ 8 ev ($\lambda \sim$ 1000-2000 A). This shortwave radiation is absorbed and emitted again by neighboring molecules. The reabsorption process is repeated a few times with partial dissipation of energy. When the excitation energy becomes equal to the energy of the first excited electronic state normal fluorescence occurs.

Birks states that this mechanism, unlike the exciton and other theories, can explain energy migration to practically any distance. In [1] Birks calculated the mean free path of the primary photons in crystals such as anthracene, stilbene and terphenyl and obtained the value 7μ. As an experimental verification of his theory he refers to reference [2]. The authors of the latter article attempted to obtain a direct photographic record of the size of the region in which energy transfer occurs in a large stilbene crystal irradiated with alpha particles from Po^{210}. They found that the transfer of excitation energy in a stilbene crystal proceeds to a distance of the order of a few millimeters.

II. The size of the region in which intermolecular energy transfer occurs in crystals can be calculated relatively simply by the use of a luminescence camera [3]. For this purpose it is sufficient to photograph the tracks of ionizing particles in these crystals. We performed such experiments with crystals of anthracene and CsI(Tl). Alpha particles from Po^{210} were used (5.3 Mev), which impinged on the crystal surface at a small angle.

In order to project the images of the tracks on the photocathode of an electron-optical image tube (EOI) we used a microscope with 200 x to 300x magnification. The total path of an alpha particle in anthracene and cesium iodide crystals is $\sim$ 34 and $\sim 27\mu$, respectively. The amplification of the EOI was quite high and permitted photographic registration of a single electron emitted from the input photocathode [4]. In all other details the experimental apparatus was similar to that described in [3].

A few tracks of alpha particles in anthracene and CsI(Tl) crystals which were obtained with a luminescence camera are shown in Figs. 1 and 2. It can be seen that the images of the tracks in both figures consist of separate dots. Each dot corresponds to a single photoelectron emitted from the photocathode of the EOI. The number of dots per unit track is determined by the luminescence yield of the crystal, the quantum yield of the EOI photocathode, the properties of the optics employed and, finally, by the agreement between the spectral sensitivity of the photocathode and the emission spectrum of the crystal. Tracks were photographed in anthracene and CsI(Tl) under identical conditions, and the emission spectra of these crystals fit entirely on the spectral sensitivity curve of an antimony-cesium photocathode. Therefore the difference of both density and total number N of dots on the track photographs depends only on the quantum luminescence yield of the crystals.

We shall now make a preliminary calculation of N in both cases for the total range of a Po^{210} alpha particle. Let E be the energy of the alpha particle and V be the energy expended by an alpha particle to produce a single quantum in the crystal. Then N is given by

$$N = \frac{E\eta\xi \sin^2(\alpha/2)}{n^2 V} \qquad (1)$$

Here η is the quantum yield of the photocathode for crystal luminescence; ξ is a factor which allows for light losses in the optical system; sin α * is the microscope aperture; and n is the refractive index of the crystal.

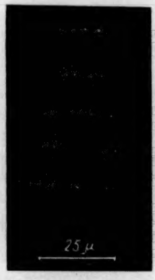

Fig. 1. Photographs of Po^{210} alpha particle tracks in an anthracene crystal.

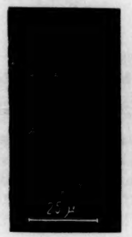

Fig. 2. Photographs of Po^{210} alpha particles in a CsI(Tl) crystal.

In this formula, all quantities are known with sufficient accuracy for both anthracene and cesium iodide: $E = 5.3 \cdot 10^6$ ev; $\eta = 5 \cdot 10^{-2}$; $\xi = 0.76$, $\sin^2 \frac{\alpha}{2} = 0.137$; $n \simeq 1.7$ for anthracene and $n = 1.78$ for cesium iodide; $V \simeq 10^3$ ev ** for anthracene [1] and $V \simeq 50$ ev ** for CsI(Tl) [1].

Inserting the calculated values in (1) we obtain

$$N \simeq 10 \text{ for anthracene}; \; N \simeq 150 \text{ for CsI(Tl)}.$$

These values of N are in completely satisfactory agreement with our experimental results.

When a median line is passed through the tracks in Figs. 1 and 2 it can be seen that no dots are more than 1μ distant from the line.

Let us consider the resolving power of our apparatus. This is determined by the resolving power of the EOI and of the microscope, and also by the quality of treatment of the crystal surface. The resolving power of the EOI was 10^{-2} cm. The microscope resolution was $d = \lambda/2n \sin \alpha \sim 0.2\mu$. Here $\lambda = 4500$ A is the mean wavelength in the crystal spectrum. Consequently, with 200 × magnification by the microscope the luminescence camera was able to resolve about 1 μ of the object.

From our experimental data it thus follows that for both anthracene and CsI(Tl) the luminescence is emitted by molecules which are separated from the path of the alpha particle by a distance which is not greater than the minimum distance which could be resolved by our apparatus (± 1 μ). This result, however, does not agree with Birks' calculation for the mean free path of the primary photons; it also disagrees sharply with [2].

---

*This refers to a "dry" (not an immersion) objective.

**In these values of V we allowed for the nonlinearity of the luminescence yield which occurs for high ionization densities.

The low luminescence yield of stilbene, the low sensitivity of the EOI photocathode in the spectral region of stilbene emission and the absorption by the optical system prevented us from obtaining entirely satisfactory photographs of the alpha particle tracks in this crystal. However, in experiments similar to [2] but employing a luminescence camera we were not able to detect excitation energy transfer in stilbene to distances which exceeded the accuracy of the measurements − 0.1 mm.* Apparently the authors of [2] did not eliminate reflections of luminescent quanta from the surfaces and inhomogeneities of the crystals.

In conclusion we wish to thank L. M. Beliaev for making the anthracene and cesium iodide crystals available and M. D. Galanin for an interesting discussion of the results.

Received June 9, 1956

LITERATURE CITED

[1] J. Birks, Scintillation Counters (Foreign Lit. Press, 1955) (Russian Translation).

[2] M. Ageno and G. Cortellessa, Nuovo Cimento 9, 196 (1952).

[3] E. K. Zavoiskii, G. E. Smolkin, A. G. Plakhov and M. M. Butslov, Doklady Akad. Nauk SSSR 100, 241 (1955).

[4] E. K. Zavoiskii, M. M. Butslov and G. E. Smolkin, Doklady Akad. Nauk SSSR 111, 5, 995 (1956).

---

* In this case we used an ordinary Jupiter-3 photographic objective with 1× 1 magnification instead of a microscope.

THE UPPER LIMIT OF THE RADIATION CAPTURE CROSS SECTION OF 275 KEV RESONANCE NEUTRONS BY Li^7

E. A. Koltypin and V. M. Morozov

(Presented by Academician A. P. Aleksandrov, June 9, 1956)

The activation cross section of Li for radiation capture of neutrons was determined by comparison with the cross section of the well-studied reaction Li^6(n, t)He^4 [1]. The comparison is facilitated by the fact that after β decay of Li^8 the resulting Be^8 nucleus is an alpha emitter and can be detected through the ionization produced by alpha particles. Such detection can be performed by the same counter which records alpha particles and tritium nuclei from the reaction Li^6(n, t)He^4 with approximately the same efficiency, since in 90% of β decays of Li^8 the Be^8 nucleus is formed in an excited state (the 3.1 Mev level) so that alpha decay produces alpha particles of energy 1.5 Mev each [2]. This energy is comparable with the energy of the alpha particles from the reaction Li^6(n, t)He^4 (~ 2 Mev). But study of Li^7 activation by the usual method (by observation of the activity after emission) is strongly hampered both by the short half-life of Li^8 (0.89 sec) and by the small anticipated cross section (in [3] the thermal neutron activation cross section was measured at 33 ± 5 millibarns).

TABLE 1

No. of counts		Duration of measurement, sec	No. of coincidences	Estimated No. of random coincidences	Effect
Proportional counter	Geiger counter				
40 200	34 2000	1500	46	29	17±7
40 250	34 4000	1500	53	30	23±7
40 000	32 5050	1500	36	28	8±6
48 600	47 2850	1800	58	41	17±8
141 400	146 3150	5400	147	122	25±12
Σ 310450			340	250	90±19

We recorded continuously the acts of β decay of Li^8 during neutron irradiation of lithium, separating the detector pulses caused by alpha particles in Be^8 decay from pulses produced by products of the reaction Li^6(n, t)He^4, by coincidences with pulses from electrons due to Li^8 β decay in the second detector. Indeed, the alpha decay of Be^8 even in the ground state takes place in ~ 10^{-16} sec, so that this process can be studied experimentally at the same time as the β decay of Li^8.

Measurements were performed with apparatus (see Fig. 1) which consisted of two gas-filled counters. The inside counter was of ordinary construction and functioned as a proportional counter. Its walls were covered with a thin layer of lithium fluoride of natural isotope content. The outside (Geiger) counter was intended to record electrons from Li^8 β decay. This counter is of unusual design; its construction is shown in the figure.

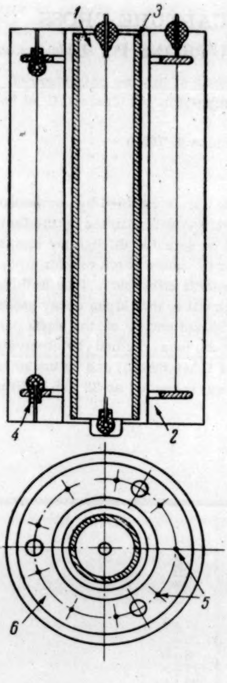

Fig. 1. 1) First counter; 2) second counter; 3) layer of LiF; 4) insulators (glass); 5) filaments; 6) rings holding filaments.

Since electrons from the β decay of Li^8 are very energetic (the upper limit of the spectrum is ~ 13 Mev) it is not necessary to have especially thin walls for the two counters.

With our assumptions regarding the efficiency of registration of alpha particles from Be^8 decay and the products of the $Li^6(n, t)He^4$ reaction the registration efficiency of β decay of Li^8 (relative to the registration of $Li^6(n, t)He^4$ depends only on the absolute efficiency of the electron count from Li^8 β decay by the outside counter. We estimated this efficiency by calculating the solid angle occupied by the outside counter with respect to the working volume of the inside counter (~ 85% of 4π) and the percentage of electrons in the β decay spectrum of Li^8 which were able to penetrate the walls of the counters into the working space of the outside counter (~ 60%, using the spectrum in [2]); consequently, the efficiency of the outside counter is $50 \mp 10\%$ – the inaccuracy of this quantity is associated with the simplifications introduced into the computation. Thus the number of Li^8 β decays recorded in a definite time interval must be doubled before comparison with the number of $Li^6(n, t)He^4$ reactions registered by the inside counter in the same time interval.

As a check of the method we measured the radiation capture cross section of thermal neutrons by Li^7. The neutrons were derived from a radium-beryllium source (~ 1.6 c) surrounded by lead in order to reduce the γ ray background. The neutrons were slowed down by paraffin.

Results derived from the measurements are given in Table 1.

Taking for the $Li^6(n, t)He^4$ reaction a thermal neutron cross section of 67 ± 7 barns [4] per nucleus of a natural mixture of lithium isotopes and taking the isotope composition into account, the data of Table 1 can be used to determine the (n, γ) cross section in Li^7 for thermal neutrons. This cross section is 42 ± 10 millibarns, in satisfactory agreement with [3] (33 ± 5 millibarns). The accuracy of these measurements is sufficient to check the possibilities of the method.

Measurements with neutrons of the resonance energy (275 kev [5]) were performed with neutrons from the $T(p, n)He^3$ reaction; the energy spread of the neutrons did not exceed ~ 15 kev. These measurements were accompanied by a proportional counter background associated with the $Li^6(n, t)He^4$ reaction for thermal neutrons present in the measuring space in small quantities. This background was determined in the individual measurements and was found to be 50 ± 5 % of the total number of counts of the proportional counter. The results are given in Table 2.

We assume that under our experimental conditions the number of coincidences associated with β decay of Li^8 did not exceed 2-3. In this case (considering that the cross section for $Li^6(n, t)He^4$ for 265 kev neutrons is 3.4 barns [1] we estimate the upper limit of the radiation capture cross section of resonance neutrons by Li^7 to be 1/4 millibarn.

TABLE 2

No. of counts		Duration of measurement, sec	No. of coincidences	Estimated No. of random coincidences	Effect
Proportional counter	Geiger counter				
6464	468480	810	6	9	—
1600	107780	190	0	2	—
Σ 8064			6	11	**Unobserved**

Received May 3, 1956

LITERATURE CITED

[1] G. V. Gorlov, B. M. Gokhberg, V. M. Morozov and G. A. Otroshchenko, Doklady Akad. Nauk SSSR 110, 6, 963 (1956) [Soviet Physics-Doklady, p. 598].

[2] W. F. Hornyak and T. Lauritsen, Phys. Rev. 77, 160 (1950).

[3] D. J. Hughes, D. Hall et al., Phys. Rev. 72, 646 (1947).

[4] R. K. Adair, Neutron Cross Sections (Foreign Lit. Press, 1951) (Russian translation).

[5] G. V. Gorlov, B. M. Gokhberg, V. M. Morozov and G. A. Otroshchenko, Doklady Akad. Nauk SSSR 111, 4, 791 (1956) [Soviet Physics – Doklady, p. 705].

THE EXCITATION OF MACROSCOPIC OSCILLATIONS BY QUANTUM FLUCTUATIONS

A. A. Sokolov, D. D. Ivanenko and I. M. Ternov

(Presented by Academician N. N. Bogoliubov, June 5, 1956)

1. The energy of a relativistic electron moving in a homogeneous magnetic field H is [1-4]

$$E_n = \sqrt{2eHc\hbar n + m^2c^4}, \tag{1}$$

where n = l + s, n is the principal, l the azimuthal and s the radial quantum number.

We can represent this energy as the sum of the energy of orbital motion of the electron (energy E_l) and the energy of radial oscillatory motion along the radius (E_s):

$$E_l \cong \sqrt{2eHc\hbar l + m^2c^4}, \quad E_s \cong \hbar\omega s = \frac{E\omega^2a^2}{2c^2}, \tag{2}$$

where a is the amplitude of radial oscillations.

When the electron makes a transition from state n to state $n' = n - \nu$ ($\nu = \nu' + \nu''$, $\nu'' = l - l'$, $\nu' = s - s'$) the orbital and oscillatory energies change as follows:

$$\frac{dE_l}{dt} = -\sum_{n',s'} \hbar\omega \left(\nu'' + \frac{\nu^2}{4l}\right) w_{nn'ss'} = -W_0 \left[1 - \frac{275\sqrt{3}}{96} \frac{\hbar\omega}{mc^2} \left(\frac{E}{mc^2}\right)^2\right], \tag{3}$$

$$\frac{dE_s}{dt} = -\sum_{n',s'} \hbar\omega\nu' w_{nn'ss'} = \frac{55\sqrt{3}}{96} W_0 \frac{\hbar\omega}{mc^2} \left(\frac{E}{mc^2}\right)^2, \tag{4}$$

where $w_{nn'ss'}$ is the spontaneous transition probability per unit time, as determined by Equation (56) of reference [2], and W_0 is the total emitted energy of a radiating electron in the classical approximation. The sum of (3) and (4) gives the total energy loss through radiation allowing for the quantum corrections accurate to ħ, which was obtained in [5, 6].

2. From (3) we see that quantum corrections to the orbital motion can be important only at very high energies $E \sim E_\mu$ ($\mu = 1/2$), where

$$E_\mu = mc^2 \left(\frac{mc^2}{\hbar\omega}\right)^\mu. \tag{5}$$

When $\hbar \to 0$ there will be no change of energy of radial oscillations, i. e., in the classical case s will remain constant even when radiation is taken into account.

Only in the quantum case ($\hbar \neq 0$) will there be a peculiar energy transfer where the orbital energy will be expended not only in radiation but also in the excitation of radial oscillations ($s \neq$ const) as a result of which the square of the amplitude of the radial oscillations will increase according to [2, 3, 7, 8]

$$a^2 = a_0^2 \frac{H(0)}{H(t)} + \frac{55}{24\sqrt{3}} \frac{e^2 tR}{mE(1-q)^2} \int_0^t \left(\frac{E}{mc^2}\right)^6 \frac{dt}{R^2}, \tag{6}$$

where a_0 is the initial amplitude of the radial oscillations; $\underline{q}$ is the exponent of the decrease of magnitude of magnetic field strength as a function of $\underline{r}$.

3. We shall now discuss the mechanism for excitation of quantum radial oscillations. For this purpose let us consider the case $q \neq 0$ where axial oscillations can arise in addition to the radial oscillations. Then

$$x = r - R = a\cos(\sqrt{1-q}\,\omega t + \varphi), \quad z = b\cos(\sqrt{q}\,\omega t + \varphi_1), \tag{7}$$

where R is the radius of the stable orbit. The amplitudes $\underline{a}$ and $\underline{b}$ can be associated with the corresponding quantum numbers ($\underline{s}$ is the radial and $\underline{k}$ is the axial quantum number) by the relations (see, for example, references [7, 8]).

$$a^2 = \frac{2c\hbar s}{eH\sqrt{1-q}}, \quad b^2 = \frac{2c\hbar k}{eH\sqrt{q}}.$$

Hence it can be seen that the quantum theory permits the following minimum change of the square of oscillation amplitude ($\Delta s = 1$):

$$\Delta(a^2) = \frac{2c\hbar}{eH\sqrt{1-q}}. \tag{8}$$

The excitation of radial oscillations will proceed as follows: the relativistic electron emits along the tangent to its orbit a photon with energy $\Delta E \sim \hbar \frac{c}{R} \nu_m$, where $\nu_m \sim \left(\frac{E}{mc^2}\right)^3$ is the index of the most probable emitted harmonic. This change of energy must result in a change of the stable orbit radius by the amount

$$\Delta R = \frac{1}{1-q} \frac{\Delta E}{E} R. \tag{9}$$

Rigorous quantum calculations in [8] [see Equation (29)] lead to the following value for the square of the amplitude of radial oscillations when one photon is emitted with energy ΔE:

$$\Delta(a^2)_q = \frac{R^2}{(1-q)^2}\left(\frac{\Delta E}{E}\right)^2; \quad (\Delta R)^2 > \Delta(x_0^2) \quad (s \neq 0); \tag{10}$$

$$\Delta(a^2)_q = 0; \quad (\Delta R)^2 < \Delta(x_0^2) \quad (s = 0). \tag{11}$$

From (10) we find that radial excitations will take place at energies $E > E_{1/5}$ ($\mu = 1/5$).

From (7) and (9) it can be seen that in the classical case the change of amplitude associated with change of the center of oscillations must also depend on the phase

$$\Delta(a^2)_{cl} = \Delta(a^2)_q - 2a\Delta R\cos(\sqrt{1-q}\,\omega t + \varphi). \tag{12}$$

If in the course of a single period of oscillation there are a few "random" changes of the oscillation center subject to the condition that the phase φ will retain its value (the classical approximation) we obtain the vanishing result (11). The quantum result (10) can be obtained only by averaging (12) over the phase φ.

Thus the excitation of radial oscillations will take place when there is statistical independence of successive processes (a Markov chain). As we know, Markov chains are fundamental in the theory of fluctuations (see, for example, the theory of Brownian motion).

A rigorous quantum method for investigating the excitation of radial betatron oscillations was used in a number of our articles on the quantum theory of the radiating electron, and a semiclassical method including averaging over the phase was used by Sands [10] in investigating the effect of quantum fluctuations on radial-phase oscillations in a synchrotron. The two methods lead to an identical result. This recalls the rigorous quantum derivation of the Lamb shift and its semiclassical interpretation by Welton (see, for example, [11-13]). Thus for high energies $E \gg E_{1/5}$ ($s = \text{const}$) we will have the very interesting case of a relativistic electron whose orbit in a magnetic field will be described by classical theory but whose radial oscillations with a macroscopic amplitude (forming a sort of "macroatom") will be described by the laws of quantum mechanics.

The "macroatom" has its own uncertainty principle. The amplitudes of the radial oscillations and of the radial momentum are of the order

$$a \sim \sqrt{\frac{c\hbar s}{eH}}, \quad p_0 \sim \frac{E}{c^2}\,\omega a \sim \sqrt{\frac{eH\hbar s}{c}}. \tag{13}$$

It is thus seen that for a possible unit change of s we shall know the amplitudes of the momentum and the coordinate only to an accuracy given by

$$\Delta p_0 \sim \frac{\partial p_0}{\partial s}\,\Delta s \sim \frac{p_0}{s}, \quad \Delta a \sim \frac{a}{s}. \tag{14}$$

However, the uncertainties in the measurement of the coordinate (Δx) and momentum (Δp) cannot both simultaneously coincide with the uncertainties Δa and Δp_0 since for $s \gg 1$ we would obtain the inequality

$$\Delta a \cdot \Delta p_0 \sim \frac{\hbar}{s} \ll \hbar,$$

which contradicts the uncertainty principle

$$\Delta x \cdot \Delta p \sim \hbar. \tag{15}$$

Therefore only one of the uncertainties can be placed equal in order of magnitude to the increase of the corresponding amplitude; the uncertainty of the second quantity can be evaluated from the uncertainty principle (15).

Then in both instances:

$$\begin{aligned} &1)\quad \Delta p \sim \Delta p_0 \sim \frac{p_0}{s}, \quad \Delta a \sim \frac{\hbar}{\Delta p} \sim a; \\ &2)\quad \Delta x \sim \Delta a \sim \frac{a}{s}; \quad \Delta p \sim \frac{\hbar}{\Delta x} \sim p_0 \end{aligned} \tag{16}$$

we are not able to use the classical approximation.

The indicated uncertainties can only arise in a time interval $\tau = 1/(w_{s,s+1})$ where $w_{s,\,s+1}$ is the transition probability with unit change of the quantum number s̲.

For $E \ll E_{1/5}$, $\tau \to \infty$, therefore we can use the classical approximation. For $E \gg E_{1/5}$ the time $\tau \sim \frac{137mc^2}{\omega E}$; therefore the indicated transitions can occur in the first few periods of radial oscillation, which in the end (i. e., as a result of many transitions) must result in a quantum character of the radial oscillations, although the transition from the classical to the quantum equations would be difficult under the existing theories.

The excitation of axial oscillations, which is possible for energies $E > E_{1/3}$ ($\mu = 1/3$) will follow the law

$$b^2 = b_0^2 \frac{H(0)}{H(t)} + \frac{13}{24\sqrt{3}} \frac{e^2\hbar R}{qmE} \int_0^t \left(\frac{E}{mc^2}\right)^4 \frac{dt}{R^2}. \tag{17}$$

M. V. Lomonosov Moscow State University

Received June 16, 1955

LITERATURE CITED

[1] D. Ivanenko and A. Sokolov, Classical Field Theory (Moscow-Leningrad, 1951), pp. 288-290.

[2] A. A. Sokolov and I. M. Ternov, J. Exptl.-Theoret. Phys. (USSR) 25, 698 (1953).

[3] A. A. Sokolov and I. M. Ternov, Doklady Akad. Nauk SSSR 92, 537 (1953).

[4] A. A. Sokolov, A. N. Matveev and I. M. Ternov, Doklady Akad. Nauk SSSR 102, 65 (1955).

[5] A. A. Sokolov, N. P. Klepikov and I. M. Ternov, Doklady Akad. Nauk SSSR 89, 665 (1953).

[6] A. A. Sokolov, N. P. Klepikov and I. M. Ternov, J. Exptl.-Theoret. Phys. (USSR) 24, 249 (1953).

[7] A. A. Sokolov and I. M. Ternov, Doklady Akad. Nauk SSSR 97, 823 (1954).

[8] A. A. Sokolov and I. M. Ternov, J. Exptl.-Theoret. Phys. (USSR) 28, 431 (1955).

[9] A. A. Sokolov, Doklady Akad. Nauk SSSR 67, 1013 (1949).

[10] M. Sands, Phys. Rev. 97, 470 (1955); A. N. Matveev, Doklady Akad. Nauk SSSR 109, 495 (1956) [Soviet Physics-Doklady, p. 443].

[11] T. Welton, Phys. Rev. 74, 1157 (1948).

[12] R. Feynman, Rev. Mod. Phys. 20, 367 (1948).

[13] A. Sokolov and D. Ivanenko, Quantum Field Theory (Moscow-Leningrad, 1952), p. 189.

MESON-MESON SCATTERING IN MESON FIELD THEORY

V. V. Sudakov

(Presented by Academician L. D. Landau, June 8, 1956)

Unlike the Green's function and the vertex part, the asymptotic expressions for which are functions of a single argument [1, 2], the same kind of asymptotic expression for meson-meson scattering depends in general on two arguments. I. T. Diatlov and K. A. Ter-Martirosian [3] have set up a system of equations which determine the asymptotic behavior of the amplitude and have found its limiting values. In the general case these equations can be solved only by numerical integration.

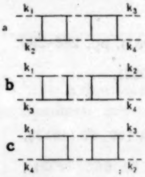

Fig. 1.

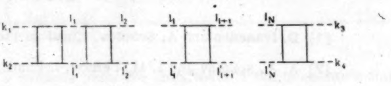

Fig. 2.

It would be possible to confine ourselves to the most interesting case where the two arguments of P coincide so that P is a function of a single argument (in this case the momenta of all four mesons k_1, k_2, k_3 and k_4 as well as their paired sums must be of the same order of magnitude). However in the set of equations given in [3] the amplitude P which depends on a single argument is not independent,and must be determined simultaneously with the P which is dependent on two arguments.

We shall show that it is nevertheless possible to obtain a simple closed expression for a P which is dependent on only a single argument (our derivation will use neutral pseudoscalar meson theory). For this purpose we consider the quantity $F(k_1, k_2, k_3, k_4)$ of [3], which is the sum of all diagrams reduced to the diagram in Fig. 1,a (we recall that the reduction of a diagram is the replacement of two squares connected by two meson lines by a single square). Each diagram of this sum is reducible with respect to the separation of momenta k_1, k_2 from k_3, k_4, i. e., it can be divided into two parts which are connected by only two meson lines, with k_1, k_2 connected to one part and k_3, k_4 to the other. Such a diagram consists of two or more parts connected by a chain of meson lines l_i, $l_i' = -l_i + k_1 + k_2$ (see Fig. 2) and not further reducible with respect to the separation of approaching pairs of meson lines l_i, l_i' and l_{i+1}, l'_{i+2} (i assumes all possible values).

We shall denote the contribution of the ith part of type n_i by f_{n_i} (assuming that we have numbered all possible irreducible parts):

$$f_{n_i}(z_i, z_{i+1}) = f_{n_i}[\max(z_i, z_{i+1})], \quad z_i = \ln(-l_i^2/m^2).$$

The contribution of this type of diagram is

$$f_{n_0, n_1, \dots, n_N}(\xi) = $$

$$= \left(\frac{-g_0^2}{4\pi}\right)^N \int_\xi^L dz_1 \int_\xi^L dz_2 \dots \int_\xi^L dz_N f_{n_0}(\xi, z_1)\, d^2(z_1)\, f_{n_1}(z_1, z_2)\, d^2(z_2) \dots d^2(z_N)\, f_N(z_N, \xi). \tag{1}$$

We divide the region of integration over $z_1, \dots\dots, n_N$ into N regions; the jth region is defined by the inequality

$$z_j \leqslant z_1, z_2, \dots, z_{j-1}, z_{j+1}, \dots, z_N; \quad j = 1, \dots, N.$$

The right-hand side of (1) goes over into the sum of N terms. In the jth term we integrate over all z_k, $k \neq j$. Then using directly the formulas obtained from (1)

$$\left(\frac{-g_0^2}{4\pi}\right)^{j-1} \int_{z_j}^L dz_1 \dots \int_{z_j}^L dz_{j-1} f_{n_0}(\xi, z_1)\, d^2(z_1) \dots d^2(z_{j-1})\, f_{n_{j-1}}(z_{j-1}, z_j) =$$

$$= f_{n_0, \dots, n_{j-1}}(z_j),$$

$$\left(\frac{-g_0^2}{4\pi}\right)^{N-j} \int_{z_j}^L dz_{j+1} \dots \int_{z_j}^L dz_N f_{n_j}(z_j, z_{j+1})\, d^2(z_{j+1}) \dots d^2(z_N)\, f_N(z_N, \xi) =$$

$$= f_{n_j, \dots, n_N}(z_j),$$

we have

$$f_{n_0, n_1, \dots, n_N}(\xi) = \sum_{j=1}^N \left(\frac{-g_0^2}{4\pi}\right) \int_\xi^L f_{n_0, \dots, n_{j-1}}(z_j)\, d^2(z_j)\, f_{n_j, \dots, n_N}(z_j)\, dz_j. \tag{2}$$

The meson-meson scattering amplitude is expressed as follows in terms of the quantities $f_{n_0, \dots, n_N}$:

$$P(\xi) = \sum_{N=0}^\infty 2^{-N} \sum_{n_0, \dots, n_N} f_{n_0, \dots, n_N}(\xi).$$

The factor 2^{-N} represents the fact that in summing over all possible irreducible parts n_j we obtain 2^N identical resulting diagrams. Inserting in

$$F(\xi) = \sum_{N=1}^\infty 2^{-N} \sum_{n_0, \dots, n_N} f_{n_0, n_1, \dots, n_N}(\xi)$$

the Expression (2) for $f(\xi)$ we obtain

$$F(\xi) = \left(\frac{-g_0^2}{8\pi}\right) \int_\xi^L P^2(z)\, d^2(z)\, dz. \tag{3}$$

The total amplitude P is expressed [3] as the sum of six squares shown in Fig. 3 and denoted by us as $R_0(\xi)$, and the sum of three $F(\xi)$ corresponding to the sets of diagrams reduced to Figs. 1a, b, c:

$$P(\xi) = R_0(\xi) + 3F(\xi). \tag{4}$$

Substituting (3) in (4) we finally obtain

$$\begin{gathered} P(\xi) = R_0(\xi) - \frac{3g_0^2}{8\pi}\int_\xi^L P^2(z)\, d^2(z)\, dz, \\ R_0 = 24(1-x), \quad x = [1 + (5g_0^2/4\pi)(L-\xi)]^{-1/5}. \end{gathered} \tag{5}$$

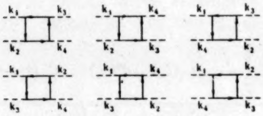

Fig. 3.

Our derivation can be extended with very insignificant complications associated with the appearance of isotopic indices to the symmetric pseudoscalar theory and gives the following equations:

$$F_{\tau_1\tau_2,\,\tau_3\tau_4}(\xi) = -\frac{g_0^2}{8\pi}\int_\xi^L P^2(z)\, d^2(z)\, dz\, [2\delta_s + 5\delta_{\tau_1\tau_2}\delta_{\tau_3\tau_4}], \tag{3'}$$

$$P_{\tau_1\tau_2\tau_3\tau_4}(\xi) = P(\xi)\delta_s, \quad \delta_s = \delta_{\tau_1\tau_2}\delta_{\tau_3\tau_4} + \delta_{\tau_1\tau_3}\delta_{\tau_2\tau_4} + \delta_{\tau_1\tau_4}\delta_{\tau_2\tau_3},$$

$$P(\xi)\,\delta_s = \rho_0\delta_s + F_{\tau_1\tau_2,\,\tau_3\tau_4}(\xi) + F_{\tau_1\tau_3,\,\tau_2\tau_4}(\xi) + F_{\tau_1\tau_4,\,\tau_2\tau_3}(\xi), \tag{4'}$$

$$P(\xi) = \rho_0(\xi) - \frac{11g_0^2}{8\pi}\int_\xi^L P^2(z)\, d^2(z)\, dz, \tag{5'}$$

where $\rho_0(\xi)\,\delta_s$ is the sum of six squares (Fig. 3);

$$\rho_0(\xi) = {}^{16}/_3\,(y-1), \quad y = [1 + (5g_0^2/4\pi)(L-\xi)]^{3/5}.$$

The integral Equations (5) and (5') reduce to the differential equations

$$\frac{dP}{dx} = -24 + {}^3/_2\left(\frac{P}{x}\right)^2, \quad P(1) = 0, \tag{6}$$

$$\frac{dP}{dy} = {}^{16}/_3 - {}^{11}/_6\left(\frac{P}{y}\right)^2, \quad P(1) = 0. \tag{6'}$$

The exact solutions of (6) and (6') are

$$P(x) = \frac{\sqrt{145}+1}{3}\, x\, \frac{1 - x^{\sqrt{145}}}{1 + [(\sqrt{145}+1)/(\sqrt{145}-1)]\, x^{\sqrt{145}}}, \tag{7}$$

$$P(y)=\frac{16}{11}\,y\,\frac{1-y^{-10/3}}{1+{}^{5}/_{11}x^{-10/3}}\,. \tag{7'}$$

It is seen from (7) and (7') that P in both cases is of the same order of magnitude as the contributions R_0 and ρ_0 from the very simple diagrams of Fig. 3. This supports the conclusion in [4] that the meson has zero charge.

In conclusion I wish to thank K. A. Ter-Martirosian for a number of valuable comments and I. Ia. Pomeranchuk and V. B. Verestetskii for fruitful discussions.

Received June 7, 1956

LITERATURE CITED

[1] L. D. Landau, A. A. Abrikosov and I. M. Khalatnikov, Doklady Akad. Nauk SSSR 95, 497, 773, 1177 (1954).

[2] A. A. Abrikosov, A. D. Galanin and I. M. Khalatnikov, Doklady Akad. Nauk SSSR 97, 793 (1954).

[3] I. T. Diatlov and K. A. Ter-Martirosian, J. Exptl.-Theoret. Phys. (USSR) 30, 416 (1956).*

[4] I. Ia. Pomeranchuk, Doklady Akad. Nauk SSSR 103, 1005 (1955).

---

* [Soviet Physics – J.E.T.P., p. 454].

ON PION PRODUCTION BY HIGH-ENERGY COSMIC RAYS

Zh. S. Takibaev, P. A. Usik and M. G. Antonova

(Presented by Academician I. E. Tamm, June 9, 1956)

According to one group of investigators [1] the multiple production of pions is probably much more frequent when particles of very high energies $E \geq 10^{12}$ ev interact with atomic nuclei. Emulsion chambers were used consisting of alternate layers of unbacked photographic emulsions and plates of a material in which the production of "jets" (very narrow showers) is studied. The fact that the number of light tracks in these showers is independent or only slightly dependent on the atomic number of the nucleus (these authors used Pb and Cu plates) apparently supports the conclusion that multiple pion production occurred. But a more detailed analysis shows that the slight dependence of the number of light tracks (in "jets" and not in showers consisting of a large number of particles) on the atomic number of the target nucleus is not alone sufficient to determine the validity of any theory.

We have investigated showers with both a small angular spread (jets) and a wide angular spread of shower particles. The analysis of a number of showers (Figs. 1 and 2) produced by interactions between high-energy cosmic ray particles with the nuclei of photographic emulsions exposed in the stratosphere in 1954 and 1955 leads us to the conclusion that in the majority of cases the observed showers cannot be explained merely by the mechanism of multiple pion production resulting from the single collision of an incident nucleon with one of the nucleons of the target nucleus. The hypothesis that mesons are generated by the collision of a primary particle with an entire "tube" of nucleons also fails to explain the observed shower parameters (n_s and $v_{1/2}$). This applies especially to the primary energy range from 10 to 1000 Bev. We present below certain data concerning several showers and the results of their analysis on the basis of the theory of multiple pion production [2].

These showers were selected from a large number (about 40,000 stars) formed in plates exposed to cosmic rays in the stratosphere at the latitude of Moscow. On the assumption that all of the shower particles of a given star were produced by the collision of an incident particle with one of the nucleons of the target nucleus we determine the energy of the primary particle striking a nucleon by the formula $E_0 = 2Mc^2/\tan^2 v_{1/2}$. It is clear that this method gives the lower limit of the primary particle energy.

Experimental data for 36 showers are given in Table 1. The emulsion was calibrated by grain densities in electron tracks of $\pi \to \mu \to e$ decays. The minimum density was also estimated from the grain density in tracks of 660-Mev protons with which the plates were irradiated at the Institute for Nuclear Problems of the Academy of Sciences, USSR.

It is clear from the data in Table 1 that the majority of the showers were not produced by nucleon-nucleon collisions. In this connection we attempted to compare the experimental results with Landau's theory, selecting for each case a suitable "tube" length. This comparison for 15 showers is given in Table 2 where

$$N = \frac{3}{2} n_s + \frac{l}{4d} - \frac{1}{2};$$

$$N'' = 0.84 \left(\frac{l}{d} + 1\right)\left(\frac{E}{Mc^2}\right)^{1/4}, \quad E'' = Mc^2 \left[\frac{N}{0.84\,(l/d + 1)}\right]^4,$$

(continued)

TABLE 1

No. of shower	Primary particle	Recoil nuclei	$N_b + N_g + n_s$	$\vartheta_{1/2}$	$E_0 = Mc^2 \frac{2}{\tan^2 \vartheta_{1/2}}$ Bev	$E' = Mc^2 \left(\frac{n_s}{1,06}\right)^4$ in Bev	$n'_s = 1.06 \left(\frac{E_0}{Mc^2}\right)^{1/4}$	$\vartheta'_{1/2} = \text{arc tan} \sqrt{2\left(\frac{1,06}{n_s}\right)^4}$
1	p	1	6+ 4+ 5	42°55′	2,1	461	1	3°38′
2	p	—	3+ 1+ 5	15°28′	24	461	2	3°38′
3	p	—	3+ 0+ 5	3°06′	633	461	5	3°38′
4	p	—	4+ 5+ 6	21°44′	12	956	2	2°31′
5	z	1	7+ 3+ 6	6°42′	135	—	—	—
6	n	1	5+ 5+ 6	2°24′	1058	956	6	2°31′
7	p	—	11+ 5+ 7	13°13′	34	1771	3	1°51′
8	p	—	11+ 5+ 7	18°07′	17,4	1771	2	1°51′
9	p	—	4+ 2+ 7	26°19′	7,5	1771	2	1°51′
10	n	—	5+ 3+ 8	25°54′	7,9	3020	2	1°25′
11	p	—	12+10+ 8	35°09′	3,7	3020	1	1°25′
12	p	—	5+ 3+ 9	9°56′	61	4838	3	1°07′
13	p	1	10+ 2+ 9	5°37′	192	4838	4	1°07′
14	p	—	9+ 3+12	15°49′	23	15300	2	36′
15	p	—	10+ 2+13	25°53′	8	$2 \cdot 10^4$	2	32′
16	p	—	8+ 2+14	9°58′	60	$2.8 \cdot 10^4$	3	28′
17	p	—	3+ 3+14	15°49′	23	$2.8 \cdot 10^4$	2	28′
18	z	—	18+ 8+15	20°53′	13	—	—	—
19	n	—	8+ 4+15	16°53′	20	$3.7 \cdot 10^4$	2	24′
20	p	—	6+ 4+17	21°55′	11,5	$6.2 \cdot 10^4$	2	20′
21	p	—	17+12+17	26°11′	8	$6.2 \cdot 10^4$	2	20′
22	n	—	15+14+20	32°34′	4,6	$1.2 \cdot 10^5$	2	14′
23	p	—	5+ 1+21	20°45′	13	$1.4 \cdot 10^5$	2	12′
24	p	—	6+ 3+23	9°38′	65	$2.1 \cdot 10^5$	3	10′
25	n	—	11+ 2+25	10°06′	59	$2.9 \cdot 10^5$	3	9′
26	p	1	16+ 9+27	18°15′	17	$3.9 \cdot 10^5$	2	8′
27	α	—	3+ 1+32	4°36′	287	—	—	—
28	p	—	12+ 5+36	18°35′	16,5	$1.2 \cdot 10^6$	2	4′
29	z	—	14+11+39	15°59′	23	—	—	—
30	p	1	16+26+44	23°05′	10	$2.8 \cdot 10^6$	2	3′
31	z	—	5+ 2+5	19°42′	14,5	—	—	—
32	p	—	4+ 2+8	24°06′	9,3	3020	2	1°25′
33	p	—	15+ 7+10	8°43′	79	7374	3	55′
34	p	—	2+ 2+11	24°06′	9,3	$1 \cdot 10^4$	2	45′
35	p	—	7+ 7+12	33°43′	4,2	$1.5 \cdot 10^4$	2	36′
36	p	—	12+ 2+7	19°38′	14,6	1771	2	1°51′

TABLE 2

No. of shower	Primary particle	Recoil nuclei	$N_b' + N_g + n_s$	$\vartheta_{1/2}$	$E_0 = \frac{2Mc^2}{\tan^2 \vartheta_{1/2}}$	Tube length $\frac{l}{d}$	$E = \frac{2Mc^2}{\tan^2 \vartheta_{1/2}} \frac{l}{d}$	N'' corresponding to the value of E_0	E'' corresponding to the value of N	$\vartheta''_{1/2}$ corresponding to the value of N	N	$\frac{\vartheta_{1/2}}{\vartheta''_{1/2}}$
1	p	—	3+ 0+5	3°06′	633	1	623	—	—	—	—	—
2	p	—	6+ 3+23	9°38′	65	7.2	468	31	792	7°20′	36	1 3
3	p	—	12+ 5+36	18°35′	17	3	51	9	$6 \cdot 10^4$	35′	53.7	31
						7.2	122.4	22	$4.5 \cdot 10^3$	3°	55.3	~6
						10	170	28	$1.7 \cdot 10^4$	5°45′	56	3,2
4	p	1	16+ 9+27	18°15′	17	7.2	122,4	22.4	$\sim 10^4$	5°5′	40.2	3.2
5	n	—	11+ 2+25	10°06′	59	7.2	42.5	31	$\sim 10^3$	6°25′	38.8	1.6
6	p	—	5+ 1+21	20°45′	13	7.2	93.6	21	567	8°40′	32.8	2.4
7	n	—	15+14+20	32°34′	4.6	7.2	33	16	465	9°25′	31.3	3.5
8	p	—	17+12+17	26°11′	8	7.2	57.6	18.4	250	12°50′	26.8	2.0
9	p	—	6+ 4+17	21°51′	11.5	7.2	82.8	20	250	12°50′	26.8	1.7
10	n	—	8+ 4+15	16°53′	20	7.2	144	23.4	151	16°10′	23.8	~1
11	p	—	3+ 3+15	15°49′	23	7.2	166	24.5	122	18°20′	22.3	0.9
12			8+ 2+14	9°58′	60	7.2	432	30	121	18°20′	22.3	<1
13			10+ 2+13	25°53′	8	7.2	58	18	92	20°40′	20.8	1.5
14	p	—	9+ 3+12	15°49′	23	7.2	166	24.5	68	23°50′	19.3	<1
15	p	1	10+ 2+9	5°37′	192	3	576	16.8	352	7°10′	14.8	~1

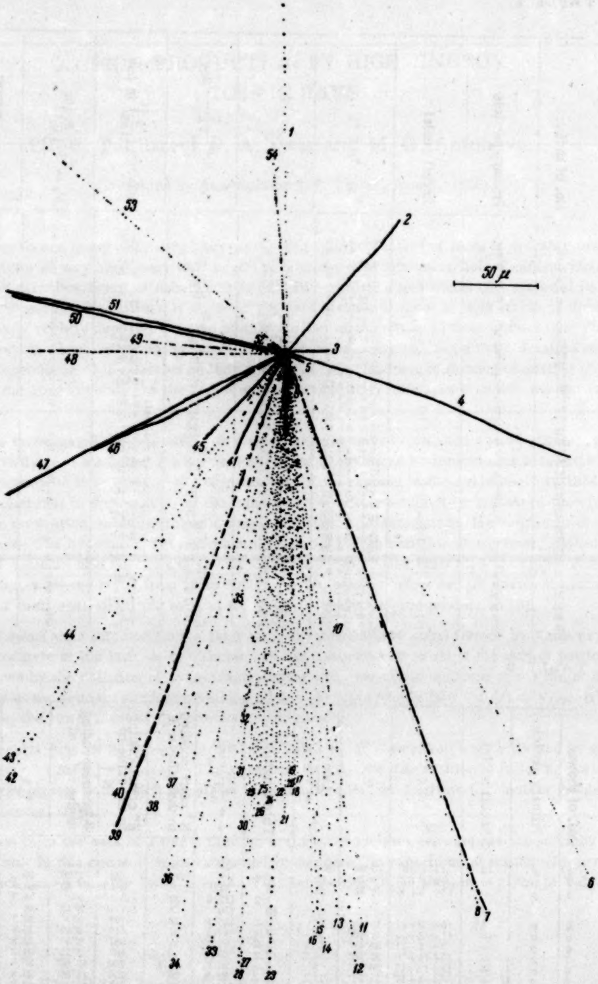

Fig. 1. Particle No. 1 of minimum ionization, assumed to be a proton, produces a star consisting of 36 light, 6 gray and 12 black tracks.

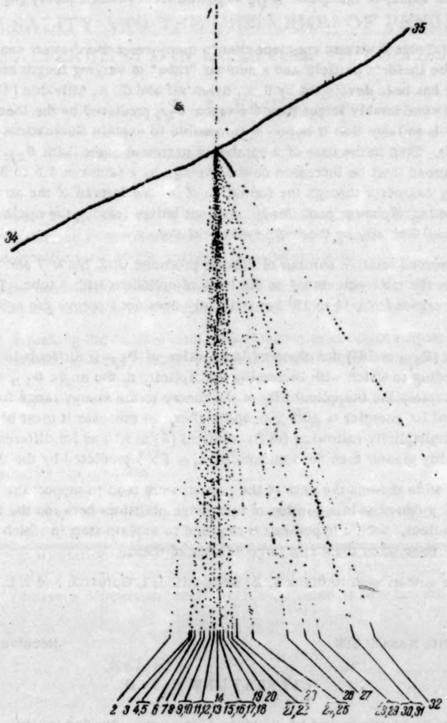

Fig. 2. A star produced by an alpha particle, consisting of 32 light, 1 gray and 3 black tracks.

$$\tan \theta''_{1/2} = \left[\frac{0,84\,(l/d+1)}{N}\right]^2 \left(2\,\frac{l}{d}\right)^{1/2}, \quad \text{when} \quad \frac{l}{d} \leqslant 37;$$

$$N'' = 1.55\left(\frac{l}{d} - 0,25\right)^{3/4}\left(\frac{E}{Mc^2}\right)^{1/4}, \quad E'' = Mc^2\,\frac{N^4}{(1.55)^4\,(l/d - 0,25)^3},$$

$$\tan \theta''_{1/2} = \frac{(1,55)^2\,(l/d - 0.25)^{3/4}}{N^2}\left(2\,\frac{l}{d}\right)^{1/2}, \quad \text{when} \quad \frac{l}{d} > 37.$$

Table 1 gives the values of E_0', n_s' and $\vartheta'_{1/2}$ expected from Fermi's theory [3] assuming nucleon-nucleon collisions.

From the data of Table 2 we can conclude that in many cases the showers can be treated as the result of a collision between the incident particle and a nuclear "tube" of varying length according to Landau's hydrodynamical theory which has been developed by S. Z. Belen'kii and G. A. Milekhin [4]. However the apex angle $\vartheta_{1/2}$ of some showers is considerably larger than the value $\vartheta''_{1/2}$ predicted by the theory for given n_s. For some showers this discrepancy is so large that it becomes impossible to explain fluctuations [5] of n_s (for example, shower No. 3 of Table 2). Even in the case of a number of narrow showers, with $\vartheta_{1/2} < 15°$, for agreement with the theory the angular spread must be increased on the average by a factor of 1.5 to 2 (see, for example, showers 2 and 5). Such widening can occur through the formation of a cone instead of the assumed cylinder of nuclear matter, or through scattering of shower particles by nucleons before leaving the nucleus. "Jets" ($\vartheta_{1/2} < 10°$) are satisfactorily explained formally by the hydrodynamical theory.

However, the observed relative number of showers produced with $l/d < 7$ and $l/d < 3$, respectively, is considerably greater than the ratio calculated on the basis of collisions with a tube. The statistical theory of meson production in the region from 10 to 10^3 Bev evidently does not improve the agreement of experiment and theory.

For wide showers ($\vartheta_{1/2} > 15°$) the observed large value of $\vartheta_{1/2}$ is difficult to explain by the theory of multiple processes according to which with increasing multiplicity n_s the angle $\vartheta_{1/2}$ of a shower should decrease. It would be possible to explain the inapplicability of the theory to the energy range from 10 to 1000 Bev by saying that it is strictly valid for energies of 10^{12} Mev and higher. In this case it must be mentioned that in the range 10-1000 Bev the multiplicity (allowing for fluctuations [5] in n_s' and for different lengths of the nucleonic "tubes" [4]) is considerably greater than the multiplicity $n_s' \sim E^{1/4}$ predicted by the theories of Fermi and Landau.

We note that for wide showers the data of the present work tend to support the presence of a compound-multiple process of pion production in a number of successive collisions between the incident particle and nucleons of the target nucleus. Such a hypothesis is required to explain stars in which light tracks are contained within a very wide cone, even when there is a large number of them.

In conclusion the authors wish to thank S. Z. Belen'kii, I. I. Gurevich and I. L. Rozental' for comments and discussions.

Physico-Technical Institute Kazakh SSR

Received April 20, 1956

LITERATURE CITED

[1] M. F. Kaplon, D. M. Ritson and W. D. Walker, Phys. Rev. 90, 716 (1953).

[2] L. D. Landau, Bull. Acad. Sci. USSR, Phys. Ser. 17, 51 (1953); S. Z. Belen'kii and L. D. Landau, Progr. Phys. Sci. (USSR) 56, 309 (1955).

[3] E. Fermi, Progr. Theor. Phys. 5, 570 (1950).

[4] S. Z. Belen'kii and G. A. Milekhin, J. Exptl.-Theoret. Phys. (USSR) 29, 20 (1955).

[5] M. I. Podgoretskii, I. L. Rozental' and S. D. Chernavskii, J. Exptl.-Theoret. Phys. (USSR) 29, 296 (1955)[Soviet Physics – J.E.T.P., p. 211].

CAUSALITY AND THE CRITERION OF PHYSICAL REALIZABILITY IN QUANTUM FIELD THEORY

L. A. Khalfin

(Presented by Academician V. A. Fok, June 23, 1956)

A number of authors [1-3] have recently discussed the limitations imposed by causality in field theory. The "dispersion" relations derived in these articles are based on very general and almost certain physical hypotheses [7] independently of the specific form of the interactions between fields.

The present article considers one more result of the causality principle. By analogy with a criterion of theoretical electronics [5] this criterion is called the criterion of physical feasibility.

For the purpose of making the fundamental idea clear let us consider a model. Let the forward scattering amplitude (or an associated quantity) f(E) be expressed by the Fourier integral

$$f(E)=\int_{-\infty}^{\infty} F(t)\,e^{iEt}\,dt, \qquad (1)$$

where F(t) satisfies "causality" in the form

$$F(t)=F(t) \text{ for } t>0; \qquad F(t)=0 \text{ for } t\leqslant 0. \qquad (2)$$

It is clear that this limitation on the function F(t) imposes definite limitations on f(E). The principle of "causality" (2) insures analytic functionality of f(E) in the half plane ImE > 0, which enables us on the basis of the Cauchy theorem to derive a "dispersion" relation, i. e., a relation between the real and imaginary parts of f(E):*

$$\operatorname{Re} f(E)=\frac{1}{\pi}\,P\int_{-\infty}^{\infty}\frac{\operatorname{Im} f(E')}{E'-E}\,dE'. \qquad (3)$$

However (3), i. e., analyticity, does not, as we shall see, exhaust all the limitations on f(E) which follow from "causality" principle (2). From (1) we obtain:

$$F_1(t)\equiv F(-t)=\frac{1}{2\pi}\int_{-\infty}^{\infty} f(E)\,e^{iEt}\,dE, \qquad (4)$$

where the newly introduced function $F_1(t)$ satisfies the "causality" principle:

$$F_1(t)=0,\quad t>0; \qquad F_1(t)=F_1(t),\quad t<0. \qquad (5)$$

---

* On the assumption that f(E) diminishes with sufficient rapidity for $|E|\to\infty$.

Let us represent f(E) as the product of the modulus $\psi(E)$ and the phase factor $e^{i\varphi(E)}$; then (4) becomes

$$F_1(t) = \frac{1}{2\pi}\int_{-\infty}^{\infty} \psi(E)\, e^{-i\varphi(E)} e^{iEt}\, dE \tag{6}$$

where $\psi(E)$ is nonnegative by definition.

The question naturally arises: what limitations are imposed by "causality" principle (5) on the permissible functions $\psi(E)$ and $\varphi(E)$? By virtue of the "dispersion" relation (3) there exists a definite connection between $\psi(E)$ and $\varphi(E)$ [5], so that $\psi(E)$ and $\varphi(E)$ cannot be given separately and independently. But this is just the "relation" itself, i. e., for its verification one must know both $\psi(E)$ and $\varphi(E)$. We wish to obtain a criterion which must be satisfied only by $\psi(E)$ possessing a definite physical meaning) in order to satisfy "causality" principle (5) . We thus have the following problem: let an arbitrary nonnegative function $\psi(E)$ be given; is it then possible to select a function $\varphi(E)$ which will satisfy "causality" principle (5)? It appears that $\psi(E)$ cannot be arbitrary. The condition which it must satisfy follows from the fundamental Paley-Wiener theorem [4].

Let $\psi(x)$ be a positive nonzero function defined for $x \in (-\infty, \infty)$ and quadratically integrable in this region. The necessary and sufficient condition for the existence of a real or complex function F(x) defined in the same region, vanishing for $x \geq x_0$ for some x_0 and such that the Fourier transform f(x) of F(x) satisfies the condition $|f(x)| = \psi(x)$ will be

$$\int_{-\infty}^{\infty} \frac{|\ln \psi(x)|}{1+x^2}\, dx < \infty. \tag{7}$$

It is of essential importance in the theorem that the Fourier integral disappear in the semi-infinite interval $[x_0, \infty]$.

The Paley-Wiener theorem for our model can be formulated as follows:

The necessary condition for satisfaction of a "causality" principle of the type [5]

$$F_1(t) = 0 \text{ for } t \geq t_0; \quad F_1(t) = F_1(t) \text{ for } t < t_0$$

is finiteness of the integral

$$\int_{-\infty}^{\infty} \frac{|\ln \psi(E)|}{1+E^2}\, dE < \infty. \tag{8}$$

on the assumption that $\psi(E)$ is quadratically integrable.

This criterion which must be satisfied by $\psi(E)$ will be called the criterion of physical realizability.

Since the theorem does not necessarily require that $t_0 = 0$ the criterion of physical realizability must be satisfied both for micro- and macro- "causality." In addition the "dispersion" relations depend essentially on satisfying micro- or macro- "causality."

The Condition (8) may not be satisfied both because the Integral (8) is improper at the upper (lower) limit and because of singular points of the integrand. In any case $\psi(E)$ cannot be allowed to vanish for any range of E. Since (18) is absolutely convergent if it converges at all, the necessary and sufficient condition for the integrability of (8) is the Cauchy criterion [6]:

a) convergence at the upper (lower) limit is insured by satisfying

$$\frac{|\ln \psi(E)|}{1+E^2} < \frac{A}{E^p}\,, \tag{9}$$

where $A > 0$, $p > 1$, i. e., if $\psi(E)$ decreases for $|E| \to \infty$ not more rapidly than e^{-E^q}, where $q < 1$;

b) convergence at the singular points of the integrand is insured by satisfying

$$\frac{|\ln \psi(E)|}{1+E^2} < \frac{A}{(E-E_0)^p}, \tag{10}$$

where E_0 is a singular point, i. e., $\psi(E_0) = 0$ and $A > 0$, $p < 1$.

Let us consider the polynomial variation of $\psi(E)$. Let $\psi(E)$ satisfy all the conditions of the theorem; then the function

$$\zeta(E) = \psi(E)\,|E|^n, \tag{11}$$

where $\underline{n}$ is a real number, if quadratically integrable also satisfies (8), for

$$\int_{-\infty}^{\infty} \frac{|\ln \zeta(E)|}{1+E^2}\,dE = \int_{-\infty}^{\infty} \frac{|\ln \psi(E)|}{1+E^2}\,dE + \int_{-\infty}^{\infty} \frac{n\,|\ln|E||}{1+E^2}\,dE, \tag{12}$$

where the first integral on the right-hand side converges by hypothesis and the second integral clearly satisfies the Cauchy criterion. We note also that by differentiation of (4) with respect to $\underline{t}$ we can obtain the polynomial variation of f(E) and causality is preserved.

The criterion of physical realizability (8) can be verified directly since the modulus $\psi(E)$ of the forward scattering amplitude is proportional to the differential scattering cross section at zero angle for a given energy E.

The criterion of physical realizability can be utilized for the following purposes.

1) In investigating the behavior of the modulus of the forward scattering amplitude (resulting from any definite interaction scheme) for $E \to \infty$ and at points where $\psi(E) \to 0$ it is possible to select physically permissible forms of interaction.

2) In checking the "dispersion" relations it is generally necessary to know the imaginary part of f(E), i. e., the total scattering cross section, for infinitely large values of E. The Criterion (8) enables us to select the physically permissible behavior of the cross section for $E \to \infty$.

Since (8) was derived from very general assumptions it is not surprising that it allows a very broad class of possible functions for $\psi(E)$. It is important to emphasize once more that the criterion of physical realizability must be satisfied both for micro- and macro- "causality."

In conclusion I wish to thank Academician V. A. Fok and Iu. V. Novozhilov for discussions and valuable comments.

All-Union Scientific Research Institute for
Prospecting Geophysics

Received June 20, 1956

LITERATURE CITED

[1] M. Gell-Mann, M. L. Goldberger and W. E. Thirring, Phys. Rev. 95, 1612 (1954).

[2] M. L. Goldberger, Phys. Rev. 97, 508 (1955); 99, 979 (1955).

[3] M. L. Goldberger, H. Miyazawa and R. Oehme, Phys. Rev. 99, 986 (1955).

[4] R. E. A. C. Paley and N. Wiener, Fourier Transforms in the Complex Domain (Am. Math. Soc., New York, 1934), p. 184.

[5] G. Bode, Circuit Theory and the Design of Feedback Amplifiers (1948).

[6] G. M. Fikhtengol'ts, Course in Differential and Integral Calculus, 2, 3 (1948).

[7] N. N. Bogoliubov, B. V. Medvedev and M. K. Polivanov, Abstracts of the All-Union Conference on High-Energy Particle Physics, Moscow, 1956.

ELECTRICAL CONDUCTIVITY AND PHOTOCONDUCTIVITY OF PHTHALOCYANINES

A. T. Vartanian and I. A. Karpovich

(Presented by Academician A. N. Terenin, June 26, 1956)

The presence of appreciable electrical conductivity in phthalocyanines which increases exponentially with temperature, was first established by one of the authors [1]. Eley [2] obtained a similar result. Electrical conductivity in phthalocyanines was observed by Vartanian in 1947; this was mentioned by A. A. Krasnovskii [3] but we carried through a detailed investigation only recently. The photo-emf of phthalocyanine films was investigated by E. Putseiko using the condenser method [4].

In the present article we give the results of an investigation of electrical conductivity and photoconductivity in nonmetallic phthalocyanine films (Phth) and in the copper (Phth-Cu), zinc (Phth-Zn) and magnesium (Phth-Mg) complexes.

The apparatus which we used was similar to that described in [5]. Films of from 0.1 to a few microns were deposited on a quartz surface by vacuum volatilization of the dye. Platinum electrodes had previously been deposited on the quartz surface separated by a 1 mm gap. Illumination took place from the quartz side. Since the electrical conductivity and photoconductivity of phthalocyanines are very sensitive to oxygen, after deposition the films were not exposed to the air but were investigated in the same vessel. Currents of the order of 10^{13} amp were measured by a dc amplifier.

The conductivity of Phth, Phth-Cu and Phth-Zn films which were vacuum-deposited and again degassed at 200° was of the order 10^{-12}-10^{-13} $\mathrm{ohm}^{-1}\mathrm{cm}^{-1}$ at room temperature and increased with rising temperature according to the law $\sigma = \sigma_0 \exp(-\epsilon/2kT)$, where $\epsilon \approx 1.7$-1.8 ev. We assume that the measured conductivity is intrinsic. One of us [1] had previously obtained for Phth and Phth-Cu the values $\sigma = 10^{-8}$ $\mathrm{ohm}^{-1}\mathrm{cm}^{-1}$ and $\epsilon = 0.87$ and 1.3 ev because of the fact that the method used for preparing and degassing the films did not permit sufficiently complete removal of oxygen from the films. Recently Eley and Parfitt [6] investigated the temperature dependence of the intrinsic conductivity of a Phth powder in a high-frequency field and obtained $\epsilon = 1.5$ ev. Our somewhat higher value (1.73 ev) is probably due to transient resistances.

One cannot prepare a film of Phth-Mg in a vacuum (10^{-4} mm) which is sufficiently free of oxygen since Phth-Mg is extremely sensitive to oxygen. Therefore the conductivity of Phth-Mg exceeded by a factor of almost 1000 the conductivity of the other phthalocyanines and the activation energy was 1.2 ev.

In oxygen at pressures from 0.5 to 450 mm at 150-200° the metallic phthalocyanines show a marked increase of electrical conductivity (10^4 - 10^5 times) and a decrease of ϵ depending on the quantity of sorbed oxygen. At an oxygen pressure of 450 mm we obtained the following values for ϵ: 1.0 ev for Phth-Cu; 0.73 ev for Phth-Zn and 0.53 ev for Phth-Mg, which are in close agreement with earlier results [1]. Thus the introduction of oxygen into films of Phth-Cu, Phth-Zn and Phth-Mg results in impurity conductivity.

Phth in oxygen also shows some (but a relatively small) increase of conductivity. Unlike the case of the other phthalocyanines the activation energy does not decrease but increases by 0.2 ev. It seems to us that the small increase of conductivity of Phth in oxygen is due to traces of the metallic complexes, which cannot be eliminated by vacuum deposition. The increased activation energy, as previously [1], is ascribed to the action of oxygen in the spaces between microcrystals.

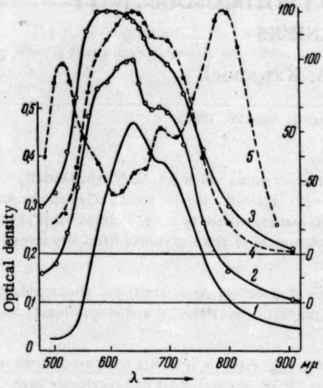

Fig. 1. Nonmetallic phthalocyanine. 1) Absorption curve of deposited film; 2) spectral distribution of photosensitivity (i_{Ph}/L) for a thin film with $n \approx 1$; 3) i_{Ph}/L for the same film as in 2 but with $n = 0.68$; 4) $i_{Ph}^{1/0.68}/L$ for the same film as in 2; 5) $i_{Ph}^{1/n}/L$ for a thick film.

The photoconductivity of carefully degassed phthalocyanine films is very small and practically noninertial. In such films space charge is found to be formed during the passage of both dark and photocurrents.

In oxygen not only the dark current but also the photocurrent is intensified. The latter, depending on the amount of absorbed oxygen, can be increased 10^2-10^3 times. But with increased oxygen content the ratio of the photocurrent to the dark current is reduced. Polarization phenomena are usually absent in such films. An appreciable time lag is observed in the establishing of a stationary photocurrent. For a single film the setting up time of a stationary photocurrent increases with reduction of the intensity of illumination. The photocurrent drops hyperbolically after illumination ceases.

For a photocurrent Ohm's law is satisfied only in fields up to 10^3 v/cm. At high voltages the photocurrent rises faster than by Ohm's law.

At temperatures from 0 to 150° the temperature dependence of the photocurrent (i_{Ph}) follows the law $i_{Ph} = a \exp(-\epsilon_{Ph}/2kT)$. For the investigated phthalocyanines ϵ_{Ph} is between the limits 0.5 to 0.65 ev. For temperatures below 0° there is a departure from the exponential law.

The photocurrent is related to the intensity L of illumination by the relation $i_{Ph} = KL^n$. For oxygen-free films n is close to 1. As the oxygen content increases n approaches 0.5. For a constant oxygen content n is independent of the wave length and remains almost constant as the intensity of illumination changes by a factor of 1000.

Because of the "nonlinearity " of the photocurrent the relative photosensitivity which is ordinarily expressed by the ratio i_{Ph}/L, is a function of the illumination intensity. However, keeping in mind that n is almost independent of the wave length (in the absorption band) and of the illumination intensity (within quite broad limits), we can take as a measure of the relative photoconductivity the expression $i_{Ph}^{1/n}/L$, which is independent of L. The spectral sensitivity curves which are calculated in this way for films whose optical density is below 0.5 (thin films) is in satisfactory agreement with the absorption spectra (Fig. 1).

The correlation which has been established for thin films between the spectral absorption curves and the relative photosensitivity is absent in thick films. Curve 5, which refers to a thick film, shows the reduction of the photocurrent yield in the strong absorption region.

In the longwave region of photosensitivity decrease a linear relation was established between the logarithm of the photosensitivity and the wave length. According to Moss [7] the wave length for which the sensitivity drops to one half of the maximum preceeding the exponential decrease ($\lambda_{1/2}$) can be used to determine the optical activation energy $\epsilon\lambda_{1/2}$ (of the longwave photoconductivity limit). The values of $\lambda_{1/2}$ were determined from the spectral photosensitivity curves for thin films.

For the purpose of determining the optical activation energy we also used the method of "photoelectric straight lines" (ϵ_{Ph}). The illumination source for these measurements was a temperature-limited tube with a

TABLE 1

Dye	$\lambda_{1/2}$ in mμ	Optical activation energy in ev	
		$\epsilon_{\lambda_{1/2}}$	ϵ_{Ph}
Phth	750	1.65	1.61
Phth−Cu	752	1.64	1.63
Phth−Zn	768	1.61	1.58
Phth−Mg	820	1.51	1.53

tungsten ribbon. For films of the same dye with different n the slope of the photoelectric lines $\log(i_{ph}/T^2) = f(1/T)$ varies. When the slope is determined from $\log(i_{ph}^{1/n}/T^2) = f(1/T)$ it is independent of n and is a characteristic constant for a given dye.

From Table 1, which contains the values of the optical activation energy obtained by both methods it follows that they are in good agreement with each other.

The activation energies obtained from the temperature dependence of the electrical conductivity are on the average 0.2 ev higher than those given in Table 1; this is additional confirmation of the presence of transient resistances in the films investigated.

Received June 14, 1956

LITERATURE CITED

[1] A. T. Vartanian, J. Phys. Chem. (USSR) 22, 769 (1948).

[2] D. D. Eley, Nature 162, 819 (1948); D. D. Eley, G. D. Parfitt, M. Y. Perry and D. H. Taysum, Trans. Farad. Soc. 49, 79 (1953).

[3] A. A. Krasnovskii, Bull. Acad. Sci. USSR, Biol. Ser. 3, 377 (1947).

[4] E. Putseiko, Doklady Akad. Nauk SSSR 59, 471 (1948).

[5] A. T. Vartanian, J. Phys. Chem. (USSR) 20, 1065 (1946).

[6] D. D. Eley and G. D. Parfitt, Trans. Farad. Soc. 51, 1529 (1955).

[7] T. S. Moss, Photoconductivity in the Elements (Butterworths, 1952).

LINEAR AND QUADRATIC ZEEMAN EFFECTS AND EXCITON DIAMAGNETISM OF COPPER OXIDE CRYSTALS

E. F. Gross, Corresponding Member of the Academy of Sciences USSR
and B. P. Zakharchenia

Numerous recent investigations [1, 2] have shown that for a number of semiconducting crystals narrow lines are observed at the continuous absorption boundary. Such a discrete spectrum is observed with special clearness when crystals are cooled to the temperature of liquid helium. Several considerations enable us to interpret these spectra as the optical spectra of exciton excitation in a crystalline lattice. This interpretation is also favored by the study of the spectral distribution of photoconductivity in CdS and HgI_2 crystals. In these experiments a number of peaks of the photoconductive effect were observed which agree with optical absorption lines at the fundemental absorption edge of the crystal [3], i. e., the effect was similar to that observed by Apker and Taft [4] in studying the external photoelectric effect in colored alkali halide films. In addition, exciton lines were observed in experiments on luminescence by Grillot et al., [5] and in our laboratory [6]. In some CdS crystals Grillot observed 7 narrow lines in the emission spectrum, of which 6 form a hydrogen-like series, and 3 of which – the shortest wave lengths – coincide with observed absorption lines [7]. In HgI_2 two narrow emission lines were observed [6] which coincide with absorption lines. These lines can reasonably be associated with the annihilation of an exciton accompanied by the emission of light.

Copper oxide crystals are among the most interesting objects for the study of exciton absorption. In thin sheets of Cu_2O at the temperature of liquid nitrogen two series of absorption lines have been observed: one in the yellow portion of the spectrum (the yellow series) and the other in the green portion (the green series). The line frequencies of these series satisfy well the series formulas of the hydrogen atom:

Yellow series $$\nu_n = \nu_\infty^y - \frac{R_{ex}^y}{n^2} = 17460 - \frac{785}{n^2}\ (\mathrm{cm}^{-1}),\ n = 1, 2, 3, \ldots$$

Green series $$\nu_n = \nu_\infty^g - \frac{R_{ex}^g}{n^2} = 18507 - \frac{1246}{n^2}\ (\mathrm{cm}^{-1}),\ n = 2, 3, \ldots$$

where ν_∞ is the limiting frequency limit of the series which corresponds to an electron transition into the free zone and R_{ex} is a constant which is analogous to the Rydberg constant. The first line of the yellow series (n = 1) departs strongly from the hydrogen-like formula.

When a crystal was cooled to 1.3°K in which case the lines were narrowed, 10 members of the yellow series were observed [7]. The higher members of the series satisfy the hydrogen-like formula with great accuracy.

The fact that the optical spectrum of an exciton is well represented by a hydrogen-like series of absorption lines is evidence that in a copper oxide crystal an exciton can be approximately represented, at least in high excited states, by Mott's model, i. e., an exciton can be regarded as a system consisting of an electron and a hole and interacting according to Coulomb's law in a medium with the dielectric constant ϵ_0 while in motion around a common center of gravity. On this model the constant R_{ex} for an exciton

$$R_{ex} = \frac{R\,(\mu/m)}{n_0^4}, \tag{1}$$

where R is Rydberg's constant; n_0 is the refractive index, which for Cu_2O is 2.5; m is the electron mass in a vacuum; μ is the effective reduced exciton mass defined by the relation $\frac{1}{\mu} = \frac{1}{\mu_1} + \frac{1}{\mu_2}$; μ_1 and μ_2 are the effective electron and hole masses, respectively.

The Coulomb interaction of the electron and hole in a medium of dielectric constant $\epsilon_0 = n_0^2$ results in increasing the radius of the exciton orbit by the factor ϵ_0 compared with the orbit of an isolated atom, so that

$$r_{ex} = \varepsilon_0 \frac{\hbar^2}{\mu e^2} n^2; \qquad (2)$$

here μ is the effective reduced exciton mass, which is 0.28 m for the yellow series. From (2) it follows that the radii of the exciton orbits for large quantum numbers attain values of a few hundred angstroms.

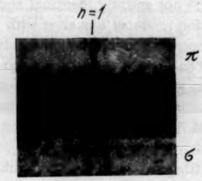

Fig. 1. Zeeman triplet of the first member of the yellow series of an exciton (π and σ components).

Due to the large size of an exciton it was possible to observe the Stark effect in exciton absorption lines in a relatively weak field applied to the crystal [8].

For the high members of the series the effect is observed in a field as low as E = 5 kv/cm. The large size of the exciton orbits permitted detection of exciton ionization by an electric field. Beginning with a field E = 6 kv/cm the gradual disappearance of the higher members of the series is observed, which are approached by the fundamental absorption edge. As the field is increased the absorption edge encloses a larger and larger number of series members, so that when E = 25-30 kv/cm only two members of the yellow series remain: n = 1 and n = 2. Such extraction of an electron by a field is known to be observed in atoms also but, as follows from the experiment of Rausch von Traubenberg [9], this occurs in very large fields of the order E = 1000 kv/cm.

When we investigated the effect of a magnetic field on the exciton spectrum we observed a phenomenon which is observable because of the large exciton orbits. The results of this investigation will be presented briefly in the present communication.

The effect of a magnetic field on an exciton spectrum* was investigated with 100μ layers of Cu_2O at 1.3°K. A spectrograph with a dispersion of 1.5 A/mm was used. Our magnet enabled us to excite a field of 30,000 oersteds in a 38 mm gap.** Under these experimental conditions we were able to establish [11, 12] that the first yellow exciton series member in a magnetic field is split into a triplet. The experiments in polarized light showed that this triplet consists as usual of an undisplaced line in the π component and a doublet in the σ component. In magnetic fields of H = 27,000 oersteds the separation of the doublet components is $\Delta\lambda = 1.0$ A (see Fig. 1).

The considerable narrowing of the lines at 1.3°K and the high-dispersion spectrograph permitted observation of Zeeman splitting not only for the narrow first line of the series (n = 1) but also of other members of the series.

We were able to establish the effect of a magnetic field on members of the yellow series with n = 3, 4, 5 and 6 [12]. The splitting of the member with n = 2 could not be established because of its great width. In the magnetic field the lines with n = 3, 4, and 5 were split into doublets. The polarization investigations showed that these doublets are observed in both the π and the σ components and that the members of the doublets coincide in both components, i. e., the patterns of splitting in the π and σ components are identical.

---

*A theoretical investigation of the Zeeman effect of an exciton was carried through by A. G. Samoilovich and L. A. Korenblit [10].

**The authors are indebted to the director of the Cryogenic Laboratory of the Physico-Technical Institute, N. M. Reinov, with whom they began these experiments and who assisted greatly in conducting them.

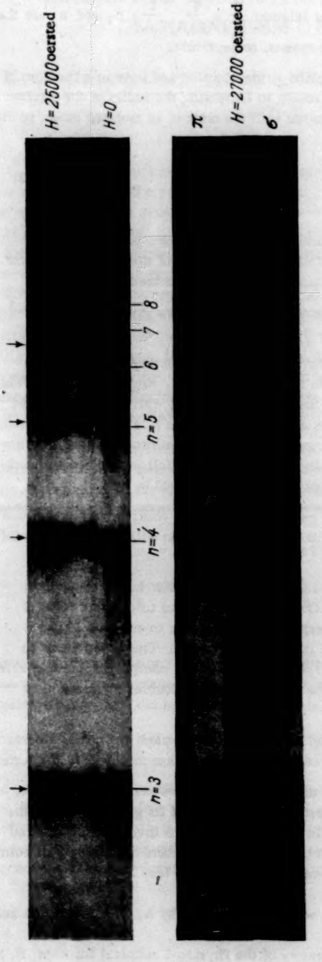

Fig. 2. Linear and quadratic Zeeman effects of the yellow series of an exciton; a) in unpolarized light; b) in polarized light.

It is not impossible, however, that the separations between the constituents of the doublets of the π and σ components are not entirely identical and that the Zeeman splitting produces a quartet with very close π and σ components which are not resolved in our spectrograms. The separation Δλ between the doublet components within the limits of experimental error remains constant for all three members of the series and is 0.84 A in a magnetic field H = = 28000 oersted. In fairly strong fields for n = 6 more complicated splitting is observed. The doublet is here complicated by the appearance of two weaker components, one on the short-wave and the other on the long-wave side of the doublet. The splitting pattern for the line with n = 6 is identical in the π and σ components. The separation between the doublet constituents is the same as for the other members of the series, which is 0.84 A at H = 28000 oersted. The new long-wave component is 0.8 A from the nearer doublet constituent; the short-wave component is separated by 0.7 A.

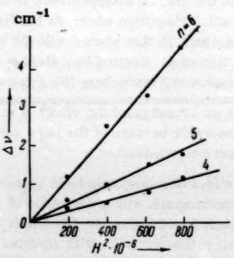

Fig. 3. Diamagnetic shift of the "center of gravity" of the Zeeman components of members of the yellow exciton series as a function of the magnetic field H.

In addition to the ordinary Zeeman splitting we observed another interesting phenomenon [12]. Members of a series which are split in a magnetic field are shifted in the short-wave direction with respect to their original position in the absence of a magnetic field. This shift is the greater, the higher the quantum number n of the corresponding series member, and is clearly noticeable in the spectrogram of Fig. 2. The magnitude of the shift for the n = 5 line is of the order 0.6 A at H = 28000 oersted.

Measurements of the shift of the "centers of gravity" of the Zeeman components (doublets) in fields of different magnitude showed that the shift increases as H^2, i. e., it is proportional to the square of the field (see Fig. 3). This indicates that besides the usual Zeeman effect the spectrum of an exciton exhibits the so-called quadratic Zeeman effect which is known to be associated with diamagnetism. It follows from the theory of the diamagnetic quadratic Zeeman effect [13] that the diamagnetic shift is proportional to the square of the radius of the electronic orbit and thus to the fourth power of the quantum number (n^4). Indeed, the change of magnetic energy resulting from the diamagnetism of the atom is

$$\Delta W = \frac{e^2}{8mc^2} r^2 H^2. \tag{3}$$

If the shift which we observed is actually due to exciton diamagnetism we should observe dependence of the shift on n^4. Fig. 4 shows that the shift of the Zeeman components in the exciton spectrum is indeed proportional to n^4 for the given field.

It follows from the above that the diamagnetic shift in the Zeeman effect of an exciton is very large since it is observed in a series member with the quantum number $n = 3$, whereas in atomic spectra this shift, as shown by the experiments of Jenkins and Segre and of Harting and Klinkenberg [14], is observed only for very high series members. An appreciable shift for sodium was observed at about $n = 20$. This shows that exciton diamagnetism is very large because of its large orbits.

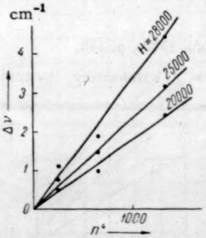

Fig. 4. Diamagnetic shift of the "centers of gravity" of Zeeman components for members of the yellow exciton series as a function of the fourth power of the quantum number n.

The diamagnetic shift in the exciton spectrum makes it possible to determine the exciton radius. It follows from our experiments that the diamagnetic shift of the center of gravity of the Zeeman components for the $n = 5$ member of the yellow exciton series is $1.8\ \mathrm{cm}^{-1}$ when $H = 28000$ oersted. Substituting these numerical values in Formula (3) we found that the exciton radius for $n = 5$ is $r_{ex} = 200$ A. The radius for the same excited exciton state as calculated from (2) on Mott's model was $r_{ex} = 280$ A, which is in good agreement with the value of r_{ex} calculated from the diamagnetic shift, if the approximate character of the calculations is taken into account.

Thus the phenomena described in this article show that in a solid there does exist a quasi-particle (the exciton) which possesses the properties of an atomic system. The similarity of its properties is such that in an exciton spectrum one can observe all the characteristic phenomena of atomic spectra, including such phenomena as the ionization of an exciton by an electric field and the diamagnetic shift of exciton lines. Our experiments show that these phenomena are easily observed in a solid since exciton orbits are much larger than orbits of isolated atoms.

We are grateful to Professor P. P. Pavinskii for friendly discussions of certain theoretical questions in connection with our experimental results.

Physico-Technical Institute, Academy of Sciences USSR

Received July 4, 1956

LITERATURE CITED

[1] E. F. Gross and N. A. Karryev, Doklady Akad. Nauk SSSR 84, 261, 471 (1952); E. F. Gross and B. P. Zakharchenia, Doklady Akad. Nauk SSSR 90, 745 (1953); E. F. Gross, B. P. Zakharchenia and N. M. Reinov, Doklady Akad. Nauk SSSR 92, 265 (1953); 99, 231 (1954); E. F. Gross and M. A. Iakobson, Doklady Akad. Nauk SSSR 102, 485 (1955); E. F. Gross and A. A. Kaplianskii, J. Tech. Phys. (USSR) 25, 1661, 2061 (1955).

[2] M. Hayachi and K. Katsuki, J. Phys. Soc. Japan 7, 599 (1952); S. Nikitine, G. Perny and M. Sieskind, Comptes. rend. 238, 67 (1954); S. Nikitine, L. Couture, M. Sieskind and G. Perny, Comptes. rend. 238, 1786 (1954); S. Nikitine and G. Perny, Comptes. rend. 240, 64 (1955); S. Nikitine, L. Couture, G. Perny and R. Reiss, Comptes. rend. 241, 629 (1955); S. Nikitine, Helv. Phys. Acta 28, 307 (1955); S. Nikitine and R. Reiss, Comptes rend. 242, 1003 (1956); S. Nikitine, R. Reiss and G. Perny, Comptes rend. 242, 1588 (1956).

[3] E. F. Gross, A. A. Kaplianskii and B. V. Novikov, J. Tech. Phys. (USSR) 26, 697 (1956); 26, 913 (1956) [Soviet Physics Technical Physics, p. 900].

[4] L. Apker and E. Taft, Phys. Rev. 79, 964 (1950); 81, 698 (1951); 82, 814 (1951).

[5] E. Grillot, M. Grillot, P. Pesteil and A. Zmerli, Comptes rend. 242, 1794 (1956).

[6] E. F. Gross, A. A. Kaplianskii and B. V. Novikov, J. Tech. Phys. (USSR) 26, 697 (1956); [Soviet Physics Technical Physics, p 674]; E. F. Gross and M. A. Iakobson, J. Tech. Phys. (USSR) 26* (1956).

[7] E. F. Gross, B. P. Zakharchenia and N. M. Reinov, Doklady Akad. Nauk SSSR 99, 231 (1954).

[8] E. F. Gross, B. P. Zakharchenia and N. M. Reinov, Doklady Akad. Nauk SSSR 97, 57, 221 (1954).

[9] H. Rausch v. Traubenberg, Z. Physik 62, 289 (1930); 71, 291 (1931).

[10] A. G. Samoilovich and L. A. Korenblit, Doklady Akad. Nauk SSSR 100, 43 (1955).

[11] E. F. Gross, B. P. Zakharchenia and N. M. Reinov, Doklady Akad. Nauk SSSR 99, 527 (1954); J. Tech. Phys. (USSR) 26, 700 (1956) [Soviet Physics – Technical Physics,

[12] E. F. Gross, B. P. Zakharchenia and N. M. Reinov, J. Tech. Phys. (USSR) 26, 700 (1956) [Soviet Physics – Technical Physics, p. 677].

[13] J. H. van Vleck, Theory of Electric and Magnetic Susceptibilities (Oxford, 1932), p. 178.

[14] F. A. Jenkins and E. Segre, Phys. Rev. 55, 52 (1939); D. Harting, and P. F. A. Klinkenberg, Physica 24, 669 (1949).

---

*[Number and page missing in original – editor's note].

THE λ POINT OF SOLUTIONS OF HELIUM ISOTOPES

B. N. Esel'son, N. G. Berezniak and M. I. Kaganov

(Presented by Academician L. D. Landau, May 28, 1956)

The lowering of the temperature T_λ of the HeI-HeII phase transition with increasing concentration of He^3 was observed a few years ago [1-3]. Various methods of recording T_λ were used to cover a wide range of concentrations x_1, thus making it possible to draw the curve $T_\lambda = T_\lambda(x_1)$.

In connection with the obtaining of data required for construction of the liquid-vapor phase diagram of the He^3-He^4 system [4, 5] there appeared another possible way of determining $T_\lambda(x_1)$. We refer to the bend in the vapor pressure versus temperature curve which should be observed at the λ point of a solution.

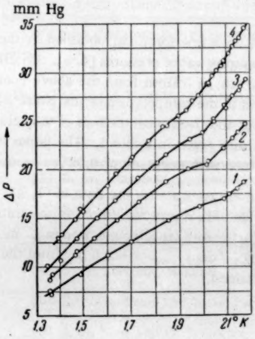

Fig. 1. ΔP as a function of temperature 1) 8.3% He^3; 2) 11.1% He^3; 3) 13.4% He^3; 4) 16.7% He^3.

Indeed, whereas in the curve for the temperature dependence of the vapor pressure for pure He^4 the λ point is characterized by a bending of the derivative dP_4^0/dT, on the curves for the partial pressures and total pressure of solutions of helium isotopes at the λ point the derivatives dP_3/dT, dP_4/dT and dP/dT undergo jumps. This follows from the general thermodynamical considerations discussed in [2] and later in [6].

If φ denotes the thermodynamical potential for a single particle of the solution, then by equating the chemical potentials for He^3 and He^4 in the two phases we easily obtain:

$$kT_\lambda \Delta \frac{\partial \ln P_3}{\partial T} = (1 - x_1)\, \Delta \frac{\partial^2 \varphi}{\partial T\, \partial x_1}, \qquad kT_\lambda \Delta \frac{\partial \ln P_4}{\partial T} = -x_1 \Delta \frac{\partial^2 \varphi}{\partial T\, \partial x_1}{}^{*}. \tag{1}$$

Multiplying the first Equation (1) by P_3 and the second by P_4 and adding we obtain

$$kT_\lambda \Delta \frac{\partial \ln P}{\partial T} = (x_n - x_1)\, \Delta \frac{\partial^2 \varphi}{\partial T\, \partial x_1}, \tag{2}$$

where x_n is the concentration in the gas phase.

---

[*] The jump of the second derivative $\partial^2 \varphi / \partial T \partial x_1$ can be associated with the jump of the specific heat Δc_p [2]:

$$\Delta \frac{\partial^2 \varphi}{\partial T\, \partial x_1} = \frac{|\Delta c_p|}{T_\lambda} \frac{\partial T_\lambda}{\partial x_1}.$$

It is also possible to exclude the jump of the derivative of the pressure from Equation (1). Then for the jump of the derivative of the concentration in the gas phase we have (for $x_n << 1$ see [2]):

$$kT_\lambda \Delta \frac{\partial x_n}{\partial T} = x_n (1 - x_n) \Delta \frac{\partial^2 \varphi}{\partial T \, \partial x_1}. \tag{3}$$

From Equation (2) it is seen that for the pure material, as was shown above $\Delta \frac{\partial \ln P}{\partial T} = 0.$

Thus the experimental observation of the break in the curve for the temperature dependence of the vapor pressure of isotope solutions permits the determination of $T_\lambda(x_1)$.

Usually the recording of such a bend in the P(T) curve is difficult but it is considerably easier when we investigate the temperature dependence of the difference in vapor pressures ΔP between that of the solution P and of pure He^4(P_4^0). In the case of the P-T curve because of the large value of dP/dT a relatively small jump of this value at the λ point will be unnoticeable. On the ΔP-T curve the value of $d/dT(\Delta P)$ is considerably reduced while the jump at the λ point remains the same.

Fig. 1 shows ΔP-T for a few solutions, obtained by the differential method of measuring vapor pressures [4, 5]. On all curves a bend appears which, as follows from the above considerations, must correspond to the temperature of the phase transition. These temperatures and the concentrations of the solutions to which they refer are given in Table 1. The bends in the curves were determined with accuracy of 0.02°.

A comparison of these results with the data of [1, 3] shows that there is considerable discrepancy both in the initial slope of the curve $T_\lambda(x_1)$ and in its subsequent course. In particular, instead of $(dT_\lambda / dx_1)_{x_1 = 0} = -2.8$ deg/mol the value -1.5°/mol is obtained.

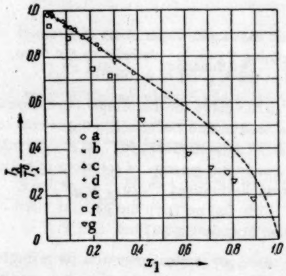

Fig. 2. T_λ / T_λ^0 as a function of the He^3 concentration $x_1 = N_3/(N_3 + N_4)$. a) Ref. [2]; b) Ref. [10]; c) Ref. [14]; d) Ref. [11]; e) the present work; f) Ref. [1]; g) Ref. [3]; the curve was calculated from a formula of Ref. [12].

TABLE 1

X_1 %	8.3	11.1	13.4	16.7	19.2	22.6	23.9	30.2	38.3
T_λ, °K	2.08	2.02	2.00	1.93	1.91	1.86	1.82	1.71	1.59

It is important to emphasize that our data are in good agreement with the values of T_λ which have been obtained recently in the study of various properties of He^3 solutions in He^4 for small concentrations [9-11]. This is illustrated by Table 2 and Fig. 2, which give the dependence of T_λ / T_λ^0 (T_λ^0 is the λ temperature of pure He^4) on concentration, obtained experimentally and calculated from a formula of Ref. [12].

We note also that the magnitude of $(dT_\lambda \; dx_1)_{x_1 = 0}$ can be obtained by using data on the density of the normal component of solutions of helium isotopes. The density of the normal component of a solution can be written as follows:

$$\rho_n (T, x_1) = \rho_n (T, 0) + x_1 \rho_4 \frac{m(T)}{m_4}, \tag{4}$$

TABLE 2

x_1, %	T_λ, °K	$\left(\frac{dT}{dx_1}\right)_{x_1=0}$ in deg/mol	Ref
<4		− 1.5	[9]
2.5	2.149	− 1.48	[10]
3.65	2.127	− 1.47	[11]
6.0	2.096		
9.2	2.045		

where m(T) is a function of temperature with the dimension of mass, which, according to [13] at a distance from T_λ coincides with the effective mass of He atoms in the solution.

Writing Equation (4) for $T = T_\lambda$:

$$\rho_n(T_\lambda, 0) + x_1 \rho_4 \frac{m(T_\lambda)}{m_4} = \rho(1\ \ )$$

and expanding $\rho_n(T_\lambda, 0)$ and $\rho(x_1)$ in powers of the concentration we obtain the quantity of interest:

$$\left(\frac{dT_\lambda}{dx_1}\right)_{x_1=0} = \frac{\partial\rho/\partial x_1 - \rho_4 m(T_\lambda)/m_4}{(\partial\rho_n(T,0)/\partial T)_{T_\lambda^0}}. \qquad (5)$$

Using the data on the temperature dependence of the normal component of a solution with the concentration 3.0 % He^3 [14] it is possible to obtain $m(T_\lambda)$ and thus also $(dT_\lambda/dx_1)_{x_1=0}$. The value of $(dT_\lambda/dx_1)_{x_1=0}$ calculated in this manner is in sufficiently good agreement with the value given above (− 1.5°/mole).

We take this opportunity to thank Professor B. G. Lazarev and Professor I. M. Lifshits for discussions of the results.

Physico-Technical Institute, Academy of Sciences USSR Received May 25, 1952

LITERATURE CITED

[1] B. M. Abraham, B. Weinstock and D. W. Osborne, Phys. Rev. 76, 864 (1949).

[2] B. N. Esel'son, B. G. Lazarev and I. M. Lifshits, J. Exptl.-Theoret. Phys.(USSR) 20, 748 (1950).

[3] J. G. Daunt and C. V. Heer, Phys. Rev. 79, 46 (1950).

[4] B. N. Esel'son, J. Exptl.-Theoret. Phys. (USSR) 26, 745 (1954).

[5] B. N. Esel'son and N. G. Beresniak, Doklady Akad. Nauk SSSR 105, 454 (1954).

[6] J. de Boer and C. J. Gorter, Physica 18, 565 (1952).

[7] H. A. Fairbank, C. A. Reynolds et al., Phys. Rev. 74, 345 (1948).

[8] J. G. Daunt and C. V. Heer, Phys. Rev. 86, 205 (1952).

[9] J. C. King and H. A. Fairbank, Phys. Rev. 91, 489 (1953).

[10] Z. Dokoupil, G. van Soest et al., Physica 20, 1181 (1954).

[11] J. G. Dash and R. D. Taylor, Phys. Rev. 99, 598 (1955).

[12] Z. Mikura, Progr. Theor. Phys. 11, 25 (1954); 14, 337 (1955).

[13] I. Pomeranchuk, J. Exptl.-Theoret. Phys. (USSR) 19, 42 (1949).

[14] N. G. Berezniak and B. N. Esel'son, Doklady Akad. Nauk SSSR 111, 2, 322 (1956) [Soviet Physics – Doklady, p. 645].

ON THE DISPERSION RELATION FOR NUCLEON-NUCLEON SCATTERING

F. M. Kuni

(Presented by Academician V. A. Fok, July 9, 1956)

A number of recent articles on quantum field theory have been concerned with the dispersion relations previously obtained for meson-nucleon scattering [1-3]. It is of interest to extend the dispersion relations to nucleon-nucleon scattering. The principal difficulties arise in connection with the calculation of the imaginary part of the forward nucleon-nucleon scattering amplitude $A_{nn}(\omega)$ in the "unphysical" region $-m < \omega < m$, where ω is the energy of the incident nucleon and m is the nucleonic mass. The imaginary part of the forward scattering amplitude $A_{na}(\omega)$ for the antinucleon-nucleon case is expressed by $A_{nn}(-\omega)$.

Using the approximate method given in [5] it was not possible to obtain an expression for $A_{nn}(\omega)$ in finite form in the region $-m < \omega < m$. The present article makes an attempt to determine $A_{nn}(\omega)$ in the range $-m < \omega < m$ for the case in which the spins of the scattering and scattered nucleons are antiparallel. The calculations were made for the charge-symmetrical theory with pseudoscalar coupling.

1. Let us consider the matrix element of the operator T which is associated with the scattering matrix S by the relation $T = i(1 - S)$ for nucleon-nucleon scattering:

$$(a_\nu^+(\mathbf{k}')\,a_\mu^+(\mathbf{q}')\,\Omega_0,\ T a_\nu^+(\mathbf{k})\,a_\mu^+(\mathbf{q})\,\Omega_0) = -i\left(\Omega_0, a_\nu(\mathbf{k}')\,a_\mu(\mathbf{q}')\left\{1-\sum_{n=0}^{\infty}\frac{(-i)^n}{n!}\int\limits_{-\infty}^{+\infty}dt_1\ldots \int\limits_{-\infty}^{+\infty}dt_n\,P\,[H_{\rm I}(t_1)\ldots H_{\rm I}(t_n)]\right\}a_\nu^+(\mathbf{k})\,a_\mu^+(\mathbf{q})\,\Omega_0\right). \tag{1}$$

Here we have used the notation: $\mathbf{k}$, ν and $\mathbf{q}$, μ are the momenta and quantum numbers (nucleon spin and charge), respectively, for the incident and scattering nucleon (we use the laboratory system of coordinates and assume $\mathbf{q} = 0$); $\mathbf{k}'$, ν and $\mathbf{q}'$, μ are the momenta and quantum numbers of the nucleons after the collision; P denotes the time ordering of the operators; $a_\nu^+(\mathbf{k})$ and $a_\mu(\mathbf{q}')$ are, respectively, the creation and annihilation operators for nucleons with momenta $\mathbf{k}$, $\mathbf{q}'$ and quantum numbers ν, μ; Ω_0 is the vacuum functional of the noninteracting meson and nucleon fields. In a charge-symmetrical theory with pseudoscalar coupling we have for the interaction Hamiltonian of the nucleon and meson fields $H_I(t)$

$$H_{\rm I}(t) \equiv \int\limits_{x_0=t}\mathfrak{H}_{\rm I}(x)\,d^3x = ig\int\limits_{x_0=t}N\,[\bar{\psi}(x)\,\gamma_5\,\tau_\alpha\,\Phi_\alpha(x)\,\psi(x)]\,d^3x - \delta m\int\limits_{x_0=t}N\,[\bar{\psi}(x)\,\psi(x)]\,d^3x - \frac{1}{2}\,\delta\mu^2\int\limits_{x_0=t}N\,[\Phi_\alpha(x)\,\Phi_\alpha(x)]\,d^3x + \frac{1}{4}\,\lambda\int\limits_{x_0=t}N\,\{[\Phi_\alpha(x)\,\Phi_\alpha(x)]^2\}\,d^3x, \tag{2}$$

where $\psi(x)$ and $\overline{\psi}(x)$ are the operators of the nucleon field; $\Phi_\alpha(x)$ is the meson field operator ; N denotes the normal product of the operators.

With the aid of the commutation relations,

$$\begin{gathered}[a_\nu(\mathbf{k}')\,a_\mu(\mathbf{q}'),\ \mathfrak{H}_I(x)]_- = S^{\mathbf{k}'\nu}_{\mathbf{q}'\mu}(x);\\ [\mathfrak{H}_I(y),\ a^+_\nu(\mathbf{k})\,a^+_\mu(\mathbf{q})]_- = -S^{+\mathbf{k}\nu}_{\mathbf{q}\mu}(y);\\ [a_\nu(\mathbf{k}')\,a_\mu(\mathbf{q}'),\ [\mathfrak{H}_I(y),\ a^+_\nu(\mathbf{k})\,a^+_\mu(\mathbf{q})]_-]_- = \Gamma^{\mathbf{k}'\nu;\ \mathbf{k}\nu}_{\mathbf{q}'\mu;\ \mathbf{q}\mu}(y);\\ S^{\mathbf{k}'\nu}_{\mathbf{q}'\mu}(x) = \frac{ig}{(2\pi)^{3/2}}\{e^{-ik'x}\,\overline{u}^\nu(\mathbf{k}')\,\gamma_5\,\tau_\alpha\,\Phi_\alpha(x)\,\psi(x)\,a_\mu(\mathbf{q}') -\\ -e^{-iq'x}\,\overline{u}^\mu(\mathbf{q}')\,\gamma_5\,\tau_\alpha\,\Phi_\alpha(x)\,\psi(x)\,a_\nu(\mathbf{k}')\} -\\ -\frac{\delta m}{(2\pi)^{3/2}}\{e^{-ik'x}\,\overline{u}^\nu(\mathbf{k}')\,\psi(x)\,a_\mu(\mathbf{q}') - e^{-iq'x}\,\overline{u}^\mu(\mathbf{q}')\,\psi(x)\,a_\nu(\mathbf{k}')\},\end{gathered} \tag{3}$$

where $S^{+\mathbf{k}\nu}_{\mathbf{q}\mu}(y)$ is the Hermitian conjugate of the operator $S^{\mathbf{k}\nu}_{\mathbf{q}'\mu}(y)$ it is easy to write the matrix element (1) as an average over the vacuum of the interacting fields of the P operator product in the Heisenberg representation:

$$i\int d^4x\,d^4y\,\langle\Omega^\Gamma_0\,|\,P\,[\mathbf{S}^{\mathbf{k}'\nu}_{\mathbf{q}'\mu}(x),\ \mathbf{S}^{+\mathbf{k}\nu}_{\mathbf{q}\mu}(y)]\,|\,\Omega^\Gamma_0\rangle - \int d^4x\,\langle\Omega^\Gamma_0|\,\mathbf{\Gamma}^{\mathbf{k}'\nu;\ \mathbf{k}\nu}_{\mathbf{q}'\mu;\ \mathbf{q}\mu}(x)\,|\,\Omega^\Gamma_0\rangle, \tag{4}$$

where

$$\begin{gathered}\mathbf{S}^{\mathbf{k}'\nu}_{\mathbf{q}'\mu}(x) = U^{-1}(x_0,0)\,S^{\mathbf{k}'\nu}_{\mathbf{q}'\mu}(x)\,U(x_0,0);\qquad \mathbf{S}^{+\mathbf{k}\nu}_{\mathbf{q}\mu}(y) = U^{-1}(y_0,0)\,S^{+\mathbf{k}\nu}_{q\mu}(y)\,U(y_0,0);\\ \mathbf{\Gamma}^{\mathbf{k}'\nu;\ \mathbf{k}\nu}_{\mathbf{q}'\mu;\ \mathbf{q}\mu}(x) = U^{-1}(x_0,0)\,\Gamma^{\mathbf{k}'\nu;\ \mathbf{k}\nu}_{\mathbf{q}'\mu;\ \mathbf{q}\mu}(x)\,U(x_0,0);\qquad \Omega^\Gamma_0 = U^{-1}(\pm\infty,0)\,\Omega_0.\end{gathered} \tag{5}$$

The unitary operator U(t, 0) satisfies the equation

$$i\,\frac{\partial U(t,0)}{\partial t} = H_I(t)\,U(t,0),\qquad U(0,0) = 1. \tag{6}$$

At t = 0 the Heisenberg representations and the interactions coincide.

2. Let us introduce the operator P_λ of the 4-dimensional energy-momentum operator of the interacting nucleon and meson fields. An important part will be played hereafter by the relations

$$\begin{gathered}\mathbf{S}^{\mathbf{k}'\nu}_{\mathbf{q}'\mu}(x) = e^{-iPz}\,\mathbf{S}^{\mathbf{k}'\nu}_{\mathbf{q}'\mu}(x-z)\,e^{iPz}\,e^{-i(k'+q')z};\\ \mathbf{S}^{+\mathbf{k}\nu}_{\mathbf{q}\mu}(y) = e^{-iPz}\,\mathbf{S}^{+\mathbf{k}\nu}_{\mathbf{q}\mu}(y-z)\,e^{iFz}\,e^{i(h'+q)z};\\ \mathbf{\Gamma}^{\mathbf{k}'\nu;\ \mathbf{k}\nu}_{\mathbf{q}'\mu;\ \mathbf{q}\mu}(x) = e^{-iPz}\,\mathbf{\Gamma}^{\mathbf{k}'\nu;\ \mathbf{k}\nu}_{\mathbf{q}'\mu;\ \mathbf{q}\mu}(x-z)\,e^{iPz}\,e^{i(k+q-k'-q')z},\end{gathered} \tag{7}$$

which can be derived on the basis of the definitions (5) and (3) of the operators $\mathbf{S}^{\mathbf{k}'\nu}_{\mathbf{q}'\mu}(x)$, $\mathbf{S}^{+\mathbf{k}\nu}_{\mathbf{q}\mu}(y)$ and the explicit expression for the operator $\mathbf{\Gamma}^{\mathbf{k}'\nu;\mathbf{k}\nu}_{\mathbf{q}'\mu;\ \mathbf{q}\mu}(x)$.

With the aid of (7) it is easy to separate out the function $(2\pi)^4\,\delta(k'+q'-k-q)$ in the matrix element (4) which expresses conservation of the 4-dimensional momentum. If then in the coefficient of $(2\pi)^4$ ×

$\times\ \delta(k' + q' - k - q)$ in the matrix element of (4) we pass to the limit $\mathbf{k}' \to \mathbf{k}$ but $\mathbf{k}' \neq \mathbf{k}$ and $\mathbf{q}' \to \mathbf{q}$ but $\mathbf{q}' \neq \mathbf{q}$ subject to the condition that $k' + q' = k + q$, we obtain an expression for the forward nucleon-nucleon scattering amplitude $F_{nn}(k)$ which for antiparallel spins of the incident and scattered particles is given by

$$F_{\mathbf{nn}}(k) = i \int d^4x \, \langle \Omega_0^{\Gamma} \,|\, P\,[\mathbf{S}_{\mathbf{q}\mu}^{\mathbf{k}\nu}(x),\ \mathbf{S}_{\mathbf{q}\mu}^{+\mathbf{k}\nu}(0)] \,|\, \Omega_0 \rangle. \tag{8}$$

3. Equation (8) actually defines the functional dependence of the forward scattering amplitude on only one variable, the energy $k_0 = \omega$ of the incident particle: $F_{nn} = F_{nn}(\omega)$, as dependence on the spatial components of the 4-vector k_λ results from $\mathbf{k}^2 = \omega^2 - m^2$, where $\underline{m}$ is the mass of the nucleon. $F_{nn}(\omega)$ cannot be continued analytically into the region above the real axis in the plane of the complex variable ω, since $F_{nn}(\omega)$ has poles above the real axis to the left of the straight line $\mathrm{Re}\,\omega = m$. Therefore in deriving the dispersion relations instead of $F_{nn}(\omega)$ the function $M_{nn}(\omega)$ is introduced [1], in which such poles to the left of $\mathrm{Re}\,\omega = m$ are moved to the lower half plane so that they are the mirror images of the poles of $F_{nn}(\omega)$ with respect to the real axis. $M_{nn}(\omega)$ is analytic in the upper half plane of the complex variable ω [4] and actually coincides with $F_{nn}(\omega)$ for $\omega > m$, and in the region $-m < \omega < m$ satisfies the equality:

$$A_{\mathbf{nn}}(\omega) \equiv \mathrm{Im}\, M_{\mathbf{nn}}(\omega) = -\,\mathrm{Im}\, F_{\mathbf{nn}}(\omega). \tag{9}$$

4. The main task in deriving dispersion relations for nucleon-nucleon scattering is the determination of $\mathrm{Im}\, M_{nn}(\omega) = -\mathrm{Im}\, F_{nn}(\omega)$ in the range $-m < \omega < m$.

We shall show that for neutron-neutron and proton-proton scattering with antiparallel spins $\mathrm{Im}\, M_{nn}(\omega) = 0$ for $-m < \omega < m$. We shall not consider questions associated with the intermediate deuteron state, which plays a part only for neutron-proton scattering. The intermediate deuteron state was taken into account in [5].

Introducing a complete system of state eigenvectors Ω_n for the operator P_λ:

$$P_\lambda \Omega_n = p_\lambda^n \Omega_n, \tag{10}$$

using (7), noting that for $t = 0$ the Heisenberg and interaction representations coincide and considering, finally, that the operator $S_{\mathbf{q}\mu}^{+\mathbf{k}\nu}(0)$ is the Hermitian conjugate of $S_{\mathbf{q}\mu}^{\mathbf{k}\nu}(0)$, after integrating over x_λ we arrive at the following expression for $\mathrm{Im}\, F_{nn}(\omega)$:

$$\begin{aligned} \mathrm{Im}\, F_{\mathbf{nn}}(\omega) = 2^3\pi^4 \sum_{n\,(\mathbf{p}^n = \mathbf{k})} \delta\,[E_n - (\omega + m)]\, |\langle \Omega_0 \,|\, S_{\mathbf{q}\mu}^{\mathbf{k}\nu}(0) \,|\, \Omega_n \rangle|^2 \,+ \\ +\, 2^3\pi^4 \sum_{n\,(\mathbf{p}^n = -\mathbf{k})} \delta\,[E_n + (\omega + m)]\, |\langle \Omega_0 \,|\, S_{\mathbf{q}\mu}^{+\mathbf{k}\nu}(0) \,|\, \Omega_n \rangle|^2. \end{aligned} \tag{11}$$

Hence it can be seen that $\mathrm{Im}\, F_{nn}(\omega)$ can be different from zero only if $E_n^2 = (\omega + m)^2$. Noting that $E_n^2 = M_n^2 + (\mathbf{p}^n)^2 = M_n^2 + \omega^2 - m^2$, where M_n is the mass of the intermediate state with energy E_n and momentum $\mathbf{p}^n$, it is easily seen that for $-m < \omega < m$ contributions to $\mathrm{Im}\, F_{nn}(\omega)$ come only from intermediate states with mass $0 < M_n < 2m$.

It can thus be stated that in each of these intermediate states there is not more than one nucleon or one antinucleon (we do not consider the bound deuteron state). But then for these intermediate states

$$\langle \Omega_0^{\Gamma} \,|\, S_{\mathbf{q}\mu}^{\mathbf{k}\nu}(0) \,|\, \Omega_n^{\Gamma} \rangle = 0; \quad \langle \Omega_0^{\Gamma} \,|\, S_{\mathbf{q}\mu}^{+\mathbf{k}\nu}(0) \,|\, \Omega_n^{\Gamma} \rangle = 0. \tag{12}$$

Indeed, considering (3) for the operators $S_{\mathbf{q}\mu}^{\mathbf{k}\nu}(0)$ and $S_{\mathbf{q}\mu}^{+\mathbf{k}\nu}(0)$ it is easily seen that the matrix element $\langle \Omega_0^\Gamma | S_{\mathbf{q}\mu}^{\mathbf{k}\nu}(0) | \Omega_n^\Gamma \rangle$ or $\langle \Omega_0^\Gamma | S_{\mathbf{q}\mu}^{+\mathbf{k}\nu}(0) | \Omega_n^\Gamma \rangle$ can differ from zero only if the intermediate state contains two nucleons or two antinucleons, disregarding, of course, a certain number of mesons and nucleon-antinucleon pairs.

We have thus shown that $A_{nn}(\omega) = -\operatorname{Im} F_{nn}(\omega) = 0$ when $-m < \omega < m$.

In conclusion I wish to express my thanks to Academician V. A. Fok and Iu. V. Novozhilov for valuable comments and detailed discussions.

Leningrad State University

Received July 4, 1956

LITERATURE CITED

[1] M. L. Goldberger, Phys. Rev. 99, 979 (1955).

[2] M. L. Goldberger, H. Miyazawa and R. Oehme, Phys. Rev. 99, 986 (1955).

[3] R. Oehme, Phys. Rev. 100, 1503 (1955).

[4] N. N. Bogaliubov , B. V. Medvedev and M. K. Polivanov, All-Union Conference on the Physics of High-Energy Particles, Moscow, 1956.

[5] V. Ia. Fainberg and E. S. Fradkin, All-Union Conference on the Physics of High-Energy Particles, Moscow, 1956.

THE INTERACTION OF VIBRATIONS OF NONPOLAR CRYSTALS WITH ELECTRIC FIELDS

V. S. Mashkevich and K. B. Tolpygo

(Presented by Academician N. N. Bogoliubov, June 1, 1956)

1. In Born's lattice model the neutral atoms of a homopolar crystal do not interact with electric fields. However, the absorption of infrared light by diamond, Si and Ge crystals [1, 2] indicates that such interaction is present. In the theory of ionic crystals, which takes the polarizability of ions into account [3], the connection between the nuclear displacements $\mathbf{u}_s^l$ and the dipole moments $\mathbf{P}_s^l$ of the electronic shells results both from the electrostatic interactions and the dependence of the exchange integrals on $\mathbf{P}_s^l$ (l is the number of a cell; $\underline{s}$ is the number of an atom in the cell). The latter effect should also occur in homopolar crystals.

2. We calculated the energy U of a homopolar crystal such as the diamond as a function of the displacements $\mathbf{u}_s^l$ and dipole moments $\mathbf{P}_s^l$ similarly to [3], but with the difference that as the grounds state instead of the states of isolated atoms we took their states in the crystal when the valence crystals form σ bonds. In the harmonic approximation we obtained

$$U(\ldots \mathbf{u}_s^l \ldots \mathbf{P}_s^l \ldots) = \sum_l \sum_{l'}^{(4)} \{d(\mathbf{u}_{12}^{ll'}\cdot\mathbf{r}_{12}^{ll'})^2 + g(\mathbf{u}_{12}^{ll'})^2 + b(\mathbf{P}_{12}^{ll'}\cdot\mathbf{u}_{12}^{ll'}) + c(\mathbf{P}_{12}^{ll'}\cdot\mathbf{r}_{12}^{ll'})(\mathbf{u}_{12}^{ll'}\cdot\mathbf{r}_{12}^{ll'})\} + \sum_{ls}\left[\frac{1}{2\alpha}(\mathbf{P}_s^l)^2 - \frac{1}{2}(\mathbf{E}_s^l\cdot\mathbf{P}_s^l) - (\mathbf{E}_s^{0l}\cdot\mathbf{P}_s^l)\right], \qquad (1)$$

where $\mathbf{u}_{12}^{ll'} = \mathbf{u}_1^l - \mathbf{u}_2^{l'}$; $\mathbf{r}_{12}^{ll'}$ is the separation of atoms $\substack{l\\1}, \substack{l'\\2}$; α is the atomic polarizability; $\mathbf{E}_s^l$ is the electric field created at lattice site $\substack{l\\s}$ by the dipole moments of all other atoms; $\mathbf{E}_s^{0l}$ is the external electric field at site $\substack{l\\s}$. $\sum\limits_{l'}^{(4)}$ denotes summation over the 4 nearest neighbors; d, g, b, c, are theoretical parameters expressed by Coulomb and exchange integrals of the interactions between nearest neighbors in the ground and excited states. Terms which are bilinear with respect to displacements and dipole moments lead to coupling between displacements and atomic dipole moments. The presence of such coupling was suggested in [2] for the purpose of explaining light absorption, but no conclusions were reached regarding the origin and form of the coupling and the parameters were not evaluated qualitatively.

3. In the adiabatic approximation the states of electronic shells of atoms (which we characterize by the dipole moments $\mathbf{P}_s^l$) follow atomic displacements without delay and according to the variation principle are determined by the minimum of U. The equation of atomic vibrations is thus written

$$m_s \ddot{u}_{sx}^l = -\frac{\partial U}{\partial u_{sx}^l}; \quad 0 = -\frac{\partial U}{\partial P_{sx}^l}. \qquad (2)$$

These equations were solved for $\mathbf{E}_s^{0l} = 0$ by substituting $\mathbf{u}_s^l = \mathbf{u}_s e^{-i\omega t + i\mathbf{k}\mathbf{r}_s^l}$; $\mathbf{P}_s^l = \mathbf{P}_s e^{-i\omega t + i\mathbf{k}\mathbf{r}_s^l}$ and expanding in powers of $|\mathbf{k}|\underline{a}$, where $\underline{a}$ is the lattice constant; as in [3] retardation in the propagation of the field $\mathbf{E}_s^l$ was taken into account.

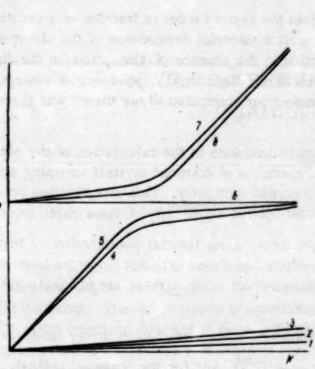

Fig. 1.

In addition to the acoustic and three optical branches for which in the zeroth approximation $\mathbf{u}_1 = \mathbf{u}_2$, $\omega(0) = 0$, $\mathbf{P}_1 = \mathbf{P}_2 = 0$ and $\mathbf{u}_1 = -\mathbf{u}_2$, $\omega(0) = \omega_0 = 0$, $\mathbf{P}_1 = -\mathbf{P}_2$, respectively, there are 2 more solutions (the so-called light vibrations) for which $\mathbf{u}_1 = \mathbf{u}_2 = 0$, $\mathbf{P}_1 = \mathbf{P}_2 \neq 0$ and $\omega = c\,|\mathbf{k}|/n$, where $\underline{n}$ is the optical refractive index associated with the polarizability α by the usual formula and $\underline{c}$ is the velocity of light. In the first and second approximations in $|\mathbf{k}|\underline{a}$ it is possible to derive a relation between $\omega(\mathbf{k})$ and the quantities $\mathbf{u}_s$, $\mathbf{P}_s$ for all branches. In the accoustic and optical branches the dipole moments $\mathbf{P}_1$ and $\mathbf{P}_2$ and the dipole moment $\mathbf{P}_1 + \mathbf{P}_2$ of a cell are not zero and for the light vibrations we obtain shifts $\mathbf{u}_1$ and $\mathbf{u}_2$ which are not zero. On the basis of the experimental values of n, ω_0 (the Raman frequency) and the elastic moduli c_{11}, c_{12} and c_{44} we determined the theoretical parameters d, g, b, c, α. If we neglect the interactions of the displacements and dipole moments (assuming $b = 0$, $c = 0$) we obtain

$$c_{14} = c_{11} - \frac{(c_{11} + c_{12})^2}{4c_{11}}, \tag{3}$$

which has already figured in the literature [4]. This is well satisfied in Ge but much worse in Si and diamond. The authors of [4] considered the fulfillment of (3) to be an indication that we can confine ourselves in the calculations to interactions inside the first coordination sphere. From the point of view of the complete theory there is no ground for neglecting the dipole moments $\mathbf{P}_1$ and $\mathbf{P}_2$. On the other hand, the dipole interaction is not limited to only the nearest coordination spheres, while the covalent interaction must be practically absent even for the second sphere. Therefore, even if (3) is satisfied by chance it cannot serve as a criterion. In calculating the vibrational spectra spectra of homopolar crystals corrections should take farther coordination spheres into account in the theory of a point lattice and also the dipole interactions.

4. A special investigation is required by the agreement of the optical and light vibrations with $c|\mathbf{k}|/n = \omega_0$. When this is considered by perturbation theory for close eigenvalues it can be shown that in the neighborhood of $|\mathbf{k}_0| = n\omega_0/c$ instead of two optical and two light vibrations there are 4 mixed vibrations with both $\mathbf{u}_1$, $\mathbf{u}_2$ and $\mathbf{P}_1 + \mathbf{P}_2$ different from zero (see Fig. 1). Thus, for the light vibrations Curves 4 and 5 for $\omega < \omega_0$ and Curves 7 and 8 for $\omega > \omega_0$ near the point ω_0 there will be considerable dispersion. If $\mathbf{k}$ has the direction of the diagonal of a cube face and $\mathbf{P}_1 + \mathbf{P}_2$ lies in the plane of this face, the corresponding light vibrations are not perturbed.

5. On the basis of these results we can explain the first-order absorption of light by homopolar crystals. The external light field induces crystal polarization $\mathbf{P}_1 + \mathbf{P}_2$. This polarization according to the equations of motion (2) leads to the gradual conversion of electrical energy into vibrational energy. The quantitative calculation of this effect gives the result that the initial "pure light" vibration ($\mathbf{u}_1 = \mathbf{u}_2 = 0$) with frequency ω close to ω_0 is represented as the superposition of vibrations 4, 7 (or 5, 8 depending on the polarization). Since these vibrations have different frequencies for identical $\mathbf{k}$, beats arise and in the time $T \sim \pi / 2(\omega_4 - \omega_7)$ the displacements $\mathbf{u}_1$ and $\mathbf{u}_2$ reach their maximum values with the simultaneous decrease of $\mathbf{P}_1 + \mathbf{P}_2$. If the vibrations were purely harmonic then in the time from T to 2T, $\mathbf{u}_1$ and $\mathbf{u}_2$ would again vanish and all of the energy would become electrical. Since T is relatively large (of the order $10^3/\omega$) the mechanical energy of vibrations 4 and 7 in time T goes into other normal modes. Therefore the difference of the squares of $\mathbf{P}_1 + \mathbf{P}_2$ for $t = 0$ and $t = T$ will be

proportional to the energy absorbed in time T. Evaluation of T gives the correct order (a fraction of a centimeter) for the depth of light penetration in the crystal $l \sim Tc$. Theory predicts essential dependence of the absorption coefficient on the direction **k** and polarization of light and in particular the absence of absorption for the direction [110] with $P_1 + P_2$ lying in this cubic face. Experimental check of the directional dependence of absorption could distinguish this first-order effect from some less intense second-order absorption whose theory was given in [2].

6. In order to explain how these effects are related to the approximations in the calculation of the potential energy (1) one of us (B. S. Mashkevich) studied the vibrational spectrum of diamond crystals assuming arbitrary quadratic dependence of $U(\ldots \mathbf{u}_s^l \ \ldots P_s^l \ldots)$ subject only to crystal symmetry. This investigation confirmed all the qualitative results of the theory, in particular the indicated optical asymmetry of these cubic crystals.

7. In connection with the fact that for homopolar crystals our theory gives inertial polarization, we investigated the possibility of the formation of polarons such as those predicted by Pekar [5]. But since the longitudinal components of the dipole moment $P_1 + P_2$ appear only in the second order in $k\,\underline{a}$ there are no stable polaron states of large radius in a diamond crystal.

The investigation of scattering of conduction electrons by vibrations using perturbation theory leads for acoustic vibrations to the temperature dependence of the mobility $u \sim T^{-3/2}$, and for the case of optical vibrations $u \sim e^{\hbar\omega_0/kT}$ for low temperatures, $u \sim T^{-3/2}$ for high temperatures.

T. G. Shevchenko Kiev State University

Received May 29, 1956

LITERATURE CITED

[1] R. J. Collins and H. Y. Fan, Phys. Rev. 93, 674 (1954).

[2] M. Lax and E. Burstein, Phys. Rev. 97, 39 (1955).

[3] K. B. Tolpygo, J. Exptl.-Theoret. Phys. (USSR) 20, 497 (1950).

[4] Yu Chang Hsien, Phys. Rev. 85, 730 (1952).

[5] S. I. Pekar, Investigations in the Electron Theory of Crystals (Moscow-Leningrad, 1951).

NUCLEON PROPAGATION FUNCTION IN THE QUADRATIC APPROXIMATION

V. G. Solov'ev

(Presented by Academician N. N. Bogoliubov, June 26, 1956)

There is no agreement with experiment for the cross sections of interactions between pions or gamma rays and nucleons which are calculated by perturbation theory in pseudoscalar symmetrical meson theory with pseudoscalar coupling. This discrepancy is associated with the fact that the perturbation series is evidently asymptotic and that the coupling constant is large. Therefore the first terms of an asymptotic expansion do not give a correct representation of the behavior of the true function. Investigations which go beyond perturbation theory are therefore very important.

Local meson theory which does not take the structure of elementary particles into account and which neglects interaction with heavy mesons and hyperons can hardly be correct for high energies where these factors must play an important part. It is of interest to establish the applicability of the theory to the region of relatively low energies.

The present work investigates the Green's function in pseudoscalar symmetrical meson theory with pseudoscalar coupling, and is principally concerned with the mathematical side of the problem. The foundation is laid for a new method of constructing approximate Green's functions; this is called the quadratic approximation. The method is intended for application to low energies. We have obtained the nucleon propagation function $G(k|0)$ and the vertex parts $\Gamma_5^\lambda(k;q)$ and $\Gamma_\mu(k;q)$ in the quadratic approximation. The vertex part $\Gamma_\mu(k;q)$ was used to obtain information concerning the nucleonic magnetic moment.

The equations for the Green's functions are very complicated; therefore we have followed Edwards and Peierls [1] in considering only the linear equations for the Green's functions, i. e., we neglect all closed nucleon-antinucleon loops. On the basis of a model investigation it was shown in [2] that Feynman's conclusion regarding the large role of pairs refers only to the region $k^2 \gg m^2$.

As we know, the Green's function of a nucleon $G(x,y|0)$ is associated with the Green's function $G_{cl}(x,y|\varphi)$ of a nucleon in the classical field φ neglecting vacuum polarization as follows:

$$G(x,y|0) = \langle T\{G_{cl}(x,y|\varphi)\}\rangle_v, \tag{1}$$

i. e., by averaging the T product of $G_{cl}(x,y|\varphi)$ over the boson vacuum. According to [3] the rule for calculating $\langle T\{f(\varphi)\}\rangle_v$; can be formulated as follows: each operator of the boson field $\varphi^\lambda(x)$ is replaced by $\varphi'^\lambda(x)$ according to the formula

$$\varphi'^\lambda(x) = \theta^\lambda(x) - i\int D(x-y)\,dy\,\frac{\delta}{\delta\theta^\lambda(y)};$$

then a functional differentiation is performed, after which $\theta^\lambda(x)$ is set equal to zero. In momentum space (1) is written symbolically as

$$G(k\,|\,0) = \{G_{\mathrm{cl}}(k\,|\,\varphi')\cdot 1\}^{\theta^\lambda - 0}_{\varphi'^\lambda(p) = \theta^\lambda(p) - iD(p)\frac{\delta}{\delta\theta^\lambda(-p)}}, \tag{1'}$$

where $D(p) = \dfrac{1}{\mu^2 - p^2 - i\epsilon}$; μ is the mass of a pion.

Using the translational invariance of kernels of the functionals [4] we write the equation for $G_{\mathrm{cl}}(k|\varphi)$ as

$$\left[m - \gamma_\mu k_\mu - \int dp\,\gamma_\mu p_\mu \varphi^\lambda(p)\frac{\delta}{\delta\varphi^\lambda(p)} - \bar{g}\gamma_5\dot{\tau}^\lambda \int dp\,\varphi^\lambda(p)\right] G_{\mathrm{cl}}(k\,|\,\varphi) = 1, \tag{2}$$

where $\bar{g} = g/(2\pi)^2$; m is the mass of a nucleon. Instead of the usual matrices of isotopic spin τ^λ, we shall use the matrices $\dot{\tau}^\lambda$, defined by the relation $g^\lambda\tau^\lambda\varphi^\lambda = g\dot{\tau}^\lambda\varphi^\lambda$.

The Green's function $G_{\mathrm{cl}}(k\,|\,\varphi)$ of a nucleon in a classical field φ is written as

$$G_{\mathrm{cl}}(k\,|\,\varphi) = \left[m + \gamma_\mu k_\mu + \int dp\,\gamma_\mu p_\mu \varphi^\lambda(p)\frac{\delta}{\delta\varphi^\lambda(p)} + \bar{g}\gamma_5\dot{\tau}^\lambda \int dp\,\varphi^\lambda(p)\right]\mathfrak{G}_{\mathrm{cl}}(k|\varphi), \tag{3}$$

and we obtain an equation for $\mathfrak{G}_{\mathrm{cl}}(k\,|\,\varphi)$;

$$\Big\{m^2 - k^2 - \int dp\,(p^2 + 2kp)\,\varphi^\lambda(p)\frac{\delta}{\delta\varphi^\lambda(p)} - \int dp_1\,dp_2\,(p_1 p_2)\,\varphi^{\lambda_1}(p_1)\varphi^{\lambda_2}(p_2)\times$$
$$\times\frac{\delta^2}{\delta\varphi^{\lambda_1}(p_1)\,\delta\varphi^{\lambda_2}(p_2)} + \frac{\bar{g}^2}{2}\int dp\,dp'\varphi^\lambda(p)\varphi^\lambda(p') + \bar{g}\gamma_5\dot{\tau}^\lambda\int dp\gamma_\mu p_\mu\varphi^\lambda(p)\Big\}\mathfrak{G}_{\mathrm{cl}}(k\,|\,\varphi) = 1. \tag{4}$$

Since Equation (4) cannot be solved exactly we use a simplified equation in which we neglect the recoil part $\int dp_1\,dp_2\,(p_1 p_2)\,\varphi^{\lambda_1}(p_1)\,\varphi^{\lambda_2}(p_2)\,\dfrac{\delta^2}{\delta\varphi^{\lambda_1}(p)\,\delta\varphi^{\lambda_2}(p_2)}$ and the interference term $-\bar{g}\gamma_5\dot{\tau}^\lambda\int dp\,\gamma_\mu p_\mu\varphi^\lambda(p)$.

We solve the simplified equation

$$\Big\{m^2 - k^2 - \int dp\,(p^2 + 2kp)\,\varphi^\lambda(p)\frac{\delta}{\delta\varphi^\lambda(p)} + \frac{\bar{g}^2}{2}\int dp\,dp'\varphi^\lambda(p')\,\varphi^\lambda(p')\Big\}\times$$
$$\times\mathfrak{G}_{\mathrm{cl}}(k\,|\,\varphi) = 1 \tag{5}$$

by the proper time method introduced by V. A. Fok [5]; we obtain

$$G_{\mathrm{cl}}(k\,|\,\varphi) = i\int_0^\infty d\nu\exp\{-\varepsilon\nu - i(m^2 - k^2)\nu\}\Big[m + \gamma_\mu k_\mu +$$
$$+\int dp\,dp'\gamma_\mu p_\mu\varphi^\nu(p)\,u_\nu(p, p')\,\varphi^\lambda(p') + \bar{g}\gamma_5\dot{\tau}^\lambda\int dp\,\varphi^\lambda(p)\Big]\times \tag{6}$$
$$\times\exp\left\{\frac{1}{2}\int dp_1\,dp_2\varphi^\lambda(p_1)\,u_\nu(p_1, p_2)\,\varphi^\lambda(p_2)\right\},$$

where

$$u_\nu(p_1, p_2) = -i\bar{g}^2 \int_0^\nu d\nu' \exp\{i\nu'(p_1^2 + p_2^2 + 2kp_1 + 2kp_2)\}.$$

Functional averaging requires solution of the functional equation. The solution of the functional equation is expressed in terms of a function which satisfies a nonlinear equation. The solution of this equation is in turn represented by the solution of a Fredholm integral equation of the second kind. The calculations yield a Green's function of the nucleon $G(k|0)$ as an integral of the determinant of the Fredholm equation with 4 independent variables.

Using the theorem that if in different spaces we have the two kernels K and Q such $\mathrm{Sp}K^n = \mathrm{Sp}Q^n$ their determinants are equal, we obtain the Green's function of a nucleon in the form

$$G(k|0) = (m + \gamma_\mu k_\mu)\, i \int_0^\infty d\nu \exp\{-\varepsilon\nu - i(m^2 - k^2)\nu\}\{\det(1 + Q)\}^{-3/2}. \tag{7}$$

Here $\det(1 + Q)$ is the determinant of the Fredholm integral equation

$$y(\omega) + \bar{g}^2 \int_0^\nu Q(\omega, \omega')\, y(\omega')\, d\omega' = f(\omega) \tag{8}$$

with the kernel

$$Q(\omega, \omega') = \pi^2 \int_0^\infty \frac{d\beta}{(1+\beta)^2}(1 - \exp\{-i\beta\lambda^2(\omega + \omega')\})\times$$
$$\times \exp\left\{-i\frac{(\omega - \omega')^2}{\omega + \omega'}\frac{k^2}{1 + \beta} - i\beta\mu^2(\omega + \omega') - \varepsilon\beta(\omega + \omega')\right\},$$

where λ is the cutoff parameter.

Calculation of the first three terms and investigation of the nth term of the expansion of $\det(1 + Q)$ in terms of the parameter show that $G(k|0)$ has only one singularity, namely, the pole at $k^2 = m^2$.

If for the calculation of $\dfrac{\delta^n G_{\mathrm{cl}}(k\,|\,\varphi)}{\delta\varphi^{\lambda_1}(q_1)\ldots\delta\varphi^{\lambda_n}(q_n)}$ we use $G_{\mathrm{cl}}(k|\varphi)$ in the form (6) and perform a functional averaging, after renormalization we obtain only part of a perturbation expansion. Therefore, in order to prevent the results of calculating cross sections for pion-nucleon interactions and other processes from reducing to the results of a perturbation calculation it is required that each nth variational derivative $\dfrac{\delta^n G_{\mathrm{cl}}(k\,|\,\varphi)}{\delta\varphi^{\lambda_1}(q_1)\ldots\delta\varphi^{\lambda_n}(q_n)}$ be functionally averaged; also that the simplified equation be solved, followed by functional averaging and renormalization. The resulting expression

$$\left\{\frac{\delta^n G(k\,|\,\Phi)}{\delta\Phi^{\lambda_1}(q_1)\ldots\delta\Phi^{\lambda_n}(q_n)}\right\}_{\Phi=0}$$

is simply related to the transition matrix element of the corresponding process.

There are greater mathematical difficulties associated with obtaining the vertex parts Γ_5^λ and Γ_μ than with $G(k|0)$. In calculating $\Gamma_\mu(k; q)$ the interaction with an electromagnetic field must be taken into account in the first perturbation approximation. After tedious calculations the vertex parts $\Gamma_5^\lambda(k; q)$ and $\Gamma_\mu(k; q)$ are obtained as

$$\begin{aligned}\Gamma_5^\lambda(k;q) = G^{-1}(k+q\,|\,0)\,\{\gamma_5\dot{\tau}^\lambda\mathfrak{G}(k\,|\,0) + \gamma_5\dot{\tau}_\lambda\int_0^\infty d\nu\int_0^\infty d\omega\,\times \\ \times\exp\{-\varepsilon\nu-\varepsilon'\omega - i\,(m^2-k^2)\,\nu - i\,[m^2-(k+q)^2]\,\omega\}\,\times \\ \times(m-\gamma_\mu k_\mu - \gamma_\mu q_\mu)\,\gamma_\mu q_\mu - i\bar{g}^2\int pd\,\times \\ \times\exp\{i\omega\,(p^2-2kp-2qp)\}\,F_{\nu,\omega}(p)]\,\{\det(1+K_{\nu,\omega})\}^{-3/2}\}\,G^{-1}(k\,|\,0),\end{aligned} \tag{9}$$

$$\begin{aligned}\Gamma_\mu(k;q) = G^{-1}(k+q\,|\,0)\,\{\tau_p\gamma_\mu\mathfrak{G}(k\,|\,0) - \int_0^\infty d\nu\int_0^\infty d\omega\,\times \\ \times\exp\{-\varepsilon\nu-\varepsilon'\omega - i\,(m^2-k^2)\,\nu - i\,[m^2-(k+q)^2]\,\omega\}\,\times \\ \times[\tau_p\,(m+\gamma_\nu k_\nu+\gamma_\nu k_\nu)\,(2k_\mu+\gamma_\nu q_\nu\gamma_\mu) - i\bar{g}^2\int dp\,\exp\{i\omega\,(p^2-2kp-2qp)\}\,\times \\ \times(\tau_N-\tau_p)\,F_{\nu,\omega}(p)]\,\{\det(1+K_{\nu,\omega})\}^{-3/2} + (\tau_p-\tau_N)\,B_\mu(k;q)\}\,G^{-1}(k\,|\,0).\end{aligned} \tag{10}$$

Here $\det(1+K_{\nu,\omega})$ is the determinant and $F_{\nu,\omega}(p)$ is the solution of the Fredholm integral equation

$$F_{\nu,\omega}(p) + \bar{g}^2\int dp'K_{\nu,\omega}(p,-p')\,F_{\nu,\omega}(p') = D(p) \tag{11}$$

with the kernel

$$\begin{aligned}K_{\nu,\omega}(p,p') = D(p)\int_0^\omega d\omega'\exp[i\omega'(p^2+p'^2+2kp+2kp'+2qp+2qp')] + \\ + D(p)\exp[i\omega\,(p^2+p'^2+2kp+2kp'+2qp+2qp')]\int_0^\nu d\nu'\,\times \\ \times\exp[i\nu'(p^2+p'^2+2kp+2kp')].\end{aligned} \tag{11'}$$

In (10) $B_\mu(k; q)$ describes the contribution to Γ_μ from the direct interaction of pions with the electromagnetic field.

We use the vertex part $\Gamma_\mu(k; q)$ to obtain information concerning the nucleonic magnetic moment. The calculations for the quadratic approximation give as the sum of the neutron and proton magnetic moments one nuclear magneton, i. e.,

$$\mu_p + \mu_n = 1,$$

where the neutron magnetic moment μ_n is not zero. This result is in quite good agreement with experiment.

Calculations of the proton and neutron magnetic moments separately or of pion scattering cross sections from nucleons etc. were not carried through because of the great mathematical difficulties associated with the solution of Fredholm integral equations.

In conclusion we wish to express our deep appreciation to Academician N. N. Bogoliubov for suggesting the problem and for his direction and assistance.

Institute for Nuclear Problems, Academy of Sciences USSR

Received June 20, 1956

LITERATURE CITED

[1] **S. Edwards and R. Peierls, Proc. Roy. Soc. (London) A, 224, 24 (1955); S. Edwards, Proc. Roy. Soc. (London) A, 228, 411 (1955); 232, 371, 377 (1955).**

[2] **V. G. Solov'ev, Doklady Akad. Nauk SSSR 108, 1041 (1956) [Soviet Physics — Doklady, p. 393].**

[3] **J. Anderson, Phys. Rev. 94, 703 (1954).**

[4] **N. N. Bogoliubov, Bull. Moscow State Univ. 1955, No. 4-5, 115.**

[5] **V. A. Fok, Physik. Z. Sowietunion 12, 404 (1937).**

LUMINESCENCE FLASHES IN ZINC SULFIDE CRYSTALS AND THE TWO-STAGE EXCITATION MECHANISM

N. A. Tolstoi

(Presented by Academician A. A. Lebedev, June 29, 1956)

1. N. A. Tolstoi and P. P. Feofilov [1] discovered luminescence flashing (LF) of the long-wave luminescence band of ZnS-Mn phosphors, but despite the obvious importance of this phenomenon for the theory of phosphorescence it has been almost neglected during recent years. A similar phenomenon was observed by N. A. Gorbacheva [2] in the phosphor $Cd_2P_2O_7$-Pb, Mn. V. V. Antonov-Ramonovskii [3] has proposed an interpretation of LF from the point of view of the stimulating effect of the exciting light. Our further investigations in this area have shown that first, LF is a much more universal phenomenon than could have been anticipated; secondly, that this phenomenon can be used as the basis for a new method of investigating local phosphor levels; thirdly, that the processes revealed by the investigation of LF should be kept in mind in constructing the theory of phosphorescence in sulfide phosphors.

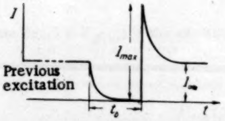

Fig. 1.

2. We recall that LF in ZnS-Mn means the following: Switching on of exciting light of constant intensity E = const (λ = 365 mμ) after decay which in turn was preceded by prolonged stationary excitation (λ = 365 mμ) induces a flash (see Fig. 1) of the orange band of Mn luminescence. The relative intensity of the flash, defined as $V = I_{max}/I_\infty$ reaches the magnitude 4 in ZnS–Mn under optimal conditions.

By constructing a "single-stage" light modulator with an electrically controlled shutter [4] we were able to investigate V as a function of the duration of the dark interval t_0 by varying the latter from 0.01 sec to practically infinite time while maintaning a constant and sufficiently good steepness of the leading edge of the light pulses ($\approx 3 \cdot 10^{-4}$ sec). V was found to have a maximum at a definite $t_0 = t_{0max}$. This "ripening" time of the flash depends strongly on temperature; in first approximation it follows the law

$$\frac{1}{t_{0\max}} \sim e^{-u/kT}. \tag{1}$$

The time t_{0max} is practically independent of the excitation intensity E(λ_{ex} = 365 mμ). Thus for sufficiently small or sufficiently large t_0 compared with t_{0max} LF may not be detected. Our new method enabled us to discover a fact which has escaped the attention of investigators of zinc-sulfide phosphors: that a considerable number of ZnS phosphors possess LF (excited with λ = 365 mμ). Thus we can give ZnS–Ni; ZnS–Ni, Ag; ZnS–Co; ZnS–Fe; ZnS–Eu; ZnS–P; some samples of ZnS–Cu (with orange luminescence) and, finally, a large fraction of "unactivated" ZnS.* At a given temperature the ripening time differs in these phosphors but always is shortened as the temperature rises. Many of them give very large values of V (for example, in ZnS–Ni we observed $V \approx 6$). In all cases LF are observed in the long-wave luminescence band; the short-wave band (Zn) shows "normal" kinetics. All of these phosphors satisfy the rule which we have noted previously [5]: the short-wave bands are more or less clearly superlinear ($I_{\infty} \sim E^{\geq 1}$), while the long-wave bands are sublinear ($I_{\infty} \sim E^{\leq 1}$). The relaxation of the short-wave and long-wave luminescence is also of unlike character: the rise of the short-wave luminescence is slower than the decay ($L_r/L_d > 1$, see [6, 7]) while the rise of the long-wave luminescence is faster than the decay ($L_r/L_d < 1$). The rise time in the presence of LF is formally even negative ($L_r/L_d < 0$).

---

*V. A. Arkhangel'skaia and P. P. Feofilov have reported to the author that they have observed LF under periodic excitation (using a tau-meter) in cooled TlCl with V ≈ 1.5. Our new method enabled us to obtain for TlCl V = 12 and with orange irradiation during the dark interval, V ≈ 45.

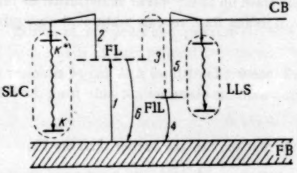

Fig. 2.

3. We shall now discuss the possible luminescence mechanism of phosphors which posses LF. We admit to begin with that the scheme which we shall consider is very crude and that many of its details must be improved and developed. Thus Fig. 2, which we use to illustrate our comments, must not be considered to have any literal physical meaning.

The first effect of exciting light 1 is to induce a transition of electrons from the filled band FB (or from the unexcited levels S and L, respectively, of the short-wave luminescence center (SLC) and the long-wave luminescence center (LLC) to local levels which we shall call feeding levels (FL).

The number of levels in the FL is limited by the fact that they are ejected from the FL to the conduction band (CB) by the secondary effect of the exciting light (2) and spontaneously move (3) to flash levels (FlL). In very strong excitation process 2 dominates and the number of electrons on FL is constant; under very weak excitation process 3 dominates (probably with the participation of quenching 6) and the number of electrons in FL is proportional to the excitation E. These limiting cases give for the intensity of the stationary short-wave luminescence $I_{\infty\,sh}$ the limiting values $I_{\infty\,sh} \sim E$ and $I_{\infty\,sh} \sim E^2$, respectively; as we know, this is in accordance with experiment.

The balance of the number of electrons in FlL is determined by the receipt of electrons from the FL (process 3), the spontaneous departure of electrons (4) and by the optical ejection of electrons (5) which results in the excitation of only LLC. When the excitation is terminated process 5 stops and the number of electrons in FlL begins to increase by process 3 which continues until the electrons in FL are exhausted; this is the "ripening" process of the flash. If process 4 is improbable the ability to produce flashes can last a very long time (for example in ZnS–Ni for days). Renewed illumination after an interruption again induces process 5, intensified as a result of the fact that the number of electrons in FlL during the first few moments is higher than the stationary number; there will be a flash of long-wave luminescence.

One of the most important experimental facts favoring this picture is the following: as the long-wave flash "ripens" a reverse phenomenon "ripens" in the short-wave portion of the spectrum, which is the slowing down of the short-wave rise that is observed under succeeding excitation. This means that the FL have already been emptied and must be filled to equilibrium again for the development of short-wave luminescence. If the dark interval t_0 is short then only a small fraction of the electrons are transferred from the FL to the FlL, the long-wave flash will be small and the rise of the short-wave luminescence will be rapid since the electron reserve in FL can immediately be "put into action" (process 2). Experiment shows that this correlation between the kinetics of the long-wave and the short-wave luminescence is not only of qualitative but also of quantitative character; the "ripening of the flash" (measured by increase of the area over the long-wave rise curve) proceeds in time exactly as the "ripening of slowness" (measured by the decrease of area over the short-wave rise curve). We believe that this correlation as well as the superlinearity and sublinearity of stationary luminescence establishes the nature of the "competition" of luminescence bands in phosphors (see [8] for example).

Let us see how our scheme agrees with other experimental facts (for example, for ZnS–Ni):

1) A rise of temperature accelerates the ripening of the flash and the ripening of slowness; the departure of electrons from FL (process 3) is accelerated.

2) Infrared irradiation during the initial stages of the dark interval accelerates the ripening of the flash and the slowness and is ineffective in the further stages; so long as the FL have electrons the infrared light can extract them and empty these levels. Infrared radiation has practically no effect on the flash intensity; such light is absorbed only by electrons in the FL.

3) Orange-green illumination in the dark period reduces the flash up to complete annihilation by removing electrons from the FIL. (Experiment shows that a phosphor with a ripening flash reveals additional absorption in the orange-green portion of the spectrum).

4) Orange-green irradiation in the initial stages of the dark interval facilitates ripening of slowness in the short-wave rise and does not affect the latter stages; this irradiation extracts electrons not only from the FIL but also from the FL when present there.

From 2) and 4) it follows, as we have postulated (see Fig. 2), that the FIL are deeper than the FL.

5) The intensity of the flash V does not depend within broad limits on the intensity of the previous excitation, but it increases with the intensity of excitation for which LF are observed; the number of electrons entering the FL as a result of previous excitation is limited; the flash intensity is determined only by process 5.

4. We are of the opinion that the study of phosphors with LF will connect the two most important classes of crystal phosphors: the "ordinary" and the "flashing", i. e., phosphors that are infrared stimulated. From this point of view ripening of LF represents "autostimulation" by the exciting light.

Received June 21, 1956

LITERATURE CITED

[1] N. A. Tolstoi and P. P. Feofilov, Doklady Akad. Nauk SSSR 68, 285 (1949).

[2] N. A. Gorbacheva, J. Exptl.-Theoret. Phys. 21, 305 (1951).

[3] V. V. Antonov-Romanovskii, Bull. Acad. Sci. USSR, Phys. Ser. 15, 637 (1951).

[4] N. A. Tolstoi, N. N. Tkachuk, M. Ia. Tsenter, Z. S. Mansyrova and A. V. Burlakov, Optics and Spectroscopy 1, 5, 719 (1956).

[5] N. A. Tolstoi and A. V. Shatilov, Optics and Spectroscopy 1, 2 (1956).

[6] N. A. Tolstoi and I. A. Litvinenko, J. Exptl.-Theoret. Phys. (USSR) 29, 507 (1955).

[7] N. A. Tolstoi and A. V. Shatilov, J. Exptl.-Theoret. Phys. (USSR) 30, 109 (1956).*

[8] V. L. Levshin, Photoluminescence of Solids and Liquids (1951), p. 373.

---

* [Soviet Physics, J. E. T. P. p. 81].

TOWARDS A GENERAL THEORY OF MESON SCATTERING

A. Brodskii

(Presented by Academician N. N. Bogoliubov June 30, 1956)

During recent years one-particle Green's functions have been represented [1, 2] as integrals of scalar functions on the basis of very general hypotheses. We give the renormalized nucleon and meson functions [1, 2] in a form which is convenient for our subsequent discussion:*

$$G(x, x') = i\left(\Psi_0, T\left(\psi(x)\bar{\psi}(x')\Psi_0\right)\right) =$$
$$= \frac{1}{(2\pi)^4}\int (dp)\, e^{ip(x-x')}\, i\int_0^\infty ds e^{-is(m^2+p^2)} \sum_{\lambda=0,1} (-\gamma p + m)^\lambda \nu_\lambda(s), \tag{1}$$

$$\mathfrak{G}(\xi i, \xi' j) = i\left(\Psi_0, T\left(\varphi_i(\xi), \varphi_j(\xi')\Psi_0\right)\right) = \frac{\delta_{ij}}{(2\pi)^4}\int (dk)\, e^{ik(\xi-\xi')} i\int_0^\infty dt\, e^{-it(\mu^2+k^2)} \nu(t), \tag{2}$$

where all quantities, just as in the following, are assumed to be renormalized.** We note that in our notation $Z_2^{-1} = \nu_1(0)$ and $Z_3^{-1} = \nu(0)$. The functions $\nu_\lambda(s)$, $\nu(t)$ which have been introduced have the following general structure:

$$\nu_\lambda(s) = \int_0^\infty \left[\delta_{\lambda 1}\delta(M^2 - m^2) + \rho_\lambda(M^2)\,\theta\left(M^2 - (m+\mu)^2\right)\right] e^{-i(M^2-m^2)s}\, dM^2, \tag{3}$$

$$\nu(t) = \int_0^\infty \left[\delta(M^2 - \mu^2) + \rho(M^2)\,\theta\left(M^2 - (3\mu)^2\right)\right] e^{-i(M^2-\mu^2)t}\, dM^2, \tag{4}$$

where $\rho_\lambda(M^2)$ and $\rho(M^2)$ are scalar functions. We now attack the problem of expressing the amplitude of meson-nucleon scattering in terms of analogous integrals. For this purpose we first write in a form which is equivalent to (2) and (3) the following quantity which directly defines the scattering amplitude [5, 6]:

$$-i\left.\frac{\delta^2 G(x, x')}{\delta I_i(\xi)\,\delta I_j(\xi')}\right|_{I=0} = -\left(\Psi_0, T\left(\psi(x)\bar{\psi}(x')\varphi_i(\xi)\varphi_j(\xi')\right)\Psi_0\right) -$$
$$- G(x, x')\,\mathfrak{G}(\xi, \xi') =$$
$$= -i\Big[G(x, x'')\,\mathfrak{G}(\xi, \xi'')\Big(\frac{\delta G^{-1}(x'', x''')}{\delta\langle\varphi_i(\xi'')\rangle} G(x''', x^{\mathrm{IV}}) \frac{\delta G^{-1}(x^{\mathrm{IV}}, x^{\mathrm{V}})}{\delta\langle\varphi_j(\xi''')\rangle} +$$
$$+ \frac{\delta^2 G^{-1}(x'', x''')}{\delta\langle\varphi_j(\xi''')\rangle} G(x''', x^{\mathrm{IV}}) \frac{\delta G^{-1}(x^{\mathrm{IV}}, x^{\mathrm{V}})}{\delta\langle\varphi_i(\xi'')\rangle} +$$
$$+ \left.\frac{\delta^2 G^{-1}(x'', x^{\mathrm{V}})}{\delta\langle\varphi_i(\xi'')\rangle\,\delta\langle\varphi_j(\xi''')\rangle}\Big)\right|_{I=0} G(x^{\mathrm{V}}, x')\,\mathfrak{G}(\xi''', \xi')\Big] \tag{5}$$

---

* We retain in general the notation of [3, 4].

** Our discussion has meaning either for the so-called regularizable theories or for unregularizable theories with cutoff. Otherwise the type of interaction is not fixed.

(integrated over the same coordinates).

We now pass to the momentum representation and introduce

$$\begin{gathered}\rho(p,\ p',\ ki,\ k'j) = \\ = \frac{-i}{(2\pi)^8}\int \exp\{-i(px - p'x' + k\xi - k'\xi')\}\ \frac{\delta^2 G(x,\ x')}{\delta I_i(\xi)\,\delta I_j(\xi')}\bigg|_{I=0}(dx)\,(dx')(d\xi)(d\xi') = \\ = -ig^2 G(p)\,\mathfrak{G}(k)\left\{\int (dp'')\,[\Gamma_{5i}(p,\ p'';\ k)\,G(p'')\,\Gamma_{5j}(p'',\ p';\ -k') + \right. \\ \left. + \Gamma_{5j}(p,\ p'';\ -k')\,G(p'')\,\Gamma_{5i}(p'',\ p';\ k)] + l(p,\ p';\ ki,\ k'j)\right\} G(p')\,\mathfrak{G}(k'). \qquad (6)\end{gathered}$$

The meaning of the notation becomes clear after comparing (6) with (5). We now consider the general conditions which must be satisfied by the functions $\rho(p,\ p';\ ki,\ k'j)$ and $l\ (p,\ p';\ ki,\ k'j)$. We first note that if $\rho(p,\ p';\ ki,\ k'j)$ corresponds to all coupling diagrams with two external meson and two nucleon lines then the term in square brackets in (6) describes the portion of these diagrams depicted in Fig. 1, while $l\ (p,\ p';\ ki,\ k'j)$ corresponds to the remaining diagrams in which the incident and scattered particles are connected by more than one line not included in the vertex part or the self-energy part; examples of such diagrams are shown in Fig. 2. For pseudoscalar mesons Fig. 2a is excluded by virtue of parity conservation. By 4-momentum conservation in the motion of particles which are described by a two-particle Green's function the Fourier component of (6) must be proportional to $\delta(p-p'+k-k')$. Furthermore, (6) must be a Lorentzian scalar consisting of components which are proportional to the isotopic tensors $\tau_i\tau_j$, $\tau_j\tau_i$, δ_{ij}; it must contain three scalars including the γ-matrices: $p\gamma$, $p'\gamma$, $(p+k)\gamma = (p'+k')\gamma$ and 6 other independent scalars p^2, p'^2, k^2, k'^2, $pk = p'k'$ and pp' or their linear combinations. Because of the symmetry of (5) with respect to the meson variables $\rho(p,\ p';\ ki,\ k'j)$ and $l\ (p,\ p';\ ki,\ k'j)$ should not change as a result of the substitutions $k \leftrightarrow -k'$, $i \leftrightarrow j$. As can bee seen from (5), with consideration of the fact that $CG^{-1T}(x,\ x')C^{-1} = G^{-1}(x,\ x')$ the functions $\rho(p,\ p';\ k,\ k')$ and $l\ (p,\ p';\ ki,\ k'j)$ must also be invariant with respect to charge conjugation, consisting in this case of transposition, the subsitution $p \leftrightarrow -p'$ and the replacements $\gamma_\alpha^T \rightarrow -\gamma_\alpha$, $\gamma_5^T \rightarrow -\gamma_5$, $\tau_i^T \rightarrow -\tau_i$; from these conditions it follows that we can assume *

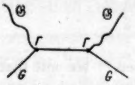

Fig. 1.

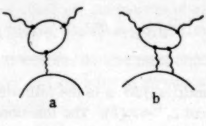

Fig. 2.

$$\left.\begin{aligned}(1+\mathrm{Int})\int dp''\,[\Gamma_{5i}(p,\ p'',\ k)\,G(p'')\,\Gamma_{5j}(p'',\ p';\ -k')] \\ l(p,\ p';\ ki,\ k'j)\end{aligned}\right\} = $$

$$= \delta(p-p'+k-k')(1+\mathrm{Int})\sum_{\lambda=0,1}(\gamma p+m)^{\lambda_1}(\gamma(p+k)+m)^{\lambda_2}(\gamma p'+m)^{\lambda_3}(\tau_i\tau_j)^{\lambda_4}\times$$

$$\times\begin{cases}\varphi^1_{\lambda_1\lambda_2\lambda_3\lambda_4}(p^2,\ p'^2,\ (p+k)^2,\ (k-k')^2;\ k^2,\ k'^2), \\ \varphi^2_{\lambda_1\lambda_2\lambda_3\lambda_4}(p^2,\ p'^2,\ (p+k)^2,\ (k-k')^2,\ k^2,\ k'^2),\end{cases} \qquad (7)$$

where $(\tau_i\tau_j)^0 = \delta_{ij}$ and Int denotes the interchanges $i \leftrightarrow j$, $k \leftrightarrow -k'$. Since $\Gamma_{5i} \sim \gamma_5\tau_i$ it is evident that $\varphi^1_{\lambda_1\lambda_2\lambda_3 0} = 0$. For scattering problems we require only the value of (6) for $\gamma p = \gamma p' = -m$, $k^2 = k'^2 = -\mu^2$, in

---

* A similar formula is obtained by Nambu [9]; the author became aware of this after the present article was completed and presented at a seminar of the Moscow State University.

connection with which we limit ourselves to a consideration of the functions $\varphi^{j}_{0\lambda_2 0\lambda_4}(-m^2, -m^2, (p+k)^2, (k-k')^2, -\mu^2, \mu^2)$ which we shall write briefly as $\varphi^{j}_{\lambda_2\lambda_4}((p+k)^2, (k-k')^2)$ and the sum of which we shall denote as $\varphi_{\lambda_2\lambda_4}((p+k)^2, (k-k')^2) = \varphi^1 + \varphi^2$. Now representing the matrix element of (5) in the form of different possible sums of products of matrix elements of less than 4 operators over intermediate states we can reach the familiar result (see [5]) that (6) can have a pole only for "real" intermediate states in which energy is conserved, while the rule for encircling the poles depends ultimately on the causality principle [5]. From an examination of different sections of the diagrams it follows that φ^1_λ and φ^2_λ can have poles for energies of the intermediate states given by $p_0 + k_0 = p'_0 = k'_0$, and φ^2 for the intermediate state energy $|p_0 - p'_0| = |k_0 - k'_0|$. In the first case the poles must, for example, be of the form

$$\frac{1}{-(p_0+k_0)^2 + M^2 - i\varepsilon} = P\,\frac{1}{-(p_0+k_0)^2 + M^2} + \pi i\delta(-(p_0+k_0)^2 + M^2), \tag{8}$$

i. e., the functions $\varphi^i((-p_0+k_0)^2)$ have a negative imaginary part and are regular for $\operatorname{Im}[-(p_0+k_0)^2] > 0$. Using now the theory formulated in [6] and passing to a relativistic notation we find that the functions $\varphi_{\lambda_2\lambda_4}$ can be represented as Stieltjes' integrals:

$$\varphi_{\lambda_2\lambda_4}((p+k)^2, (p-p')^2) = \int_0^\infty\!\!\int_0^\infty \frac{d\omega'_{\lambda_2\lambda_4}(M_1^2)\, d\omega''_{\lambda_2\lambda_4}(M_2^2)}{[(p+k)^2 + M_1^2 - i\varepsilon]\,[(k-k')^2 + M_2^2 - i\varepsilon]}, \tag{9}$$

where $\omega(M)$ are nondecreasing functions of limited change. It follows from a study of the diagrams that $M_1^2 = m^2$, or $M_1^2 \geq (m+\mu)^2$ and $M_2^2 > (2\mu)^2$.• Introducing now, as in (3) and (4), the functions $\nu_{\lambda_2\lambda_4}(t_1, t_2)$:

$$\begin{aligned}\nu_{\lambda_2\lambda_4}(t_1, t_2) = \int_0^\infty dM_1^2 \int_0^\infty dM_2^2 \exp\{-i[(M_1^2 - m^2)t_1 + (M_2^2 - (2\mu)^2)t_2]\} \times \\ \times [\delta(M_1^2 - m^2) + \theta(M_1^2 - (m+\mu)^2]\,\theta(M_2^2 - (2\mu)^2)\,\rho_{\lambda_2\lambda_4}(M_1^2, M_2^2),\end{aligned} \tag{10}$$

we can write (6) in the form

$$\begin{aligned}\rho(p, p'; ki, k'j)\Big|_{\substack{\gamma p = \gamma p' = -m \\ k^2 = k'^2 = -\mu^2}} = + ig^2\delta(p, p' + k - k')\, G(p)\,\mathfrak{G}(k) \times \\ \times \Big\{(1 + \mathrm{Int}) \sum_{\lambda = 1,2} (\gamma k)^{\lambda_2} (\tau_i\tau_j)^{\lambda_4} \int_0^\infty dt_1 \int_0^\infty dt_2 \exp\{-i[((p+k)^2 + m^2)t_1 + \\ + ((k-k')^2 + 4\mu^2)t_2]\,\nu_{\lambda_2\lambda_4}(t_1, t_2)\}\Big\}\, G(p')\,\mathfrak{G}(k').\end{aligned} \tag{11}$$

We now insert (11) into the general expression for the matrix element of the scattering T matrix given in [7, 8]. As a result we obtain

$$\begin{aligned}(p\sigma, ki\,|\,T\,|\,p'\sigma', k'j) = \frac{g^2}{(2\pi)^4}\,\bar{u}(p\sigma)\Big\{(1 + \mathrm{Int}) \sum_{\lambda = 1,2} (\gamma k)^{\lambda_2} (\tau_i\tau_j)^{\lambda_4} \int_0^\infty dt_1 \int_0^\infty dt_2 \times \\ \times \exp\{-i[((p+k)^2 + m^2)t_1 + ((k-k')^2 + 4\mu^2)t_2]\}\,\nu_{\lambda_2\lambda_4}(t_1, t_2)\Big\} \times \\ \times u(p'\sigma')\,|_{p+k = p'+k'}.\end{aligned}$$

• In [6] another limiting condition is given: $\sup\limits_{y \to \infty} |y\,\varphi(iy)| < \infty$; we assume that this is satisfied for regularized functions. Moreover, in (10) and (11) it is assumed that the energy-momentum vector in intermediate states is time-like and that the integration over M_1^2 is thus taken from 0; if this condition is not satisfied the integration must be taken from $-|M_{10}^2|$. The spectral representation of (6) is analytically continued on the real semi-axis going around the poles from above [$-i\epsilon$ in (9)].

Thus on the basis of very general assumptions, without resorting to the field equations, we have introduced 4 functions of 2 parameters which give the scattering completely*; the dependence on the momenta is to a considerable extent separated out, and this enables us to make a number of predictions regarding the behavior of the scattering cross section without specifying the type of interaction.

We now indicate the conditions which determine the relation between the different spectral functions of the two-particle and one-particle Green's functions. On the basis of Schwinger's equation [3] with the supplementary causality condition, for pseudoscalar coupling we can find that

$$\delta(p-p')\,G(p)=\frac{1}{\gamma p+m}\Big\{\delta(p-p')-\frac{ig^2}{(2\pi)^4}\gamma_5\tau_i\int\frac{(dk)\,(dk')}{\gamma(p-k)+m}\gamma_5\tau_j\times \\ \times\,[\delta_{ij}\mathfrak{G}(k)G(p)\delta(p-p')\,\delta(k'-k)+\rho(p-k+k',\,p';\,ki,\,k'j)]\Big\}. \tag{12}$$

Inserting the above expressions into (12) and integrating over k, k', with results which are too complicated to give here, we obtain a relation between the spectral functions of the one-particle and two-particle Green's functions. The writing of the scalar functions using parameters such as proper time obviated several difficulties associated with divergences in the integration over momenta. Another condition is associated with the fact that, as follows from an examination of (5), the half sum of the limits which (5) approaches when $(x_0-x_0') \longrightarrow \pm 0$ and also the half sum of the limits of the derivative of (5) with respect to ξ_0 or ξ_0' as $\xi-\xi_0' \longrightarrow \pm 0$ must be separately equal to zero. Hence it follows that

$$\lim_{\alpha\to 0}\int k_0\sin\alpha k_0\cdot\rho(p,p';\,ki,\,k'j)\,dk_0=\lim_{\alpha\to 0}\int\sin\alpha p_0\cdot\rho(p,\,p';\,ki,\,k'j)\,dp_0=0, \tag{13}$$

where α approaches zero after integrating. These conditions establish the relation between the residues of the function ρ at the different poles.

The author is grateful to D. D. Ivanenko for his continued interest and to N. N. Bogoliubov and W. Thirring for comments.

LITERATURE CITED

[1] H. Lehman, Nuovo Cimento 4, 11, 342 (1954).

[2] M. Gell-Mann and F. E. Low, Phys. Rev. 95, 1300 (1954).

[3] J. Schwinger, Proc. Nat. Acad. Sci. US 37, 452, 455 (1951).

[4] J. Schwinger, Phys. Rev. 82, 5, 664 (1951).

[5] M. Gell-Mann, M. L. Goldberger, and W. E. Thirring, Phys. Rev. 95, 1612 (1954).

[6] N. I. Akhiezer and I. M. Glazman, Theory of Linear Operators in Hilbert Space (Moscow, 1950), p. 211.

[7] H. Lehmann, Symanzik, and W. Zimmerman, Nuovo Cimento Ser. 10, 1, 205 (1955).

[8] A. Klein, Phys. Rev. 99, 3, 998 (1955).

[9] Y. Nambu, Phys. Rev. 100, 1, 394 (1955).

Received June 27, 1956

M. V. Lomonosov Moscow State University

---

* The value of g^2 in (11) can be associated with the value of the pseudovector coupling constant, considering for p-scattering the limiting case of small k as was done in [8].

MEASUREMENTS OF THE Li^6 (n,t) He^4 CROSS SECTION FOR NEUTRONS WITH ENERGIES FROM 9 TO 700 KEV

G. V. Gorlov, B. M. Gokhberg, V. M. Morozov, and G. A. Otroshchenko

(Presented by Academician A. P. Aleksandrov, July 21, 1956)

At the beginning of 1953, following the measurements of the total cross sections for the interactions of monoenergetic neutrons with Li^6 and Li^7 [1], we measured the cross section of $Li^6(n,t)He^4$ in the neutron energy range from 9 to 700 kev.

Monoenergetic neutrons in this range were obtained from the reaction $T(p,n)He^3$. The angular distribution and dependence of neutron energy on the angle of emission in this reaction are given in [2]. The tritium target at the center of the measuring room was a molybdenum disk 0.2 mm thick bearing a titanium film of 280 $\mu g/cm^2$. The titanium film was saturated with tritium to an atomic coefficient of 1.8. When protons of ~ 1200 kev struck the target their energy loss in the titanium film was ~ 28 kev. The protons were accelerated by an electrostatic generator [3]. In order to obtain neutrons with energies from 9 to ~ 350 kev the protons were accelerated to 1214 kev, and monoenergetic neutrons in the given range could be separated out at different angles with the proton beam. By increasing the proton energy we were able to obtain neutrons of higher energies. The neutron fluxes were monitored by three "long" boron counters; the absolute value of the fluxes was determined by comparison with a standard neutron source.

Measurements were performed in a room of the dimensions 3 × 3 × 2.5 m. The walls of the room were made of a mixture of paraffin and borax.

Investigation of the neutron background scattered from the walls of the room showed that at angles from 0 to 80° the background did not exceed a few percent of the principal neutron flux at a given angle. At large angles (> 140°) the background was a considerable fraction of the flux, reaching 60%. Since the experimental conditions made the background very stable and it was measured with high statistical accuracy we were able to take this background into account without greatly increasing the over-all error of the measurements.

In order to measure the relative change of cross sections for $Li^6(n,t)He^4$ we constructed a small ionization chamber with helical electrodes of 25 mm length and 20 mm diameter. On the electrodes there was deposited ~ 0.5 g of lithium fluoride containing an enriched mixture of lithium isotopes (Li^6 content ~ 92%). The cylindrical shell of the chamber and the hemispherical bottom and cover were made of copper 0.3 mm thick. The chamber was filled with commercial argon at 10 atmospheres and was operated at 150 v. The features of the pulse characteristic of this chamber were unimportant to us since it was intended for measurements of relative change of cross sections and the reaction energy of $Li^6(n,t)He^4$ is considerably greater than neutron energies in the investigated range.

In order to measure the absolute cross section for $Li^6(n,t)He^4$ we prepared three flat ionization chambers. The chambers contained platinum disks bearing thin films (~ 150 $\mu g/cm^2$) of lithium fluoride containing an enriched mixture of lithium isotopes (Li^6 content ~ 92%). The diameter of the deposited films was ~ 5 cm. The separation of the electrodes in the chambers was 10 mm. The 0.5 mm steel shell of each chamber was sealed at its ends with a 0.1 mm nickel foil. The chambers were filled with commercial argon to a pressure of ~ 4 atmos and were operated at ~ 350 v. The number of Li^6 nuclei in each chamber was determined by weighing. The flat ionization chambers intended for absolute measurements had quite satisfactory pulse characteristics. In determining the number of pulses corresponding to the total number of reaction events in the chamber, extrapolation of the chamber characteristics to zero for the discriminator gave an error not exceeding 5%.

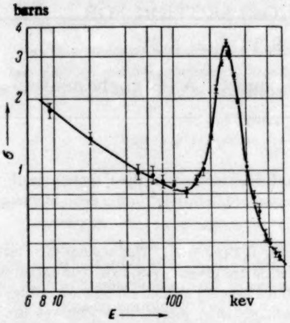

Fig. 1.

For measurements of the relative change of the cross section the helix ionization chamber was placed on a rotatable optical bench at a distance of 15 cm from the center of the target. By rotation of the optical bench, the chamber could be placed at any angle to the proton beam from 0 to 170°. The chamber was surrounded by a cadmium screen for shielding from thermal neutrons. The background of epicadmium neutrons was determined by measurements at different distances between the chamber and target (15, 30, and 60 cm), since at these distances the absolute value of the background was practically constant. The calculations took into account the intrinsic chamber background; it should be noted that the number of background pulses in the majority of cases did not exceed 3% of the total number of chamber counts and only at ~ 170° did it reach 10%. In addition we took into account the neutron scattering in the target backing (this is important only at large angles, where the intensity of the neutron flux drops sharply). The flux of neutrons scattered in the backing was calculated at 1.5% of the direct neutron flux. About 80% of these scattered neutrons have energies from 30 to 200 kev.

Measurements of the absolute cross section for $Li^6(n,t)He^4$ were performed for 100 and 265 kev neutrons. Background determination and shielding from thermal neutrons were similar to those for the measurement of relative change of the cross section.

The flat chambers possessed worse energy resolution than the coil chamber. Therefore, in measurements of the cross section with 265 kev neutrons (at the cross section peak), knowing the shape of the curve from relative measurements, we introduced a correction for the resolving power of the flat ionization chamber. The ratio of cross sections for 265 and 100 kev in the relative and absolute measurements agreed within 3%.

The measurements are presented in Fig. 1. The horizontal axis gives neutron energies in the laboratory system; the vertical axis gives the cross section for $Li^6(n,t)He^4$. At each point the statistical errors of the relative measurements are indicated. The cross section for 265 kev neutrons is 3.4 ± 0.3 barns. The error in the absolute measurements is greater than the error in the relative measurements because the flux of the standard neutron source was known to within ~ 7%. For low neutron energies (E_n < 50 kev) the cross section increases. Extrapolation into the thermal region according to the 1/v law does not conflict with the known value of the $Li^6(n,t)He^4$ cross section for thermal neutrons.

Blair and Holland investigated the energy dependence of the $Li^6(n,t)He^4$ cross section for neutrons from 150 to 625 kev, also using an electrostatic generator. Their results were published in the collection [4]. Comparison with our data gives good agreement for the cross section peak and the shape of the curves, but the location of the peak in their data differs from ours by 15 kev in the direction of lower energies. It should be noted that this difference lies within the limits of the resolving power of both experiments (~ 25 kev).

These results for the dependence of the $Li^6(n,t)He^4$ cross section on neutron energy, in conjunction with our data for the total cross section of neutron interaction with Li^6 in the same energy range [1], permit certain conclusions regarding the state of the intermediate Li^7 nucleus. As will be seen, resonance for 265 kev neutrons is due basically to the p-wave interaction of neutrons with the Li^6 nucleus, i. e., interference between the s-wave interaction and the potential interaction is weak. Therefore, without great error we can represent the total cross section σ_{tot} of neutron interactions with Li^6 close to resonance by the sum of the potential cross section σ_0 and the resonance cross section

$$\sigma_{tot} = \sigma_0 + \frac{\pi}{k^2}\,\frac{2I+1}{6}\,\frac{\Gamma_n\Gamma}{(E_0-E)^2+\Gamma^2/4}, \qquad (1)$$

where $\underline{k}$ is the wave number of a neutron with energy E; E_0 is the neutron resonance energy; $\Gamma = \Gamma_t + \Gamma_n$; Γ_t and Γ_n are partial reaction widths; I is the total spin of the intermediate nucleus. Similarly we can write the cross section $\sigma(n,t)$ of the reaction $Li^6(n,t)He^4$ as

$$\sigma(n, t) = \sigma' + \frac{\pi}{k^2}\,\frac{2I+1}{6}\,\frac{\Gamma_n\Gamma_t}{(E_0 - E)^2 + \Gamma^2/4}, \qquad (2)$$

where σ' is the fraction of the cross section due to the effect of other levels of the excited Li^7 nucleus (principally a level in the thermal region). Unfortunately it is very difficult to evaluate σ_0 and σ' objectively. Therefore, we have calculated σ_0 from scattering by a solid sphere (0.7 barns) and σ' from the cross section of $Li^6(n,t)He^4$ in the thermal region using the $1/v$ law (estimated at ~ 0.3 barns). The ratio of the resonance terms in (1) and (2) makes it possible to determine Γ_n/Γ_t:

$$\frac{\sigma_{tot} - \sigma_0}{\sigma(n, t) - \sigma'} = 1 + \frac{\Gamma_n}{\Gamma_t}. \qquad (3)$$

Using our measurements of σ_{tot} and $\sigma(n,t)$ and the indicated estimates of σ_0 and σ' we obtain from (3) $\Gamma_n/\Gamma_t = 1.87$. Inserting this ratio in (1) we obtain for $I = {}^3/_2;\ {}^5/_2;\ {}^7/_2$ the values $\sigma_{tot} = 6.5;\ 9.5;\ 12.4$. As can be seen, $I = {}^5/_2$ gives very good agreement with experiment. $I = {}^5/_2$ corresponds to values of the orbital angular momentum l of a neutron from 1 to 4. Thus in the production of a given excited level of a Li^7 nucleus with spin $I = {}^5/_2$ the s-wave interaction plays no part. At the same time the contribution of neutrons with large angular momentum increases strongly with l. Therefore, we assume that in the production of a given level of an intermediate Li^7 nucleus in the reaction under investigation the p-wave interaction is almost exclusively involved. Roberts et al. [5] come to the same conclusion on the basis of their measurements of the angular distribution of tritons in the $Li^6(n,t)He^4$ interaction. Johnson, Willard, and Bair [6], using our measurements of the total cross section for neutron interactions with Li^6 and the data of Blair and Holland [4] for $Li^6(n,t)He^4$ also conclude that a predominant part is played by the p-wave interaction in the production of the given excited state of Li^7.

LITERATURE CITED

[1] G. V. Gorlov, B. M. Gokhberg, V. M. Morozov, and G. A. Otroshchenko, Doklady Akad. Nauk SSSR 110, 6, 963 (1956).[Soviet Physics – Doklady, p. 598].

[2] B. M. Gokhberg, G. V. Gorlov, V. M. Morozov, and V. A. Shigin, J. Tech. Phys. (U.S.S.R.) 26, 5, 986 (1956) [Soviet Physics – Technical Physics, p. 964].

[3] G. V. Gorlov, B. M. Gokhberg, V. M. Morozov, and G. A. Otroshchenko, Doklady Akad. Nauk SSSR 102, 2, 237 (1955).

[4] Neutron Cross Sections, Atomic Energy Commission Report AECU 2040 (Office of Technical Services, Washington, D. C., 1952).

[5] J. H. Roberts, L. Darlington, and J. Haugsnes, Phys. Rev. 82, 2, 299 (1951); L. E. Darlington, J. Haugsnes, H. M. Mann, and J. H. Roberts, Phys. Rev. 90, 6, 1049 (1953).

[6] C. H. Johnson, H. B. Willard, and J. K. Bair, Phys. Rev. 96, 4, 985 (1954).

Received May 3, 1956

INTERACTIONS OF FAST PIONS AND NUCLEI

L. P. Kudrin and B. A. Nikol'skii

(Presented by Academician L. A. Artsimovich July 21, 1956)

The interaction of high-energy nucleons and pions with a nucleus can be regarded as a convenient instrument for the study of the properties of the nucleus. It may be expected that when the wavelength of the incident particle is smaller or comparable with the internucleonic separations in the nucleus, experiments on the interaction of the fast particles with nuclei will be sensitive to such nuclear characteristics as the distribution of nucleons in the nucleus or the energy spectrum of the nuclear nucleons. However, since we know too little about the structure of the nucleus, an exact calculation of the interaction of nucleons and pions with nuclei is impossible at present. Therefore, our conclusions about nuclear properties can at present be based only on models, the plausibility of which is determined by comparing experiments and calculations.

The present work compares with experiment the calculation of the inelastic scattering of 160-Mev π^--mesons by photographic emulsion nuclei assuming individual meson-nucleon interactions inside the nucleus. This hypothesis is favored by the data which we have for inelastic pion scattering in nuclei.

Experimental Results

In this work we used a beam of π^--mesons, with energy E_π = 188 ± 6 Mev, extracted from the synchrocyclotron of the Institute for Nuclear Problems of the Academy of Sciences USSR. After traversing a deflecting magnet and collimator, the π^--meson beam entered a film emulsion stack consisting of 30 layers of 395μ thickness and 70 mm diameter each. We used a type "R" NIKFI (Cine-Photographic Scientific Research Institute) emulsion. In order to facilitate the tracing of particle tracks traversing a few layers, the emulsions were imprinted with an x-ray reference grid consisting of lines with ~ 35μ thickness and ~ 3 mm spacing. We selected "stars" located in the emulsion stack in such a way that the π^--mesons which produced them had to traverse a distance of 4.3 ± 0.9 cm, losing 28 ± 6 Mev. Thus the experimental results refer to π -mesons of energy E_π = = 160 Mev. We found altogether 1185 cases of interactions between π^--mesons of the indicated energy and emulsion nuclei. Of these we observed an inelastically scattered charged pion in 323 cases. The method chosen for finding cases of pion interactions consisted of area scanning with 450 × magnification. Therefore we did not in effect record elastic pion-nuclear interactions or 0-pronged stars in cases where the inelastically scattered pion lost less than 80 Mev.* Identification of pion scattering was accomplished by determining the gradient of on-track grain density; energies were determined from grain densities and ionization ranges in those cases where the pion track was contained within the emulsion stack.

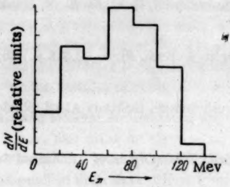

Fig. 1. Energy spectrum of pions scattered in the angular range θ = 90-180°.

---

* The number of such cases was small and allowance for them cannot change the conclusions of this work.

From examination of 323 cases of inelastic pion interactions with emulsion nuclei we obtained the energy and angular distributions of scattered π^--mesons.

For further interpretation of the experimental material Fig. 1 gives the energy spectrum of pions scattered at angles $\theta = 90\text{-}180°$. This spectrum has a mean energy $E_{\text{exp}} = 64 \pm 3$ Mev and a half width

$$\Delta E_{\text{exp}} = \sqrt{\frac{(\bar{E}-E_i)^2}{n-1}} = (30.9 \pm 3) \text{ Mev}.$$

Calculation of 160-Mev π^--Meson Interactions with Emulsion Nuclei

We calculated the energy and angular spectra of 160-Mev π^--mesons scattered by emulsion nuclei on the assumption that the characteristics of meson-nucleon collisions in a nucleus are similar to the corresponding characteristics of interactions between π^--mesons and free nucleons.

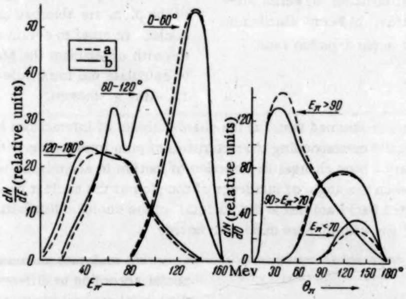

Fig. 2. Comparison of angular and energy spectra of a pion colliding with a single nuclear nucleon in the reactions: a) $\pi^- + p \rightarrow \pi^- + p$; b) $\pi^- + n \rightarrow \pi^- + n$. The momentum distribution of the nucleons corresponds to a degenerate Fermi gas with $E_{\text{max}} = 30$ Mev.

In order to determine the sensitivity of our results to the assumed energy and angular dependence of meson-nucleon collisions in a nucleus we compared the corresponding calculated π^--meson distributions after a single collision with a moving nuclear proton and neutron. The results are given in Fig. 2. Since the π^--meson scattering cross sections on protons and neutrons have different angular and energy dependence it follows from Fig. 2 that the calculations of pion scattering at the indicated energy by nuclear nucleons are insensitive to the cross section characteristics for interactions of pions and nuclear nucleons.

Figure 3 shows the energy and angular spectra of π^--mesons scattered by nuclear neutrons and protons on the assumption that nuclear nucleons have the momentum distribution of a degenerate Fermi gas with maximum energies of 30 and 20 Mev. Figure 3 shows that pion scattering by nuclear nucleons is also insensitive to the details of the nuclear nucleon energy distribution.

In describing experiments on elastic scattering of pions by nuclei according to the optical model it was necessary to use the real part of the pion-nucleus interaction potential:

$$V(r) = \begin{cases} V_0 \text{ for } r \le R, \\ 0 \text{ for } r > R, \end{cases}$$

where R is the nuclear radius.

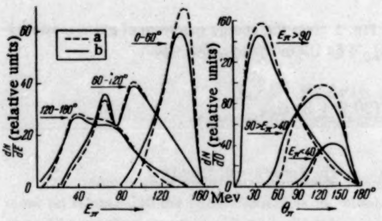

Fig. 3. Energy and angular spectra of π^--mesons colliding with a single nuclear nucleon: a) Fermi distribution with E_{max} = 20 Mev; b) Fermi distribution with E_{max} = 30 Mev. The neutron-proton ratio corresponds to A ~ 100.

It is obvious that V is the average pion-nucleus interaction potential which must also appear in experiments on inelastic pion scattering by nuclei.

The insensitivity of the angular and energy spectra of pions scattered by nuclear nucleons to the details of the meson-nucleon interaction in the nucleus enables us to obtain a quite reliable estimate of the magnitude of V from experiments on inelastic pion scattering by nuclei.

In order to determine the mean interaction potential between pions and nuclei one must estimate the number of pions undergoing 1, 2, etc. collisions with nuclear nucleons, as well as the changes in the spectrum of scattered pions resulting from the fact that a fraction of the pions are absorbed and do not emerge from the nuclei. In order to obtain results suitable for comparison with experiment the Monte Carlo method was used to calculate the intranuclear cascade produced by 160-Mev π^--mesons.

In this calculation it was assumed that: a) the characteristics of interactions between pions and nuclear nucleons do not differ from the corresponding characteristics of pion interactions with free nucleons; b) in passing through the nuclear boundary a pion changes its direction of motion in accordance with the magnitude of the mean nuclear potential; when the angle of incidence of the pion at the nuclear boundary is sufficiently large the particle may be reflected backward inside the nucleus; c) the nucleon distribution inside the nucleus was that of a degenerate Fermi gas with 30 Mev maximum energy.

TABLE 1

π-meson energy in Mev	Sign of pion	V	Reference
48	+	—15	[1]
62	—	—18	[2]
62	+, −	—20	[3]
60—105	+, —	—19	[4]
125	—	—30	[5]

We took into account the absorption of pions by nuclei according to different models and showed that the results are insensitive to the possible assumptions regarding the character of pion absorption by nuclei. The calculations were based on 517 instances of interactions between π^--mesons and emulsion nuclei. Since the emulsions consisted of heavy (A ~ 100) and light (A ~ 14) nuclei the calculation covered the characteristics of both types of nuclei.

From a knowledge of the mean energy and relative numbers of particles experiencing 1, 2, etc. collisions with nuclear nucleons and emerging from a nucleus a comparison with experiment permits an evaluation of the mean nuclear potential for π^--mesons with $\overline{E}_{exp}$ = 160 Mev.

The calculation showed that the energy spectrum of pions issuing from nuclei in the angular range θ = = 90-180° has a half-width of ΔE_{calc} = 31± 2.5 Mev and mean energy before leaving the nuclei of $\overline{E}_{calc}$ = = 88 ± 5 Mev. Thus the mean interaction potential of π^--mesons with 160 Mev was $V = \overline{E}_{exp} - \overline{E}_{calc} = -(24 \pm 6)$ Mev. This value of V is in agreement with the mean interaction potential between pions and nuclei which is obtained from experiments on elastic pion-nucleus scattering.

The values of V obtained from experiments on elastic pion-nucleus scattering are given in Table 1.

It should be noted that the determination of the mean interaction potential between 160-Mev pions and nuclei from experiments on elastic scattering is of considerable difficulty and has not yet been accomplished, because nuclei are practically transparent to pions at this energy.

In conclusion the authors wish to thank Professor I. I. Gurevich for discussion of the results, Corresponding Member of the Academy of Sciences USSR M. G. Meshcheriakov for making it possible to perform the experiments on the synchrocyclotron of the Institute for Nuclear Problems of the Academy of Sciences USSR, A. E. Ignatenko and A. I. Mukhin for their assistance with the irradiation of the nuclear emulsions, and S. A. Ali-Zade, G. V. Kolganova, and A. A. Kondrashina for other assistance.

LITERATURE CITED

[1] A. M. Shapiro, Phys. Rev. 84, 1063 (1951).

[2] A. Minguzzi, Nuovo Cimento 12, 799 (1954).

[3] L. M. Lederman, H. Byfield, and J. O. Kessler, Phys. Rev. 90, 344 (1953).

[4] E. C. Fowler and W. B. Fowler et al., Phys. Rev. 91, 135 (1953).

[5] J. O. Kessler and L. M. Lederman, Phys. Rev. 94, 689 (1954).

Received May 31, 1956

ON AN INTERMEDIATE SYSTEM FORMED DURING THE SCATTERING OF ELEMENTARY PARTICLES

M. S. Livshits

(Presented by Academician N. N. Bogoliubov July 9, 1956)

1. In the present article we attempt to investigate the properties of an intermediate system which is formed during the collision of two elementary particles subject to the assumption that the interaction between the particles results from a quasi-charge coupling the corresponding fields. We use the expression [1]

$$S_0(W)=\frac{1+\frac{iP}{2}\varphi(W)}{1-\frac{iP}{2}\varphi(W)}(\hbar=c=1) \tag{1}$$

for the scattering matrix in the simplest case of two-particle collisions $a_1 + a_2 \rightarrow C \rightarrow a_2 + a_1$ (the angular momentum l and the spins of particles a_1 and a_2 are zero), which is a generalization of the Wigner-Eisenbud formula [2]. In (1) P denotes the total decay probability of the intermediate system C; $\varphi(W)$ is defined by

$$\varphi(W)=((A-WI)^{-1}\mathbf{e}_0, \mathbf{e}_0), \tag{2}$$

where A is the self-adjoint energy operator of a "closed box"; $\mathbf{e}_0$ is a unit vector; $W=\sqrt{m_1^2+p^2}+\sqrt{m_2^2+p^2}\cdot$ $\cdot\,(m_1 \geq m_2)$ is the total energy of the system.

We shall seek P and $\varphi(W)$ using as an example the scattering of a photon by an electron where the electron "at first" absorbs a photon with 4-momentum k_2', and "later" emits a photon with 4-momentum k_2''. For this purpose we consider the corresponding second-approximation scattering matrix elements [4]:

$$S^{(2)}_{i\rightarrow f}=\frac{ie^2}{2\sqrt{\omega'\omega''}}\,\bar{u}''\left\{\hat{e}''\,\frac{i\hat{f}_1-m}{f_1^2+m^2}\,\hat{e}'\right\}u'\,(2\pi)^4\,\delta(k_1'+k_2'-k_1''-k_2'') \tag{3}$$

and go over to the new variables

$$\mathbf{k}=\mathbf{k}_1+\mathbf{k}_2,\quad \zeta=\frac{k_{2z}}{|k_2|},\quad W=|\mathbf{k}_2|+\sqrt{m^2+|\mathbf{k}_1|^2},\quad \alpha=\arctan\frac{k_{2y}}{k_{2x}}, \tag{4}$$

where $\mathbf{k}_1$, $\mathbf{k}_2$ are the electron and photon momenta.

The volume element is transformed according to

$$d\mathbf{k}\,dW\,d\zeta\,d\alpha\rightarrow\frac{d\mathbf{k}_1 d\mathbf{k}_2}{|k_2|^3}(\mathbf{v}_1-\mathbf{v}_2,\mathbf{k}_2),$$

and the matrix $S^{(2)}$ in the new representation is

$$(\zeta'\alpha'|S^{(2)}|\zeta''\alpha'')=\sqrt{\frac{|\mathbf{k}_2'|^3\,|\mathbf{k}_2''|^3}{(\mathbf{v}_1'-\mathbf{v}_2',\mathbf{k}_2')(\mathbf{v}_1''-\mathbf{v}_2'',\mathbf{k}_2'')}}\,S^{(2)}_{i\rightarrow f}.$$

Since in the c.m. system $\mathbf{k}' = \mathbf{k}'' = 0$, after some simple transformations the scattering matrix for this system can be written as *

$$(\zeta'\alpha' \,|\, S^{(2)} \,|\, \zeta''\alpha'') = \frac{il^2}{2}(2\pi)^4 \frac{W_1 W_2}{W_1 + W_2} u''^* \{\hat{e}''(m\beta - WI)^{-1}\hat{e}'\} u', \tag{5}$$

where

$$\beta = \left\| \begin{matrix} 1 & & & \\ & 1 & & \\ & & -1 & \\ & & & -1 \end{matrix} \right\|, \quad W_1 = p = |\mathbf{k}_1| = |\mathbf{k}_2|, \quad W_2 = \sqrt{m^2 + p^2}.$$

For small values of the product $P\varphi(|x|)$, Eq. (1) becomes

$$S_0 - I \cong iP((A - WI)^{-1}\mathbf{e}_0, \mathbf{e}_0). \tag{6}$$

From (5) and (6), averaging over all photon and electron polarizations, we have

$$\begin{gathered} P = \alpha \frac{W_1 W_2}{W_1 + W_2} \quad \left(\alpha = \frac{e^2}{2\pi}\right), \\ \varphi(W) = \overline{u''^* \{\hat{e}''(m\beta - WI)^{-1}\hat{e}'\} u'} = \frac{1}{4}\operatorname{Sp}(m\beta - WI)^{-1} = \frac{W}{m^2 - W^2}. \end{gathered} \tag{7}$$

Since $W = p + \sqrt{m^2 + p^2}$, we can write $\varphi(W)$ as

$$\varphi(W) = -\frac{1}{2p}. \tag{8}$$

2. If we assume that (7) and (8) remain valid for particles of any mass m_1 and m_2 ($m_1 \geq m_2$) the scattering matrix S_0 will be

$$S_0 = \frac{1 - \frac{i\alpha}{2}\,\frac{W_1 W_2}{(W_1 + W_2)\,2p}}{1 + \frac{i\alpha}{2}\,\frac{W_1 W_2}{(W_1 + W_2)\,2p}} = \frac{v_1 + v_2 - \frac{i\alpha}{4}}{v_1 + v_2 + \frac{i\alpha}{4}},$$

where $W_1 = \sqrt{m_1^2 + p^2}$; $W_2 = \sqrt{m_2^2 + p^2}$; α is the coupling constant between the corresponding fields. It is interesting to note that for $m_1 = m_2$ this function differs only in sign from the scattering matrix which Heisenberg used [5] to determine the mass of a stable "atomic nucleus" composed of two identical particles. From (8) we can obtain the energy operator A of the intermediate system regarded as a "closed box" and the vector $\mathbf{e}_0$. Using the relation $W = \sqrt{m_1^2 + p^2} + \sqrt{m_2^2 + p^2}$, we have

$$\varphi(W) = -\frac{1}{\sqrt{\zeta^2(W) - m_2^2}}; \quad \zeta = \frac{1}{2}\left(W - \frac{\mu_1\mu_2}{W}\right), \tag{9}$$

where $\mu_1 = m_1 - m_2$, $\mu_2 = m_1 + m_2$.

To construct A and $\mathbf{e}_0$ we introduce wave functions $f(\lambda)$ of the form $f(\lambda) = \begin{pmatrix} f_1(\lambda) \\ f_2(\lambda) \end{pmatrix}$ ($\mu_1 \leq \lambda \leq \mu_2$) and define the scalar product by

$$(f, g) = \frac{1}{2m_2}\int_{\mu_1}^{\mu_2} [f_1^*(\lambda) g_1(\lambda) + f_2^*(\lambda) g_2(\lambda)]\, d\lambda. \tag{10}$$

---

* We have omitted δ functions.

Futhermore, we consider the operators M and σ defined by

$$Mf(\lambda) = \lambda f(\lambda), \quad \sigma f(\lambda) = \begin{pmatrix} f_1(\lambda) \\ -f_2(\lambda) \end{pmatrix} \quad (\mu_1 \leqslant \lambda \leqslant \mu_2). \tag{11}$$

In was shown in [6] that $\varphi(W)$ determines the corresponding operator A and vector $\mathbf{e}_0$ to within a unitary equivalence-class. Hence it follows that A and $\mathbf{e}_0$ can be constructed according to

$$Af(\lambda) = \sigma Mf(\lambda), \quad e_{01}(\lambda) = e_{02}(\lambda) = \frac{\sqrt{m_2/\pi}}{\sqrt[4]{m_2^2 - \zeta^2(\lambda)}} \quad (\mu_1 \leqslant \lambda \leqslant \mu_2). \tag{12}$$

Indeed, from (10), (11), and (12) it follows that

$$\begin{aligned} ((A - WI)^{-1}\,\mathbf{e}_0, \mathbf{e}_0) &= \frac{1}{2\pi}\int_{\mu_1}^{\mu_2}\left(\frac{1}{t - W} + \frac{1}{-t - W}\right)\frac{dt}{\sqrt{m_2^2 - \zeta^2(t)}} = \\ &= \frac{1}{2\pi}\int_{\mu_1}^{\mu_2}\frac{dt}{(t - W)\sqrt{m_2^2 - \zeta^2(t)}} + \frac{1}{2\pi}\int_{-\mu_2}^{-\mu_1}\frac{dt}{(t - W)\sqrt{m_2^2 - \zeta^2(t)}} = \\ &= -\frac{1}{2\sqrt{\zeta^2(W) - m_2^2}}. \end{aligned} \tag{13}$$

The last equality was obtained from the theory of residues for the function $F(\lambda) = \dfrac{1}{(t - \lambda)\sqrt{\zeta^2(\lambda) - m_2^2}}$.

Now knowing A and $\mathbf{e}_0$ we can write the equation for the decay of the intermediate system C. According to [1] this equation is

$$i\frac{df}{dt} = H^* f,$$

where

$$H^* f = M\sigma f - \frac{iP}{2}(f, \mathbf{e}_0)\mathbf{e}_0.$$

From (11) and (12) it follows that if the masses of both particles are greater than zero, A has a continuous spectrum filling the ranges $m_1 - m_2 \leq \lambda \leq m_1 + m_2$ and $-m_1 - m_2 \leq \lambda \leq m_2 - m_1$. This fact enables us to prove [7] that if at some instant of time we eliminate the incident wave then for t → ∞ the number of particles formed in C will approach a nonzero limit and they will thus be practically stable particles.* The only exception is the case $m_2 = 0$ in which the spectrum of A reduces to the two points $\pm m_1$.

Let us now assume that the spins of particles a_1 and a_2 are $^1/_2$ and 0, respectively. Taking (5) as an example again, we introduce 4-vectors and consider the 4th-order diagonal matrix

$$\tilde{\varphi}(W) = \| ((M\beta - WI)^{-1} e^{(j)}, e^{(k)}) \|,$$

where $e^{(j)}$ (j = 1, 2, 3, 4) are orthogonal unit vectors with the components

$$e_k^{(j)} = \sqrt{\frac{2m_2}{\pi}}\,\frac{1}{\sqrt[4]{m_2^2 - \zeta^2(\lambda)}}\,\delta_{jk} \quad (j, k = 1, 2, 3, 4;\ \mu_1 \leqslant \lambda \leqslant \mu_2).$$

---

* This refers to stability against decay into the particles a_1 and a_2.

The diagonal elements $\tilde{\varphi}_{jj}(W)$ are

$$\tilde{\varphi}_{11}(W) = \tilde{\varphi}_{22}(W) = \frac{1}{\pi}\int_{\mu_1}^{\mu_2} \frac{dt}{(t - W)\sqrt{m_2^2 - \zeta^2(t)}},$$

$$\tilde{\varphi}_{33}(W) = \tilde{\varphi}_{44}(W) = \frac{1}{\pi}\int_{\mu_1}^{\mu_2} \frac{dt}{(-t - W)\sqrt{m_2^2 - \zeta^2(t)}}.$$

It is easily verified that $\varphi(W) = \frac{1}{4}\operatorname{Sp}\tilde{\varphi}(W)$. According to (1) the scattering matrix $\tilde{S}_0(W)$ can be written as

$$\tilde{S}_0(W) = \frac{1 + \frac{iP}{2}\tilde{\varphi}(W)}{1 - \frac{iP}{2}\tilde{\varphi}(W)}.$$

The decay equation of the intermediate system can be written as

$$i\,\frac{df}{dt} = M\beta f - \frac{iP}{2}Jf,$$

where

$$Jf = \sum_{j=1}^{4}(f, e^{(j)})\,e^{(j)}.$$

The equation of motion of the intermediate system can easily be written in relativistically invariant form. Thus, for example, the equation of motion of the system C regarded as a closed box will be

$$i\,\frac{\partial f}{\partial t} = [(\vec{\alpha}\mathbf{k}) + M\beta]\,f,$$

where $\mathbf{k} = \mathbf{k}_1 + \mathbf{k}_2$ is the momentum of the system.

Hence it follows that M plays the part of the rest mass. The particles of C thus possess a continuous spectrum of virtual rest masses in the range $m_1 - m_2 \leq \lambda \leq m_1 + m_2$ $(m_1 \geq m_2 > 0)$.

LITERATURE CITED

[1] M. S. Livshits, Doklady Akad. Nauk SSSR 111, 1, 67 (1956) [Soviet Physics, Doklady, p. 620].

[2] E. P. Wigner and L. Eisenbud, Phys. Rev. 72, 29 (1947).

[3] J. M. Blatt and V. F. Weisskopf, Theoretical Nuclear Physics (Foreign Lit. Press, 1954).

[4] A. I. Akhiezer and V. B. Berestetskii, Quantum Electrodynamics (1953).

[5] W. Heisenberg, Z. Physik 123, 1-2 (1944).

[6] M. S. Livshits, Doklady Akad. Nauk SSSR 97, 3 (1954).

[7] M. S. Livshits, J. Exptl.-Theoret. Phys. (U.S.S.R.) 31, 121 (1956) [Soviet Physics – J.E.T.P., p. 91].

Received June 2, 1956

Odessa Hydrometeorological Institute

SPECTROPHOTOMETRIC METHOD OF INVESTIGATING DISPERSION AND ABSORPTION BY SOLIDS

M. P. Lisitsa

(Presented by Academician A. N. Terenin July 9, 1956)

Quantitative investigations of the absorption spectra of solids encounter a number of difficulties associated with exact allowance for scattered light. In studying the possiblities for a complete account of reflection losses we developed a method which permits the plotting of a reliable absorption curve, and also of a dispersion curve in the same spectral region. The principal variations of the method follow.

Variation I. Let a parallel light beam with intensity I_0 impinge on an absorbing plane-parallel layer. If the intensities of transmitted and reflected beams are denoted by I_d and I_r, respectively, complete allowance for multiple reflections inside the layer leads to the relations [1]

$$\frac{I_d}{I_0} = \frac{(1-R)^2 e^{-Kd}}{1-R^2 e^{-2Kd}} = D, \tag{1}$$

$$\frac{I_r}{I_0} = \frac{R\,[1-e^{-2Kd}\,(2R-1)]}{1-R^2 e^{-2Kd}} = \mathfrak{R}, \tag{2}$$

where K is the absorption coefficient; d is the layer thickness; R is the coefficient of surface reflection; D and $\mathfrak{R}$ are the transmission and reflection coefficients of the entire layer.

Formulas (1) and (2) are valid for all angles of incidence, but we shall consider only the simplest case of normal incidence. We know that then

$$R = \frac{n^2+\kappa^2-2n+1}{n^2+\kappa^2+2n+1}, \tag{3}$$

where n and κ are the real and imaginary parts of the complex index of refraction $\mathfrak{N} = n - i\kappa$ with

$$\kappa = \frac{K\lambda}{4\pi}. \tag{4}$$

Determining D and $\mathfrak{R}$ experimentally with the aid of (1) and (2) we first obtain R and K:

$$R = \frac{D^2-\mathfrak{R}^2+2\mathfrak{R}+1+\sqrt{(D^2-\mathfrak{R}^2+2\mathfrak{R}+1)^2-4\mathfrak{R}\,(2-\mathfrak{R})}}{2\,(2-\mathfrak{R})}, \tag{5}$$

$$K = \frac{1}{2d}\ln\frac{R\,[R\,(\mathfrak{R}-2)+1]}{\mathfrak{R}-R}; \tag{6}$$

then by the formula

$$n = \frac{1+R+\sqrt{4R-(1-R)^2\kappa^2}}{1-R}, \tag{7}$$

which was derived from (3) we calculate the refractive index. κ is determined from (6) and (4).

In investigations of anisotropic substances, both in this and the following variations, the measurements must be made with polarized light.

Variation II differs from the preceding in that D and R are directly measured quantities. The initial formulas are (1) and (2). The shortcoming of this variation compared with the other is the need for preparing an additional sample in the form of a wedge or with one polished surface. Only then can one determine R by eliminating reflection from the opposite face.

We obtain the absorption coefficient K from (1):

$$K = \frac{1}{d} \ln \frac{2DR^2}{-(1-R)^2 + \sqrt{(1-R)^4 + 4D^2R^2}}. \tag{8}$$

Calculating κ from (8) and (4) we then determine the refractive index from (7).

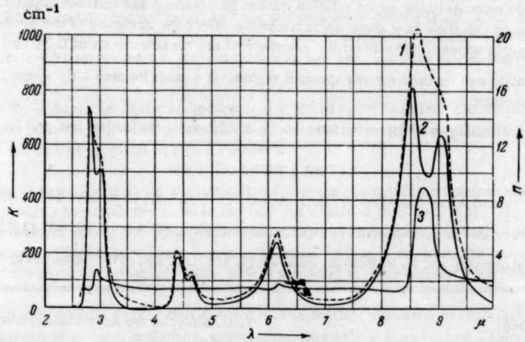

Fig. 1.

This variation was used to plot a dispersion curve and an absorption curve for gypsum. We used the data of G. A. Zaitsev and B. S. Neporent [2], taking the case in which the electric vector of the incident light wave was parallel to the direction of the fibrous cleavage structure of the crystal. The results of these calculations are given in Fig. 1. Curve 1 represents the absorption coefficient with complete neglect of reflection. It corresponds to transmission Curve II in Fig. 3 of [2]. Curve 2 of Fig. 1 represents the true absorption calculated from (6) and Curve 3 gives the dispersion of the refractive index.

It is striking not only that there is a large quantitative discrepancy in the absorption as given by Curves 1 and 2, but also that there is a strong qualitative difference between the two curves. While the two extreme intense absorption bands of Curve 2 are split into two components, Curve 1 and the corresponding Curve II of [2] do not show this splitting although it must occur. G. A. Zaitsev and B. S. Neporent attempted to detect the splitting but their attempts to resolve the 3300-3600 cm^{-1} band by using large dispersion (with an LiF prism) and smaller sample thickness (to 2μ) were not successful. They were also unable to resolve the 1100-1200 cm^{-1} band. This failure is entirely due to reflection, which is especially large in the absorption band. Increased dispersion of the spectroscopic instrument and reduced thickness of the sample in this and similar instances cannot in principle improve the result. Only the simultaneous use of experimental findings and the relationships given above permits a strict allowance for reflection losses and the construction of the true absorption and dispersion curves.

It is predicted in [2] that the peak of one of the unresolved components of the 1150 cm^{-1} band should be around 1120 cm^{-1}. On our calculated Curve 2 this peak is at 1105 cm^{-1}, thus differing from the prediction by

15 cm^{-1}. For this spectral region such a discrepancy is not large but the possibility remains that it is actually smaller.

In concluding the presentation of the results it should be mentioned that the numerical values of the refractive index and of the absorption coefficients near 1150 and 3450 cm^{-1} may differ a little from the actual values. The transmissivity of the sample investigated in [2] was very low here so that it was difficult to determine it with the required accuracy from Fig. 3 of [2]. In addition, low transmissivity appreciably increases the errors for D [3]; as a result of such errors the dispersion curve was spread considerably around 8.75 μ. The disappearance of the band in Curve 3 around 4.5 μ results from the absence of the corresponding band in the reflection spectrum. This interesting effect deserves further study, as was correctly pointed out in [2].

A test of the second variation convincingly emphasizes its great possibilities. The first variation has just as good possibilities. But the most attractive is a third variation which is based on use of transmitted light beams alone. Here it is necessary to measure D for two samples of different thicknesses and then solve a set of two equations like (1). Unfortunately, the exact solution cannot be obtained and suitable approximations must be used. Only further study can show how these approximations affect the accuracy of the method. The accuracy of the first two variations depends entirely on the accuracy of the measurements of D, $\mathfrak{R}$ and R.

The above method can be used for any spectral region. It cannot be used only where interference effects must be taken into account.

The author is profoundly grateful to Professor A. A. Shishlovskii for his interest and for discussions.

LITERATURE CITED

[1] M. P. Lisitsa and A. A. Shishlovskii, Bull. Acad. Sci. U.S.S.R., Phys. Ser. 17, 5, 660 (1953).

[2] G. A. Zaitsev and B. S. Neporent, J. Exptl.-Theoret. Phys. (U.S.S.R.) 29, 857 (1955).

[3] V. M. Chulanovskii and N. P. Penkin, Bull. Acad. Sci. U.S.S.R., Phys. Ser. 1945, 3, 206.

Received April 9, 1956

T. G. Shevchenko Kiev State University

ENRICHMENT OF RADIOACTIVE ISOTOPES OF IODINE, GERMANIUM, ARSENIC, AND ANTIMONY BY (γ,n) REACTIONS

A. N. Murin, V. D. Nefedov, V. I. Baranovskii, and D. K. Popov

(Presented by Academician A. P. Vinogradov July 13, 1956)

We here communicate the results of a few experiments on enrichment of radioactive isotopes by irradiation of a number of elements with gamma rays produced by the synchrotron of the Lebedev Physics Institute of the Academy of Sciences USSR [1]. The cross sections for (γ,n) reactions are usually small. Thus, for example, the maximum cross section for $Sb^{123}(\gamma,n)Sb^{122}(F\gamma = 14.8$ Mev) is only $0.362\cdot 10^{-24}$ cm^2 with an integral cross section of the order of 2 Mev·barns; For $As^{75}(\gamma,n)As^{74}$ the integral cross section is about 0.8 Mev·barns; for $I^{127}(\gamma,n)I^{126}$ it is ~ 2 Mev·barns. Thus the preparation of samples with high specific activity requires suitable variations of the Szilard-Chalmers method. Investigations in this area are very few in number and are represented by [2-5].

In addition to the isotope aspect, the radiochemical study of (γ,n) reactions can be important for the chemistry of radioactive atoms in the high-energy region, since the recoil energy in a (γ,n) reaction exceeds by three orders of magnitude the energy supplied in a (n,γ) reaction.

For the purpose of enrichment we, in the majority of cases, used organic compounds which had previously been employed successfully to enrich the radioactive isotopes obtained from (n,γ) [6]. The samples were irradiated for 48 hours by bremsstrahlung from the synchrotron of the Physics Institute of the Academy of Sciences USSR with 265 Mev maximum. Targets were placed on a cylindrical surface 2 cm from the beam axis and did not disturb the course of the main experiments. Only 10% of the total gamma intensity was used.

Special control experiments showed that there was practically no neutron background in the beam. Our results for the enrichment of arsenic, antimony, germanium, and iodine are given in Table 1. *

It should be noted that prolonged irradiation of targets leads to considerable radiation-chemical decomposition of the compounds; this, of course, reduces the corresponding enrichment factors. It must also be pointed out that a number of short-lived impurities are formed, so that the samples must be stored for 36 hours after irradiation or purified by additional operations.

We consider it our pleasant duty to thank Professor P. A. Cherenkov and Professor V. I. Gol'danskii as well as P. S. Baranov for valuable advice and assistance in the irradiation of the samples.

LITERATURE CITED

[1] V. I. Veksler, Atomic Particle Accelerators (Acad. Sci. USSR Press, 1956).

[2] W. H. Barkas, P. R. Carlson, J. E. Henderson, and W. H. Moore, Phys. Rev. 58, 577 (1940).

[3] D. Ch. Hoffman and Don S. Martin, J. Phys. Chem. 56, 1097 (1952).

---

* In this table, the tabulated values of the enrichment factors and radioisotope yields are the averages of five well reproduced experiments; typical values are given for the activity of the samples.

TABLE 1

Element	Compound	Reaction	Method of enrichment	Activity in pulses per min			Yield %	Enrichment factor	Half-life (days)		E_β, Mev	
				original solution	impoverished fraction	enriched fraction			Measured (av)	Tab.	Meas.	Tab.
I	KIO_3	$I^{127}(\gamma,n)I^{126}$	Extraction of iodine by carbon tetrachloride from an iodic acid solution of potassium iodate diluted with HNO_3	2600	2250	340	13	10^3	13.7	13.7	0.87	0.87
Ge	$(C_6H_5)_4Ge$	$Ge^{70}(\gamma,n)Ge^{69}$	Adsorption of inorganic germanium from a solution of irradiated $(C_6H_5)_4Ge$ in dioxane, on MnO_2	575	205	370	64	10^3-10^4	1.6	1.65	1.1	1.215
Sb	$(C_6H_5)_3SbCl_2$		Adsorption of inorganic antimony on chromium hydroxide from an alcohol solution of the irradiation sample	2730	375	2355	86	10^3-10^4	2.8	2.83	1.8	1.94 1.36
		$Sb^{123}(\gamma,n)Sb^{122}$	Extraction of inorganic antimony by 2N HCl from an ether solution of the irradiated sample	530	320	235	44	10^3				
As	$(C_6H_5)_3AsCOOH$	$As^{75}(\gamma,n)As^{74}$	Adsorption of inorganic arsenic on $Al(OH)_3$ from an alcohol solution of the irradiated sample	600	430	160	29	10^3	17.3	17.8	0.92 1.4 0.6	0.92 1.36 0.69
	$(C_6H_5)_3As$		Adsorption of inorganic arsenic on $Fe(OH)_3$ from an alcohol solution of the irradiated sample	478	294	174	36	10^3				
			Extraction of inorganic arsenic from an ether solution of the irradiated sample in 6N HCl	537	380	152	34	10^3-10^4				

[4] H. Morinaga and D. J. Zaffarano, Phys. Rev. 93, 1422 (1954).

[5] J. Pouli and P. Süe, Comptes rend. 240, 2226 (1955); 241, 197 (1955).

[6] A. N. Murin and V. D. Nefedov (Collection) Tracers in Analytic Chemistry (Acad. Sci. USSR Press, 1955), p. 75; Collection of Articles on Radiochemistry, Leningrad State University (1955).

Received July 2, 1955

V. G. Khlopin Radium Institute
Academy of Sciences USSR
A. A. Zhdanov Leningrad State University

SATURATION MEASUREMENTS OF ULTRASONIC ABSORPTION IN ETHYL ACETATE USING AN IMPULSE METHOD WITH TWO FIXED DISTANCES

V. F. Nozdrev and V. D. Sobolev

(Presented by Academician V. V. Shuleikin November 29, 1955)

The most complete representation of the structure of liquids or of the processes which take place in them through ultrasonic measurements is obtained when the measurements include the relaxation region, for which the dispersion and anomalous absorption of ultrasound are characteristic.

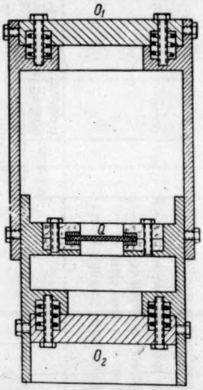

Fig. 1

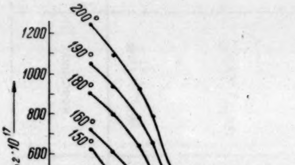

Fig. 2

Some articles are available concerning the investigation of the acoustic properties of liquids which relax in experimentally attainable frequency regions [1, 8]. Recently A. M. Sultanov and one of the present authors [2] detected and investigated two relaxation regions in ethyl acetate between 3 and 30 Mc at temperatures from −40° to +40°.

There are no measurements of absorption in relaxing liquids at temperatures above the boiling point. But such measurements are very important for an understanding of the nature of liquid relaxation. We have taken the first step toward the investigation of absorption in relaxing liquids from the saturation curve at high pressures and temperatures.

In our experiments we used an impulse method of measuring absorption with the pulse generator built in the laboratory of the Moscow Regional Pedagogical Institute under the supervision of one of the present authors [3, 4].

We developed and applied a new impulse technique for measuring ultrasonic absorption, the method of two fixed distances, which permits the covering of broad temperature and pressure ranges and avoids difficulties in constructing the mechanism which shifts the reflector, while maintaining a perfect seal of the experimental vessel. This method is a combination of the methods of the fixed and variable distances.

A quartz plate Q fastened in a holder (Fig. 1) transforms an electrical into an ultrasonic pulse and radiates in the direction of two reflectors O_1 and O_2 which are at different distances from the quartz.

The signals are reflected back to the quartz at different times and produce two spatially separated pulses on the oscilloscope screen.

The absorption coefficient is calculated from the formula

$$\alpha = \frac{\Delta A}{20\,\Delta l\,\log e}, \qquad (1)$$

where ΔA is the change in amplitude of sonic pressure in decibels; Δl is the difference in the acoustic paths of the pulses reflected by the first and second reflectors.

In absorption measurements within the region where high ultrasonic absorption is observed we used the impulse method of a single fixed distance which was developed by V. F. Iakovlev [5].

Trial absorption measurements using the double fixed-distance method in normal butyl alcohol for the range 0°-90° and in toluene for the range 20°-270° gave good agreement with the results of other methods [6, 7] of measuring absorption.

Our measuring chamber was a steel autoclave designed for pressures of the order of a few hundred atmospheres at above 300°.

Ultrasonic absorption in ethyl acetate was measured by the saturation curve at seven frequencies between 5 and 15 Mc.

Our data gave the temperature and frequency dependence of the absorption (Fig. 2). Figure 2 shows that α/ν^2 decreases sharply as the frequency increases from 5 to 9 Mc and changes only slightly with further increase of frequency. A comparison of our results for the frequency dependence of α/ν^2 with the relaxation theory leads to the conclusion that the frequency range which we investigated includes the region where relaxation of volume viscosity occurs and the region where α/ν^2 is approximately constant.

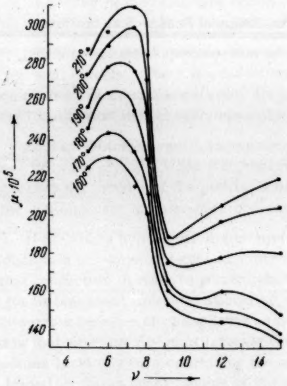

Fig. 3

We obtained a frequency dependence for excess absorption per wavelength (Fig. 3) that establishes the presence of a relaxation process in ethyl acetate from 160° to 210°, which is confirmed by the pronounced peaks of the curves. Our experiment shows that this process continues up to the critical point [9].

Our measurements of ultrasonic absorption provided the possibility of calculating the characteristics of the detected relaxation process. From the peaks of the curves of excess absorption per wavelength we obtained relaxation times that decrease from 2.65×10^{-8} to 2.12×10^{-8} sec as the temperature rises from 160° to 210°, which is of the same order of magnitude as the relaxation time in acetic acid [8].

According to the relaxation theory the anomalous absorption of ultrasound and the relaxation of volume viscosity must be accompanied by dispersion. Our calculations show that the latter quantity increases slowly with temperature from 0.08 to 0.1%. This indicates dispersion in ethyl acetate is practically unchanged over a broad temperature range and is small in accordance with the relaxation theory. The change of α/ν^2 with frequency also leads to the conclusion that ultrasonic absorption in ethyl acetate agrees qualitatively with the phenomenological relaxation theory.

It is impossible, considering the state of the problem, to make any conclusive statement regarding the molecular mechanism of the relaxation process. However, on the basis of the characteristics which we observed, it can be assumed that the relaxation process in ethyl acetate is associated with molecular excitation, which, as in the case of acetic acid [8], does not involve a change of volume. The activation energy of the relaxation process which is obtained on the basis of this hypothesis has the average value 1.824 kcal/mole, which is close in order of magnitude to the relaxation activation energy of acetic acid.

In order to determine the molecular mechanism of relaxation during the passage of ultrasonic waves in ethyl acetate we believe it is necessary to carry out a complicated investigation using ultrasonic and spectroscopic methods. Such investigations are now being performed in our laboratory.

LITERATURE CITED

[1] I. G. Mikhailov and V. A. Solov'ev, Progr. Phys. Sci. (U.S.S.R.) 1953, No. 5.

[2] V. F. Nozdrev and A. M. Sultanov, Doklady Akad. Nauk SSSR 104, 6 (1955).

[3] V. F. Nozdrev and N. I. Koshkin, Doklady Akad. Nauk SSSR 92, 4 (1953).

[4] V. F. Nozdrev, N. I. Koshkin, and V. F. Iakovlev, Doklady Akad. Nauk SSSR 96, 2 (1954).

[5] V. F. Iakovlev, Ultrasonic Investigations of Matter, 1, Moscow Regional Pedagogical Institute 1955.

[6] V. F. Nozdrev and V. I. Stremousov, Doklady Akad. Nauk SSSR 96, 3 (1954).

[7] T. M. Ledneva, Dissertation, Moscow State University, 1953.

[8] I. Lamb and I. M. Pinkerton, Proc. Roy. Soc. A 199, 114 (1949).

[9] V. D. Sobolev, Dissertation, Moscow Regional Pedagogical Institute (1955).

Received November 11, 1955

Moscow Regional Pedagogical Institute

IONIC CONDUCTIVITY OF KI(Tl) PHOSPHORS

L. M. Shamovskii, A. A. Dunina and M. I. Gosteva

(Presented by Academician A. F. Ioffe, July 19, 1956)

From a comparison of the properties of pure alkali halide crystals and the corresponding thallium-activated phosphors Bonanomi and Rossel [1] concluded that the activator does not play an important part in the actual luminescence process. The pure salts at low temperatures (~ 77°K) luminesce brightly when light is absorbed even without activators. For these salts as well as for ordinary types of phosphors it is characteristic that the spectral luminescence curve is independent of the exciting energy. They are used as detectors in radioactivity counters because the scintillation pulses in such crystals increase proportionately to the energy of the ionizing radiation [2]. An activator, which creates a system of electron-acceptor levels, only stabilizes the luminescence process, since it reduces the probability of nonradiative recombinations of electrons and holes in the crystal lattice.

In addition to nonradiative recombinations of electrons and holes photochemical processes take place in pure crystals. It has been shown that the latent image in silver halide salts appears either on the surface of the crystals or at dislocations [3, 4]. These surfaces are able to localize photoelectrons. Under the influence of the local potential gradients which thus arise, mobile cations move to the localization sites of the electrons and are neutralized thus precipitating silver atoms and their colloidal clusters. Sensitizers such as Ag_2S, which are precipitated mainly at dislocations, serve as acceptors for holes and hinder their recombination with electrons or chemical interactions between the metal and halide atoms precipitated on the surfaces.

Something of the same kind occurs in alkali halide crystals. Here, however, besides the electron-acceptor levels associated with dislocations there are also electron trap levels within the lattice in the form of F centers.

It is a reasonable hypothesis that deep cooling of the crystals sharply reduces the equilibrium concentration of structural defects. There is a reduction of the concentration of mobile cations and of their rate of migration. The movement of cations is necessary for photolysis in crystals. Under these conditions, dislocations, are important as the localization sites of electrons and holes and of their radiative recombinations, i. e., luminescence.

Both in photolysis and in luminescence the localization of electrons on contact surfaces creates local gradients within the crystal. When the product of the concentration of migrating cations by their mobility is much larger than the product of the positive hole concentration and mobility, photolytic processes occur predominantly; in the opposite case luminescence predominates.

If the above hypotheses are correct the activator in alkali halide phosphors, in addition to its ability to produce a micro-heterogeneous structure in single crystals with deep electron (or hole) levels, must suppress cation conduction in order to prevent photolysis.* It has long been known that any type of loosening of the crystal (of its polygonal structure) associated with plastic deformation or the introduction of impurities results in a considerable increase of cation (structure-sensitive) conduction [6].** But from these facts it does not at all follow that any impurity must increase ionic conductivity even if the impurity develops a crystal mosaic. The literature lacks any data concerning the effect of activators on ionic conductivity of phosphors; such data would be important for an understanding of the luminescence mechanism of alkali halide phosphors.

For electrical conductivity measurements we choose pure KI crystals and KI(Tl) phosphors grown from a melt by the Stockbarger method. From these specimens small cubes measuring ~ 0.5 cm^3 were cut. Two opposing faces of each crystal were covered with a thin layer of colloidal graphite and platinum electrodes were applied.

---

* This is implied by our ideas about the structure of these phosphors and the luminescence mechanism [5].

** Alkali halide crystals possess unipolar cation conductivity below 400-500°C [6].

The sample was clamped in a quartz spring with flat end surfaces and heated in a regulated electric furnace. Thermostatic control was maintained within ± 5°. The electrical conductivity was measured with alternating current from a 1000 cycle audiofrequency generator by a bridge and ac amplifier. The electrode potential did not exceed 10 v so that during the measurements the sample temperature could not rise due to Joule heat.

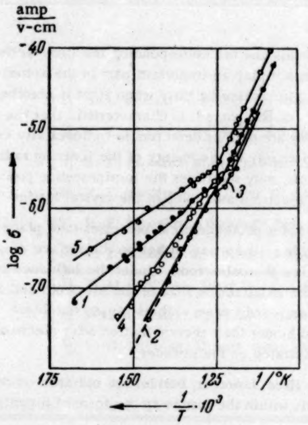

Fig. 1.

The results of conductivity measurements as a function of temperature are given in Fig. 1 in logarithmic coordinates. Curve 1 represents the experimental findings for pure KI. These practically coincide with the measurements by Lehfeldt [7]. According to our data the intrinsic conductivity of KI is

$$\sigma = 1.5\cdot 10^5 \exp(-3890/kT)\ \text{amp/v-cm}$$

and in the structure-sensitive part

$$\sigma = 3.68 \exp(-15576/kT)\ \text{amp/v-cm}$$

The dashed line 2 in Fig. 1 is the extrapolation of the intrinsic conductivity of the crystal to lower temperatures. Such conductivity would correspond to an "ideal" crystal containing only equilibrium structural defects of thermodynamical character.

Curve 3 represents the conductivity of KI(Tl) with 0.01% by weight of TlI (in the melt). In the low temperature branch a considerable reduction of conductivity is observed. Curve 3 almost coincides with Curve 2 for an "ideal" crystal. The high-temperature part of the curve has approximately the same slope as for pure KI, but somewhat lower electrical conductivity. However, no quantitative conclusions can be derived from this difference because it corresponds to a temperature difference of 6.5°, which is almost within the limits of experimental error.

For a KI(Tl) phosphor with 0.1% of TlI by weight (Curve 4) the structure-sensitive conductivity increases somewhat but still remains considerably below the values for the pure sample.

Curve 5 characterizes the conductivity of a KI(Tl) phosphor with high activator content (10% TlI by weight). In this instance the electrical conductivity of the crystal increases considerably both in the structure-sensitive part and in the intrinsic conductivity part and is higher by comparison with a pure KI crystal. It is quite probable that the rise of structure-sensitive conductivity results from multimolecular layers of TlI on intercrystalline surfaces. At high temperatures evaporation of the activator is observed in this phosphor, whereas for small proportions TlI is not removed even when heated in a vacuum. The rise of intrinsic conductivity of this sample compared with a pure crystal can apparently be explained by a 2.5% increase of the lattice parameter.

Our investigations enable us to draw the following conclusions:

1) When small quantities of the TlI activator are added the structure-sensitive conductivity of KI crystals drops sharply. In its effect this is equivalent to the deep cooling of pure crystals. A considerable drop of cation conductivity reduces the photolytic yield and increases the luminescence yield, i. e., the activator shifts the limits of luminescence quenching of the crystal into a higher temperature region.

2) The presence of an activator in a crystal does not essentially change the equilibrium concentration of the structural defects and their mobility, because the intrinsic conductivity of a crystal containing a small amount of activator remains practically the same as for pure crystals. But these defects (vacant cation and anion sites) remain less stable in a phosphor as localization sites for holes and electrons because of the presence of deeper electron-acceptor levels [9] (barrier layers on contact surfaces).

3) With considerable activator concentration the ionic conductivity rises sharply especially in the structure-sensitive region. Concentration quenching is manifested (in KI(Tl) for luminescence with the maximum at 410 mμ), which can be accounted for by the increasing importance of photochemical processes. It is clear that the temperature and concentration quenching of luminescence is associated with cation conductivity that competes with hole conductivity.

4) At low temperatures unactivated crystals acquire the properties of typical phosphors for the same reason, the decrease of ionic conductivity. Luminescence becomes possible then when a crystal possesses contact surfaces with more or less deep localization levels for electrons and holes, where even without the presence of an activator they can recombine and emit radiation.

5) The characteristics which have been established indirectly confirm the concept of a luminescence mechanism based on the microheterogeneous phosphor structure and double activator distribution. When the properties of typical phosphors are investigated it is necessary to take into account both electron-hole conductivity and ionic conductivity.

All-Union Minerals Institute

Received June 6, 1956

LITERATURE CITED

[1] I. Bonanomi and I. Rossel, Helv. Phys. Acta. 25, 7, 725 (1952).

[2] R. Swank, Ann. Rev. Nucl. Sci. 3, 111 (1954).

[3] N. Mott and R. Gurney, Electronic Processes in Ionic Crystals (Foreign Lit. Press, 1950).*

[4] I. Mitchell, Z. Physik. 138, 3-4, 381 (1954).

[5] L. Shamovskii, Optics and Spectroscopy (USSR) 1, 3, 407 (1956).

[6] R. M. Barrer, Diffusion in and through Solids (Foreign Lit. Press, 1948).*

[7] W. Lehfeldt, Z. Physik. 85, 717 (1933).

[8] W. Runciman and E. Steward, Proc. Phys. Soc. A 66, 484 (1953).

[9] L. Shamovskii and L. Rodionova, Doklady Akad. Nauk SSSR 92, 939 (1953).

---

* Russian translation.

ON THE THEORY OF DIELECTRIC POLARIZATION

M. N. Shakhparonov

(Presented by Academician V. V. Shuleikin, June 30, 1956)

Let us consider a macroscopic spherical sample of dielectric A with $N = \sum_{i=1}^{k} N_i$ molecules of components 1, 2,. . ., k, occupying volume V in a vacuum. Outside the sample there is a distribution of fixed charges which in the absence of the sample generate the field $\mathbf{E}_0$. The field $\mathbf{E}_0$ induces in the sample the electric moment $\mathbf{M}_{E_0} = \alpha_m \mathbf{E}_0$. The macroscopic polarizability of the sample α_m can be represented as a sum $\alpha_m = \alpha_m^c + \alpha_m^s$ where α_m^s is the part of the polarizability which depends on the dielectric surface; α_m^c is independent of the surface. We shall derive an equation which enables us to compute α_m^c and α_m^s from experimental information concerning the dielectric constant of dielectric A.

α_m^c and α_m^s can be divided into induction and orientational components:

$$\alpha_m^c = (\alpha_m^c)_{\text{or}} + (\alpha_m^c)_{\text{in}}, \tag{1}$$

$$\alpha_m^s = (\alpha_m^s)_{\text{in}} + (\alpha_m^s)_{\text{in}}. \tag{2}$$

The orientational components are associated with the presence of dipoles in the molecules of some of the dielectric constituents. The induction components result from the electronic and atomic polarizability of the molecules.

An electrostatic calculation [1] yields the following general expression for the macroscopic polarizability of a spherical sample:

$$\alpha_m = \alpha_m^c + \alpha_m^s = \left(\frac{3}{\varepsilon + 2}\right)\left(\frac{\varepsilon - 1}{4\pi}\right)V, \tag{3}$$

where ϵ is the dielectric constant of A in a static field. On the other hand statistical calculations for a very general molecular model of a dielectric [2-4] show that

$$\left(\frac{3}{\varepsilon + 2}\right)\left(\frac{\varepsilon - 1}{4\pi}\right)V = \left(\frac{3}{\varepsilon_\infty + 2}\right)\left(\frac{\varepsilon_\infty - 1}{4\pi}\right)V + \frac{\overline{M_s^2}}{3kT}, \tag{4}$$

where ϵ_∞ is the dielectric constant of A for high frequencies; $\mathbf{M}_s$ is the part of the total electric moment $\mathbf{M}_{E_0}$ which is associated with a definite molecular configuration for which it is independent of the external field $\mathbf{E}_0$. In the deduction of (4) it is assumed that there is no dielectric saturation.

From (1 - 4) it follows that:

$$(\alpha_m^c)_{\mathrm{or}} + (\alpha_m^s)_s = \frac{\overline{M_s^2}}{3kT}, \tag{5}$$

$$(\alpha_m^c)_{\mathrm{in}} + (\alpha_m^s)_{\mathrm{in}} = \left(\frac{3}{\varepsilon_\infty + 2}\right)\left(\frac{\varepsilon_\infty - 1}{4\pi}\right)V. \tag{6}$$

According to [2] $\mathbf{M}_S$ can be represented as the sum: $\mathbf{M}_S = \mathbf{M} + \mathbf{M}_s$, where $\mathbf{M}_s$ accounts for the effect of the spherical surface. If the spherical sample of dielectric A were surrounded by an infinite medium consisting of the same dielectric A, $\mathbf{M}_s$ would be zero. Therefore

$$(\alpha_m^c)_{\mathrm{or}} = \frac{\overline{M^2}}{3kT}, \tag{7}$$

where $\mathbf{M}$ is the electric moment of any given molecular configuration of the spherical sample of A when this sample is imbedded in a finite medium consisting of A. By definition:

$$\mathbf{M}_s = \sum_{i=1}^{k} \sum_{j=1}^{N_i} \vec{\mu}_{ij}; \tag{8}$$

μ_{ij} is the dipole moment of molecules (ij) in the absence of field $\mathbf{E}_0$. μ_{ij} includes the moment induced by all other molecules of the dielectric and depends not only on the position and orientation of molecules (ij) but also on the position and orientation of the other molecules of the sample. Using (8) we obtain

$$\overline{\mathbf{M}_s^2} = \sum_i \sum_j \overline{(\mu_{ij}\mathbf{M}_s)} = \sum_i \sum_j \overline{(\mu_{ij} \langle \mathbf{M}_s \rangle_{\mu_{ij}})}, \tag{9}$$

where $\langle \mathbf{M}_S \rangle_{\mu_{ij}}$ is the statistical mean value of moment $\mathbf{M}_S$ of the sample in a vacuum for fixed μ_{ij}. The replacement of $\mathbf{M}_S$ by $\langle \mathbf{M}_S \rangle_{\mu_{ij}}$ denotes neglect of the fluctuations of $\mathbf{M}_S$. If it is assumed that there is no distant orientational order in the sample and that its size is large compared with the distances at which the correlation between molecular orientations are important, the fluctuating changes of $\mathbf{M}_S$ can be ignored. Under these conditions [2-4]

$$\langle \mathbf{M}_s \rangle_{\mu_{ij}} = \left(\frac{3}{\varepsilon + 2}\right)\left(\frac{3\varepsilon}{2\varepsilon + 1}\right) \langle \mathbf{M} \rangle_{\mu_{ij}}, \tag{10}$$

where $\langle \mathbf{M} \rangle_{\mu_{ij}}$ denotes the statistical mean of $\mathbf{M}$ of the sample surrounded by dielectric A for fixed μ_{ij}. From (9) and (10) it follows that

$$\overline{\mathbf{M}_s^2} = \left(\frac{3}{\varepsilon + 2}\right)\left(\frac{3\varepsilon}{2\varepsilon + 1}\right)\overline{\mathbf{M}^2}. \tag{11}$$

Insertion of (11) and (7) in (5) gives

$$(\alpha_m^s)_{\mathrm{or}} = -\frac{2(\varepsilon - 1)^2}{(\varepsilon + 2)(2\varepsilon + 1)} \frac{\overline{M^2}}{3kT}. \tag{12}$$

By the Clausius-Mosotti equation:

$$\alpha_m^c = \sum_i N_i \bar{\alpha}_i = \left(\frac{3}{\varepsilon+2}\right)\left(\frac{\varepsilon-1}{4\pi}\right)V, \tag{13}$$

where $\bar{\alpha}_i$ is the average polarizability of molecules of type $\underline{i}$. A comparison of (3) and (13) shows that for substances which obey the Clausius-Mosotti equation $\alpha_m^s = 0$. We know that (13) is broadly applicable to dielectrics in high frequency fields (the Lorentz-Lorenz equation).

Therefore [see Equation (6)] we have

$$(\alpha_m^s)_{\text{ln}} \approx 0 \tag{14}$$

$$(\alpha_m^c)_{\text{ln}} \approx \sum_i N_i \alpha_i \approx \left(\frac{3}{\varepsilon_\infty+2}\right)\left(\frac{\varepsilon_\infty-1}{4\pi}\right)V. \tag{15}$$

Using (4), (7), (11) and (13) we obtain α_m^c:

$$\alpha_m^c = \frac{3}{4\pi}\left(\frac{2\varepsilon+\varepsilon_\infty}{3\varepsilon}\right)\left(\frac{\varepsilon-1}{\varepsilon_\infty+2}\right)V. \tag{16}$$

Subtracting (16) from (3) we obtain

$$\alpha_m^s = -\frac{(\varepsilon-1)^2(\varepsilon-\varepsilon_\infty)}{\varepsilon(\varepsilon_\infty+2)(\varepsilon+2)}\,\frac{V}{2\pi}. \tag{17}$$

Comparing (17) and (12) and taking (14) into account we have

$$(\alpha_m^c)_{\text{or}} = \frac{\overline{M^2}}{3kT} = \frac{V}{4\pi}\,\frac{(\varepsilon-\varepsilon_\infty)(2\varepsilon+1)}{\varepsilon(\varepsilon_\infty+2)}. \tag{18}$$

We now assume that the volume V contains one gram-molecule of dielectric A, i.e., $V = V_M = \frac{m}{\rho}$. We introduce the quantity $P = 4/3\,\pi\,\alpha_m^c$. According to (16) the molecular polarization P is given by

$$P = \left(\frac{\varepsilon-1}{\varepsilon_\infty+2}\right)\left(\frac{2\varepsilon+\varepsilon_\infty}{3\varepsilon}\right)V_M. \tag{19}$$

Equation (19) enables us to calculate the molecular polarization of polar and nonpolar dielectrics without distant orientational order. It thus becomes possible to calculate P for substances which do not obey the Clausius-Mosotti equation (except ferroelectrics).

If dielectric A is nonpolar, then $\varepsilon \approx \varepsilon_\infty$ and (19) becomes the familiar formula

$$P = \frac{\varepsilon-1}{\varepsilon+2}\,\frac{m}{\rho}. \tag{20}$$

In high frequency fields P equals the molecular refraction R.

It follows from (18) that the orientational part of the molecular polarization P_{or} is given by

$$P_{or} = \left(\frac{\varepsilon - \varepsilon_\infty}{3\varepsilon}\right)\left(\frac{2\varepsilon + 1}{\varepsilon_\infty + 2}\right) V_M = \frac{4\pi \overline{M^2}}{9kT}\ . \tag{21}$$

All molecules of type i are equivalent a priori. Therefore $\overline{M}^2$ can be represented as a sum:

$$\overline{M^2} = \sum_{i=1} N_i \overline{\mu_i^2}. \tag{22}$$

Using (15), (18) and (22) we obtain

$$P = \frac{4\pi}{3} N_A \sum_i x_i \left(\overline{\alpha_i} + \frac{\overline{\mu_i^2}}{3kT}\right), \tag{23}$$

where N_A is Avagadro's number; x_i is the concentration of molecules i in molar fractions.

We neglect short-range forces and the interaction energy between polar molecules. This is permissible for rarefied polar gases and dilute solutions of polar substances in nonpolar solvents. Then $\overline{\mu_i^2} \approx \mu_i^2$, $\epsilon \approx \epsilon_\infty$ and (23) becomes the familiar Debye equation.

M. V. Lomonosov Moscow State University

Received June 25, 1956.

LITERATURE CITED

[1] C. J. F. Böttcher, Theory of Electric Polarization (Amsterdam, 1952).

[2] J. G. Kirkwood, J. Chem. Phys. 7, 911 (1939).

[3] F. E. Harris and B. J. Alder, J. Chem. Phys. 21, 1031 (1953).

[4] F. E. Harris, J. Chem. Phys. 23, 1663 (1955).

SPONTANEOUS LATTICE DEFORMATION IN FERROGMAGNETIC TRANSITIONS

K. P. Belov and N. K. Panina

(Presented by Academician P. L. Kapitsa, July 21, 1956)

1. When a ferrogmagnetic substance is cooled below the Curie point a spontaneous lattice deformation takes place at the same time as the spontaneous magnetization. This was explained theoretically for the first time by Fowler and Kapitsa [1]. The spontaneous lattice deformation of ferromagnetics is of considerable interest since this phenomenon reveals a direct relation between the exchange energy which causes ferromagnetism and interatomic spacing.

The value of the spontaneous magnetization can now be obtained for many ferromagnetics without special difficulty, but the literature contains almost no information on the spontaneous lattice deformation.

In the present note we indicate a method of obtaining the spontaneous lattice deformation of ferromagnetics from measurements of the temperature dependence of magnetostriction and give the values obtained for a few alloys.

2. In [2], on the basis of the theory of phase transitions of the second kind, which was developed by Soviet authors [3, 4], we showed that the thermodynamic potential of a ferromagnetic near the Curie point can be represented as

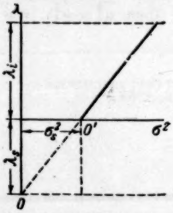

Fig. 1.

$$\Phi = \Phi_0 + a\sigma^2 + b\sigma^4 + cp + dp^2 + e\sigma^2 p - H\sigma.$$

Here σ is the specific magnetization; p is the mechanical stress; $H\sigma$ is the energy of the magnetic field; a, b, c, d and e are the thermodynamic coefficients, with d and e proportional to the elastic modulus and magnetostrictive constant, respectively. From the condition $\partial\Phi/\partial p = \omega$, where ω is the relative change of volume we obtain

$$\omega = c + 2dp + e\sigma^2.$$

Limiting ourselves to p = 0 and omitting the constant we have

$$\omega = e\sigma^2.$$

For a linear deformation, considering that $\sigma = \sigma_s + \sigma_i$, where σ_s is the spontaneous magnetization and σ_i is the true magnetization, we can write

$$\lambda = {}^1/_3 e(\sigma_s + \sigma_i)^2. \tag{1}$$

Thus the dependence of λ on the square of the spontaneous and true magnetizations, which was previously obtained on the basis of models [1], also follows from rigorous thermodynamic considerations. We shall represent this dependence graphically. In the absence of spontaneous magnetization there is no spontaneous deformation (for H = 0); let this state correspond to the point 0 in Fig. 1. When spontaneous magnetization occurs (for example, when cooled below the Curie point) spontaneous deformation also takes place, which from (1) is given by

$$\lambda_s = {}^1/_3 e\sigma_s^2. \tag{2}$$

This corresponds to the point 0'. If, in addition, we apply a magnetic field, we have true magnetization σ_i and the accompanying magnetostriction λ_i added to the spontaneous lattice deformation λ_s as σ_i is increased.

In practice we cannot directly measure λ_s, which is hidden in a ferromagnetic. In an applied field we observe only λ_i. This corresponds to the fact that in Fig. 1 the origin is shifted to the point 0'. It follows from Fig. 1 that when the magnetostriction λ_i is measured as a function of the square of the magnetization, then by extrapolating the straight line $\lambda_i(\sigma_i^2)$ to the axes we can determine not only the spontaneous magnetization but also the spontaneous deformation of the ferromagnetic lattice, which results from the exchange forces.

3. Fig. 2 gives the magnetostriction curves, – the square of the magnetization for an alloy of 31% Ni, 5% Co and 64% Fe at different temperatures in fields higher than for technical saturation. Measurements were made with a remote wire transducer the construction of which was described in [5]. The figure shows that at three temperatures the magnetostriction λ_i depends linearly on the square of the true magnetization. This magnetostriction, which accompanies the true magnetization, is isotropic.

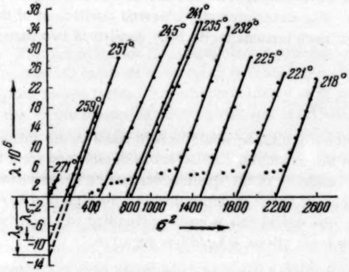

Fig. 2. Dependence of magnetostriction, which accompanies true magnetization, on σ^2 for an alloy consisting of 31% Ni, 5% Co and 64% Fe.

Extrapolating the straight lines in Fig. 2 to the horizontal axis we obtain the values of the spontaneous magnetization σ_s. This method of obtaining σ_s is similar to the familar method of determining σ_s from the curves of the magnetocaloric effect. When the lines of Fig. 2 are continued until they intersect with the vertical axis the last section gives values of the spontaneous lattice deformation λ_s. Thus from curves such as those in Fig. 2 it is easy to determine σ_s and the corresponding value of λ_s for each given temperature.

4. The form of temperature dependence of λ_s near the Curie point can be determined from thermodynamical considerations. Substituting in (2) the familar relation

$$\sigma_s^2 = \frac{\alpha_0'}{\beta}(\theta - T),$$

which also follows from the theory of phase transitions of the second kind [6], we obtain

$$\lambda_s = \frac{1}{3}\,\frac{\alpha_\theta' e}{\beta}(\theta - T), \tag{3}$$

i. e., near the Curie point λ_s like σ_s^2 must depend on T linearly.

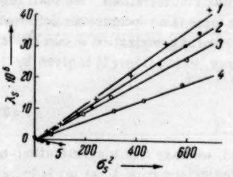

Fig. 3. Dependence of λ_s on σ_s^2 for alloys: 1) 32% Ni, 68% Fe; 2) 31% Ni, 5% Co, 64% Fe; 3) 33% Ni, 64% Fe; 4) 36% Ni, 64% Fe; 5) 97.6% Ni, 2.49% Si.

In experiments on alloys this linearity is not always observed; this is associated with inhomogeneity of alloy concentration [2]. Concentration inhomogeneity in an alloy results in "smearing out" of the ferromagnetic transition, so that the graphs of $\sigma_s^2(T)$ and $\lambda_s(T)$ are curved. Experiment shows, however, that the dependence of λ_s and σ_s^2 on T is identical. This indicates that (2), which establishes a linear dependence of λ_s on σ_s^2, must also be observed for inhomogeneous ferromagnetics. Fig. 3 provides good confirmation of this conclusion for all of the alloys which we investigated.

5. The value of the spontaneous lattice deformation enables us to determine the ferromagnetic anomalous thermal expansion in ferromagnetics. The experimentally observed coefficient of thermal expansion α for each ferromagnetic body consists of two parts:

$$\alpha = \alpha_{\sigma_s = 0} \pm \frac{d\lambda_s}{dT}. \tag{3}$$

Here $\alpha_{\sigma_s} = 0$ is the coefficient of thermal expansion which a substance would have if spontaneous magnetization were absent; $d\lambda_s/dT$ is the ferromagnetic anomaly of the expansion coefficient as determined from the temperature dependence of the spontaneous lattice deformation. The sign of the second term is determined by the sign of $d\lambda_s/dT$ during heating. For nickel this is positive (leading to a positive anomaly α); for Invar alloys, $d\lambda_s/dT$ is negative.

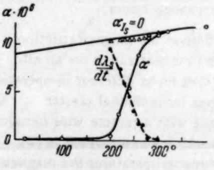

Fig. 4.

Fig. 4 gives the temperature dependence of α for Invar alloy (31% Ni, 5% Co, 64% Fe) obtained with a Shevenar dilatometer. Adding in Fig. 4 to the ordinate α (for each given temperature) the experimental value of $d\lambda_s/dT$ we obtain the temperature dependence $\alpha_{\sigma_s} = 0$, which in first approximation agrees with the dependence of α on T for nonferromagnetic metals. This construction thus shows that the anomalous thermal expansion in ferromagnetics is determined by the spontaneous lattice deformation which occurs during the ferromagnetic transition.

M. V. Lomonosov Moscow State University

Received July 20, 1956

LITERATURE CITED

[1] R. Fowler, P. Kapitza, Proc. Roy. Soc. (London) A124, 1 (1929).

[2] K. P. Belov, Physics of Metal and Metallography, Acad. Sci. USSR, Ural Branch 2, 3 (1956).

[3] L. D. Landau and E. Lifshits, Statistical Physics (1940).

[4] V. L. Ginzburg, J. Exptl.-Theoret. Phys. (USSR) 19, 36 (1949).

[5] K. P. Belov and V. V. Shmidt, J. Tech. Phys. (USSR) 23, 44 (1953).

[6] S. V. Vonsovskii and Ia. S. Shur, Ferromagnetism (1948).

ELASTIC SCATTERING OF GAMMA RAYS WITH ENERGY TO 120 Mev BY PROTONS

B. B. Govorkov, V. I. Gol'danskii, O. A. Karpukhin,
A. V. Kutsenko and V. V. Pavlovskaia

(Presented by Academician I. E. Tamm, August 15, 1956)

The investigation of the angular distribution and absolute cross sections for elastic γp scattering is one of the possible methods of studying both the electromagnetic structure of protons and the nature of their interaction with meson fields. The simplest theory of gamma scattering by protons was advanced by Powell [1]. In this theory the scattering center (with spin 1/2) was regarded as a point and was characterized only by charge and mass; the complicated internal structure of the proton was considered purely phenomenologically by introducing a static anomalous magnetic moment. Powell thus obtained the Klein-Nishina formula with additional terms containing the difference between the magnetic moment and a nuclear magneton.

It is quite clear that in the scattering of gamma rays by nucleons, especially at energies $h\nu \gtrsim m_\pi c^2$ pions play an essential part (see, for example, [2]). But allowance for the latter depends on specific assumptions regarding the properties of the meson fields and the character of their interaction with nucleons. Therefore the predictions of theoretical articles which employ different specific meson theories [3-5] and ideas concerning the nucleon isobar ($I = 3/2$, $T = 3/2$) [6-9] require extensive experimental checking.

Despite the interest of elastic γp scattering, until the end of 1955 not a single experimental article appeared concerning the Compton effect involving protons. The main reason for the scarcity of experimental work is the extreme smallness of the cross section for elastic γp scattering (the Thomson cross section is

$$\sigma_{\text{Thomson}} = \frac{8}{3}\pi\left(\frac{e^2}{Mc^2}\right)^2 = 1,93\cdot 10^{-31}\ \text{см}^2),$$

and a considerably larger cross section can be expected only for energies near the isobar maximum ($h\nu \approx 340$ Mev), where the difficulties of detection also increase because of the large gamma background from the decay of π^0 mesons. Because of this last circumstance the first experiments on elastic γp scattering [10, 11] as well as our experiments described below were performed at gamma-ray energies which did not exceed the threshold for photoproduction of pions.* In this energy region the total elastic γp scattering cross sections according to all theoretical predictions almost coincide with the Thomson cross section; therefore considerable interest attaches not to the total cross sections but to the angular distribution of the scattered gamma rays. However with regard to the angular distribution of elastic γp scattering the results of [10], in which strong forward scattering was observed (at maximum gamma-ray energy of 98 Mev $\sigma(45°)/\sigma(30°) \lesssim 4,5$) disagreed with [11], whose authors did not detect this effect. Therefore, although during the final stages of preparation of our experiments these papers [10, 11] were published, we considered it fully advisable to carry through our measurements of the angular distribution in the elastic scattering of gamma rays to 120 Mev by protons.

---

* As was reported during a symposium at the European Center for Nuclear Investigations (Cern) at Geneva in June 1956 by G. Bernardini et al., very recently the Compton effect has been studied for protons and at higher energies. Their results and the improved results of [11], which were reported in May 1956 at the Moscow Conference on the Physics of High-Energy Particles by V. Weisskopf, have not yet been published.

The experiments were performed on the 265 Mev synchrotron of the P. N. Lebedev Physics Institute of the Academy of Sciences USSR. In order to reduce the background of the individual counters and the chance coincidence count, instantaneous switching-off of the accelerating resonator voltage was replaced by gradual reduction so that the synchrotron pulses had a duration of 1000 μ sec instead of the usual 30 μ sec. The electron spectrum at the synchrotron target was approximately triangular with its base from 75 to 119 Mev and its peak at 97 Mev.

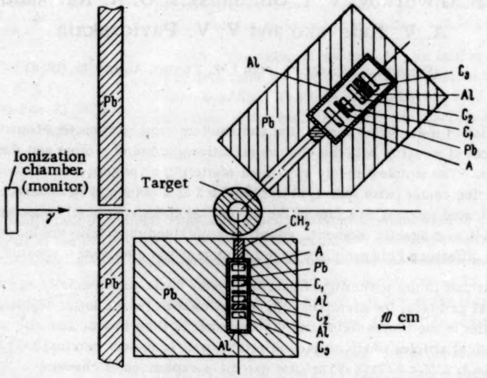

Fig. 1. Diagram of apparatus.

Elastic γp scattering at these energies was studied by recording only scattered gamma rays with a telescope of scintillation counters. A general diagram of the apparatus is given in Fig. 1.

Observations were made with two telescopes simultaneously at 90° and 90°, 45° and 90°, 45° and 135°, in the laboratory system. Each telescope consisted of four liquid scintillation counters filled with a solution of terphenyl in toluene (3 g per liter). The first counter of each telescope, connected for anticoincidences in order to reduce the background of penetrating pairs, was followed by a lead converter of 6.2-7 g/cm² thickness; between the third and fourth counters there was a 5.4-6 g/cm² aluminum filter. The gamma threshold, which was determined by the thickness of the second and third counters and the Al filter, was ~ 40 Mev for both telescopes.

For detection of light pulses from the scintilators we used FEU-19-II photomultipliers. The operating potential of the photomultipliers reached 4-4.5 kv; thus the FEU output going directly to a RK-50 cable (with wave resistance ρ = 150 ohms) consisted of pulses with 10 v amplitude. From the FEU output the pulses were fed directly by a long cable (~ 50 m) to the coincidence selector where they were shaped by meter sections of RK-50 cable; the resulting resolution time was $\tau \approx 9 \cdot 10^{-9}$ sec. Fig. 2 shows a typical coincidence curve observed when delays were introduced into the channel of one of the counters operating for triple coincidences.

The coincidence selector was constructed on the principle of diode circuits with preshaping of pulses at the input. The nonlinear elements were DGTs-8 germanium diodes. The apparatus was designed to make it possible to control all counters, and to count double, triple and quadruple coincidences and their combinations. Thus all kinds of verifying measurements were possible.

We used liquid hydrogen contained in a cylinder made of PS-4 foam polystyrene, with inside diameter 108 mm, outside diameter 208 mm and walls of about 200 mg/cm². The counting rate from the empty target

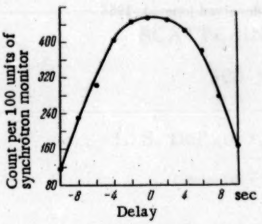

Fig. 2. Triple coincidence count of telescope with different delays in one of the channels.

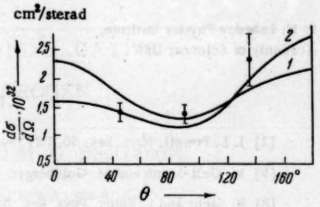

Fig. 3. Angular distribution of elastic γp scattering: 1) According to Powell's formula [1]; 2) from interference between data for zero-energy photons and Ritus' calculations [8] for photons above 190 Mev.

varied from 50 to 80% of the rate from the target when filled with liquid hydrogen. The effective working space of the target for the telescope disposition was determined by comparing the counting rate for recording of π^0 mesons from a "point" graphite source and the foam polystyrene target filled with liquid nitrogen (these experiments were performed with a bremsstrahlung spectrum of 265 Mev maximum). In order to convert the data to absolute values we determined the counting rate of gamma rays from photoproduction of π^0 mesons in hydrogen (at 265 Mev) and measured the bremsstrahlung flux (at $h\nu_{\max}$ = 119 and 265 Mev) with graphite detectors activated by the reaction $C^{12}(\gamma n)C^{11}$ and especially calibrated by us in separate experiments.

For the cross section calculations it was assumed in first approximation that the differential angular cross section at 90° of gamma rays from π^0 meson decay is simply double the cross section for emission of π^0 mesons at this angle; for $h\nu_{\max} = 250$ Mev this is $2.4\cdot 10^{-30}$ cm² /effect · quantum · sterad [12]. The efficiency of the telescopes for recording gamma rays from π^0 meson decay and elastic γp scattering (averaged over the spectrum of these gamma rays) was taken as about the same. For comparison of the data for 45° and 135° with 90° we introduced correction factors (0.92 for 45° and 1.08 for 135°) to allow for the energy differences of the scattered gamma rays.

Our results are shown in Fig. 3. The cross section at 90° ($d\sigma/d\Omega = (1.35 \pm 0.13)\cdot 10^{-32}$ cm²/sterad) is in good agreement with [10]. However, in distinction from this other work, our experiments established predominant scattering of photons into the backward hemisphere (for 45° $d\sigma/d\Omega = (1.40 \pm 0.17)\cdot 10^{-32}$ cm²/sterad; for 135° $(2.25 \pm 0.45)\cdot 10^{-32}$ cm²/sterad). These results indicate even at gamma energies below 120 Mev an analysis of the proton Compton effect based only on the static anomalous magnetic moment [1] and yielding a somewhat excessive cross section in the forward hemisphere is unsatisfactory. Even at these energies there is apparently interference of gamma-ray scattering from the proton as a point charge and from its nucleon isobar, i. e., because of the asymmetric meson cloud in the p state the nucleons have a dynamic magnetic moment.

The authors are indebted to V. I. Veksler, Corresponding Member of the Academy of Sciences USSR, for his constant interest and valuable discussions. We wish to thank, A. I. Shal'nikov, Corresponding Member of the Academy of Sciences USSR, N. I. Ginzburg, N. N. Khoroshilov and other members of the low temperature department of the physics faculty of the Moscow State University for assistance in the experiments with liquid hydrogen. We also thank the synchrotron crew of the Physics Institute of the Academy of Sciences USSR.

While the present article was being set in type Professor D. Frisch of MIT was kind enough to send us the text of a detailed article by the authors of [11] which they had submitted to the Physical Review. This article shows that for gamma rays from 90 to 130 Mev a considerable reduction is observed in the scattering cross section at 45° compared with the Thomson cross section; this is in qualitative agreement with our results.

P. N. Lebedev Physics Institute,
Academy of Sciences USSR

Received June 14, 1956

LITERATURE CITED

[1] J. L. Powell, Phys. Rev. 75, 32 (1949).

[2] M. Gell-Mann and M. Goldberger, Phys. Rev. 96, 1433 (1954).

[3] R. Sachs and L. Foldy, Phys. Rev. 80, 824 (1950).

[4] R. H. Capps and R. Sachs, Phys. Rev. 96, 540 (1954).

[5] R. Capps and W. Holladay, Phys. Rev. 99, 931 (1955).

[6] S. Minami, Progr. Theor. Phys. 9, 108 (1953).

[7] R. Huddlestone, Bull. Am. Phys. Soc. 28, 3, JA 14 (1953).

[8] V. I. Ritus, Report at All-Union Conference on the Quantum Electrodynamics and Theory of Elementary Particles, March 1955.

[9] N. Austern, Phys. Rev. 100, 1522 (1955).

[10] C. Oxley and V. Telegdi, Phys. Rev. 100, 435 (1955).

[11] G. Pugh, R. Gomez, D. Frisch and G. Janes, Phys. Rev. 100, 1245 (1955).

[12] V. Goldschmidt-Clermont, L. S. Osborne and M. B. Scott, Phys. Rev. 89, 329 (1953).

SCATTERING OF POSITIVE AND NEGATIVE 300-Mev PIONS BY HYDROGEN

L. S. Dul'kova, I. B. Sokolova and M. G. Shafranova

(Presented by Academician D. V. Skobel'tsyn August 4, 1956)

In the present work nuclear emulsions are used to study the scattering of positive and negative pions by hydrogen.

Type "R" NIKFI plates loaded with lithium acetate were irradiated in the synchrocyclotron of the Institute for Nuclear Problems of the Academy of Sciences USSR. The average energy of the positive mesons in the plates was 295 ± 10 Mev, and 300 ± 15 Mev for the negative mesons. The methods of treating and scanning the plates and the preliminary results were reported earlier [1]. At present we have found 105 instances of elastic scattering of negative mesons and 149 instances of scattering of positive mesons from 10° to 170°.

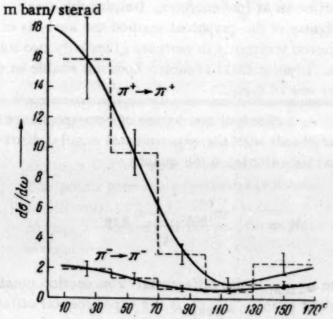

Fig. 1. Angular distributions of $\pi^{\pm}$-mesons scattered by hydrogen. Solid curves represent the functions $f(\theta) = a + b \text{ cps } \theta + c \cos^2 \theta$, where a, b, c are experimental coefficients.

For evaluation of the integral elastic scattering cross section we introduced the following corrections: for efficiency of area scanning (10%), for omission of events in the glass and on the emulsion surface (5%) and for omission of instances in which the scattering plane forms a large angle with the plane of the emulsion; this last correction amounts to 35% of the total number of events and is independent of the scattering angle.

With the indicated corrections we obtained the following values of the integral cross sections:

$$\sigma(\pi^- + p \to \pi^- + p) = (11 \pm 2)\text{m barn};$$
$$\sigma(\pi^+ + p \to \pi^+ + p) = (63 \pm 10)\text{m barn}.$$

The angular distributions for these processes were analyzed on the assumption that scattering occurs in the state with isotopic spins 3/2 and 1/2 with only s and p waves participating.

Consequently, the angular distribution function can be represented as

$$f(\theta) = a + b\cos\theta + c\cos^2\theta.$$

The method of least squares was used to obtain the coefficients a, b and c in mbarn/sterad for scattering of $\pi^{\mp}$-mesons: $a_- = 0.57 \pm 0.16$; $a_+ = 2.6 \pm 0.60$; $b_- = 0.59 \pm 0.20$; $b_+ = 7.5 \pm 1.1$; $c_- = 0.96 \pm 0.28$; $c_+ = 8.0 \pm 1.8$. The corresponding angular distributions are shown in Fig. 1. The scattering phases were determined by Ashkin's graphical method [25]. The required (for the analysis) scattering cross section of negative pions with charge exchange was taken to be the difference between the total cross section for $\pi^- + p$ scattering as measured in [2] by the transmission method and the elastic scattering cross section which we obtained.

We obtained the following phases:

$$\alpha_3 = -32^\circ \pm 8^\circ$$
$$\alpha_{31} = -12^\circ \pm 3^\circ$$
$$\alpha_{33} = 141^\circ \pm 10^\circ$$

$$\swarrow (1) \quad (2) \searrow$$

$$\begin{array}{ll} \alpha_1 = 12^\circ & \alpha_1 = 12^\circ \\ \alpha_{13} = 10^\circ & \alpha_{13} = -10^\circ \\ \alpha_{11} = -20.5^\circ & \alpha_{11} = 21.5^\circ \end{array}$$

The errors in the phases were obtained by varying the diameters of the circles whose intersection determines the phases in Ashkin's method.

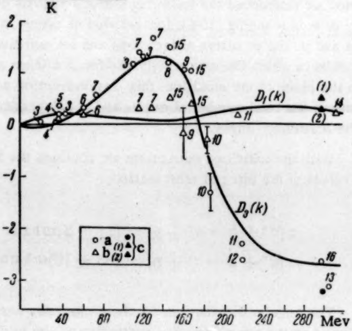

Fig. 2. Comparison of the forward scattering amplitude obtained from the dispersion relations with experiment: a) $\sin 2\alpha_3 + \sin 2\alpha_{31} + 2 \sin 2\alpha_{33}$; b) $\sin 2\alpha_1 + \sin 2\alpha_{11} + 2 \sin 2\alpha_{13}$; c) our experiment.

In analyzing the data on π^+ meson scattering we chose the Fermi solution, which follows from experiments at low energies. Despite the great ambiguity of the graphical method the analysis of π^- meson scattering in our case gives only two solutions. Experimental accuracy does not enable us to select one of these.

As a check of the degree of correspondence of the phases with the experimental angular distribution we calculated the quantity

$$M = \sum_{i=1}^{10} \frac{(\sigma_{i\,\mathrm{scat}} - \sigma_{i\,\mathrm{exp}})^2}{\xi_i^2},$$

where $\sigma_{i\,\mathrm{scat}}$ is the differential cross section obtained from the phases; $\sigma_{i\,\mathrm{exp}}$ is the experimental differential cross section and ξ_i is the error of measurement.

For Solution (1) M = 7; for Solution (2) M = 11 instead of the expected value M = 4. These values of M favor Solution (1) but do not enable us to reject Solution (2).

The phase shifts obtained are in satisfactory agreement with the deductions from the dispersion relations for meson scattering.

Fig. 2 shows the energy dependence of the forward scattering amplitude for states with isotopic spin 3/2(D_3) and 1/2 (D_1).

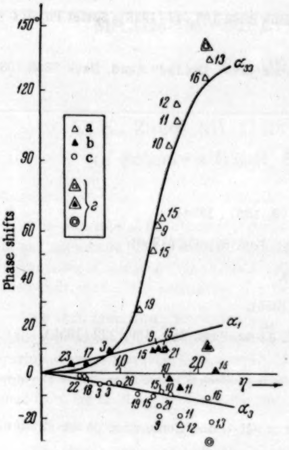

Fig. 3. Phase shifts as a function of pion momentum; η is the pion momentum in the c. m. system in units μc. The upper curve was obtained by Chew and Low for phase α_{33}. The straight lines $\alpha_1 = 0.16\,\eta$ and $\alpha_3 = 0.11\,\eta$ were obtained by Orear. The points give the experimental results of different authors [3-23]. a) α_{33}; b) α_1; c) α_3; d) is the present experiment.

The solid curves up to E = 240 Mev were calculated from the causality relation of Anderson et al. [24] and extended by us to E = 300 Mev. In agreement with Orear, we took for low energies $\alpha_3 = -0.11\,\eta$; $\alpha_1 = 0.16\,\eta$. The experimental points were taken from various authors [3-16]. Our results at E = 300 Mev for π^+ mesons and both solutions for π^- mesons agree with the calculated curve within the limits of experimental error.

A comparison of our phases with the phases for other energies is given in Fig. 3.

It should be noted that experiment gives only one value for the phase α_1, which remains constant during variation of the coefficients within the limits of their errors. This value of α_1 does not agree with Orear's line, but the error, which it is difficult to determine, may be large.

The phase α_3 is negative and even when the largest error is allowed for it lies considerably below Orear's line with the slope $0.11\,\eta$.

The value obtained for the phase α_{33} confirms the resonance character of the interaction in the state J = = 3/2, I = 3/2 and disagrees with the theoretical curve of Chew and Low. It also follows from experiment that the p phases for isotopic spin 1/2 at 300 Mev make an essential contribution to the scattering.

The low accuracy of the experiment does not enable us to allow for the possible addition of a d wave. Inclusion of the d wave gives an angular distribution for $\pi^+ + p$ scattering in the form:

$$F(\theta) = (2.9 \pm 2.3) + (8.7 \pm 2.2)\cos\theta + (8.0 \pm 5.9)\cos^2\theta + \\ + (0.17 \pm 4.04)\cos^3\theta + (3.4 \pm 7.5)\cos^4\theta.$$

Errors in the coefficients of the last two terms are so large that they do not exclude the possibility of a zero value, i. e., the absence of a d wave. If the d wave makes an essential contribution the analysis of the experimental findings leads to some change of the s and p phases. This may result in agreement of phases α_1 and α_3 with Orear's lines. But it is possible that for the given energy there is already a nonlinear dependence of the phases on momentum, i. e., the effective interaction radius begins to exert some influence.

The authors are grateful to I. M. Frank, Corresponding Member of the Academy of Sciences USSR, I. Ia. Barit and K. D. Tolstoi for their assistance, to V. Ia. Fainberg and V. I. Ritus for valuable advice and to the laboratory staffs of the Physics Institute and of the Electrophysical Laboratory of the Academy of Sciences USSR who assisted with the scanning of the plates.

P. N. Lebedev Physics Institute,
Academy of Sciences USSR

Received August 28, 1956

LITERATURE CITED

[1] L. S. Dul'kova, T. A. Romanova et al., Doklady Akad. Nauk SSSR 107, 43 (1956) [Soviet Physics – Doklady, p. 154].

[2] A. E. Ignatenko, A. I. Mukhin, E. B. Ozerov and B. M. Pontecorvo, Doklady Akad. Nauk SSSR 103, 395 (1955).

[3] J. Orear, Phys. Rev. 96, 176 (1954).

[4] J. Tinlot and A. Roberts, Phys. Rev. 95, 137 (1954).

[5] J. P. Perry and C. E. Angell, Phys. Rev. 91, 1289 (1933).

[6] D. Bodansky, A. M. Sachs and J. Steinberger, Phys. Rev. 93, 1367 (1954).

[7] H. L. Anderson, F. Fermi, P. Martin and D. E. Nagle, Phys. Rev. 85, 936 (1953).

[8] R. A. Grandey and A. F. Clark, Phys. Rev. 97, 791 (1955).

[9] H. L. Anderson and M. Glicksman, Phys. Rev. 100, 268 (1955).

[10] H. L. Anderson, W. C. Davidson, M. Glicksman and U. E. Kruse, Phys. Rev. 100, 279 (1955).

[11] M. Glicksman, Phys. Rev. 94, 1335 (1954).

[12] U. Taft, Phys. Rev. 101, 1116 (1956).

[13] A. I. Mukhin, E. B. Ozerov and B. M. Pontecorvo, Report at All-Union Conference on the Physics of High-Energy Particles, Moscow, 1956.

[14] V. G. Zinov and S. M. Korenchenko, Report at the All-Union Conference on the Physics of High-Energy Particles, Moscow, 1956.

[15] L. Ashkin, I. P. Blaster, F. Feine and M. O. Stern, Phys. Rev. 101, 1149 (1956).

[16] R. Margulies, Phys. Rev. 99, 673 (A) (1955).

[17] J. Orear, Phys. Rev. 96, 174 (1954).

[18] J. Orear, Phys. Rev. 98, 239 (A) (1955).

[19] J. Orear, Phys. Rev. 96, 1417 (1954).

[20] H. L. Anderson, E. Fermi, R. Martin and D. E. Nagle, Phys. Rev. 91, 155 (1953).

[21] H. A. Bethe, F. Hoffman, N. Metropolis, E. F. Alei, Phys. Rev. 95, 1586 (1954).

[22] S. L. Whetstone and H. Stork, Phys. Rev. 102, 251 (1956).

[23] M. C. Rinehart, K. C. Rogers and M. Lederman, Phys. Rev. 99, 673 (A) (1955).

[24] H. L. Anderson, W. C. Davidon and U. E. Kruse, Phys. Rev. 100, 339 (1955).

[25] J. Ashkin and S. H. Vosko, Phys. Rev. 91, 1248 (1953).

MAXIMUM AMPLIFICATION FACTOR AND NOISE OF PHOTOMULTIPLIERS

E. K. Zavoiskii, Corresponding Member of the Academy
of Sciences USSR, M. M. Butslov and G. E. Smolkin

The principle of the electron-optical amplification of light enables us to attain an amplification factor η of any magnitude [1]. It is easily seen, however, that this factor has a limiting value $\eta_{\lim}$ which permits the photographing of a minimum possible signal – that of a single electron emitted from the input photocathode of a photomultiplier. Further increase of η has practically no meaning.

We shall tentatively determine $\eta_{\lim}$ from the formula $\eta_{\lim} = n\sigma$. Here $\underline{n}$ is the number of electrons striking unit screen area which is required for obtaining a normal photograph with optical density ≈ 0.2-0.4. Experiment shows that (see, for example, [2]) in such instances when the electron energy is $\approx 2 \cdot 10^4$ ev the number is $\approx 10^9$. σ is the area of the circular image on the screen when one electron is recorded. It is determined from the resolving power of the instrument and in our case has the value $\approx 10^{-4}$ cm^2. Consequently, $\eta_{\lim} \approx 10^5$.

The photographing of a single electron was achieved experimentally with a Type 95 photomultiplier. For this purpose we first used the electrons of dark emission from the input photocathode (intrinsic noise). This noise produces a certain background on the fluorescent screen of the multiplier. Visual observation shows that this background consists of individual localized flashes of a luminophor like scintillation (Fig. 1a). The emitting area of the screen during a flash is $\approx 10^{-4}$ cm^2. The flash duration is determined by the fluorescent period of the screen.

A number of experiments (on relative flash brightness, the effect of a weak light source and of a γ specimen on the photocathode, etc) showed that in the range of operating voltages (from 8 to 20 kv) the majority of flashes on the screen did not correspond to individual electrons emitted by the input photocathode but to entire groups (bunches) of electrons. It was thus established that the dark emission of a SbCs photocathode has two different components: "single-electron" and "multi-electron" emission which are readily seen to be of different nature.

The separation of the single-electron component by minimum optical density of a negative involves a number of difficulties due to noise from other cathodes and thus does not enable us to decide the question of the possible recording of a single electron.

For the reliable separation and recording of a single electron and for the explanation of the emission character of the multi-electronic noise component we defocused the electronic image in the input stage of the multiplier. The diameters of the diffuse circles of flashes depended on the degree of defocusing and on the component $U_0^{\perp}$ of initial electron velocity perpendicular to the instrumental axis. Under defocusing a flash is resolved into a group of individual points, each of which corresponds to a single input electron. This is confirmed by the fact that the brightness of points in the group is almost identical.

Fig. 1 contains a number of photographs obtained by the method described. a, b, c, d demonstrate the gradual defocusing of multi-electronic flashes. e, f are photographs of individual defocused flashes.

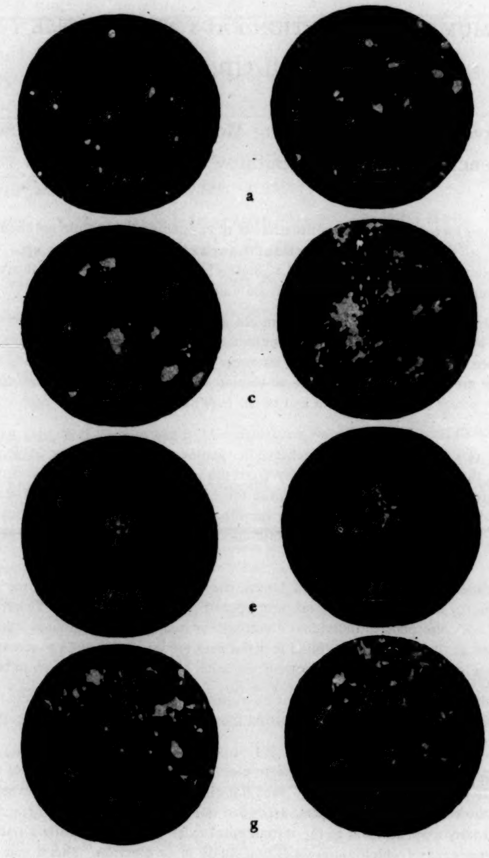

Fig. 1. a, b, c, d are photographs of the background on the screen of a photomultiplier, obtained by defocusing the electronic image; e, f are photographs of individual resolved groups of electrons; g, h are photographs of individual photoelectrons.

Photograph g was obtained by illuminating one half of the photocathode with weak light without defocusing. Photograph h was obtained with strong defocusing while other conditions remained unchanged. If we exclude the points resulting from noise (some of these are indicated by arrows) it can be seen that the size, brightness and number of the remaining points is the same in both photographs. This indicates that the points correspond to individual photoelectrons leaving the illuminated portion of the photocathode. In these experiments the amplification factor $\eta = 3 \cdot 10^5$. But with such high amplification the background noise may be a serious disturbance when a single electron is being recorded. Its source is principally the dark emission of the photocathodes; the noise of the input cathode induces the greatest background on the output screen since this noise passes through the entire amplification channel.

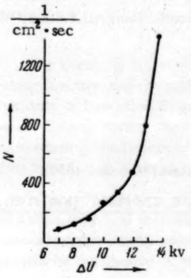

Fig. 2. The number N of electron groups as a function of the potential difference ΔU of a stage.

By defocusing the electron image at the input we succeeded in obtaining quantitative information concerning both components of the dark current of a SbCs photocathode. We took a series of photographs of the background with a definite time of exposure and obtained a count per unit area and per unit time. These measurements whowed that with a potential difference $\Delta U = 12$ kv for the stage the SbCs photocathode emits $\sim 20 \frac{1}{cm^2 \cdot sec}$ individual electrons at room temperature. It was also shown that under the same conditions a photocathode emits $\sim 500 \frac{1}{cm^2 \cdot sec}$ local electron groups (bunches). The number δ of electrons in a group may vary from 2-3 to 15-20. The largest number of groups consist of 7-12 electrons.

The different origins of these two currents is shown first of all by their temperature dependence. When a photocathode was cooled in liquid nitrogen the single-electron current disappeared completely, thus indicating that it is of thermoelectronic origin.* At the same time the multi-electronic component of the dark current remained practically unchanged.

With respect to the emission mechanism of the multi-electronic component interest attaches to the potential difference ΔU of a stage and to the spread of initial electron velocities U_0 and the mean time τ during which electrons of a single group are emitted. The current as a function of ΔU is shown in Fig. 2. As ΔU increases, the number of electron groups $N \frac{1}{cm^2\text{-}sec}$ increases following the law $\sim a\,(\Delta U)^5$.

An estimate of the perpendicular component of initial electron velocities $U_0^{\perp}$ was made from the known velocity spectrum of the photoelectrons. For this purpose point-source light was projected on the photocathode and the sizes of the diffused circles due to this source and due to individual electron bunches were compared under a certain amount of defocusing. The maximum value of $U_0^{\perp}$ was ~ 10 ev.

The time τ was studied by a high-frequency sweep of the electronic image on the input of the photomultiplier which was described in detail in [7]. Preliminary measurements gave a value below 10^{-11} sec.

Data available at present are insufficient to determine the origin of the multi-electronic dark current of a SbCs photocathode: whether it is cold emission from inhomogeneities (spherulites) of the photocathode or bombardment of the cathode by heavy ions.

Thus on the basis of the experimental facts presented above it may be considered proved that the maximum electron-optical amplification factor has been attained and that further increase of sensitivity will be reached by raising the quantum yield of the photocathode. The recording of a single electron makes it possible to study the phenomena which accompany the departure of one photoelectron (or a secondary electron) from the input photocathode. This method, combined with a method which is widely used at the present time [7], reveals new experimental possibilities for the investigation of ultra-fast processes. We have also shown that the thermoelectronic current of the photocathode is small and cannot cause disturbances in such investigations. The level of the multi-electronic noise component is also quite small and can be greatly reduced by pulsed feeding.

---

*It should be noted that our measurement of the thermoelectronic current differs considerably from the values obtained by other authors: $10^{-16} \frac{amp}{cm^2}$ [3, 4]; $10^{-15} - 10^{-14} \frac{amp}{cm^2}$ [5, 6] etc.

Received August 27, 1956

LITERATURE CITED

[1] E. K. Zavoiskii, M. M. Butslov, A. G. Plakhov and G. E. Smolkin, Atomic Energy(U.S.S.R.) 1956, No. 4, 35.

[2] I. S. Stekol'nikov, Oscilloscopes (1949).

[3] G. Morton, RCA Review 10, 525 (1949).

[4] F. Boeshoten, M. W. Milatz and C. Smit, Physica 20, 193 (1954).

[5] R. W. Engstrom, J. Optical Soc. Amer. 37, 420 (1947).

[6] N. O. Chechik, S. M. Fainshtein and G. M. Lifshits, Electron Multipliers (Moscow, 1954).

[7] E. K. Zavoiskii and S. D. Fanchenko, Doklady Akad. Nauk SSSR 108, 2, 218 (1956) [Soviet Physics – Doklady, p. 285].

THE TRANSMISSION OF RADIATION THROUGH AN INHOMOGENEOUS MEDIUM

V. V. Sobolev

(Presented by Academician V. A. Ambartsumian, August 5, 1956)

35.

In the theory of radiation transmission it is usually assumed that the optical properties of a medium (the scattering function and the ratio of the scattering coefficient to the absorption coefficient) are constant. In the majority of cases met in practice these quantities change in passing from one point to another. For example, in the earth's atmosphere the scattering function is strongly dependent on altitude; in stellar atmospheres the ratio of the scattering coefficient of a line to the absorption coefficient in the continuous spectrum is depth-dependent. We thus have the problem of radiation transmission in a medium with changing optical properties.

We here consider the special case of radiation in a semi-infinite medium consisting of plane-parallel layers with a spherical scattering function. The ratio of the scattering coefficient to the sum of the scattering and true absorption coefficients (i. e., the probability that a quantum will survive an elementary scattering event) will be denoted by λ and will be regarded as a function of the optical depth τ.

Our problem is now the solution of the following integral equation for the function $B(\tau)$:

$$B(\tau) = \frac{\lambda(\tau)}{2} \int_0^\infty B(\tau') \operatorname{Ei}|\tau - \tau'|\, d\tau' + g(\tau), \tag{1}$$

where the function $g(\tau)$ depends directly on the sources of radiation. The light intensity which leaves a medium at the angle arc cos η to the normal is expressed in terms of $B(\tau)$ by

$$I(\eta) = \int_0^\infty B(\tau) e^{\tau/\eta} \frac{d\tau}{\eta}. \tag{2}$$

The problem can also be solved by a method based on the probability that a photon will escape from the medium (1). We denote by $p(\tau, \eta)\, d\omega$ the probability that a quantum absorbed at the optical depth τ will escape from the medium (in general, after multiple scattering) at the angle arc cos η to the normal within the solid angle $d\omega$. When $p(\tau, \eta)$ is known the intensity of the escaping radiation for any light sources can be obtained from

$$I(\eta) = 4\pi \int_0^\infty \frac{g(\tau)}{\lambda(\tau)} p(\tau, \eta) \frac{d\tau}{\eta}. \tag{3}$$

The function $p(\tau, \eta)$ is defined by the integral equation

$$p(\tau, \eta) = \frac{\lambda(\tau)}{4\pi} e^{-\tau/\eta} + \frac{\lambda(\tau)}{2} \int_0^\infty p(\tau', \eta) \operatorname{Ei} |\tau - \tau'| \, d\tau', \tag{4}$$

which is a special case of (1) (for $g(\tau) = \frac{\lambda(\tau)}{4\pi} e^{-\tau/\eta}$, i. e., when the medium is illuminated by parallel rays).

In principle the solution of (4) presents the same difficulties as the solution of (1). But for the determination of $p(\tau, \eta)$ we can set up still another equation. We shall obtain the probability of escape of a quantum from the depth $\tau + \Delta\tau$, i. e., the quantity $p(\tau + \Delta\tau, \eta)$. For this purpose we consider the quantum as escaping from the depth τ and then traversing an additional layer of small thickness $\Delta\tau$ (with or without absorption in this layer). When λ = const the medium without the additional layer does not differ from the medium plus the layer; therefore we can write:

$$p(\tau + \Delta\tau, \eta) = p(\tau, \eta)\left(1 - \frac{\Delta\tau}{\eta}\right) + 2\pi \int_0^1 p(\tau, \eta') \frac{\Delta\tau}{\eta'} \, d\eta' \, p(0, \eta). \tag{5}$$

When λ depends on τ the Relation (5) does not hold true. But in such case we can write a more general relation than (5). We consider the set of media in which the probability of quantum survival is $\lambda(\tau + \alpha)$, where α is a parameter. The probability of quantum escape from a medium characterized by a definite value of α will be denoted by $p(\tau, \eta, \alpha)$.

It is obvious that after removing a layer of thickness $\Delta\tau$ from the medium we have a medium with quantum survival probability $\lambda(\tau + \alpha + \Delta\tau)$ and with quantum escape probability from depth τ given by $p(\tau, \eta, \alpha + \Delta\tau)$. Instead of (5) we now obtain:

$$\begin{aligned} p(\tau + \Delta\tau, \eta, \alpha) = p(\tau, \eta, \alpha + \Delta\tau)\left(1 - \frac{\Delta\tau}{\eta}\right) + \\ + 2\pi \int_0^1 p(\tau, \eta', \alpha + \Delta\tau) \frac{\Delta\tau}{\eta'} \, d\eta' \, p(0, \eta, \alpha). \end{aligned} \tag{6}$$

Hence it follows that

$$\frac{\partial p}{\partial \tau} - \frac{\partial p}{\partial \alpha} = -\frac{1}{\eta} p(\tau, \eta, \alpha) + 2\pi \int_0^1 p(\tau, \eta', \alpha) \frac{d\eta'}{\eta'} \, p(0, \eta, \alpha). \tag{7}$$

The quantity $p(0, \eta, \alpha)$ in Equation (7) can be represented as

$$p(0, \eta, \alpha) = \frac{\lambda(\alpha)}{4\pi} \left[1 + 2\eta \int_0^1 \rho(\eta, \eta', \alpha) \, d\eta'\right], \tag{8}$$

where

$$\rho(\eta, \zeta, \alpha) = \frac{\pi}{\eta\zeta} \int_0^\infty e^{-\tau/\zeta} p(\tau, \eta, \alpha)\, d\tau. \tag{9}$$

The magnitude of $\rho(\eta, \zeta, \alpha)$ is the luminous coefficient of the medium illuminated by parallel rays at angle arc cos ζ to the normal. If the parallel rays produce illumination πS of the surface which is perpendicular to them, the intensity of radiation diffusively reflected by the medium is

$$I(\eta, \zeta, \alpha) = S\rho(\eta, \zeta, \alpha). \tag{10}$$

From (7) and (8) we can obtain a single equation for $\rho(\eta, \zeta, \alpha)$. Multiplying (7) by $e^{-\tau/\zeta}$ and integrating over τ between 0 and ∞ we obtain

$$\left(\frac{1}{\eta} + \frac{1}{\zeta}\right) \rho(\eta, \zeta, \alpha) - \frac{\partial \rho}{\partial \alpha} = \frac{\pi}{\eta} p(0, \eta, \alpha) \left[1 + 2\zeta \int_0^1 \rho(\eta', \zeta, \alpha)\, d\eta'\right]. \tag{11}$$

Inserting (8) in (11) and assuming symmetry of $\rho(\eta, \zeta, \alpha)$ with respect to η and ζ (which results from (1 - 4) with $g(\tau) = \frac{\lambda(\tau)}{4} Se^{-\tau/\zeta}$), we have instead of (11):

$$(\eta + \zeta)\rho(\eta, \zeta, \alpha) - \eta\zeta \frac{\partial \rho}{\partial \alpha} = \frac{\lambda(\alpha)}{4} \varphi(\eta, \alpha)\varphi(\zeta, \alpha), \tag{12}$$

with the notation

$$\varphi(\eta, \alpha) = 1 + 2\eta \int_0^1 \rho(\eta, \eta', \alpha)\, d\eta'. \tag{13}$$

It follows from (12) and (13) that

$$\rho(\eta, \zeta, \alpha) = \int_\alpha^\infty \frac{\lambda(\alpha')}{4} \varphi(\eta, \alpha')\varphi(\zeta, \alpha') e^{-(\alpha'-\alpha)\left(\frac{1}{\eta} + \frac{1}{\zeta}\right)} \frac{d\alpha'}{\eta\zeta}, \tag{14}$$

$$\varphi(\eta, \alpha) = 1 + \frac{1}{2} \int_0^1 \frac{d\zeta}{\zeta} \int_\alpha^\infty \lambda(\alpha')\varphi(\eta, \alpha')\varphi(\zeta, \alpha') e^{-(\alpha'-\alpha)\left(\frac{1}{\eta} + \frac{1}{\zeta}\right)} d\alpha'. \tag{15}$$

Thus our problem becomes the determination of $\varphi(\eta, \alpha)$ from (15). When $\varphi(\eta, \alpha)$ is known (14) can be used to obtain the luminous coefficient for any of the media under consideration. To obtain the luminous coefficient for the original medium we must in (14) set $\alpha = 0$.

Let us consider some special cases.

1. When λ = const, then φ is independent of α and instead of (14) and (15) we have:

$$\rho(\eta, \zeta) = \frac{\lambda}{4} \frac{\varphi(\eta)\varphi(\zeta)}{\eta + \zeta}, \tag{16}$$

$$\varphi(\eta) = 1 + \frac{\lambda}{2} \eta \varphi(\eta) \int_0^1 \frac{\varphi(\zeta)}{\eta + \zeta} d\zeta. \tag{17}$$

Equations (16) and (17) were obtained earlier by V. A. Ambartsumian [2].

2. Let $\lambda = \lambda_0$ for $0 \leq \tau \leq \tau_0$ and $\lambda = \lambda_1$ for $\tau_0 \leq \tau < \infty$. From (14) and (15) we obtain

$$\rho(\eta, \zeta, \alpha) = \frac{\lambda_0}{4} \int_\alpha^{\tau_0} \varphi(\eta, \alpha') \varphi(\zeta, \alpha') e^{-(\alpha' - \alpha)\left(\frac{1}{\eta} + \frac{1}{\zeta}\right)} \frac{d\alpha'}{\eta\zeta} + $$
$$+ \rho_1(\eta, \zeta) e^{-(\tau_0 - \alpha)\left(\frac{1}{\eta} + \frac{1}{\zeta}\right)}, \tag{18}$$

$$\varphi(\eta, \alpha) = 1 + \frac{\lambda_0}{2} \int_0^1 \frac{d\zeta}{\zeta} \int_\alpha^{\tau_0} \varphi(\eta, \alpha') \varphi(\zeta, \alpha') e^{-(\alpha' - \alpha)\left(\frac{1}{\eta} + \frac{1}{\zeta}\right)} d\alpha' + $$
$$+ \frac{\lambda_1}{2} \eta \varphi_1(\eta) \int_0^1 \varphi_1(\zeta) e^{-(\tau_0 - \alpha)\left(\frac{1}{\eta} + \frac{1}{\zeta}\right)} \frac{d\zeta}{\eta + \zeta}, \tag{19}$$

where $\rho_1(\eta, \zeta)$ and $\varphi_1(\eta)$ are defined by (16) and (17) for $\lambda = \lambda_1$. Equation (18) gives the luminous coefficient of a semi-infinite medium with $\lambda = \lambda_1$ on which there is superimposed a layer of arbitrary optical thickness $\tau_0 - \alpha$ with $\lambda = \lambda_0$ $(0 \leq \alpha \leq \tau_0)$.

3. Assuming in (18) and (19) that $\lambda_1 = 0$, $\tau_0 - \alpha = t$, $\tau_0 - \alpha' = t'$, we obtain .

$$\rho(\eta, \zeta, t) = \frac{\lambda}{4} \int_0^t \varphi(\eta, t') \varphi(\zeta, t') e^{-(t - t')\left(\frac{1}{\eta} + \frac{1}{\zeta}\right)} \frac{dt'}{\eta\zeta}, \tag{20}$$

$$\varphi(\eta, t) = 1 + \frac{\lambda}{2} \int_0^1 \frac{d\zeta}{\zeta} \int_0^t \varphi(\eta, t') \varphi(\zeta, t') e^{-(t - t')\left(\frac{1}{\eta} + \frac{1}{\zeta}\right)} dt'. \tag{21}$$

Equation (20) defines the luminous coefficient of a medium of optical thickness t with constant λ. We have arrived at new equations for the functions $\rho(\eta, \zeta, t)$ and $\varphi(\eta, t)$ in the problem which was earlier examined in detail.

By virtue of (8) and (13) Equation (7) becomes

$$\frac{\partial p}{\partial \tau} - \frac{\partial p}{\partial \alpha} = -\frac{1}{\eta} p(\tau, \eta, \alpha) + \frac{\lambda(\alpha)}{2} \varphi(\eta, \alpha) \int_0^1 p(\tau, \eta', \alpha) \frac{d\eta'}{\eta'}. \tag{22}$$

Using (22) the intensity of radiation escaping from the medium $I(\eta, \alpha)$ according to (3) can be expressed in terms of $\varphi(\eta, \alpha)$ for different light sources. This can be done relatively simply when $g(\tau)$ is a polynomial or exponential function of τ.

A. A. Zhdanov Leningrad State University

Received June 2, 1956

LITERATURE CITED

[1] V. V. Sobolev, Astr. Jour. (USSR) 28, 5 (1951).

[2] V. A. Ambartsumian, Doklady Akad. Nauk SSSR 37, 257 (1943).

AN ASYMPTOTIC INVESTIGATION OF THE VERTEX PART IN QUANTUM ELECTRODYNAMICS

V. Z. Blank and D. V. Shirkov

(Presented by Academician N. N. Bogoliubov, June 15, 1956)

In the present note the renormalization group method, which has already been used to improve the perturbation formulas for Green's functions [1], is employed to improve the formulas for the vertex part.

Unlike the Green's functions, the vertex operator has a quite complicated matrix structure and depends on two 4-momenta. It can in general be expanded in products of different numbers of Dirac matrices. Since we are aiming at obtaining an asymptotic expression for the vertex operator in the infrared and ultraviolet regions, we shall confine ourselves from the very beginning to a consideration of the Γ^n term proprtional to the matrix γ^n, which will clearly be a scalar function of three independent scalar arguments p^2, q^2, k^2 ($p - q = k$):

$$\Gamma^n = \gamma^n \Gamma(p^2, q^2, k^2). \tag{1}$$

As usual we transfer the multiplicative arbitrariness of the vertex function to the arguments of the Γ function, introducing an auxiliary momentum and going over to dimensionless arguments:

$$\Gamma\left(\frac{p^2}{\lambda^2}, \frac{q^2}{\lambda^2}, \frac{k^2}{\lambda^2}, \frac{m^2}{\lambda^2}, e^2\right). \tag{2}$$

We first regard Γ as a function of p^2 by fixing the remaining arguments. Then the functional equation for the vertex part can be written as

$$\begin{gathered}\Gamma(x, y, z, u, e^2, e^2 d_l^0) = \\ = \Gamma(t, y, z, u, e^2 d_l^0) \cdot \frac{\Gamma\left(\frac{x}{t}, \frac{y}{t}, \frac{z}{t}, \frac{u}{t}, e^2 d(t, u, e^2), e^2 d_l^0\right)}{\Gamma\left(1, \frac{y}{t}, \frac{z}{t}, \frac{u}{t}, e^2 d(t, u, e^2), e^2 d_l^0\right)}.\end{gathered} \tag{3}$$

Here d_l^0 is the longitudinal part of the photon Green's function, which we shall regard as independent of momentum. The Lie differential equation corresponding to (3) will be

$$\begin{gathered}\frac{\partial}{\partial x} \ln \Gamma(x, y, z, u, e^2, e^2 d_l^0) = \\ = \frac{1}{x}\left[\frac{\partial}{\partial \xi} \ln \Gamma\left(\xi, \frac{y}{x}, \frac{z}{x}, \frac{u}{x}, e^2 d(x, u, e^2), e^2 d_l^0\right)\right]_{\xi=1}.\end{gathered} \tag{4}$$

Integrating, we obtain

$$\ln \frac{\Gamma(x, y, z, u, e^2, e^2 d_l^0)}{\Gamma(x_0, y, z, u, e^2, e^2 d_l^0)} = I(x, y, z, u, e^2, e^2 d_l^0 \mid x^0) \equiv$$

$$\equiv \int_{x_0}^{x} \frac{dx'}{x'} \left[\frac{\partial}{\partial \xi} \ln \Gamma\left(\xi, \frac{y}{x'}, \frac{z}{x'}, \frac{u}{x'}, e^2 d(x', u, e^2), e^2 d_l^0\right)\right]_{\xi=1}. \tag{5}$$

We now regard $\Gamma(x_0, y, z, \ldots)$ as a function of z, and obtain

$$\ln \frac{\Gamma(x, y, z, u, e^2, e^2 d_l^0)}{\Gamma(x_0, y_0, z_0, u, e^2, e^2 d_l^0)} = I(x, y, z, u, e^2, e^2 d_l^0 \mid x_0) + I(x_0, y, z, u, e^2, e^2 d_l^0 \mid y_0) + I(x_0, y_0, z, e^2, e^2 d_l^0 \mid z_0). \tag{6}$$

We note that (5) and (6) are considerably simplified when for the determination of Γ we used second-order perturbation theory:

$$\Gamma_0(x, y, z, u, e^2, e^2 d_l^0) = 1 + e^2 \left[\Lambda_t\left(\frac{x}{u}, \frac{y}{u}, \frac{z}{u}\right) - \widetilde{\Lambda}_t(u)\right] + e^2 d_l^0 \left[\Lambda_l\left(\frac{x}{u}, \frac{y}{u}, \frac{z}{u}\right) - \widetilde{\Lambda}_l(u)\right], \tag{7}$$

and, in particular, in this case the integrals which contain Λ_l are calculated explicitly.

We shall consider the specific case of the ultraviolet asymptotic expression

$$|k^2| \gg |p^2|, \ |q^2| \gg m^2$$

or

$$|z| \gg |x|, \ |y| \gg |u|. \tag{8}$$

The corresponding second-order perturbation calculations were carried out by A. A. Abrikosov [2] and V. V. Sudakov [3]. They obtained

$$\Lambda_l = 0; \quad \Lambda_t\left(\frac{x}{u}, \frac{y}{u}, \frac{z}{u}\right) = -\frac{1}{8\pi^2} \ln\left|\frac{z}{x}\right| \ln\left|\frac{z}{y}\right|. \tag{9}$$

Here, as previously in similar instances, the "mass" variable u dropped out.

Condition (8) requires, unlike (6) that the integration over z be performed last. The final expression, symmetrized with respect to x and y, will be

$$\ln \frac{\Gamma(x, y, z. e^2)}{\Gamma(x_0, y_0, z_0, e^2)} = 3\left[\ln \frac{z}{z_0} - \frac{12\pi^2}{e^2} \ln \frac{d(z, e^2)}{d(z_0, e^2)}\right] + \frac{3}{2} \ln(x_0 y_0) \ln \frac{d(z, e^2)}{d(z_0, e^2)} + \frac{3}{2}\left[\ln \frac{z}{x_0} \ln \frac{d(y, e^2)}{d(y_0, e^2)} + \ln \frac{z}{y_0} \ln \frac{d(x, e^2)}{d(x_0, e^2)}\right] + \frac{3}{4}\left[\ln \frac{x_0}{x} \ln \frac{d(y, e^2)}{d(y_0, e^2)} + \ln \frac{y_0}{y} \ln \frac{d(x, e^2)}{d(x_0, e^2)}\right]. \tag{10}$$

This formula is valid subject to fulfillment of the following conditions:

$$\begin{gathered} 1-\frac{e^2}{12\pi^2}\ln z \gg e^2, \\ \ln z > \ln x, \quad \ln y \geqslant \ln x_0, \ \ln y_0, \ \ln z_0. \end{gathered} \tag{11}$$

Here z_0, x_0, $y_0 \gg u$, $\ln x_0 \sim \ln y_0$, but $\ln z_0$ cannot be much greater than $\ln x_0$, $\ln y_0$.

We now note that for $e^2 \ln z \ll 1$ we arrive at the formula previously obtained by V. V. Sudakov [3] through summation of a number of principal Feynman diagrams and by V. Z. Blank [4] through an approximate solution of the Schwinger equation by the proper time method.

We now proceed to the infrared asymptotic expression and consider the case where

$$p^2 = q^2 \to m^2, \quad k^2 < 0. \tag{12}$$

The corresponding second-order perturbation calculations were performed by A. A. Abrikosov [3]. He obtained

$$\Lambda_l\left(\frac{x}{u}, \frac{z}{u}\right) = \frac{1}{8\pi^2}\ln\left|\frac{u}{x-u}\right|; \tag{13}$$

$$\Lambda_t\left(\frac{x}{u}, \frac{z}{u}\right) = \frac{1}{8\pi^2}\varphi\left(\frac{z}{u}\right) + \frac{1}{8\pi^2}\psi\left(\frac{z}{u}\right)\ln\left|\frac{u}{x-u}\right|; \tag{14}$$

where

$$\varphi\left(\frac{z}{u}\right) = \frac{1-2u/z}{\sqrt{1-4u/z}}\left(\ln\left|1-\frac{z}{2u}\right|\right)^2; \tag{15}$$

$$\psi\left(\frac{z}{u}\right) = \frac{2-4u/z}{\sqrt{1-4u/z}}\ln\left[1-\frac{z}{2u}+\frac{|z|}{2u}\sqrt{1+\frac{4u}{|z|}}\right]-1. \tag{16}$$

Performing suitable integrations we obtain

$$\begin{gathered} \ln\frac{\Gamma(x, \ z, \ u, \ e^2, \ e^2 d_l^0)}{\Gamma(x_0, z_0, u, e^2, \ e^2 d_l^0)} = \\ = \frac{e^2}{8\pi^2}\ln\left|\frac{x_0-u}{x-u}\right|\Phi\left(\frac{z}{u}, \frac{z_0}{u}, u\right) + \frac{e^2}{8\pi^2}\Psi\left(\frac{z}{u}, \frac{z_0}{u}, \frac{x_0}{u}, u\right). \end{gathered} \tag{17}$$

Here

$$\Psi\left(\frac{z}{u}, \frac{z_0}{u}, \frac{x_0}{u}u\right) = \int_{z_0}^{z} d(z', u, e^2)\left[\frac{\partial\varphi(z'/u)}{\partial z'}dz' + \ln\left|\frac{u}{x_0-u}\right|\frac{\partial\psi(z'/u)}{\partial z'}dz'\right], \tag{18}$$

and the index of the infrared singularity

$$\Phi\left(\frac{z}{u},\ \frac{z_0}{u},\ u\right)=\int_{z_0}^{z} d\left(z',\ u,\ e^2\right)\frac{\partial\psi\left(z'/u\right)}{\partial z'}\,dz'+\psi\left(\frac{z_0}{u}\right)+d_l^0 \tag{19}$$

after some small transformations and neglecting small terms of the order e^2 can be written as

$$\beta\left(\frac{k^2}{m^2}\right)=\frac{e^2}{8\pi^2}\,\Phi\left(\frac{k^2}{m^2},\ \frac{k_0^2}{m^2},\ \frac{m^2}{\lambda^2}\right)=\frac{e^2}{8\pi^2}\,d_l^0-3\ln\left|1-\frac{e^2}{24\pi^2}\,\psi\left(\frac{k^2}{m^2}\right)\right|. \tag{20}$$

In the limiting case of large k^2, when $(e^2/12\pi^2\ln(k^2/m^2)\sim 1$, we obtain

$$\beta\left(\frac{k^2}{m^2}\right)=\frac{e^2}{8\pi^2}\,d_l^0+3\ln d\left(\frac{k^2}{m^2},\ e^2\right). \tag{21}$$

On the other hand, when

$$\frac{e^2}{12\pi^2}\ln\frac{k^2}{m^2}\ll 1$$

we arrive at the result:

$$\beta\left(\frac{k^2}{m^2}\right)=\frac{e^2}{8\pi^2}\left[d_l^0+\psi\left(\frac{k^2}{m^2}\right)\right], \tag{22}$$

which Abrikosov obtained [2] by summing principal Feynman diagrams.

We have considered the principal asymptotic expressions for the vertex part when Γ^n is proportional to the matrix γ^n. When higher orders in e^2 are taken into account it may be necessary to consider components of Γ^n of different matrix structure. However, from the above investigation it follows that corresponding considerations can be extended to such cases also.

It is also clear that the renormalization group method can also be used for more complicated functions such as those corresponding to various scattering processes.

In conclusion the authors wish to acknowledge their indebtedness to N. N. Bogoliubov for a number of valuable suggestions.

M. V. Lomonosov Moscow State University
and
V. A. Steklov Mathematics Institute,
Academy of Sciences USSR

Received June 14, 1956

LITERATURE CITED

[1] N. N. Bogoliubov and D. V. Shirkov, Doklady Akad. Nauk SSSR 103, 203, 391 (1955); A. A. Logunov, J. Exptl.-Theoret. Phys. (USSR) 30, 793 (1956) [Soviet Physics – J. E. T. P., p. 766].

[2] A. A. Abrikosov, J. Exptl.-Theoret. Phys. (USSR) 30, 96 (1956) [Soviet Physics – J. E. T. P., p. 71].

[3] V. V. Sudakov, J. Exptl.-Theoret. Phys. (USSR) 30, 87 (1956) [Soviet Physics – J. E. T. P., p. 65].

[4] V. Z. Blank, Doklady Akad. Nauk SSSR 107, 389 (1956) [Soviet Physics – Doklady, p. 184].

PHOTOPRODUCTION OF SLOW π^--MESONS IN COMPLEX NUCLEI

E. G. Gorzhevskaia and N. M. Panova

(Presented by Academician D. V. Skobel'tsyn, June 25, 1956)

INTRODUCTION

The interaction of photons with nuclei which results in meson production has been studied insufficiently. Investigations have been made principally of the dependence of the cross section for photoproduction of mesons on the atomic number of the target [1, 2] and the energy and angular distributions of the photomesons [3]. As has been shown in some articles [4-6], photoproduction of mesons in nuclei is for the larger part accompanied by nuclear disintegrations ("stars"). But the characteristics of this process have not yet been studied. Only recently did an article appear [7] which partially remedied this lack.

It was the purpose of the present work to study the mechanism of photoproduction of π^- mesons in complex nuclei. In particular we wished to determine whether photoproduction of mesons in complex nuclei involves a single nucleon or whether the process is more complicated; we also wished to attempt to obtain information concerning the interaction of a slow meson with the residual nucleus.

EXPERIMENTAL

We used NIKFI Type "R" emulsions irradiated in the synchrotron of the Physics Institute of the Academy of Sciences by a photon beam with $E_{max} = 250$ Mev. The emulsions were impregnated with heavy water so that a simultaneous study was made of the photoproduction of π^- mesons in deuterium [8].

We selected nuclear disintegrations that contained a meson track which terminated in the emulsion. In the great majority of cases the π^- meson produced a star when stopped; thus identification was not difficult.[*] Because of such choice of pions the energy of the majority of mesons did not exceed 6-8 Mev.

In each case we determined the energy of the meson and particles in the star which accompanied meson creation and measured the angle between their directions of flight and the direction of the photon beam. All singly-charged particles were regarded as protons.[**] The energies of particles stopped in the emulsions were obtained from the range-energy curves calculated for the loaded emulsion. The energies of particles escaping from the emulsions were determined by measuring the grain densities of the tracks. The emulsion nuclei in which mesons were produced were divided by the "potential barrier" method [6, 9] into "light" (C, N, O) and "heavy" (Ag, Br, I) nuclei.[***]

---

[*] It should be noted that a short meson track which does not produce a star at its termination cannot be identified unambiguously. However, it is known that such cases comprise about 30%. This was taken into consideration in obtaining cross sections.

[**] The fact that an insignificant fraction of singly-charged particles which we regarded as protons may actually be deuterons does not affect our conclusions.

[***] This method of separation may possibly exaggerate the number of heavy nuclei somewhat at the expense of the light nuclei.

RESULTS

In an area of 830 cm^2 of the emulsions we found 262 stopped mesons. Seventy-five of these were assigned to π^- meson production in light nuclei and 163 to heavy nuclei. In 24 cases the nucleus in which the meson was created could not be identified.

We obtained the following cross sections for π^- meson production with energies up to 4 Mev in light and heavy emulsion nuclei (correcting for the geometry and for mesons which did not produce stars): for a light nucleus $(2.2 \pm 0.33) \times 10^{-29}$ cm^2; for a heavy nucleus $(8.8 \pm 0.9) \times 10^{-29}$ cm^2.

In obtaining the cross sections we assumed that the unidentified stars are divided in the same ratio as the identified stars. We note for comparison that the cross section for meson production with such energies in deuterium is $(0.33 \pm 0.07) \times 10^{-29}$ cm^2.*

TABLE 1

Number of prongs	0	1	2	3	4	5	6
Number of cases among heavy nuclei	50	92	20	1	0	0	0
Number of cases among light nuclei	0	9	38	18	5	4	1

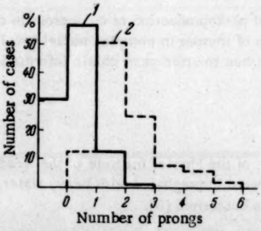

Fig. 1. Prong distribution in stars which accompanied the emission of mesons from heavy (1) and light (2) nuclei.

Fig. 1 and Table 1 give the prong distribution in stars which accompanied π^- meson production in light and heavy nuclei; the meson and recoil nucleus tracks are not included. It can be seen that, first, a large fraction of double-pronged stars and practically all stars with more than 2 prongs belong to light nuclei and, secondly, in a large number of instances the production of a slow π^- meson in a heavy nucleus is accompanied by the emission of only one proton. The angular distribution of these protons in the laboratory system has an appreciable maximum in the direction of the photon beams. With increased proton energy the peak becomes sharper.

Discussion of Results and Summary

The following are the most important experimental results.

1. We established the presence of a sharp peak in the angular distribution of high-energy protons which accompany photomeson production.

2. We determined the ratio of cross sections for π^- meson production in heavy and light emulsion nuclei for low energies.

Fig. 2 gives for comparison the angular distribution of protons with energies above 20 Mev from heavy nuclei and from deuterium which accompanied the production of π^- mesons with energies below 10 Mev.* Both distributions are of the same character, but the angular distribution of protons from deuterium has a sharper peak. The difference between our distribution and the distribution of protons from deuterium indicates the important effect of nucleon motion within the nucleus.

Fig. 3 gives curves obtained by A. M. Baldin and A. I. Lebedev* for angular distribution of fast (≥ 20 Mev) protons accompanying slow (≤ 10 Mev) mesons from nuclei.**

---

*Private communication.

**A Gaussian distribution was assumed for nucleonic momenta in the nucleus: $\rho(p) = (\beta/\pi)^{3/2} e^{-\beta p^2}$. Curve $\beta = 0.745$ corresponds to $1/2m\beta = 14$ Mev [13]. The curves were computed according to the independent particle model of Lax and Feshbach [10].

The good agreement with experiment of the calculated curve for $\beta = 0.745$ indicates that at least in the 30% of cases considered a photon produces a meson by interacting with one of the nuclear nucleons, whereupon the photon momentum is transferred mainly to the nucleon at which the meson is created.

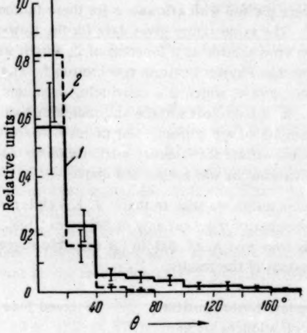

Fig. 2. Angular distribution of protons with energies above 20 Mev from heavy nuclei (1) and from deuterium (2).

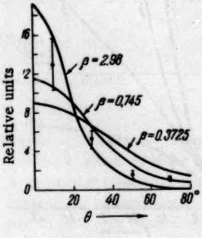

Fig. 3. Angular distribution of protons with energies above 20 Mev. The solid curves were calculated by A. M. Baldin and A. I. Lebedev from the independent particle model and Gaussian momentum distribution.

According to the calculations of Baldin and Lebedev in 60% of the cases the production of slow π^- mesons in the primary event is accompanied by a proton with energy above 20 Mev. In our experiments these comprised about 30 % of all cases of π^- meson production in heavy nuclei.

The character of the angular distribution of these protons indicates that the great majority of them did not interact with the nucleus. The probability that a particle produced at any point in a nucleus will escape without collisions can be obtained from simple geometrical considerations and depends on the nuclear radius R and the mean free proton path λ in the nuclear substance. The value of λ for protons can be obtained from the optical model [11, 14] and for energies 20-50 Mev is about $(2\text{-}4) \cdot 10^{-13}$ cm. For heavy emulsion nuclei it can be assumed that $R = 6.7 \cdot 10^{-13}$ cm. In this case the probability of proton escape without interaction is 25-40 %, whence it is easily seen that the fraction of single protons with energies above 20 Mev must be 0.15-0.24 of the total number of π^- meson productions in heavy nuclei, which agrees well in order of magnitude with the experimental value 0.3. We neglected meson absorption since the mean free path for mesons of such small energy is $\gg R$. *

Our result is a clear proof of the independent particle model.

The ratio of the cross sections for meson production with energy up to 4 Mev in light and heavy emulsion nuclei is 0.25 ± 0.06 according to our data. Baldin and Lebedev estimated that the ratio must be considerably lower if it is considered that the meson is emitted in the form of a free particle in the Coulomb field of a point charge. In this case even by the $A^{2}/_{3}$ law the ratio must be $\sigma_l / \sigma_h = 0.2\,(Z_l \,/\, Z_h)^{2}/_{3} = 0.06$, where 0.2 is the ratio of the Coulomb factors. This discrepancy can evidently be attributed to a specific interaction between the meson and nucleus within a region of the order of nuclear size and also principally to the fact that the Coulomb field in the nucleus differs from the field of a point charge.

---

* According to [12] for a meson with energy of the order 20 Mev the mean free path is $16 \cdot 10^{-13}$ cm.

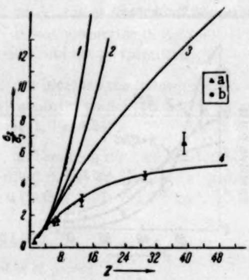

Fig. 4. Dependence of the cross section for low-energy meson production on the atomic number of the nucleus. a) our data; b) data of V. M. Popova, N. G. Semashko and F. R. Iagudina.

Fig. 4 gives curves for the dependence of the cross section for pion production with 2 Mev energy on Z as calculated by Baldin and Lebedev. Curves 1 and 2 were plotted, neglecting nuclear size and the nuclear interaction potential, for functions proportional to Z and $Z^{2/3}$, respectively. Curves 3 and 4 were plotted with allowance for these factors, respectively. The same figure gives data for the slow-meson production cross section as a function of Z, which were obtained from the Physics Institute synchrotron.* The points fit well on Curve 4, which is a convincing argument for meson production on the nuclear surface and indicates that the hypotheses employed are correct. Our points fit this curve less well. But the difference is easily attributable to inaccuracy in identifications, as was mentioned above.

In conclusion we wish to thank V. I. Veksler, Corresponding Member of the Academy of Sciences USSR, for directing this work and A. M. Baldin for valuable suggestions and discussions of the results.

P. N. Lebedev Physics Institute,
Academy of Sciences USSR

Received June 20, 1956

LITERATURE CITED

[1] R. F. Mozely, Phys. Rev. 80, 493 (1951).

[2] K. M. Littauer and D. Walker, Phys. Rev. 82, 746 (1951).

[3] J. Steinberger and A. S. Bishop, Phys. Rev. 86, 171 (1952).

[4] R. D. Miller, Phys. Rev. 82, 260 (1951).

[5] S. Kikuchi, Phys. Rev. 86, 41 (1952).

[6] R. M. Lebedev, Dissertation, Phys. Inst. Acad. Sci. USSR (1953).

[7] E. P. George, Proc. Phys. Soc. 69, 434 A, 110 (1956).

[8] M. I. Adamovich, G. V. Kuz'micheva, V. G. Larionova and S. P. Kharlamov, Doklady Akad. Nauk SSSR 102, 715 (1955).

[9] M. G. K. Menon, H. Muirhead and O. Rochat, Phil. Mag. 41, No. 317, 583 (1950).

[10] M. Lax and H. Feshbach, Phys. Rev. 81, 189 (1951).

[11] A. M. Lane and C. F. Wandel, Phys. Rev. 98, 1524 (1955).

[12] F. H. Tenney and J. Tinlot, Phys. Rev. 92, 974 (1953).

[13] K. A. Brueckner, R. J. Eden and N. C. Francis, Phys. Rev. 98, 1445 (1955).

[14] R. Serber, Phys. Rev. 72, 1114 (1947).

---

*Private communication from V. M. Popova, N. G. Semashko and F. R. Iagudina.

DOUBLE-RESONANCE CURVES OF A REFLECTION GRATING

L. N. Deriugin and G. Kh. Fridman

(Presented by Academician M. A. Leontovich, November 6, 1956)

It has previously [1] been shown that peculiar resonance phenomena occur on reflection gratings, especially when the rulings are narrow compared with the wavelength ($a \ll \lambda/2$ or $k\alpha \ll 1$, where 2a is the ruling width, λ is the wavelength, $k = 2l/\lambda$, $2l$ is the grating space and $\alpha = a/l$). In particular a special case of surface resonance (C) was found when the amplitudes of the glancing waves and fields in the rulings exceed the field of the incident wave manyfold. This can rightly be called double resonance since it is resonance with respect to the two parameters k and θ (where $\theta = 2\pi h/\lambda$ and h is the depth of the rulings). For normal incidence it occurs when the space $2l$ equals a whole number of wavelengths λ and the ruling depth h is a little larger than a half wave. However, the change of amplitudes of the glancing waves and fields in the rulings away from resonance, that is, the resonance curves, were not investigated. We give an approximate treatment of this problem below.

For an analysis of the resonance curves it is useful to start not with a set of equations for the waves in the grooves (rulings) [1, 2] but with equations for the partial waves in the upper half plane, which were obtained in [3]. The latter equations are distinguished by the fact that they have no singularities at the surface resonance points. This circumstance makes the analysis considerably easier. Moreover, since at double resonance (and close to it) the fundamental resonance field consists of glancing waves whose amplitudes are many times greater than the amplitudes of the remaining waves in the upper half plane, the field in the upper half plane can be approximated by using only glancing, incident and reflected waves.

We write Equations (17) of [3] in the following form:

$$\sum_{m=0}^{\infty} \bar{u}_{nm} H_m = b_n \quad (n = 0, 1, 2, \ldots), \tag{1}$$

where H_m is the amplitude of the m-th partial wave in the upper half plane (the amplitude of the incident wave is taken as unity),

$$\bar{u}_{nm} = \begin{cases} 2u_{nm} & n \neq m, \\ 2u_{mm} - \pi\delta_m, & n = m, \end{cases} \quad m \neq 0; \qquad \bar{u}_{n0} = \begin{cases} u_{n0}, & n \neq 0, \\ u_{00} - \pi\delta_0, & n = 0, \end{cases} \quad m = 0,$$

$$b_n = \begin{cases} -(u_{00} + \pi\delta_0), & n = 0, \\ -u_{n0}, & n \neq 0, \end{cases} \qquad \delta_n = \sqrt{1 - \left(\frac{n}{k}\right)^2}.$$

Then

$$u_{nm} = \frac{t_0}{\pi\alpha} \frac{\sin n\pi\alpha \sin m\pi\alpha}{nm} + 2\frac{nm}{\pi\alpha} \sin n\pi\alpha \sin m\pi\alpha \sum_{i=1}^{\infty} \frac{t_i}{(n^2 - p_i^2)(m^2 - p_i^2)}. \tag{2}$$

For narrow rulings ($k\alpha << 1$) and for values of n and m of the order k, Equation (2) for u_{nm} can be simplified and with accuracy to within $k\alpha$ becomes

$$u_{nm} = j\tan\theta\cdot\pi\alpha - j\cdot 2\frac{\pi\alpha^4}{k}n^2m^2\sigma, \quad \sigma = \sum_{i=1}^{\infty}\frac{1}{i^3} = 1{,}18. \tag{3}$$

In this approximation (1) becomes a set of two equations with two unknowns: H_0 (the amplitude of the mirror wave) and H_1 (the amplitude of the glancing wave).

The solution, using (3), is written as:

$$H_1 = \frac{2\pi u_{10}}{(2u_{11} - \pi\delta_1)(u_{00} - \pi) - 2u_{01}},$$

$$H_0 = -1 - \frac{2\pi(2u_{11} - \pi\delta_1)}{(2u_{11} - \pi\delta_1)(u_{00} - \pi) - 2u_{01}^2}. \tag{4}$$

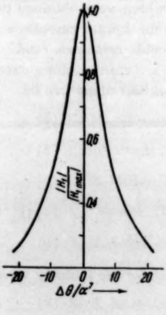

Fig. 1. Dependence of $|H_1| / |H_{1max}|$ on depth for $2l = \lambda$.

Let us consider surface resonance when $2l = \lambda$ ($k = 1$), and obtain θ_{opt} for which H_1 reaches an (absolute) maximum, i. e., double resonance occurs. Assuming $k = 1$ (and thus $\delta_1 = 0$) and inserting (3) in (4) we obtain

$$H_1 = \frac{1}{-\left(1 - \frac{2\alpha^3\sigma}{\tan\theta}\right) - j\cdot 2\alpha^4\sigma}. \tag{5}$$

Hence it can be seen that

$$H_{1\,\max} = j\frac{1}{\alpha^4\cdot 2\sigma}$$

and

$$H_0 = -1$$

$$\text{for } \tan\theta_{opt} = \alpha^3\cdot 2\sigma. \tag{6}$$

This result differs from that obtained in [1]. by only a constant factor, which can be attributed to an inaccurate approximation of the field in the upper half plane.

Let us study the change of the resonance field upon departure from double resonance, i. e., as k differs from 1 and θ from θ_{opt}.

We shall consider three cases:

A. The dependence of H_1 on $\Delta\theta$ for $k = 1$, i. e., on the depth of the rulings for the optimum spacing.

Considering the smallness of α and $\Delta\theta$ we have $\tan\theta = \tan(\theta_{opt} + \Delta\theta) = \alpha^3\cdot 2\sigma + \Delta\theta$. Inserting this expression in (5) we obtain after some transformations

$$\frac{|H_1|}{|H_{1\max}|} = \frac{1}{\sqrt{1 + \left[\frac{\Delta\theta}{\alpha^7\cdot 4\sigma^2}\right]^2}} \tag{7}$$

The graph of (7) is given in Fig. 1. The formula and the graph show that the resonance field depends strongly on $\Delta\theta$. For example, the width of the resonance curve at the 0.7 level is proportional to $\alpha^7 (\Delta\theta_{0.7} \sim \alpha^7)$.

The curve has the shape which is usual for oscillations. But it does not show the usual resonance relation of inverse proportionality between the width of the resonance curve and the amplitude of the resonance field. In the present case $\Delta\theta_{0.7} \sim \alpha^7$, and $|H_{1\,\max}| \sim 1/\alpha^4$. This can be attributed to a change of coupling between the resonance field of the grating and the field of the incident wave as θ departs from θ_{opt}.

B. The dependence of H_1 on Δk for $\theta = \theta_{\text{opt}}$, i. e., on the spacing at optimum ruling depth.

Since $\delta_1 = \sqrt{1-(1/k)^2}$ for $k = 1 + \Delta k$ and small Δk we have $\delta_1 = \sqrt{2\Delta k}$. Using the latter fact and also $\tan\theta_{\text{opt}} = \alpha^3 \cdot 2\sigma$, and inserting (3) in (4) we obtain after some transformations, accurate to higher powers of α.

$$\frac{|H_1|}{|H_{1\max}|} = \begin{cases} \dfrac{1}{1+\sqrt{\dfrac{\Delta k}{\alpha^{16}\cdot 32\sigma^4}}} & \text{for } \Delta k > 0, \\[2ex] \dfrac{1}{\sqrt{1+\dfrac{|\Delta k|}{\alpha^{16}\cdot 32\sigma^4}}} & \text{for } \Delta k < 0. \end{cases} \tag{8}$$

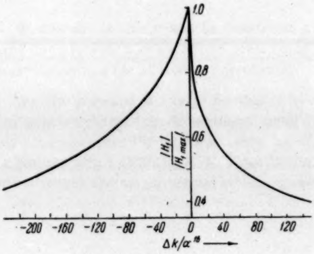

Fig. 2. Dependence of $|H_1|/|H_{1\max}|$ on the relative spacing for $\theta = \theta_{\text{opt}}$.

The graph of (8) is given in Fig. 2. The formula and the graph show that the dependence of the resonance field on the period is even stronger $(\Delta k_{0.7} \sim \alpha^{16})$, than on the depth $(\Delta\theta_{0.7} \sim \alpha^7)$. This curve also differs essentially from ordinary resonance curves in its shape: it is asymmetrical, has a sharp peak with a vertical tangent and approaches zero slowly. The width of the resonance curve is not inversely proportional to the amplitude of the resonance field since $\Delta k^{0.7} \sim \alpha^{16}$, while $|H_{1\,\max}| \sim 1/\alpha^4$. This difference results from the special character of resonance at a reflection grating since a change of Δk changes the structure of the field in the upper half plane and its relation to the field of the incident wave. The right-hand part of the curve $(\Delta k > 0)$ corresponds to the transformation of a glancing plane wave into a plane wave reflected at an angle to the grating. The left-hand part $(\Delta k < 0)$ corresponds to the transformation of a glancing plane wave into an inhomogeneous plane wave.

C. The dependence of H_1 on $\Delta\lambda$ for $h = h_{\text{opt}}$ and $2l = \lambda_0$, i. e., on frequency for optimum (and fixed) depth and spacing.

Change of λ is accompanied by a change of $\theta = 2\pi h/\lambda$ and $k = 2l/\lambda$. But since the dependence of H_1 on Δk is considerably stronger $(\Delta k_{0.7} \sim \alpha^{16})$, than on $\Delta\theta \, (\Delta\theta_{0.7} \sim \alpha^7)$ it can be assumed, up to higher powers of α, that a change of λ is accompanied only by a change of $\underline{k}$ and that $\theta = \theta_{\text{opt}}$. Therefore everything that was said for case B applies equally to the present case. Only when (8) and the graph of Fig. 2 are used it should be considered that $\Delta k = -\Delta\lambda/\lambda$.

We note in conclusion that rhese results enable us through the coupling equations of [3] to obtain resonance curves also for the fields in the rulings.

Received August 27, 1956

LITERATURE CITED

[1] L. N. Deriugin, Doklady Akad. Nauk SSSR 94, 2, 203 (1954).

[2] L. N. Deriugin, Doklady Akad. Nauk SSSR 93, 6, 1003 (1953).

[3] L. N. Deriugin, Doklady Akad. Nauk SSSR 87, 6, 913 (1952).

ON POSITRON ANNIHILATION IN METALS

V. I. Karpman and I. Z. Fisher

(Presented by Academician M. A. Leontovich, October 5, 1956)

1. In [1] the lifetime of positrons in various media was studied. It was established that there is two-photon annihilation in metals and that the lifetime depends only slightly on the kind of metal. For all the metals investigated it was found that $\tau \sim 1\text{-}2 \cdot 10^{-10}$ sec. In discussing the possibility of interpreting their data for metals as a result of direct annihilation of positrons with free electrons the authors of [1] arrive at the following value for τ:

$$\tau = (\pi r_0^2 c N)^{-1}, \tag{1}$$

where $r_0 = e^2/mc^2$ and N is the density of free electrons. The values of τ which are calculated herefrom exceed experimental values by 1 to 2 orders. On the other hand, the experimental values of τ are very close to the lifetime of parapositronium. Hence it was concluded that a positron which is slowed down in a metal before annihilation is first bound to a free electron to form positronium.

Dixon and Trainor [2] also exclude the possibility of annihilation in metals without the formation of positronium.

In the present note it will be shown that a correct calculation of the lifetime of a positron which is annihilated directly with a free electron gives completely satisfactory agreement with experiment. The formation of positronium in a metal is very improbable.

2. The presence of a large number of free electrons must result in strong screening of the Coulomb field of any positive charge introduced into a metal. Since the relaxation time for the interaction of electrons is surely not longer than the relaxation time for electron-lattice interactions ($\sim 10^{-13}$ sec at room temperature), for a positron which exists for $\sim 10^{-10}$ sec in the metal, the screening can be regarded as stable. Then in the Debye-Hueckel approximation the screening radius for a degenerate electron gas is [3]

$$r_D = \frac{\sqrt{\pi}}{2}\left(\frac{\hbar^2}{me^2}\right)^{1/2}(3\pi^2 N)^{-1/6}, \tag{2}$$

and for the ratio of the positronium radius in a vacuum, $r_p = 2\hbar^2/me^2$, to the screening radius we obtain

$$\frac{r_p}{r_D} = \frac{4}{\sqrt{\pi}}\left(\frac{\hbar^2}{me^2}\right)^{1/2}(3\pi^2 N)^{1/6}. \tag{3}$$

Assuming $N = \nu \cdot 10^{22}$, where $\nu \sim 1\text{-}10$, we obtain $(r_p/r_D) = 1.4\,\nu^{1/6}$. Thus $r_p \geqslant r_D$ and the formation of positronium in a metal in the same form as it exists in a vacuum is impossible. Moreover, it is very likely that bound electronic states in such a strongly screened Coulomb field are altogether impossible (see also [4], p. 112). If it is assumed that a bound state could be formed,the screening would produce such extensive smearing of the wave function for the relative motion of the positronium components that its lifetime would be much longer than the vacuum value $\tau \sim 10^{-10}$ sec.

It is therefore reasonable to assume that positron annihilation in metals occurs without positronium formation and directly with a free electron. We can neglect the possibility of positron annihilation with electrons of the atom cores according to [5].

3. It was shown in [6] that in the time $\tau \sim 10^{-13}$ sec the positrons in metals are slowed down to thermal velocities. Therefore the velocity of the great majority of free electrons is considerably greater than the velocity which is able to annihilate a positron. Thus we can assume approximately that the relative velocity of an electron-positron pair for large separations is equal to the electron velocity $\underline{v}$ with respect to the lattice. Then the annihilation cross section neglecting the electron-positron Coulomb interaction, averaged over the spins of the particles, will be [7]

$$\sigma = \frac{\pi r_0^2 c}{v}. \tag{4}$$

This easily gives Equation (1) above, which was used in reference [1]. Since the slow electrons play the principal part in annihilation it is essential to allow for the electron-positron interaction. The interaction can be regarded approximately as of pure Coulomb character, neglecting screening by free electrons, since the annihilation cross section is determined by the wave function of relative electron-positron motion for $r = 0$ and at small distances the screening is inconsequential. An account of the interaction requires in the right-hand side of (4) a factor equal to the ratio of the square of the modulus of an electron wave function in a Coulomb field to that of a free electron taken at the location of the positron [8] (see also [9] p. 497). Instead of (4) we then obtain

$$\sigma = \frac{2\pi^2 r_0^2 c^2 \alpha}{v^2}\left[1 - \exp\left(-\frac{2\pi\alpha c}{v}\right)\right]^{-1}; \quad \alpha = \frac{1}{137}. \tag{5}$$

But it is easily seen that even for $\underline{v}$ equal to the electron velocity on the Fermi surface the exponential in (5) is vanishingly small so that we finally have

$$\sigma = 2\alpha\left(\frac{\pi r_0 c}{v}\right)^2 = 2\alpha^3\left(\frac{\pi\hbar}{mv}\right)^2, \tag{6}$$

where $\underline{m}$ is the true electron mass.

4. The probability per unit time of positron annihilation with electrons at infinity having velocities from $\mathbf{v}$ to $\mathbf{v} + d\mathbf{v}$ will be

$$dw = (\sigma v)\cdot 2\left(\frac{\mu}{2\pi\hbar}\right)^3 d^3\mathbf{v}, \tag{7}$$

where μ is the effective electron mass. The total annihilation probability $\mathbf{W}$ per unit time is obtained by integrating (7) over a volume in velocity space bounded by the Fermi surface. Considering this surface to be spherical and μ as slightly dependent on velocity we obtain after integration and using (6):

$$w = \frac{\alpha^3 \mu^3}{\hbar m^2} v_0^2, \tag{8}$$

where v_0 is the electron velocity on the Fermi surface. When v_0 is expressed in terms of the concentration of free electrons [10, 11]

$$N = \frac{8\pi}{3} \frac{m}{\mu} \left(\frac{\mu v_0}{2\pi\hbar}\right)^3, \tag{9}$$

we obtain instead of (8):

$$w = \frac{\pi^2 \alpha^3 \hbar}{m} \left(\frac{\mu}{m}\right)^{5/3} \left(\frac{3N}{\pi}\right)^{2/3}. \tag{10}$$

Hence we have for the mean lifetime of a positron in a metal

$$\tau = \frac{1}{w} = \frac{m}{\pi^2 \alpha^3 \hbar} \left(\frac{m}{\mu}\right)^{5/3} \left(\frac{3N}{\pi}\right)^{2/3}. \tag{11}$$

Denoting again $N = \nu \cdot 10^{22}$ and substituting the values of the constants we finally obtain

$$\tau = 5.0 \left(\frac{m}{\mu}\right)^{5/3} \nu^{-2/3} \cdot 10^{-10} \text{ sec} . \tag{12}$$

5. Assuming in (12) $\mu \approx m$ and $\nu \sim 5$, we obtain $\tau \sim 1\text{-}2 \cdot 10^{-10}$ sec in agreement with experiment. Further improvement of the numerical value for τ is difficult both because the exact value of μ is unknown and because of insufficient information regarding the true density of free electrons in specific metals. The determination of N from the number of electrons per atom cannot be regarded as justified.

As a numerical illustration of (12) we shall use data for N and μ in [10, 11]. In these articles the quantities of interest were determined from optical data and from the electronic portion of the specific heat of four metals: Al, Cu, Ag and Au. The results of the computations are given in Table 1.

TABLE 1

	$\nu = N \cdot 10^{-22}$	μ/m	$\tau_{\text{theor}} \cdot 10^{-10}$ sec	$\tau_{\text{exp}} \cdot 10^{-10}$ sec
Al	5,4	1.7	0.61	1.5±0.3
Cu	3,3	2.4	0.96	1.2±0.5
Ag	5.7	1.05	1.6	1.5±0.6
Au	5.1	1.05	1.6	1.2±0.3

One should, of course, keep in mind that the initial data used in [10, 11] for computing N are not sufficiently reliable, as the writers themselves note; therefore it is impossible at the present time to explain the small discrepancies between τ_{theor} and τ_{exp} in Table 1. It must also be remembered that greater accuracy cannot be expected of the free-electron model.

We note, finally, that from the method used to obtain (11) it follows that for two-photon annihilation of protons in metals there must be no temperature dependence of τ and that two or more lifetimes are impossible (unlike nonconducting media). These circumstances are in agreement with experiment [1].

The authors take this opportunity to thank V. L. Ginzburg, Corresponding Member of the Academy of Sciences USSR, who brought the problem to their attention and who made interesting comments in a discussion of the results.

Minsk Pedagogical Institute
and
V. I. Lenin Byelorussian State University

Received April 17, 1955

LITERATURE CITED

[1] R. Bell and R. Graham, Phys. Rev. 90, 644 (1953).

[2] W. Dixon and L. Trainor, Phys. Rev. 97, 733 (1955).

[3] L. Landau and E. Lifshits, Statistical Physics (Moscow, 1951).

[4] N. Mott and R. Gurney, Electronic Processes in Ionic Crystals (Foreign Lit. Press, 1950).

[5] S. De Benedetti et al., Phys. Rev. 77, 205 (1950).

[6] G. Garwin, Phys. Rev. 91, 1571 (1953).

[7] A. Akhiezer and V. Berestetskii, Quantum Electrodynamics , Moscow, 1953.

[8] A. Sakharov, J. Exptl.-Theoret. Phys. (USSR) 18, 631 (1948).

[9] L. Landau and E. Lifshits, Quantum Mechanics (Moscow, 1948).

[10] V. Ginzburg, Doklady Akad. Nauk SSSR 97, 999 (1954).

[11] V. Ginzburg and G. Motulevich, Progr. Phys. Sci. (USSR) 55, 469 (1955).

SPARK CHANNEL BROADENING IN AIR AT ABOUT 2×10^6 AMPERES

V. S. Komel'kov and D. S. Parfenov

(Presented by Academician A. P. Aleksandrov, August 21, 1956)

1. The spark channel under investigation existed in an air gap during the discharge of a shock circuit consisting of 48 condensers with an operating voltage of 50 kv and total capacity of $132\,\mu$f.* The investigation was conducted at 40 kv, giving a spark current up to $1.7 \cdot 10^6$ amperes with an initial steep rise of 10^{12} amperes per second. At 50 kv voltage the current reached $2 \cdot 10^6$ amperes. The current was measured with a Rogovskii loop and OK-17M double oscilloscope. For voltage measurements we used a mixed divider connected in parallel with the electrodes, which were constructed of two copper hemispheres separated by 30 mm. An opening in one of the hemispheres contained an auxiliary electrode for excitation of the discharge by a pulse supplied from a high-speed photographic recorder. The IKhF photographic recorder consists of a small mirror rotated by an electric motor, objectives and a slit which revealed a small portion near the middle of the spark channel image; this was scanned on film at the rate of $3.0 \cdot 10^5$ cm/sec. Each point of the image was exposed $3 \cdot 10^{-8}$ sec. This photographic scanning was insufficient for analysis of phenomena associated with fast asymmetrical channel expansions and had to be supplemented by photographs obtained through the use of Kerr cells. The exposure for each photograph was $0.2\,\mu$ sec. Data obtained by both methods are in good agreement.

The initial phases of the process (to $10\,\mu$ sec) were the most interesting. Photographing of these with Kerr cells was very difficult because the succeeding stages illuminated the films. The luminous background was reduced by an electrically operated shutter which interrupted the light field of the cells $15\,\mu$ sec after breakdown of the spark gap.

The relation between the Kerr photographs and the current in the spark channel was established by simultaneous oscillographic recording of the current and voltage at one of the cells at the instant of photographing.

2. Unlike the monotonic channel expansion observed during the relatively short initial current rise of 10^9-10^{10} amperes per second [1-5], in our case we observed during the channel expansion four characteristic phases which are easily distinguished in Figs. 1 and 2; these are schematic copies of the scanning photographs and Kerr photographs.

In the first phase, which sometimes last $0.7\,\mu$ sec, the expansion of the channel proceeds at the rate of more than $2 \cdot 10^6$ cm/sec. The rate then drops to $4 \cdot 10^5$ cm/sec. In this stage the current density reaches its highest values for the entire discharge (10^7 amperes/cm^2 and higher), which were previously observed only in the electrical explosion of wires. The discharge channel in the first phase has one visible boundary.

The second phase reveals a new diffuse boundary which is clearly visible within the inner discharge zone in the scanning and Kerr photographs. While the boundaries of the outer zone in the scanning photographs are a direct continuation of the discharge boundaries in the first phase and are propagated with the same velocity, the boundaries of the inner zone are at first almost motionless and only after 0.5-1.0 μ sec do they begin to move with increasing speed. Within 1.5-2.0 μ sec the outer and inner zones come in contact again.

---

*This work was done in 1954 and 1955.

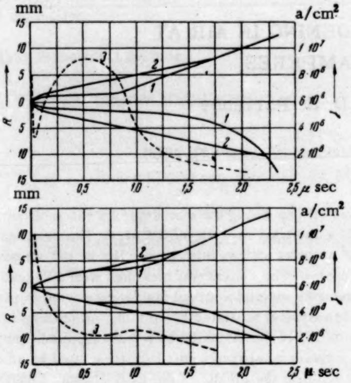

Fig. 1. Photographic scanning of spark discharge channels. p = 1 atmos; U_{op} = 10 kv; δ = 30 mm. 1) inner discharge zone; 2) outer discharge zone; 3) current density in inner discharge zone.

From the Kerr photographs (Fig. 2A) we see that the inner filament is strongly distorted while the outer zone retains its cylindrical symmetry until the two zones fuse. Assuming that the current flows predominantly in the inner bright zone we can obtain the current density here. This reaches values of the order (2.5-9.0) · 10^6 amp/cm^2.

The touching of the inner and outer boundaries gives rise to a peculiar phenomenon which develops in the third phase. At the points of contact nuclei of perturbations (shock waves) are formed which are propagated in all directions with the initial velocity (0.8-1.2) · 10^6 cm/sec. Within 2-3 μ sec the velocity of the waves drops to 5 · 10^5 cm/sec. The transparency of the gas at the boundary of the perturbation waves is reduced; this hinders further observation of the internal structure of the discharge. Fig. 2B gives an idea of the outer discharge boundaries during this period, showing that the cylindrical symmetry of the channel almost disappears and that it becomes more and more distorted.

The channel then expands at a continuously diminishing rate (fourth phase) which by the 60th microsecond amounts to 2.2 · 10^5 cm/sec. During this period of time the channel diameter becomes 12 cm. The rate of expansion of the channel gradually decreases, oscillating aroung an average value. The period of the oscillations is close to the current period τ = 18 μ sec.

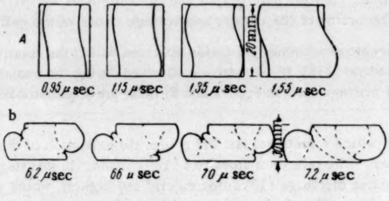

Fig. 2. Schematic representations of a discharge channel photographed with Kerr cells.

The discharge current has the shape of a damped sine wave (Fig. 3) during all four phases of the channel expansion. The potential (Fig. 3) and the longitudinal gradients in the discharge gap are maintained anomalously high (compared with an arc) for 6-7 μ sec. Initially the gradients reach 5-6 kv/cm (after subracting the inductive component) and at the end of the fourth period they drop to 0.5-1.0 kv/cm.

3. The first phase of the discharge described above differs from the initial phases of previously investigated less powerful sparks only in increased rate of channel expansion and current density, while the phenomenological

picture of the channel expansion in strong discharges remains the same. In the first period the shock wave front and the boundaries of the high-temperature zone practically coincide [2, 3]. They separate in the second stage when the intrinsic magnetic field of the current at the discharge boundary and the resultant pressure on ionized particles reach $4 \cdot 10^5$ oerst and $5 \cdot 10^4$ atmos, respectively.

The breaking-away of the shock wave also denotes that the conductivity behind its front is too low to assure the flow of the large circuit currents. In our case with a wave velocity of $4 \cdot 10^5$ cm/sec the temperature at the front, derived from certain known relationships [6], does not exceed $9 \cdot 10^4$ °K, that is, it is high enough to excite luminescence and partial ionization of the gas but too low for the required conduction. It is obvious that the high-temperature zone in which the main current flows is the inner discharge zone which is constricted by the magnetic field. The mean temperature of this zone can be determined from the equilibrium conditions of the magnetic and gas-kinetic pressures and from Saha's equation. As Schlüter showed [7], it follows from the equilibrium conditions that

$$T = 1.56 \cdot 10^9 \frac{I^2}{N_i} \text{ ev},$$

where T is the mean gas temperature in volts, I is the discharge current in amperes and N_I is the number of ions and electrons per unit length of the current filament.

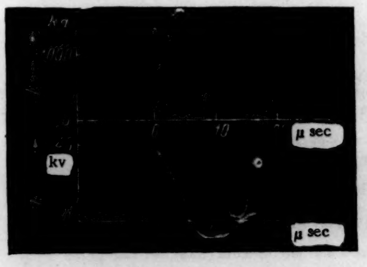

Fig. 3. Oscillograms of discharge current and spark gap potential.

From a graphical solution of this equation and Saha's equation which gives the relation $N_i = f(T)$ we find that the gas temperature (calculated for nitrogen) is 17 and 33 ev for the cases of Figs. 1A and 1B, respectively (for the times 0.8 and 1 μ sec). For the computations it was assumed that the gas density in the filament was the same as in an undisturbed medium. Since the gas density behind the front is actually considerably lower the values obtained must be regarded as the lower limit of possible temperatures.

An estimate of the mean inner zone temperature from energy balance is less accurate due to errors in measuring the longitudinal channel gradients and because of the assumptions required for computing the energy expended in radiation, ionization, heating and dissociation of the gas (the energy of the shock wave can be neglected). The last three components can be determined to the same approximation as above. To compute the radiated energy we require information concerning the depth, transparency and temperature of the radiating surface layer, the determination of which is an independent complicated problem. A rough indirect estimate of the temperature of the emitting surface can be obtained from the velocity of the shock waves formed through contact of the inner filament with the cold gas at the outer channel boundary (third phase); this gives 18 ev for a wave-front velocity of 10^6 cm/sec.

The intense illumination of the gas at the contact of the two zones is in all probability associated with the dissociation of nitrogen and formation of its oxides, which again indicates surface temperatures higher than 7 ev.

At a surface layer temperature of the order of 10 ev the light peak is shifted in the direction of the short-wave emission ($\lambda < 300$ A) which will be completely absorbed inside the channel. Schwicker and others [8] established the possibility of this absorption for waves with $\lambda = 1000$ A.

The sealed-in radiation may naturally be neglected in the balance equation. Making this assumption we obtain a temperature in the channel that is 3-5 times greater than the values obtained above, which are evidently close to the actual values.

The temperature rise of the current filament ceases as the steep current rise is reduced and the channel, in expanding, draws new and colder particles into the inner zone.

The cause of the expansion may be: 1) diffusion of hot particles from the central regions of the current filament; 2) ionization of the outer gas layers by radiation from the discharge; 3) breakdown along the channel in the layer of excited and partially ionized particles.

All of these factors result ultimately in expansion of the conduction zone. It is difficult to say which process predominates. Yet it is certain that the magnetic field of the discharge, by slowing down the channel expansion, permits heating the gas to higher temperatures than have ever been observed.

With the increase of the magnetic field the instability of the channel increases. This is noticeable even in the second discharge phase, where the channel becomes distorted into the shape of a spiral curve. Unilateral "bulges" which appear in the third phase aggravate the instability and crooked shape of the channel. Instability of the channel is understandable if we consider that any asymmetry (distortion of the original breakdown trajectory, of current distribution within the filament, random fluctuations of conduction, etc.) is reinforced by the magnetic field which exerts pressure on the filament of the order of 10^4 kg/cm.

The authors wish to thank B. P. Surnin, who photographed the spark channel using Kerr cells.

Received July 26, 1956

LITERATURE CITED

[1] I. S. Abramson and E. S. Marshak, J. Tech. Phys. (USSR) 12, 632 (1942).

[2] I. S. Abramson, N. M. Gegechkori, S. I. Drabkina and S. L. Mandel'shtam, J. Exptl.-Theoret. Phys. (USSR) 17, 862 (1947).

[3] N. M. Gegechkori, J. Exptl.-Theoret. Phys. (USSR) 21, 493 (1951).

[4] J. B. Higham and I. M. Meek, Proc. Phys. Soc. 63, 369B (1950).

[5] I. E. Allen and I. Craggs, Brit. J. Appl. Phys. 5, 446 (1954).

[6] L. D. Landau and E. M. Lifshitz, The Mechanics of Continuous Media (Moscow, 1954).

[7] A. Schlüter, Z. Naturforsch. 5a, 72 (1950).

[8] B. Ganger, Der Electrische Durchschlag von Gasen (1953).

NUCLEAR LEVELS OF Li^6

Iu. L. Sokolov, M. M. Sulkovskaia, E. A. Al'bitskaia
and E. I. Karpushkina

(Presented by Academician L. A. Artsimovich, August 28, 1956)

Using a method which we have already described [1], we investigated the interactions between fast deuterons and Li^6 and Li^7 nuclei. For registration of the reaction products we used E-1 Ilford plates with lithium introduced directly into the emulsions. The plates, which contained about 2×10^{21} atoms of lithium per cm^3 of dry emulsion, were irradiated with deuterons of energy 17.5 ± 0.25 Mev whose range was contained within the emulsions.

Among the numerous reactions detected in the plates we identified the following reactions with Li^6 and Li^7:

$$\mathrm{Li}^6(\mathrm{d},\ 2\mathrm{d})\,\mathrm{He}^4; \qquad \mathrm{Li}^6(\mathrm{d},\ \mathrm{d}',\ \mathrm{p},\ \mathrm{n})\,\mathrm{He}^4;$$

$$\mathrm{Li}^7(\mathrm{d},\ \mathrm{t},\ \mathrm{d}')\,\mathrm{He}^4; \qquad \mathrm{Li}^7(\mathrm{d},\ \mathrm{t},\ \mathrm{p},\ \mathrm{n})\,\mathrm{He}^4.$$

The reaction $\mathrm{Li}^6(\mathrm{d},\ 2\mathrm{d})\,\mathrm{He}^4$. An investigation of this reaction, which we had observed previously [1], showed that in this case, in addition to the observed levels at 2.2 and 4.5 Mev there are also levels at 5.9, 7.4 and 8.3 Mev (Fig. 1).* All of these levels must have zero isotopic spin since the decay products of the Li^6 nucleus are an alpha particle and a deuteron (which have zero isotopic spin).

The reaction $\mathrm{Li}^6(\mathrm{d},\ \mathrm{d}',\ \mathrm{p},\ \mathrm{n})\,\mathrm{He}^4$. The value of Q for this reaction is -3.7 Mev so that decay of the excited Li^6 nucleus does not in this case take place from the 2.2 Mev level. The next level which can be excited by an elastically scattered deuteron is evidently ~ 4.5 Mev. However we did not detect stars associated with this level. This is due in all probability to the short ranges of the particles which are involved, thus making it impossible to identify the corresponding stars.

All the stars which we found belonging to the reaction $\mathrm{Li}^6(\mathrm{d},\ \mathrm{d}',\ \mathrm{p},\ \mathrm{n})\,\mathrm{He}^4$ are associated with the decay of excited nuclei from higher levels whose energy is ~ 5.9 and 7.4 Mev. The isotopic spins of these levels must be zero since in this reaction the excitation of the Li^6 nucleus is produced by a deuteron.

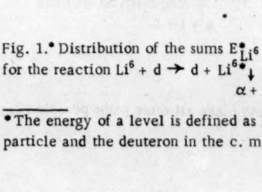

Fig. 1.* Distribution of the sums $E^*_{\mathrm{Li}^6}$ for the reaction $\mathrm{Li}^6 + \mathrm{d} \rightarrow \mathrm{d} + \underset{\alpha + \mathrm{d}'}{\underset{\downarrow}{\mathrm{Li}^{6*}}}$

---

*The energy of a level is defined as $E^* = \epsilon_\alpha + \epsilon_d + |Q|$, where ϵ_α and ϵ_d are the kinetic energy of the alpha particle and the deuteron in the c. m. system of the excited Li^6 nucleus and Q is the reaction energy.

The reaction $Li^7(d, t, d')He^4$. This reaction can evidently occur in two ways:

$$\begin{tikzcd}
 & t + \mathrm{Li}^{6*} \arrow[d] & \\
 & \alpha + d & (I) \\
\mathrm{Li}^7 + d \arrow[ruu] \arrow[rd] & & \\
 & d + \mathrm{Li}^{7*} \arrow[d] & \\
 & \alpha + t & (II)
\end{tikzcd}$$

and thus enables us to determine the location of a few Li^6 and Li^7 levels. But the analysis of stars belonging to the $Li^7(d, t, d')He^4$ reaction is complicated for the same reasons as in the case of $Li^6(d, 2d)He^4$ [1]. In the present instance we do not know in advance to which of the above reaction paths a given star belongs. It was therefore assumed that the reaction followed the possible paths alternately. It is clear that the coupled sums $E^*_{\mathrm{Li}^6} = \varepsilon_\alpha + \varepsilon_d + |Q_{\mathrm{Li}^6}|$ and $E^*_{\mathrm{Li}^7} = \varepsilon_\alpha + \varepsilon_t + |Q_{\mathrm{Li}^7}|$* found in this way must be grouped (according to one of the paired quantities) around values corresponding to the nuclear energy levels of Li^6 and Li^7. The analysis of all stars belonging to this reaction showed, first, that both reaction paths (I) and (II) are possible and that they are of approximately equal probability. The sums E* were grouped around the values 2.2, 4.5, 5.9, 7.4 and 8.3 Mev. A weak group is also observed at 9.2 Mev (Fig. 2). All of the levels mentioned corresponding to the first reaction path of $Li^7(d, t, d')He^4$, which leads to the formation of an excited Li^6 level that then decays into an alpha particle and deuteron, must possess zero isotopic spins.

It must be noted that the literature [2] contains indications that the Li^6 nucleus has a level at 8.37 Mev (the existence of which has been reliably established). Isotopic spin T = 1 has been ascribed to this level, which is inconsistent with our findings.

The reaction $Li^7(d, t, p, n)He^4$. This reaction can in principle follow the three following paths:

$$\begin{tikzcd}
 & t + \mathrm{Li}^{6*} \arrow[d] & \\
 & \alpha + p + n & (I) \\
\mathrm{Li}^7 + d \arrow[ruu] \arrow[r] \arrow[rdd] & p + \mathrm{Li}^{8*} \arrow[d] & \\
 & \alpha + t + n & (II) \\
 & n + \mathrm{Be}^{8*} \arrow[d] & \\
 & \alpha + t + p. & (III)
\end{tikzcd}$$

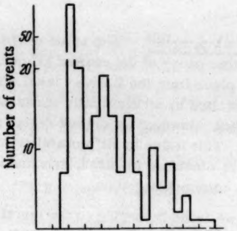

Fig. 2. Distribution of the sums $E^*_{\mathrm{Li}^6}$ for the reaction $\mathrm{Li}^7 + d \rightarrow t + \mathrm{Li}^{6*} \downarrow \alpha + d'$

The excitations which are possible in this case ($E_{d\,\max}$ = 17.5 Mev) make all three paths possible (Q_{Li^6} = − 3.7 Mev, Q_{Li^8} = − 4.5 Mev and $Q_{\mathrm{Be}^8} \cong -20$ Mev)

---

* See note on Fig. 1.

When we calculate the nuclear levels of Li^6 for stars belonging to this reaction (assuming the first reaction path) the sums $E^*_{Li^6} = \epsilon_\alpha + \epsilon_p + \epsilon_n + |Q_{Li^6}|$ which are obtained are grouped around the values 5.2, 6.7 and 8.3 Mev; these are in sufficiently good agreement with the known energy levels of Li^6. We also find a quite numerous group of sums $E^*_{Li^6}$ from 9 to 10.5 Mev. It can be assumed that we are here observing one broad level or, as is more likely to be correct, two levels are superimposed, one near ~ 9.5 Mev, the other near ~ 10.1. Since these levels were located with insufficient accuracy it can clearly be assumed that the excitation energies of 9.2 and 9.5 Mev which were found for the reactions $Li^7(d, t, d')He^4$ and $Li^7(d, t, p, n)He^4$, respectively, are actually the same level at ~ 9.3 Mev. This level must clearly possess isotopic spin $T = 0$.

The levels at 5.2 and 6.7 Mev have isotopic spin $T = 1$, which is not inconsistent with the possibility for decay of the excited Li^6 nucleus into an alpha particle, proton and neutron. These levels, like the level at ~ 10.1 Mev, were not observed in other reactions investigated by us that lead to the formation of excited Li^6 nuclei with isotopic spin $T = 0$. It can therefore be assumed that the 10.1 Mev level, if it exists, has isotopic spin $T = 1$. The level which we detected at 8.3 Mev (observed quite clearly) can in this instance have either isotopic spin $T = 1$ or $T = 0$. But the data given above for the reaction $Li^7(d, t, d')He^4$ lead to the assumption that the isotopic spin is $T = 0$.

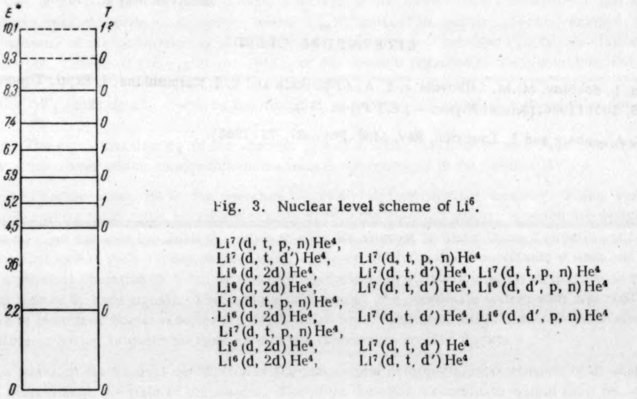
E*
T
10.1
1?
9.3
0
8.3
0
7.4
0
6.7
1
5.9
0
5.2
1
4.5
0
3.6
2.2
0
0
0
$Li^7(d, t, p, n)He^4$,
$Li^7(d, t, d')He^4$, $Li^7(d, t, p, n)He^4$
$Li^6(d, 2d)He^4$, $Li^7(d, t, d')He^4$, $Li^7(d, t, p, n)He^4$
$Li^6(d, 2d)He^4$, $Li^7(d, t, d')He^4$, $Li^6(d, d', p, n)He^4$
$Li^7(d, t, p, n)He^4$,
$Li^6(d, 2d)He^4$, $Li^7(d, t, d')He^4$, $Li^6(d, d', p, n)He^4$
$Li^7(d, t, p, n)He^4$,
$Li^6(d, 2d)He^4$, $Li^7(d, t, d')He^4$
$Li^6(d, 2d)He^4$, $Li^7(d, t, d')He^4$

Fig. 3. Nuclear level scheme of Li^6.

In conclusion the following interesting characteristic of the reactions $Li^6(d, t, d')He^4$ and $Li^7(d, t, p, n)He^4$ should be noted. In investigating the reaction path of $Li^7(d, t, d')He^4$ which leads to the formation of excited Li^6 nuclei, we observed a number of levels of this nucleus with isotopic spin $T = 0$, which resulted from the fact that these nuclei decayed into an alpha particle and deuteron.

The first reaction path of $Li^7(d, t, p, n)He^4$ which we investigated

$$\begin{tikzcd} Li^7 + d + t + Li^{6*} \arrow[d] \\ \alpha + p + n \end{tikzcd}$$

also leads to the formation of excited Li^6 nuclei with the observed levels able in this instance to possess either isotopic spin T = 0 or T = 1. But in studying the sums $E^*_{Li^6}$ which we found for the reaction $Li^7(d, t, p, n)He^4$ we observed that in this instance (as was discussed above) levels are found at 5.2, 6.7, 8.3 and 9.5-10 Mev. The levels at 5.2 and 6.7 Mev are known to have T = 1; the level at 8.3 Mev must clearly possess isotopic spin T = 0. But the other levels of Li^6 with T = 0, which from energy considerations could have been observed, namely 5.9 and 7.4 Mev with T = 0, were not detected (more accurately there was a very weak hint of a level at 7.4 Mev, but 5.9 Mev was definitely absent).

Our results regarding the observation of excited nuclear levels of Li^6 can be represented in the scheme of Fig. 3.

In this scheme it is striking that beginning with $E^*_{Li^6}$ = 3.6 Mev (we were unable to detect this level) the levels of Li^6 are separated by approximately equal distances averaging 0.8 Mev.

The authors thank Professor I. I. Gurevich, A. I. Baz' and G. M. Budianskii for discussions of a number of questions, and Z. M. Kudriashova, L. S. Baturina and M. I. Ovsiannikova for scanning the plates.

Received May 31, 1956

LITERATURE CITED

[1] Iu. L. Sokolov, M. M. Sulkovskaia, E. A. Al'bitskaia and E. I. Karpushkina, J. Exptl.-Theoret. Phys. (USSR) 30, 6, 1007 (1956) [Soviet Physics – J.E.T.P., p. 740].

[2] F. Ajzenberg and T. Lauritsen, Rev. Mod. Phys. 27, 77 (1955).

ON RELATIVISTIC INVARIANCE IN QUANTUM THEORY

Iu. M. Shirokov

(Presented by Academician N. N. Bogoliubov, June 27, 1956)

1. The purpose of the present paper is an investigation of the general requirements which must be satisfied by any relativistic quantum theory. These requirements can be expressed as commutation relations which are more general than the familar invariance conditions of quantum theory [1, 2]. In quantum field theory these relations are not satisfied.

2. One of the causes of difficulties in field theories is the nonquantum description of space-time relations. For example, the energy-momentum tensor $\hat{T}_{\mu\nu}(x)$ defined in quantum electrodynamics cannot be treated as the operator of the corresponding classical quantity because such treatment leads to violation of the uncertainty principle. Indeed, if the $T_{10}(x)$ component of this tensor is regarded as the momentum density operator then $\hat{p}_1 = \int_{\Delta V} T_{10}(x)dx\,dy\,dz$ will be the momentum operator concentrated in the small volume $\Delta V = \Delta x \Delta y \Delta z$. The eigen function ψ_λ of the operator $\hat{p}_1$ will describe the state in which the momentum p_1 is known exactly and the matter which creates this momentum is concentrated in the volume ΔV.

Thus in contemporary theory the operators $\hat{T}_{10}(x)$ and $\hat{p}_1$ lack physical meaning. This is very strange since the electromagnetic field enters into them exactly as into the classical quantities which are designated by the same letters. The cause of the difficulty appears when we attempt to find a thought experiment for measurement of p_1. The first step in such a measurement must be the establishment of a coordinate system and a metric, which is a physical operation that can be accomplished either by filling the points of space with clocks and measuring rods or by light signals. The exact establishment of a coordinate system with arbitrarily small distances by the use of quantized bodies requires momenta which are of unlimited magnitude and uncertainty. This makes it impossible to obtain an exact measurement of the momentum density $T_{10}(x)$.

In a quantum mechanical description of the space-time continuum,measurements of distances and time intervals must change the state of the system. Therefore the chosen coordinate system must be described by special dynamical variables, thus rendering possible the existence of states with an undefined coordinate system. The coordinate system must, for example, be completely undefined for the vacuum state.

The impossibility of violation of the uncertainty principle must be insured by suitable commutation relations.

3. At the present time the equations of relativistic quantum theory are subjected only to the requirement of invariance with respect to transformations of the inhomogeneous Lorentz group which lead to the following commutation relations for the operators of momentum p_μ and angular momentum $M_{\mu\nu}$ [1, 2]:

$$[M_{\mu\nu}, M_{\lambda\sigma}] = i(\delta_{\mu\sigma} M_{\lambda\nu} + \delta_{\mu\lambda} M_{\nu\sigma} + \delta_{\nu\sigma} M_{\mu\lambda} + \delta_{\lambda\nu} M_{\sigma\mu}),$$
$$[M_{\mu\nu}, p_\lambda] = i(p_\nu \delta_{\mu\lambda} - p_\mu \delta_{\nu\lambda}), \quad (p_\mu, p_\nu) = 0. \tag{1}$$

However the exclusive use of Cartesian coordinate systems implies the physical assertion that filling a bounded region around the origin with clocks and measuring rods is equivalent to measuring distances and time intervals in all space; this necessarily leads to the possibility of exact measurements of momentum in a bounded volume, which is inadmissible in quantum mechanics.

Indeed, the physical assignment of a coordinate system in one region does not predetermine the accuracy with which the coordinate system will be established at a distance from this region. The mathematical account of this fact must consist of allowing for all "degrees of freedom" of change of the coordinate system, that is, imposing on the theory the requirement of invariance with respect to all curvilinear coordinates.

4. A precise mathematical formulation can be obtained for the foregoing physical considerations. Let us assume that:

I. The theory is quantized. This means that any state of the physical system is describable by a wave function (state vector) and that the equations of motion are linear with respect to this function.

II. The theory is relativistic. This means that space and time form a four-dimensional continuum with a pseudo-Euclidean metric.

It follows from II that the correct theory must be invariant with respect to transformations to any curvilinear coordinate systems:

$$x^{\mu} = f^{\mu}(x') \tag{2}$$

These transformations form a group. In accordance with I, to each Transformation (2) there must correspond a linear transformation of the wave function (state vector) Ψ:

$$\Psi_q = U_{qq'}(f)\,\Psi_{q'}, \tag{3}$$

in which the matrices U(f) must form a representation of the group of (2). Infinitely small Transformations (2) and (3) have the respective forms:

$$x^{\mu} = x'^{\mu} + \xi^{\mu}(x'), \tag{4}$$

$$\Psi = \left\{1 + i\int dx\,\xi^{\mu}(x)\,R_{\mu}(x)\right\}\Psi'. \tag{5}$$

where $R_{\mu}(x)$ is an operator which is independent of $\xi^{\mu}(x)$.

We now perform four transformations in succession:

$$x^{\mu} = x'^{\mu} + \xi_1^{\mu}(x'), \tag{6}$$

$$x'^{\mu} = x''^{\mu} + \xi_2^{\mu}(x''), \tag{7}$$

the inverse of (6) and the inverse of (7).

As a result we obtain up to the second order:

$$x^{\mu} = x^{(\mathrm{IV})\mu} + \xi_2^{\nu}(x^{(\mathrm{IV})})\frac{\partial \xi_1^{\mu}(x^{(\mathrm{IV})})}{\partial x^{(\mathrm{IV})\nu}} - \xi_1^{\nu}(x^{(\mathrm{IV})})\frac{\partial \xi_2^{\mu}(x^{(\mathrm{IV})})}{\partial x^{(\mathrm{IV})\nu}} \equiv \\ \equiv x^{(\mathrm{IV})\nu} + \xi_3^{\mu}(x^{(\mathrm{IV})}). \tag{8}$$

By definition, the resulting transformation for Ψ must satisfy the condition

$$\Psi = \left\{1 + i\int dx\, \xi_1^{\mu}(x) R_{\mu}(x)\right\}\left\{1 + i\int dx' \xi_2^{\nu}(x') R_{\nu}(x')\right\} \times \\ \times \left\{1 + i\int dx'' \xi_1^{\lambda}(x'') R_{\lambda}(x'')\right\}^{-1}\left\{1 + i\int dx''' \xi_2^{\sigma}(x''') R_{\sigma}(x''')\right\}^{-1} \psi^{(\mathrm{IV})} = \\ = \left\{1 + i\int dx\, \xi_3^{\mu}(x) R_{\mu}(x)\right\}\psi^{(\mathrm{IV})}. \tag{9}$$

Inserting $\xi_3^{\mu}(x)$ from (8) into (9) and making use of the arbitrariness of $\xi_1^{\mu}(x)$ and $\xi_2^{\mu}(x)$ we obtain commutation relations for $R_{\mu}(x)$:

$$[R_{\mu}(x), R_{\nu}(x')] = i\left\{R_{\nu}(x)\frac{\partial}{\partial x^{\mu}} - R_{\mu}(x')\frac{\partial}{\partial x'^{\nu}}\right\}\delta(x - x'). \tag{10}$$

The Relations (10) are the desired invariance conditions of the theory with respect to transformations to arbitrary curvilinear coordinates. In the relativistic theory only such wave functions are permissible for which it is possible to define an operator $R_{\mu}(x)$ which satisfies (10). The operator $R_{\mu}(x)$ is actually defined in accordance with (5) at the point $\underline{x}$ of space. In this it differs essentially from the operators "defined at a point" of the existing field theory in connection with which it is impossible to prove that the parameter "x" on which they depend is identical with a coordinate of space.

Let us clarify the physical meaning of the operator $R_{\mu}(x)$. Setting in (5)

$$\xi^{\mu}(x) = \mathrm{const},$$

we obtain

$$\int dx\, R_{\mu}(x) = p_{\mu}, \tag{11}$$

and with

$$\xi^{\mu}(x) = \varepsilon^{\mu}_{\nu} x^{\nu}$$

we obtain

$$\int dx\,(x_{\mu} R_{\nu}(x) - x_{\nu} R_{\mu}(x)) = M_{\mu\nu}. \tag{12}$$

5. The next step in the construction of the correct theory must be the obtaining of irreducible unitary representations of the group of (2), that is, quantities which are covariant with respect to this group and which are admissible as wave functions. A wave function of a regular representation of the group of (2) is a functional of $f^{\mu}(x)$ in (2):

$$\psi = \psi[f^{\mu}(x)], \tag{13}$$

and the operator $R_{\mu}(x)$ has the form

$$R_{\mu}(x) = \frac{1}{i}\,\frac{\partial f^{\nu}(x)}{\partial x^{\mu}}\,\frac{\delta}{\delta f^{\nu}(x)}\,. \tag{14}$$

Since $R_{\mu}(x)$ does not commute with the operator $f^{\mu}(x)$ which selects a system of coordinates, momentum measurements in a bounded volume are possible only in an undefined coordinate system.

6. The assignment of a coordinate system is equivalent to the identification of individual points of the continuum and makes no stipulations regarding the metric properties of space which must be described by the metric tensor. For the wave function (13) the metric tensor is an operator of the form

$$\begin{aligned} g_{\mu\nu}(x) &= \frac{\partial f^{\lambda}(x)}{\partial x^{\mu}}\,\frac{\partial f^{\sigma}(x)}{\partial x^{\nu}}\int dy\, g^{0}_{\lambda\sigma}(y)\,\delta(y - f(x)) = \\ &= \frac{\partial f^{\lambda}}{\partial x^{\mu}}\,\frac{\partial f^{\sigma}}{\partial x^{\nu}}\, g^{0}_{\lambda\sigma}(f(x)), \end{aligned} \tag{15}$$

where $g^{0}_{\lambda\sigma}(y)$ is the metric tensor in some single coordinate system. The tensor $g_{\mu\nu}(x)$ also does not commute with $R_{\mu}(x)$. In the special theory of relativity $g^{0}_{\lambda\sigma}$ can be pseudo-Euclidean.

7. In the transition to the general theory of relativity, $g^{0}_{\mu\nu}(x)$ must be regarded as a functional variable of the wave function. The extension of the theory to allow for gravitation will result naturally from a correct quantum-mechanical description of the properties of space-time. In assuming that $g^{0}_{\mu\nu}(x)$ is pseudo-Euclidean we clearly perform the operation, inadmissible in quantum mechanics, of simply dropping the degrees of freedom which exist in gravitation; such simple discarding is inconsistent with the uncertainty relation between the conjugate coordinate and momentum which correspond to a degree of freedom.

8. It is of interest to note that the relations (10) were actually first taken into account by Tomonaga [4]. Indeed, for the functional $\psi[t_{xyz}]$ it is possible to define an operator $R_{\mu}(x)$ which satisfies (10):

$$\begin{aligned} R(\mathbf{x}, t) &= i\delta(t - t_{xyz})\,\frac{\partial t_{xyz}}{\partial \mathbf{x}}\,\frac{\delta}{\delta t_{xyz}} \\ R_{0}(\mathbf{x}, t) &= i\delta(t - t_{xyz})\,\frac{\delta}{\delta t_{xyz}}\,. \end{aligned} \tag{16}$$

Then in the equation

$$i\,\frac{\delta}{\delta t_{xyz}}\,\psi = H(x)\,\psi \tag{17}$$

the wave function is covariant with respect to the functional variable t_{xyz}.

9. In the deduction of the Relations (10) the number of dimensions of space is not important. Therefore the invariance conditions of nonrelativistic quantum theory with respect to coordinate transformations of tridimensional space are of the same form as (10) with the single difference that the δ function is tridimensional and the indices run through the values i, j = 1, 2, 3.

These conditions are fulfilled in nonrelativistic quantum mechanics. For example, for a nonrelativistic wave function $\psi(x)$ the operator $R_i(y)$ has the form

$$R_i(y) = \frac{1}{i}\,\delta(x-y)\frac{\partial}{\partial x_i} - \frac{1}{2i}\frac{\partial\delta(x-y)}{\partial y_i} \tag{18}$$

Therefore the foregoing considerations do not affect nonrelativistic quantum mechanics. The profound difference between these theories lies in the fact that in field theory the coordinates are c-numbers while in nonrelativistic quantum mechanics they are operators.

10. At the present time it is widely held that in order to overcome the difficulties of field theories some fundamentally new physical ideas are needed. From the viewpoint which has been presented a more immediate task is not the search for new ideas but a correct formulation of old physical ideas of relativity and the quantum properties of matter.

M. V. Lomonosov Moscow State University

Received June 11, 1956

LITERATURE CITED

[1] V. Bargmann and E. Wigner, Proc. Nat. Acad. Sci. (USSR) 34, 211 (1948).

[2] P. A. M. Dirac, Rev. Mod. Phys. 21, 392 (1949).

[3] I. M. Gel'fand and M. A. Naimark, J. Phys. 10, 93 (1946); Bull. Acad. Sci. USSR, Math. Ser. 11, 411 (1947).

[4] S. Tomonaga, Progr. Theoret. Phys. 1, 27 (1946).

EMISSION SPECTRUM OF CORONENE IN SOLUTIONS AT LOW TEMPERATURES

E. V. Shpol'skii and L. A. Klimova

(Presented by Academician L. A. Artsimovich, October 9, 1956)

1. In a number of previous articles from our laboratory [1-3] and those written by Bowen and Brocklehurst [4, 5] it was shown that some condensed aromatic polynuclear hydrocarbons in solutions of normal paraffins (beginning with n-pentane) frozen at 77°K, yield fluorescence and phosphorescence spectra in such narrow bands that they can be called "lines." In these articles eleven aromatic hydrocarbons were mentioned whose spectra present such a picture. It was pointed out that this picture appears whenever the solvent freezes in crystalline form; on the other hand, in solvents which on freezing become a transparent vitreous mass (special mixtures, alcohols) the spectrum becomes diffuse [3, 5]. Finally, it was shown that the most favorable conditions for the spectral structure are found in the paraffins in which the size of the c axis of an elementary cell of the crystal is close to the size of the emitting molecules.

In view of the fact that our earlier photographs of spectra were taken with apparatus whose resolving power was insufficient to reveal all details we took new photographs with instruments of considerably higher resolving power (an ISP 51 triple-prism glass spectrograph with a long-focus camera, of linear dispersion 6.3 A/mm at at 4000 A, and a spectrograph with a diffraction grating, of linear dispersion 6.3 A/mm over the entire spectrum).

2. As was indicated previously [1] the fluorescence spectrum of coronene taken under the indicated conditions is characterized by close pairs of lines whose components are separated by an amount which is constant for a given solvent (86 cm^{-1} in hexane, 70 cm^{-1} in heptane and 38 cm^{-1} in octane).

Let us consider the spectrum in hexane, for example (see Fig. 1). This reveals a weak line at 4262 A which on the basis of its relation to the absorption spectrum [5, 10] * must represent a O' → O" transition. But this line (like the corresponding lines in heptane and in octane) is not actually the shortest wave length since there is a line in the violet direction at 4246 A, which is thus separated by only 86 cm^{-1}. If these two lines are taken as a basis and the differences are found between the frequencies of these and suitably chosen succeeding lines the entire spectrum including its long-wave region, which is rich in lines, can be divided into two series which are duplicates with regard to the succession of frequencies but are separated by 86 cm^{-1} (Fig. 1, a). The same result is obtained in the other two solvents, heptane and octane, but with shifts of 70 and 38 cm^{-1}, respectively,** (Fig. 1, b). It is very important that when the series thus found in the different solvents are compared it is found that with the exception of a few individual frequencies the series coincide (Table 1). Since the solvent thus affects only the magnitude of the relative shift of the two series these series themselves must naturally be associated with the radiating molecule, that is, with coronene. Unfortunately, we do not know either the Raman spectrum or the infrared spectrum of coronene. We may hope to make some use of a structural analogy between

---

* No reference [10] appears in the original text – translator's note.

** We omit for the time being the finer details of the spectra such as the appearance of satellites at 15-20 cm^{-1} from the principal line as well as the complex character of the doublets in the long-wave region (each line in turn is split into two components).

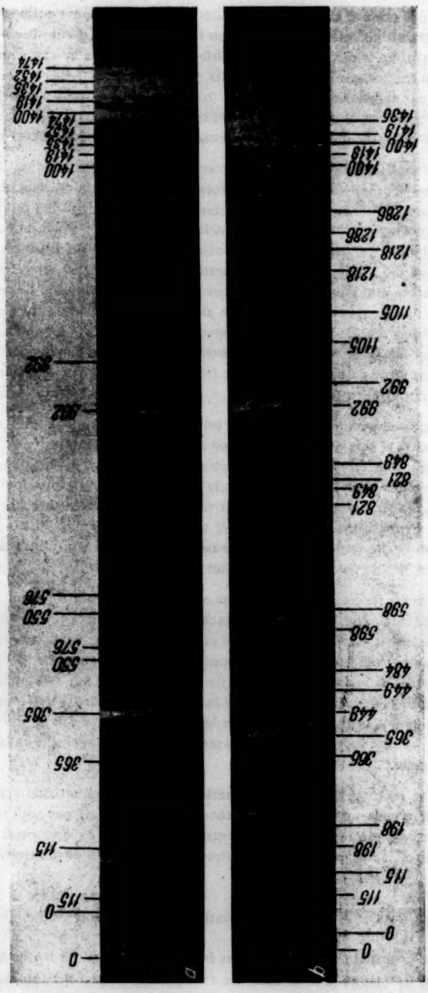
a
0
115
365
385
550
576
852
1400
1418
1419
1436
1452
1474
b
0
115
198
365
449
484
598
821
849
992
1105
1218
1286
1400
1418
1419
1436

Fig. 1.

coronene and benzene since both of these flat molecules belong to the same point symmetry group D_{6h}. For this class group theory establishes selection rules which forbid a $O' \rightarrow O''$ transition from symmetry [8]. In free benzene molecules (in the gaseous state) this prohibition is removed by antisymmetric vibrations e_{2g}* (606 cm^{-1}) which deform the molecule. In a coronene molecule the $O' \rightarrow O''$ transition should also be forbidden by symmetry [8] but under our conditions in a frozen crystalline solution the prohibition may be removed by the perturbing effect of the solvent. Since the transition probability is small in any event the corresponding line will be weak and its intensity must also depend considerably on the solvent. This is what is actually observed.

It appears however that the analogy with benzene goes much further than was to be expected. Indeed, Table 1 shows that the frequencies which are most strongly represented in the vibrational spectrum of benzene are also present in the spectrum of coronene. First there is the frequency of the fully symmetrical vibration a_{1g} (the "breathing" frequency) of the hydrocarbon skeleton at 992 cm^{-1} which in both spectra is of an intensity which far exceeds the others.** There is also the frequency 3070 [5], which within the limits of error agrees with the frequency 3062 of the fully symmetrical vibrations of the hydrogen atoms of benzene. In Table 1 we find a number of frequencies, which are close to the benzene frequencies in the last column, that are observed almost exclusively in its Raman spectrum. The table also gives more than 25 frequencies that are characteristic of but are not found in either the Raman or infrared spectrum of benzene. Among these we note the strong line 365 cm^{-1} whose origin has not been established. It should also be noted that among these frequencies we do not find frequencies which are close to the characteristic frequencies of normal paraffins [6]. It must be understood that this statement does not refer to low frequencies (< 100 cm^{-1}), which are not known at all.

3. Besides its fluorescence, coronene in frozen solutions emits yellow-green light of long duration ($\tau = 9$ sec). The interpretation of this persistent emission as a forbidden triplet-singlet transition can now be regarded as experimentally proved. The phosphorescence spectrum of coronene is given in Figs. 4 and 5 of a previous communication [3], where the weak lines unfortunately did not appear. Despite the great complexity of this spectrum compared with the fluorescence spectrum, it can also be separated into two series with a relative shift. This is rendered feasible by the different intensities of the two spectra. The shift is different from the shift in the fluorescence spectrum in the same solvent. Thus in hexane it is 58 cm^{-1} instead of 86 for fluorescence; in heptane it is 52 instead of 70 and in octane it is 13 instead of 38 cm^{-1}.

Since in this case, as for fluorescence, transitions occur to vibrational levels of the lower singlet state, it must be expected that the frequency differences of each series will reproduce the vibrations which are obtained from the fluorescence spectra. We find confirmation of this in Table 1. Here asterisks denote the vibrational frequencies which are indeed common to the fluorescence and phosphorescence spectra. It is of interest that these are just the frequencies which are absent from the benzene spectrum. We believe that this can confidently be attributed to a change in molecular configuration in the (di free radical) triplet state and the associated change of molecular symmetry, which leads in turn to a change of the selection rules. The fact that the molecule must have different symmetry in the triplet and singlet states has frequently been shown from analysis of the phosphorescence spectrum of benzene [7].

4. The origin of the relative shift of the two series which is characteristic of a given solvent is not yet understood. A number of hypotheses have been advanced [3, 5, 8] but all are open to serious objections. The solution of this important problem requires broad diversification of the experimental conditions: study of the spectra of a large number of substances of different structures, the effect of substitutions, the effect of temperature, etc.

---

*Here and hereinafter, as well as in Table 1, the notations and numbering of the vibrations of benzene follow Herzberg [9].

**The very diffuse shape of this line in Fig. 1 results from the halo induced by the 992 cm^{-1} line, whose intensity is approximately 100 times greater than the average intensity of the remaining spectral lines.

TABLE 1

In hexane	In heptane	In octane	Av.	From the data in Ref. [5] for coronene in heptane	Similar frequencies of benzene (from the Raman spectrum)
118	115	111	115*	—	
—	—	—	—	295	
367	366	364	365*	365	
447	453	448	449*	420	
—	—	484	484*	480	
550	—	—	—	550	
600	—	596	598	615	ν_{18} ($C_\parallel$ $e_{2g} = 605$)
—	822	820	821	825	
851	—	847	849	850	ν_{11} ($H_\perp$ $e_{1g} = 848{,}9$)
990	995	992	992	995	ν_2 (CC $a_{1g} = 991{,}6$)
—	—	1030	—	—	
—	—	1068	—	—	
—	1082	—	—	—	
—	—	1105	—	—	
1152	1154	—	1153*	1155	
1175	1171	—	1173	—	ν_{17} ($H_\parallel$ $a_{2g} = 1175$)
1200	—	1200	1200	—	
1218	—	1218	1218*	1220	
—	1262	—	—	—	
1286	1286	1284	1286*	1290	
1402	1403	1399	1400*	1405	
1419	1419	1418	1419	—	
1435	1436	1434	1435*		
1452	1451	1452	1452	—	
1474	1475	1473	1474		ν_{13} (CC $e_{1u} = 1475$) **Infrared benzene spectrum (1478-1485)**
1715	1716	1715	1715*	1715	$\nu_2 + 2 \times 365 = 992 + 730 = 1722$
1734	1734	1734	1734	—	
1786	1788	1788	1787	—	
—	—	1800	1800*	—	
—	—	1810	—	—	
1884	1882	1879	1882*	—	**Infrared frequency 1880**
1898	1894	—	1896	1900	**(?)**
—	1913	—	—	—	
—	—	2022	—	2020	
—	—	—	—	2215	
2346	2344	2346	2345	2345	$2\nu_2 + 365 = 2349$ (?)
2365	2363	2364	2364	—	
—	—	—	—	2525	
—	—	2776	—	—	
—	—	2790	2790*	—	
—	—	2808	2800*	2810	
—	—	—	—	3070	ν (CH) $a_{1g} = 3062$)
—	—	—	—	3250	
—	—	—	—	3720	

The authors are deeply grateful to P. P. Feofilov for the use of his spectrograph and diffraction grating to photograph the spectrum of coronene.

V. I. Lenin Moscow State Pedagogical Institute

Received October 9, 1956

LITERATURE CITED

[1] E. V. Shpol'skii, A. A. Il'ina and L. A. Klimova, Doklady Akad. Nauk SSSR 87, 935 (1952).

[2] E. V. Shpol'skii and L. A. Klimova, Bull. Acad. Sci. USSR, Phys. Ser. 673 (1954).

[3] E. V. Shpol'skii and L. A. Klimova, 4th Conference on Luminescence, June 20-25, 1955; Bull. Acad. Sci. USSR, Phys. Ser. 20, 471 (1956).

[4] E. J. Bowen and B. Brocklehurst, J. Chem. Soc. 1954, 3875.

[5] E. J. Bowen and B. Brocklehurst, J. Chem. Soc. 1955, 4320.

[6] N. Sheppard and D. M. Simpson, Quart. Rev. Chem. Soc. 7, 1, 19 (1953).

[7] P. Pesteil and A. Zmerli, Ann. Physik. 10, 1079 (1955).

[8] J. Sidmann, J. Chem. Phys. 23, 365 (1955).

[9] G. Herzberg, Vibrational and Rotational Spectra of Polyatomic Molecules (Foreign Lit. Press, 1949) (Russian Translation).

SOVIET PHYSICS – "DOKLADY" VOL. 1, NO. 6 SEPTEMBER, 1957

(Translation of all papers in the "Physics" Sections of the Proceedings of the
Academy of Sciences of the USSR, Vol. 111, Nos. 1-6, November-December, 1956)

CONTENTS

	Page	Russian Issue No.	Russian Page
Polarization of Low-Energy Protons Scattered by Carbon. B. V. Gavrilovskii, V. Ia. Golovnia, K. V. Karadzhev, A. P. Kliucharev, and V. I. Man'ko	611	1	59
On the Theory of a Real Gas with Noncentral Particle Interaction. A. E. Glauberman	615	1	63
On the Scattering Matrix of an Intermediate System. M. S. Livshits	620	1	67
An Investigation of the N Component of Extensive Air Showers. S. N. Nikol'skii, Iu. N. Vavilov and V. V. Batov	625	1	71
Nonlinearity and Conformal Reciprocity. Andrei Popovich	628	1	74
On the Theory of Concentration Quenching of Fluorescent Solutions. B. Ia. Sveshnikov	633	1	78
The Polarization of Protons Scattered Elastically by C^{12}. P. V. Sorokin and A. Ia. Taranov	637	1	82
The Effect of a Longitudinal Magnetic Field on Impulsive Gas Discharges with Large Currents. A. L. Bezbatchenko, I. N. Golovin, D. P. Ivanov, V. D. Kirillov, and N. A. Iavlinskii	640	2	319
The Energy Spectrum of He^3 Dissolved in He II. N. G. Berezniak and B. N. Esel'son.	645	2	322
Triplet-Quintet Transitions in the Atomic Spectrum of Silicon. N. A. El'iashevich and O. N. Nikitina	649	2	325
On the Intermolecular Transfer of Excitation Energy in Crystals. E. K. Zavoiskii and G. E. Smolkin	652	2	328
The Upper Limit of the Radiation Capture Cross Section of 275 Kev Resonance Neutrons by Li^7. E. A. Koltypin and V. M. Morozov	655	2	331
The Excitation of Macroscopic Oscillations by Quantum Fluctuations. A. A. Sokolov, D. D. Ivanenko, and I. M. Ternov	658	2	334
Meson-Meson Scattering in Meson Field Theory. V. V. Sudakov	662	2	338
On Pion Production by High-Energy Cosmic Rays. Zh. S. Takibaev, P. A. Usik, and M. G. Antonova	666	2	341
Causality and the Criterion of Physical Realizability in Quantum Field Theory. L. A. Khalfin	671	2	345
Electrical Conductivity and Photoconductivity of Phthalocyanines. A. T. Vartanian and I. A. Karpovich	675	3	561
Linear and Quadratic Zeeman Effects and Exciton Diamagnetism of Copper Oxide Crystals. E. F. Gross and B. P. Zakharchenia	678	3	564
The λ Point of Solutions of Helium Isotopes. B. N. Esel'son, N. G. Berezniak, and M. I. Kaganov	683	3	568

CONTENTS (continued)

	Page	Russian Issue No.	Russian Page
On the Dispersion Relation for Nucleon-Nucleon Scattering. F. M. Kuni	686	3	571
The Interaction of Vibrations of Nonpolar Crystals with Electric Fields. V. S. Mashkevich and K. B. Tolpygo	690	3	575
Nucleon Propagation Function in the Quadratic Approximation. V. G. Solov'ev	693	3	578
Luminescence Flashes in Zinc Sulfide Crystals and the Two-Stage Excitation Mechanism. N. A. Tolstoi	698	3	582
Towards a General Theory of Meson Scattering. A. Brodskii	701	4	787
Measurements of the $Li^6(n, t)He^4$ Cross Section for Neutrons with Energies from 9 to 700 Kev. G. V. Gorlov, B. M. Gokhberg, V. M. Morozov, and G. A. Otroshchenko	705	4	791
Interactions of Fast Pions and Nuclei. L. P. Kudrin and B. A. Nikol'skii	708	4	795
On an Intermediate System Formed During the Scattering of Elementary Particles. M. S. Livshits	712	4	799
Spectrophotometric Method of Investigating Dispersion and Absorption by Solids. M. P. Lisitsa	716	4	803
Enrichment of Radioactive Isotopes of Iodine, Germanium, Arsenic, and Antimony by (γ, n) Reactions. A. N. Murin, V. D. Nefedov, V. I. Baranovskii, and D. K. Popov	719	4	806
Saturation Measurements of Ultrasonic Absorption in Ethyl Acetate Using an Impulse Method with Two Fixed Distances. V. F. Nozdrev and V. D. Sobolev	722	4	808
Ionic Conductivity of KI(Tl) Phosphors. L. M. Shamovskii, A. A. Dunina, and M. I. Gosteva	725	4	811
On the Theory of Dielectric Polarization. M. N. Shakhparonov	728	4	815
Spontaneous Lattice Deformations in Ferromagnetic Transitions. K. P. Belov and N. K. Panina	732	5	985
Elastic Scattering of Gamma Rays with Energy to 120 Mev by Protons. B. B. Govorkov, V. I. Gol'danskii, O. A. Karpukhin, A. V. Kutsenko, and V. V. Pavlovskaia	735	5	988
Scattering of Positive and Negative 300-Mev Pions by Hydrogen. L. S. Dul'kova, I. B. Sokolova and M. G. Shafranova	739	5	992
Maximum Amplification Factor and Noise of Photomultipliers. E. K. Zavoiskii, M. M. Butslov, and G. E. Smolkin	743	5	996
The Transmission of Radiation Through an Inhomogeneous Medium. V. V. Sobolev	747	5	1000
An Asymptotic Investigation of the Vertex Part in Quantum Electrodynamics. V. Z. Blank and D. V. Shirkov	752	6	1201
Photoproduction of Slow π^--Mesons in Complex Nuclei. E. G. Gorzhevskaia and N. M. Panova	757	6	1205
Double-Resonance Curves of a Reflection Grating. L. N. Deriugin and G. Kh. Fridman	761	6	1209

CONTENTS (continued)

		Russian	
	Page	Issue No.	Page
On Positron Annihilation in Metals. V. I. Karpman and I. Z. Fisher	765	6	1212
Spark Channel Broadening in Air at About 2×10^6 Amperes. V. S. Komel'kov and D. S. Parfenov.	769	6	1215
Nuclear Levels of Li^6. Iu. L. Sokolov, M. M. Sulkovskaia, E. A. Al'bitskaia, and E. I. Karpushkina	773	6	1219
On Relativistic Invariance in Quantum Theory. Iu. M. Shirokov	777	6	1223
Emission Spectrum of Coronene in Solutions at Low Temperatures. E. V. Shpol'skii and L. A. Klimova.	782	6	1227

The expanded program of the American Institute of Physics comprises translation of four leading Soviet physics journals, as listed below. These translations, by competent, qualified scientists, will provide all research laboratories and libraries with accurate and up-to-date information of the results of research in the U.S.S.R.

Soviet Physics — Technical Physics

A translation of the "Journal of Technical Physics" of the Academy of Sciences of the U.S.S.R. The 1956 volume, which was originally announced as containing eighteen issues, is instead being issued monthly, in expanded issues. All issues of the original Russian journal for 1956 will be translated. Approximately 4,000 Russian pages. Annually, $90.00 domestic, $95.00 foreign.

Soviet Physics — Acoustics

A translation of the "Journal of Acoustics" of the Academy of Sciences of the U.S.S.R. Four issues per year, approximately 500 Russian pages. Annually, $20.00 domestic, $22.00 foreign. The 1955 issues of "Journal of Acoustics" U.S.S.R. will also be published. Will consist of two volumes, approximately 500 pages, and the subscription price will be $20.00 for the set.

Soviet Physics "Doklady"

A translation of the "Physics Section" of the Proceedings of the Academy of Sciences of the U.S.S.R. Six issues per year, approximately 900 Russian pages. Annually $25.00 domestic, $27.50 foreign.

Soviet Physics — JETP

A translation of the "Journal of Experimental and Theoretical Physics" of the Academy of Sciences of the U.S.S.R. Twelve issues per year, approximately 2,600 Russian pages. Annually $60.00 domestic, $64.00 foreign. Back issues of Volume 1 and 2 are available at a special price of $30.00 for both to subscribers to Volume 3.

Subscriptions should be addressed to the American Institute of Physics, 57 East 55th Street, New York 22, N.Y.